NORWEGIAN ENVIRONMENT AGENCY

Monitoring Report M-1735 | 2020

Monitoring ocean acidification in Norwegian seas in 2019

MADE BY:
Institute of Marine Research, NORCE Norwegian Research Centre, University of Bergen, Norwegian Institute for Water Research

COLOPHON

Executive institution (the institution is responsible for the content in this report)

Institute of Marine Research, NORCE Norwegian Research Centre, University of Bergen, Norwegian Institute for Water Research

Project manager for the contractor

Melissa Chierici

Contact person in the Norwegian Environment Agency

Gunnar Skotte

M-no	Year	Pages	Contract number
1735	2020	152	17078007

Publisher

Norwegian Environment Agency

The project is funded by

Norwegian Environment Agency

Author(s)

Jones, E., M. Chierici, I. Skjelvan, M. Norli, H. Frigstad, K.Y. Børsheim, H.H. Lødemel, T. Kutti, A.L. King, K. Sørensen, S. K. Lauvset, K. Jackson-Misje, L.B. Apelthun, T. de Lange, T. Johannsessen, C. Mourgues, R. Bellerby.

Title - tittel

Monitoring ocean acidification in Norwegian seas in 2019 / Havforsuringsovervåking i norske farvann i 2019

Summary - sammendrag

This is the annual report from 2019 based on the program: ‘Monitoring ocean acidification in Norwegian waters’ and ‘Monitoring of ocean acidification in the coastal zone’ funded by the Norwegian Environment Agency. The measurements are performed by the Institute of Marine Research (IMR), Norwegian Institute for Water Research (NIVA), NORCE Norwegian Research Centre (NORCE) and the Univsersity of Bergen (UiB). The measurements cover the North Sea/Skagerrak, the Norwegian Sea, and the seasonally ice-covered Barents Sea. In 2019, the program “Monitoring of ocean acidification in the coastal zone” included five fixed water column station, four lines with underway surface measurements (discrete and/or continuous) and seven cold-water coral reefs. This report presents and discusses some time series data for the period 2011-2019.

Denne rapporten gjelder undersøkelser av havforsuring i 2019 utført av Havforskningsinstituttet (IMR), Norsk institutt for vannforskning (NIVA), NORCE Norwegian Research Centre (NORCE) og Univsersitetet i Bergen (UiB) på oppdrag fra Miljødirektoratet. Måleområdet i rapporten går fra Skagerrak/Nordsjøen, Norskehavet og til nordlige deler av Barentshavet. I 2019 inkluderte prosjektet “Overvåking av havforsuring i kystsonen” målinger fra fem faste dypstasjoner, fire overflatelinjer (diskrete og kontinuerlige målinger) og sju kaldtvannskorallrev. I denne rapporten presenteres og diskuteres tidsserier fra perioden 2011-2019.

4 emneord

Karbonmålinger, mellomårlig-og sesongs-variasjon, biogeokjemiske prosesser

4 subject words

Carbonate system, interannual and seasonal variability, biogeochemical processes

Front page photo

E Jones (IMR)

Tromsø, mai 2020

Authors:
Elizabeth Jones*, Melissa Chierici*, Ingunn Skjelvan**, Marit Norli***, Helene Frigstad***, Knut Yngve Børsheim*, Helene Hodal Lødemel*, Tina Kutti*, Andrew Luke King***, Kai Sørensen***, Siv K. Lauvset**, Kristin Jackson-Misje****, Lise B. Apelthun****, Tor de Lange****, Truls Johannessen****, Claire Mourgues*, Richard Bellerby***.

*Havforskningsinstituttet (IMR), **NORCE Norwegain Research Centre (NORCE), ***Norsk institutt for vannforskning (NIVA), ****Universitetet i Bergen (UiB)

This report should be cited: Jones, E., M. Chierici, I. Skjelvan, M. Norli, H. Frigstad, K.Y. Børsheim, H.H. Lødemel, T. Kutti, A.L. King, K. Sørensen, S. K. Lauvset, K. Jackson-Misje, L.B. Apelthun, T. de Lange, T. Johannsessen, C. Mourgues og R. Bellerby. 2019. Monitoring ocean acidification in Norwegian seas in 2019, Rapport, Miljødirektoratet, M-1735|2020.

Content

Summary

This is the annual report of the 'Monitoring ocean acidification in Norwegian waters' program for 2019 funded by the Norwegian Environment Agency. The report is based on measurements of A_T, C_T, pCO_2 and pH made by the Institute of Marine Research (IMR), Norwegian Institute for Water Research (NIVA), NORCE Norwegian Research Centre (NORCE), and University of Bergen (UiB) with new data from 2019. IMR conducted water column measurements along repeat transects in the North Sea/Skagerrak (Torungen–Hirtshals), at two sections in the Norwegian Sea (Svinøy-NW, Gimsøy-NW), and at two sections in the Barents Sea (Fugløya-Bjørnøya and in the northern Barents Sea). The water column of the Norwegian Sea was also investigated by NORCE-UiB, which performed seasonal studies and continuous surface pCO_2 and surface and subsurface pH measurements at Station M. NIVA performed seasonal cruises for surface water measurements between Oslo-Kiel (North Sea/Skagerrak), Bergen-Kirkenes and Tromsø-Longyearbyen (Barents Sea opening) and present data on both seasonal and interannual basis. In addition, monthly measurements at coastal sites at Skrova, in Lofoten, and Arendal, in Skagerrak (IMR), were carried out. All sampling positions are shown in ***Figure 1***.

The project 'Monitoring of ocean acidification in the coastal zone' is performed by the partners NIVA, IMR, NORCE and Akvaplan-niva (ApN) on behalf of the Norwegian Environment agency. The aim of the project is to increase the knowledge on the status, natural variability and trends (on a longer perspective) of ocean acidification in the coastal zone in Norway. The monitoring program started in July 2019 and included measurements from five fixed water column stations, four underway surface platforms (discrete or continuous) and seven coral reefs, focused in three study regions: Hardanger, Troms/Finnmark and Isfjorden in Svalbard (***Figure 45***). The first results from this project are included as ***Chapter 3.5*** and ***Table 11-17*** in ***Appendix 6.2*** in the current report, and the results for 2019 demonstrate the large seasonal and regional variability in ocean acidification variables in Norwegian coastal waters, especially in the surface waters.

This report includes carbonate chemistry data and ancillary variables such as salinity, temperature, and inorganic nutrient concentrations to provide baseline observations of variability attributed to oceanographic and anthropogenic processes, such as the influence of mixing of water masses, freshwater/meltwater inputs, oceanic CO_2 uptake, and biological production and respiration. The data provide information that can be used in projections of future CO_2 emission scenarios and estimates in changes in the depth of the calcium carbonate ($CaCO_3$) saturation horizon. However, to determine the individual drivers of ocean acidification and their regional, seasonal and interannual variability, integrated monitoring including measurements or proxies for biological productivity, ocean physics, and land-ocean exchanges, in both surface water and in the water column is essential.

North Sea/Skagerrak

Winter sampling along the Torungen-Hirtshals section (***Figure 4***) and monthly sampling at the coastal station Arendal was carried out in the Skagerrak region (***Figure 6***). Variability in the carbonate system was driven by salinity changes as a result of freshwater inputs from riverine and Baltic Sea sources with salty waters from the southern North Sea and Atlantic Ocean. At the deepest (600 m) part of the region, temperature and salinity increased by 0.22 °C yr^{-1} and 0.02 yr^{-1}, respectively, since 2010, which is part of the observed long-term variations of exchange of Atlantic water that occur in 5-8 year cycles t these depths in the Skagerrak region (***Figure 13***). This impacted pH and Ω aragonite, which showed decreasing trends of 0.008 yr^{-1}

and 0.01 yr^{-1}, respectively. Freshwater had a large influence on surface waters in the Skagerrak (***Figure 8***) between Oslo and Kiel in spring and summer, but lowest salinities occurred in November as a likely result of increased freshwater inputs and mixing with fresher water originating in the Baltic Sea. pH and Ω aragonite were lowest in winter from freshwater inputs and mixing (***Figure 9***). The seasonal variability in surface water pCO_2 was likely strongly driven by phytoplankton production, as shown by the spring bloom that peaked in mid-March in the Skagerrak (***Figure 11***) pCO_2 increases in autumn and winter from vertical mixing and transport of carbon-rich sub-surface waters.

Norwegian Sea

Data from the Norwegian Sea were collected from two oceanographic sections Svinøy-NW and Gimsøy-NW and from the fixed station Station M and the coastal station Skrova. The distribution of pH and Ω aragonite along the Svinøy-NW and Gimsøy-NW sections shows high values in the biologically productive surface waters overlying the shelf (***Figure 16***, ***Figure 18***). Variability in the surface layer results from freshwater inputs, biological production and mixing with sub-surface Atlantic water. Low pH (8.01) and lowest Ω aragonite (0.90) were found in the deep basin of the Norwegian Sea. The saturation horizon for aragonite was located between 1500 m and 2000 m depth. Variations in Ω aragonite in the deep Norwegian Sea from 2011 to 2019 show interannual variability related to the presence of cold and fresh Arctic water and warmer Atlantic water mass. Measurements from Station M show increases in surface water pH and Ω aragonite from April to highest values in August due to biological activity. The surface pH and Ω aragonite were lowest in February-March (***Figure 20***) when CO_2-rich water is mixed up from below and temperature is low. Over the years, the deep water masses have warmed, while pH and Ω aragonite have decreased (***Figure 27***), and the saturation horizon has fluctuated around 2000 m depth. The C_T in the full water depth has increased over the last 9 years, which is connected to an increasing uptake of CO_2 from the atmosphere. Consequently, winter sea surface pCO_2 has increased by nearly 20 µatm since 2011 (***Figure 20a***), reflecting the atmospheric increase of approximately 2 µatm per year. Winter surface water pH and Ω aragonite are decreasing significantly over these 9 years: 0.0033 yr^{-1} and 0.015 yr^{-1}, respectively. Monthly measurements at coastal station Skrova in Vestfjorden show strong seasonal signals in the upper 100 m as a result of warming, freshening and biological processes during spring and summer (***Figure 26***). By early autumn, Ω aragonite starts to decrease due to reduced biological production, cooling and mixing with CO_2-rich sub-surface water.

The Barents Sea

Sampling was carried out along the Fugløya-Bjørnøya and Vardø-N transects in the Barents Sea. The latter transect is sampled in conjunction with the IMR-PINRO Barents Sea ecosystem surveys 'ØKOTOKT'. Highest pH and high Ω aragonite reflect the biological carbon uptake that occurred in the coastal waters near Fugløya (***Figure 34***). Lowest Ω aragonite occurred in the cold and fresh Arctic water. From 2012 to 2019, variability in pH and Ω aragonite is associated with fluctuations in Atlantic and Arctic water (***Figure 42***). Since 2016, the cooling and freshening trend at 300-400 m depth was accompanied by a reduction in Ω aragonite. In the northern Barents Sea, surface layer pH was highest with high Ω aragonite in the Arctic water in the north (***Figure 35***). Lowest pH and low Ω aragonite were found at 50-100 m depth in the north, likely due to increased CO_2 from microbial degradation of organic matter and the release of high-CO_2 brines from sea ice. Seasonal coverage of surface waters between Tromsø-Longyearbyen showed that variability in carbonate chemistry across the Barents Sea opening is controlled by freshwater inputs, biological production during summer, and water mass circulation. Surface waters have freshened since 2013. The underway data from MS *Norbjørn* show that pCO_2 was high during winter (January-February) in open water, and lower near the Norwegian and Svalbard coast, which is strongly connected to salinity and temperature influences. The underway sensor data from MS *Trollfjord* between Kirkenes and Bergen show a seasonal cycle for temperature and salinity, in which summertime was warmer and fresher. The coastal region near Kirkenes was low in salinity year-round, and also exhibited low pCO_2 values.

<u>The Norwegian Coastal zone</u>

In 2019, the project 'Monitoring of ocean acidification in the coastal zone' collected measurements from several sites in the coastal areas of Norway and Svalbard (***Figure 45***). Two sites in the Hardanger area showed strong seasonality in the upper 100 m (***Figure 47***) driven by river input and rain, with influences from the coastal current in the north. Surface pH and Ω aragonite are low during winter and increases with increasing biological production. Ω aragonite follows later than pH due to the low temperature in late winter/early spring. Cold water coral reefs sampling included 2 wall reefs in Hardanger and 5 sill or hill reefs in northern Norway. The carbonate chemistry varied greatly both seasonally and within the day due to freshwater inputs and strong biological uptake to give high pH values and Ω aragonite in the surface layer (***Figure 51-52***). Below 80 m (at the depths at which the corals grow), net bacterial respiration of organic matter and mixing with Atlantic water increased C_T and was usually accompanied by lowest pH and Ω aragonite. Malangen fjord, located in the northern Norwegian Sea, showed large spatial variability in hydrographic variables and oxygen saturation, cDOM fluorescence and pCO_2 in late summer/autumn 2019 from surface underway measurements (***Figure 54***). The variability in pCO_2 was partly driven by freshwater input (reduced pCO_2 near the Straumsfjorden coastal station associated with low salinity and high cDOM) and water mass cooling, that began at the end of September and continued to cool through October. This corresponded to low C_T and A_T in surface waters (***Figure 55***), and Ω aragonite in this period was mostly at or below saturation (0.5-1.9), meaning that these surface waters could be corrosive to organisms with calcium carbonate shells. On Svalbard, large seasonal variability is observed in the hydrography and carbonate chemistry in Adventfjorden (IsA station), a small branch of the larger Isfjorden on the west Spitsbergen coast. Ω aragonite variability was influenced by organic matter remineralisation and mixing in winter and CO_2 uptake through primary production in summer (***Figure 63***). Towards the mouth of Isfjorden (SVR1/IsG station), lowest pH and Ω aragonite were found below 50 m in higher salinity waters more characteristic of Atlantic Water (***Figure 64***). Decreases in surface pH and Ω aragonite over two months are related to a cooling and freshening of surface waters.

Extended Norwegian Summary

Denne rapporten beskriver overvåking av havforsuring i norske farvann i 2019 og arbeidet er gjort av Havforskningsinstituttet (IMR), Norsk institutt for vannforskning (NIVA), NORCE Norwegian Research Centre (NORCE) og Universitetet i Bergen (UiB) på oppdrag fra Miljødirektoratet innenfor programmet 'Havforsuringsovervåking i norske farvann', som startet i 2013. Rapporten er basert på diskrete målinger av total alkalinitet (A_T), totalt uorganisk karbon (C_T) og pH, samt kontinuerlige målinger av pCO_2 og pH. Både overflaten og vannsøylen er målt og målefrekvens, variabler og dyp er beskrevet i ***Tabell 1***. IMR har samlet inn vannsøyleprøver fra faste snitt i Skagerrak (Torungen–Hirtshals), i Norskehavet (Svinøy-NW og Gimsøy-NW), i Barentshavet (Fugløya-Bjørnøya og stasjoner i det nordlige Barentshavet), og fra kyststasjonene Arendal og Skrova. Norskehavet er også undersøkt av NORCE-UiB, som har samlet prøver fra vannsøylen på Stasjon M og gjort kontinuerlige overflate- og blandingslagsmålinger fra samme posisjon. NIVA har gjort overflatemålinger i vestlige deler av Barentshavet (Tromsø-

Longyearbyen), Bergen-Kirkenes og Skagerrak samt deler av Oslofjorden (Oslo-Kiel). Alle målepunkt er vist i ***Figur 1***.

Prosjektet 'Overvåkning av havforsuring i kystsonen' blir utført av partnerne NIVA, HI, NORCE og Akvaplan-niva på oppdrag fra Miljødirektoratet. Formålet med prosjektet er å øke kunnskapen om status, naturlig variasjon og trender (på lengre sikt) av havforsuring i kystområdene i Norge. Overvåkingsprogrammet startet i juli 2019 og inkluderer målinger av fem vannsøylestasjoner, fire plattformer for overflatemålinger (diskret og kontinuerlig) og syv korallrev, med fokus på tre studieområder: Hardanger, Troms/Finnmark, og Isfjorden på Svalbard (***Figur 45***). Resultatene fra 2019 viser den betydelige variasjonen over sesong og regioner i havforsuringsvariabler i norske kystvann, spesielt i overflatelaget. Resultatene for 2019 er gitt i ***Kapittel 3.5*** og datatabeller ***11-17*** i ***Appendiks 6.2***.

Rapporten inkluderer karbonatsystemdata (A_T, C_T, pH, pCO_2) og tilleggsdata som salt, temperatur og næringssalt. Karbonatsystemet påvirkes av ulike prosesser som blanding av vannmasser (f.eks. atlantisk vann, kystvann, smeltevann), biologisk produksjon, respirasjon og opptak av atmosfærisk CO_2. Det er viktig å få kunnskap om den naturlige variabiliteten i systemet for å detektere små menneskeskapte endringer, og målingene i programmet komplementerer hverandre i så henseende. Vannkolonnemålingene som tas årlig og gir over tid informasjon om mellomårlige variasjoner og trender i karbonatsystemet. Vannkolonnemålingene som tas hver/annenhver måned gir grunnleggende kunnskap om sesongvariasjonen til systemet, og kontinuerlige overflatemålinger gir oss en god prosessforståelse. Rapporten presenterer målinger gjort i 2019, men her diskuteres også målinger fra tidligere år og hvordan trender i de ulike havområdene utvikler seg.

De dominerende vannmassene i det norske havområdet er kyststrømmen, atlanterhavsvann og polarvann, og en stor del av den observerte variasjonen mellom sesonger og fra år til år er drevet av endringer i det innstrømmende atlantiske vannet og av blanding med ferskt kystvann, polarvann eller smeltevann. For å få full oversikt over enkeltfaktorene bak havforsuring, regional variabilitet og sesong- og mellomårlige endringer trengs en bred overvåkning som inkluderer målinger/estimat for biologisk produksjon, havfysikk i overflate og dyp og utveksling mellom land og hav, og ikke minst trengs langsiktighet i overvåkningen.

<u>Nordsjøen/ Skagerrak</u>

Vinterprøvetaking langs snittet Torungen-Hirtshals (***Figur 2***, ***Figur 4***) og månedlig prøvetaking på kyststasjonen Arendal ble utført i Skagerrak-regionen (***Figur 2***, ***Figur 6***). Variabiliteten i karbonatsystemet ble drevet av saltholdighetsendringer som følge av tilførsel av ferskvann fra elver og Østersjøen og saltvann fra den sørlige Nordsjøen og Atlanterhavet. De dypeste delene av vannsøylen (600 m) består av kaldt, eldre vann med forhøyet C_T fra nedbrutt organisk materiale. Øvre havlag var preget av lav A_T og C_T som et resultat av den ferske kyststrømmen og biologisk aktivitet. Høyeste pH og aragonittmetning forekom i de øvre 50 m. I den dypeste delen av vannsøylen (600 m) har temperaturen og saltholdigheten økt med henholdsvis 0,22 °C år $^{-1}$ og 0,02 år $^{-1}$ siden 2010, som var et kaldt år (***Figur 13***). Denne trenden reflekterer at dypvannet i Skagerrak blir skiftet ut med innstrømmende atlanterhavsvann med en syklus på 5-8 år. Dette påvirket pH og aragonittmetningen (Ω aragonitt), som viste negative trender på henholdsvis 0,008 år $^{-1}$ og 0,01 år $^{-1}$.

Om våren og sommeren påvirket ferskvann overflatevannet i Skagerrak (***Figur 8***) mellom Oslo og Kiel, men laveste saltholdighet ble målt i november sannsynligvis fra økt elveavrenning og blanding med vann fra Østersjøen. pH varierte fra høyeste verdier i mai, på grunn av primærproduksjon, til laveste verdier i november, på grunn av ferskvannstilførsel og vinterblanding (***Figur 9***). Ω aragonitt var lavest (1.13) om vinteren og hadde høyere verdier (2.22) om sommeren og høsten. Indre Oslofjord var undermettet med aragonitt (Ω aragonitt <1) i november, mens ytre Oslofjord var undermettet i februar, når det var økt ferskvannstilførsel, økt vertikalblanding og lav biologisk produksjon. Sesongvariasjonen i overflate-pCO_2 var sannsynligvis sterkt drevet av planteplanktonproduksjon, og under vårblomstringen i Skagerrak som toppet seg i midten av mars minket pCO_2 til <300 µatm (F***igur 11***). Etter den produktive sesongen økte pCO_2 på grunn av tilførsel av ferskere vann og oppvarming, noe som tyder på at karbonatsystemet er sterkt påvirket av fysiske og geokjemiske prosesser. I løpet av høsten og vinteren økte pCO_2 ytterligere på grunn av vertikal blanding og transport av karbonrikt vann til overflaten.

Norskehavet

Data fra Norskehavet ble samlet inn fra de to oseanografiske snittene Svinøy-NW og Gimsøy-NW, fra Stasjon M og fra kyststasjonen Skrova. Langs Svinøy-NW er pH høy (8,07) i det biologisk produktive og relativt kalde overflatevannet i den norske kyststrømmen (***Figur 16***). Lavest pH (7,99-8,01) finnes i det atlantiske vannet på 50-500 m dybde som strekker seg fra sokkelen og ut i de dypere delene av Norskehavet. Ω aragonitt var høyest (1,93) som et resultat av biologisk karbonopptak i overflatelagene, og variasjonen i denne variabelen kom fra ferskvannstilførsel, biologisk produksjon og blanding med atlantisk vann. Lav pH (8,01) og laveste Ω aragonitt (0,90) ble funnet i det dype bassenget i Norskehavet. Metningshorisonten for aragonitt lå på 1900 m ved Svinøy-NW. Langs Gimsøy-NW snittet ble høyeste pH (8,07) og høy Ω-aragonitt (1,75) funnet nærmest kysten i det varme og produktive overflatevannet som ligger over sokkelen (***Figur 18***). Laveste pH (7,96) og laveste Ω aragonitt ble funnet i de dypeste delene av Norskehavet som er fylt med vannmassen kalt Norwegian Sea Deep Water. Metningshorisonten for aragonitt var på mellom 1500 m og 2000 m dybde ved Gimsøy-NW-snittet. Variasjoner i Ω aragonitt i det dype Norskehavet fra 2011 til 2019 er knyttet til blanding av kaldt, ferskt arktisk vann og varmere atlantisk vann.

På Stasjon M var overflate-pH og -Ω aragonitt lavest i februar-mars (***Figur 20***) når temperaturen var lav og dypere vann rikt på CO_2 fra remineralisert organisk materiale blandes opp til overflaten. pH og Ω aragonitt øker i overflaten fra april til høyeste verdier på henholdsvis 8,17 og 2,87 i august på grunn av biologisk aktivitet. I løpet av de siste 9 årene har de dype vannmassene blitt varmere, mens pH og Ω aragonitt har avtatt (***Figur 27***), og metningshorisonten for aragonitt (Ω aragonitt = 1) har svingt rundt 2000 m dybde. C_T i hele vanndypet har økt de siste 9 årene, og dette er koblet til et økende opptak av CO_2 fra atmosfæren. Vinterverdier av pCO_2 i overflata har økt med nesten 20 µatm i løpet av de siste 9 årene (***Figur 20a***), som gjenspeiler den atmosfæriske økningen på omtrent 2 µatm per år. I denne perioden har vinterverdier av pH og Ω aragonitt i overflatevann avtatt betydelig: henholdsvis 0,0033 år $^{-1}$ og 0,015 år $^{-1}$. Månedlige målinger ved Skrova kyststasjon i Vestfjorden viser sterke sesongsignaler i de øvre 100 m. Oppvarming, tilførsel av ferskere vann og biologiske prosesser i løpet av våren og sommeren fører til økende Ω aragonitt-verdier opp til 2,31-2,40 i de øvre 10 m fra juli til september (***Figur 26***). I løpet av tidlig høst begynner Ω aragonitt å avta på grunn av redusert biologisk produksjon, avkjøling og blanding med CO_2-rikt overflatevann.

Barentshavet

Prøvetaking ble utført langs Fugløya-Bjørnøya og Vardø-N snittet i Barentshavet. Det sistnevnte transektet er prøvetatt i forbindelse med IMR-PINRO Barents Sea økosystemundersøkelser 'ØKOTOKT'. Vann i nærheten av Fugløya er påvirket av den ferske norske kyststrømmen, og de dypeste lagene inneholder varmt og salt atlantisk vann. I nærheten av Bjørnøya skaper tilsig av kaldere og ferskere arktisk vann sterke horisontale gradienter i saltholdighet og temperatur i de øvre 200 m ved Polarfronten på rundt 74 °N.

Høyeste pH på 8,08 og høy Ω aragonitt på 1,75-1,80 ble observert i kystvannet nær Fugløya og dette reflekterer biologisk karbonopptak (***Figur 34***). Laveste pH på 7,98 ble funnet i bunnvannet på 200 m dybde ved 71,75 °N. Den laveste Ω aragonitt på 1,34-1,36 ble funnet i det kalde og ferske arktiske vannet. Fra 2012 til 2019 er variasjon i pH og Ω aragonitt knyttet til svingninger i atlantisk og arktisk vann (***Figur 42***). Siden 2016 har trenden med avkjøling og ferskere vann på 300-400 m dyp fått følge av en reduksjon i Ω aragonitt til laveste verdier på 1,44-1,57. I det nordlige Barentshavet hadde arktisk overflatevann i nord høyest pH på 8,23 og høy Ω aragonitt på 1,88 (***Figur 35***). Høyeste Ω aragonitt (1,91) ble funnet i den sentrale delen av seksjonen, der biologisk produksjon hadde redusert C_T og fortynning av A_T fra sjøis smeltevann var relativt redusert. Laveste pH og Ω aragonitt på henholdsvis 7,99 og 1,15-1,21 ble funnet på 50-100 m dyp i nord, sannsynligvis på grunn av økt CO_2 fra mikrobiell nedbrytning av organisk materiale og frigjøring av vann med svært høyt saltinnhold og CO_2 fra havis.

Sesongdekning av overflatevann mellom Tromsø og Longyearbyen viste at variasjonen i karbonatkjemi i Barentshavsåpningen ved 69-78 °N styres av ferskvannstilførsel, biologisk produksjon om sommeren og sirkulasjon. Overflatevannet har blitt ferskere siden 2013. Ω aragonitt viser en tydeligere trend i de sørlige delene av transektet med en årlig økning på 0,018 siden 2015. pH viser en tydeligere trend i de nordlige delene av transektet med en årlig reduksjon på 0,002 (***Figur 40-41***).

Underveismålingene fra MS *Norbjørn* viser at pCO_2 var høy (~405 µatm) gjennom vinteren i åpent vann (januar-februar), og lavere langs kysten av Norge og Svalbard. Dette er sammenfallende med endringer i saltholdighet og temperatur i kystsonen. De laveste verdiene av pCO_2 ble observert langs kysten av Svalbard om sommeren (<300 µatm). Det var få sensordata for pH i 2019, men de viste høyere pH om sommeren nær Svalbard (opp mot 8,3) og lavere verdier i åpent vann, som sannsynligvis er drevet av primærproduksjon. Underveismålingene fra MS *Trollfjord* mellom Kirkenes og Bergen viser en sesongsyklus for temperatur og saltholdighet, med varmere og ferskere vann om sommeren. Kysten utenfor Kirkenes har spesielt lav saltholdighet og er også preget av lavere pCO_2, så lavt som 200 µatm fra august til oktober. Vårblomstringen startet i april i sør og bevegde seg nordover gjennom mai og juni. pCO_2 målingene fra august til oktober viste store regionale forskjeller. I denne tidsperioden viste målingene en forskjell fra >70 °N der de lå mellom 300-400 µatm og <70 °N der de lå mellom 350-450 µatm, med saltholdighet og temperatur som de største påvirkningene på karbonatsystemet.

<u>Den norske kystsonen</u>

I 2019 samlet prosjektet 'Overvåking av havforsuring i kystsonen' målinger fra flere lokaliteter i kystområdene i Norge og på Svalbard. To lokaliteter i Hardanger viste sterk sesongvariasjon i de øvre 100 m (***Figur 47***). Ferskvannstilførsel fra elver og regn påvirket overflatesjiktet (<10 m) og den nordlige stasjonen var mer påvirket av kystvannet enn den lenger sør. Det dype vannet på begge stasjoner hadde atlantisk karakter. pH viste en mer definert syklus for de grunneste vannmasene med økning i verdien på grunn av primærproduksjon. Overflate-pH og -Ω aragonitt var lave om vinteren og økte med økende biologisk produksjon. Ω aragonitt økte senere på året enn pH på grunn av den lave temperaturen senvinters / tidlig vår.

Prøvetaking av kaldtvannskoraller inkluderte 2 veggrev i Hardanger og 5 terskel- eller bakkerev i Nord-Norge. Ved veggrevene i Hardanger ble det observert høy variabilitet i karbonatkjemivariabler både fra sesong til sesong og i løpet av dagen i de øvre 80 m. Ferskvannstilførsel reduserte saltholdigheten og høy planteplanktonproduksjon reduserte C_T, og dette førte til høye pH- og Ω aragonitt-verdier i overflatesjiktet (***Figur 51-52***). Dypere enn 80 m (der hvor korallene vokser) førte økt respirasjon og blanding med atlantisk vann til økte C_T-verdier og dette ble vanligvis ledsaget av lavere pH og Ω aragonitt sammenlignet med resten av vannsøylen. Ved de nordnorske revene vises stor regional variabilitet (***Figur 58***) med kaldere og ferskere bunnvann ved de nordlige korall-lokalitetene (Korallen, Fugløyrevene) sammenlignet med de sørlige lokalitetene (Steinaværrevet, Hola). Det kalde, ferske vannet i nord er preget av lavere C_T og A_T sammenlignet med de sørlige lokalitetene der atlantisk vann er dominerende og C_T og A_T er høyere. Høyere pH ble funnet i bunnvannet i nord og Ω aragonitt var mer variabel. Korallvekst kan påvirke A_T og C_T gjennom opptak av uorganisk karbon, og dette varierer sannsynligvis mellom rev og tid på døgnet.

I Malangenområdet, i det nordlige Norskehavet, var det stor regional variasjon i hydrografiske variabler og oksygenmetning, cDOM fluoresence og pCO_2 på sensommeren/høst 2019 (***Figur 54***). I nærheten av Straumsfjorden kyststasjon var vannet merkbart ferskere og kaldere, og pCO_2 varierte mellom 300 til 400 µatm, som er typisk for regionen. Variasjonen i pCO_2 var til dels drevet av ferskvannstilførsel (redusert pCO_2 i nærheten av Straumsfjorden kyststasjon i vann med lav saltholdighet og høy cDOM) og avkjøling av vannmassene fra september til oktober. Det var betydelig sesongvariasjon i overflatelaget (0 m) ved Straumsfjorden kyststasjon, med lav saltholdighet (14-25), høy DOC og lave næringssaltkonsentrasjoner fra februar til juli, i perioden med høy avrenning i den nærliggene Målselv. I denne perioden var det lave verdier av C_T og A_T i overflatelaget (***Figur 55***), og Ω aragonitt varierte mellom 0,5 til 1,9. Det betyr at disse vannmassene kan i perioder ha en negativ innvirkning på organismer med kalkskall som lever i overflatevannet.

På Svalbard observeres stor sesongvariabilitet i hydrografi og karbonatkjemi i Adventfjorden (IsA stasjon), som er en liten gren av den større Isfjorden på vestkysten av Spitsbergen. Største sesongvariasjon er observert i de øvre 50 m der Ω aragonitt varierte fra 1,4 til 2,3 fra november til juli, sannsynligvis på grunn av remineralisering av organisk materiale og blanding om vinteren og CO_2-opptak gjennom primærproduksjon om sommeren (***Figur 63***). Ved munningen av Isfjorden (IsG stasjon) ble de laveste pH- og Ω aragonitt-verdiene på henholdsvis 8,07 og 1,7 funnet på mer enn 50 m dyp, der saltholdigheten er høy og karakteristisk for Atlanterhavsvann (***Figur 64***). Nedgang i overflate-pH og Ω aragonitt over to måneder er relatert til avkjøling og ferskere overflatevann.

1. Introduction

The marine acidification program in its current form was established in 2013 by the Norwegian Environment Agency. The background for the initiative was based on the fact that the global oceans currently absorb about 25% of the anthropogenic carbon dioxide (CO_2) emitted annually from combustion of fossil fuels and deforestation (e.g., Takahashi et al. 2009; Le Quéré et al. 2016; 2018; Friedlingstein et al. 2019). Oceanic uptake of CO_2 affects the inorganic carbon system of the ocean, with a subsequent reduction in seawater pH and the degree of saturation of calcium carbonate minerals, e.g. aragonite and calcite. Ocean acidification is occurring at a higher rate compared to changes determined during the last 55 million years. It is expected that ocean acidification will affect the structure and function of numerous marine ecosystems, and thus also have significant consequences for harvestable marine resources. Therefore, it is important to monitor the degree of ocean acidification.

The northernmost Norwegian seas have a naturally high content of inorganic carbon, and in addition, the low temperatures enhance the CO_2 solubility in seawater. Oceanic uptake of atmospheric CO_2 leads to an increased concentration of hydrogen ions and lower availability of carbonate minerals in seawater. As a result, the content of carbonates in high latitude waters is low compared to more southern areas, and we expect the higher latitude seas will be the first regions to experience lower levels of seawater carbonates as a result of ocean acidification. For example, the Arctic Ocean will become undersaturated with respect to calcium carbonate during this century if CO_2 emissions continue as they are today (AMAP 2013; Steinacher et al., 2009).

The ocean carbonate system is an important part of the global carbon cycle. About 90% of the inorganic carbon in the ocean is in the form of hydrogen carbonate (HCO_3^-), 9% is in the form of carbonate (CO_3^{2-}) and about 1% exists as dissolved CO_2. When CO_2 from the air is absorbed by the sea, the gas becomes dissolved in the seawater and carbonic acid (H_2CO_3) is formed. This also causes hydrogen ions (H^+) to be released. Carbonic acid is rapidly transformed into hydrogen carbonate and carbonate ions, which are naturally present in the seawater and form the so-called carbonate system (Eq.1).

$$CO_2 + H_2O \leftrightarrow H_2CO_3 \leftrightarrow H^+ + HCO_3^- \leftrightarrow H^+ + CO_3^{2-} \qquad \text{Equation 1}$$

Overall, uptake of CO_2 by the ocean leads to increases in the hydrogen ion concentration and decreases the availability of carbonate minerals in seawater. This results in a decrease in seawater pH; thus the process has been called ocean acidification. The surface pH of the global oceans is generally around 8, but the natural variations are large and are influenced by, for example, temperature, primary production, respiration and physical processes like mixing of different water masses. It is worth noting that the oceans will not become acidic (pH lower than 7) but rather it will become less basic. In the marine environment, it is the reduction of available carbonates that creates the most concern. Carbonate forms an important building block for many marine organisms, primarily those with calcium scales and shells, and calcium carbonate is formed only biologically (Eq. 2) while the dissolution is a chemical process (Eq. 3). When large quantities of CO_2 are absorbed, the concentration of carbonate ions (CO_3^{2-}) in seawater is reduced, and then calcium carbonate ($CaCO_3$) is likely to dissolve and the shells of some organisms becomes chemically unstable (Orr et al., 2005).

$$Ca^{2+} + 2HCO_3^- \leftrightarrow CaCO_3(s) + H_2CO_3 \qquad \text{Equation 2}$$

$$CaCO_3(s) \leftrightarrow Ca^{2+} + CO_3^{2-} \qquad \text{Equation 3}$$

Organisms with calcium carbonate (chalk) shells and skeletons will have reduced ability to survive when carbonate concentration is reduced as a result of CO_2 uptake. According to Talmange and Gobler (2009), Andersen et al. (2013) and Agnalt et al. (2013), ocean acidification can weaken a number of economically important shellfish species, and Mortensen et al. (2001), Turley et al. (2007) and Järnegren and Kutti (2014) show that this could also be the case for the large deposits of cold water corals that are found along the Norwegian coast. It has also been found that non-calcareous organisms can be adversely affected by changes in CO_2 or low pH. Further, there are also organisms that respond positively to high CO_2 content and low pH (Dupont and Pörtner, 2013). It is therefore difficult to predict which organisms will be the most effected to changes in ocean chemistry and pH, and thus, it is very important to study the natural variations of the ocean carbonate system in order to monitor the development of carbonate concentration and the degree of saturation of the two most common types of calcium carbonate in the ocean; aragonite and calcite.

2. Methods and Data

The aim of the Ocean Acidification (OA) monitoring program is to get an overview of the status and development of OA in Norwegian waters. The program will facilitate future monitoring of the effects of OA on marine ecosystems. Most of the data is available in international databases such as CDIAC (http://cdiac.ornl.gov/oceans/CARINA/) and SOCAT (www.socat.info). The data are also published in the database "Vannmiljø" (www.vannmiljo.miljodirektoratet.no) of the Norwegian Environment Agency, as well as archived in the Norwegian Marine Data Centre (NMDC).

In 2017, the OA monitoring program and the Ecosystem Monitoring in Coastal Water (ØKOKYST) program coordinated the monitoring activities, based on the need to increase the climate relevance of the latter program. ØKOKYST aims to monitor the environmental status of selected areas along the Norwegian coast. This effort included monthly sample collection of macronutrients (ammonia, phosphate, nitrate, silicate, total nitrogen and total phosphorous), chlorophyll-a concentration, and dissolved organic carbon using FerryBox on MS *Trollfjord* and MS *Color Fantasy*. This monitoring also included continuous FerryBox data for temperature, salinity and chlorophyll-a fluorescence among others. The reporting, however, has been done separately in the 'ØKOKYST' reports, and will not be repeated in this report, but some chlorophyll-a fluorescence data has been used to discuss the seasonal variation in carbonate chemistry. Similar coordination of sampling has been arranged for the seasonal monitoring at Arendal and Skrova coastal stations.

Table 1
A summary of transects and cruises where sampling was performed in 2019.

Section/station (sample type)	**Sampling month**	**Depth**	**Variables**	**Institution**	**Financing**
Torungen-Hirtshals (discrete)	January	Water column	A_T, C_T	IMR	Environment Agency
Svinøy-NW (discrete)	January	Water column	A_T, C_T	IMR	Environment Agency
Gimsøy-NW (discrete)	March, May	Water column	A_T, C_T	IMR	Environment Agency
Fugløya-Bjørnøya (discrete)	January	Water column	A_T, C_T	IMR	Environment Agency
NE Barentshav (discrete)	September	Water column	A_T, C_T	IMR	Environment Agency/ FRAM
Tromsø-Longyearbyen/ Ny-Ålesund **(continuous)**	January-March, August-December (pCO_2) June-July, September-December (pH)	Surface	pCO_2, pH	NIVA	Environment Agency
Bergen-Kirkenes (continuous)	September-November	Surface	A_T, C_T, pH	NIVA	Environment Agency
Oslo-Kiel (**continuous**)	January-May, September-December (pCO_2) February, September-November(pH)	Surface	pCO_2, pH	NIVA	Environment Agency
Station M (discrete)	January, April, May, June, November	Water column	A_T, C_T	NORCE/ UiB	Environment Agency
Station M (continuous)	January-April, June-November	Surface	pCO_2	NORCE/ UiB	Environment Agency /RCN
Coastal station Skrova (discrete)	January - December	Water column	A_T, C_T	IMR	Environment Agency
Coastal station Arendal (discrete)	January - October	Water column	A_T, C_T	IMR	Environment Agency

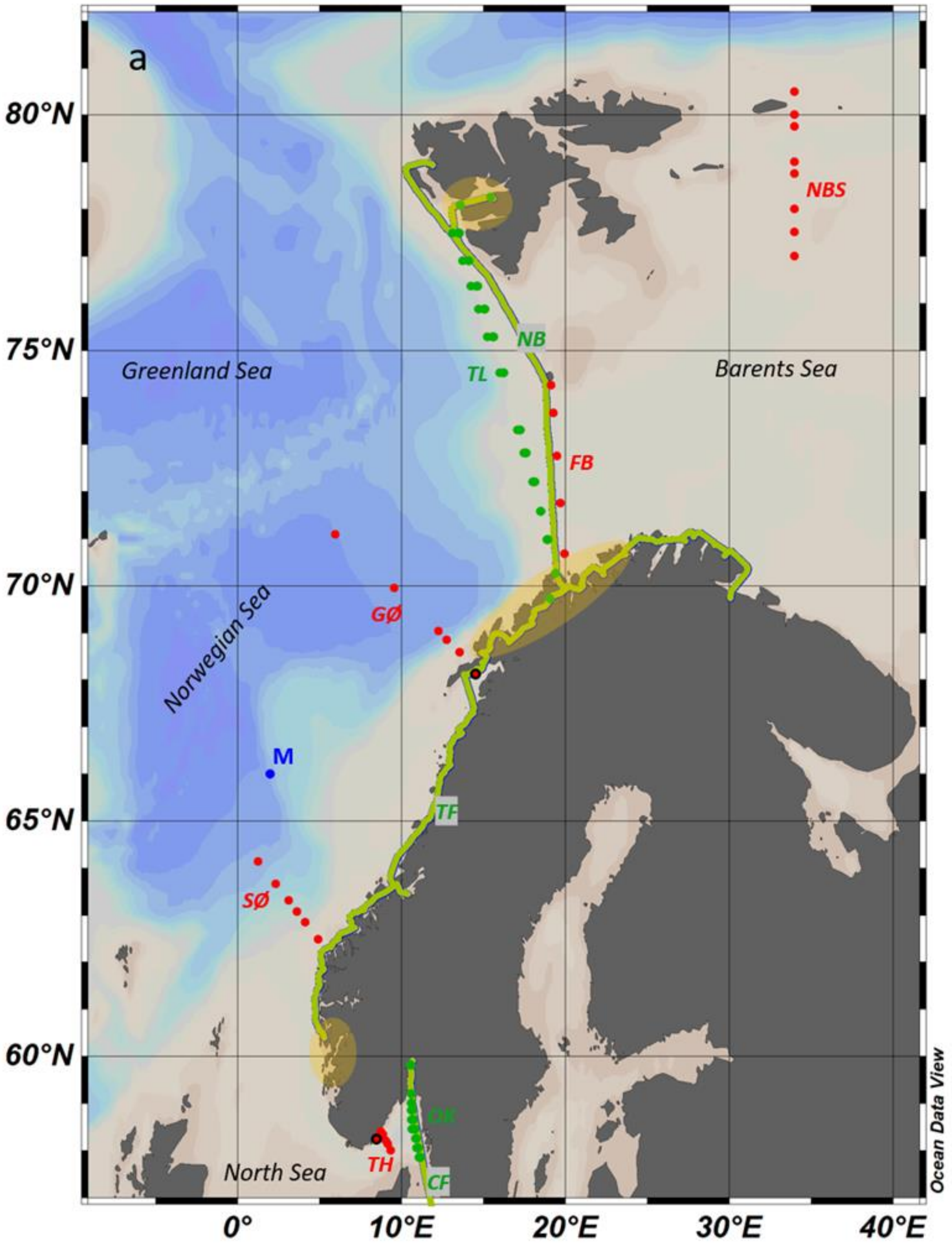

Figure 1a. *Map showing the stations being part of the program Ocean Acidification Monitoring of Norwegian waters in 2019. Red dots show transects were IMR sampled the water column; TH=Torungen-Hirtshals, SØ=Svinøy-NW, GØ=Gimsøy-NW, FB=Fugløya-Bjørnøya, and NBS=Northern Barents Sea. Red dots with black outline show the coastal stations Arendal in the south and Skrova in the north. Green dots show transects where NIVA has collected surface samples; OK=Oslo-Kiel, TL=Tromsø-Longyearbyen. Light green lines indicate NIVA's surface underway sensor measurements; CF=Color Fantasy, TF=Trollfjord, and NB=Norbjørn. Blue dot indicates Station M where NORCE and UiB have sampled the water column. The yellow areas show the areas of interest for the program Ocean Acidification of Coastal Waters in 2019 (**Chapter 3.5**).*

Figur 1a. *Kart over stasjoner som har inngått i programmet Havforsuringsovervåkning av norske farvann 2019. Røde prikker viser snitt der IMR har tatt prøver fra hele vanndypet; TH=Torungen-Hirtshals, SØ=Svinøy-NV, GØ=Gimsøy-NV, FB=Fugløya-Bjørnøya, NBS=stasjoner i nordøstlige Barentshav. Røde prikker med svart kant viser kyststasjoner; Arendal i sør og Skrova i nord. Grønne prikker viser NIVA sine overflatestasjoner; OK=Oslo-Kiel, TL=Tromsø-Longyearbyen. Lysegrønne linjer viser NIVAs underveis-sensor målinger; CF=Color Fantasy, TF=Trollfjord og NB=Norbjørn. Blå prikk viser stasjon der NORCE og UiB har tatt prøver fra hele vanndypet; M=Stasjon M. De gule områdene viser områdene som inngår i programmet Havforsuring i kystsonen i 2019 ((**kapittel 3.5**).*

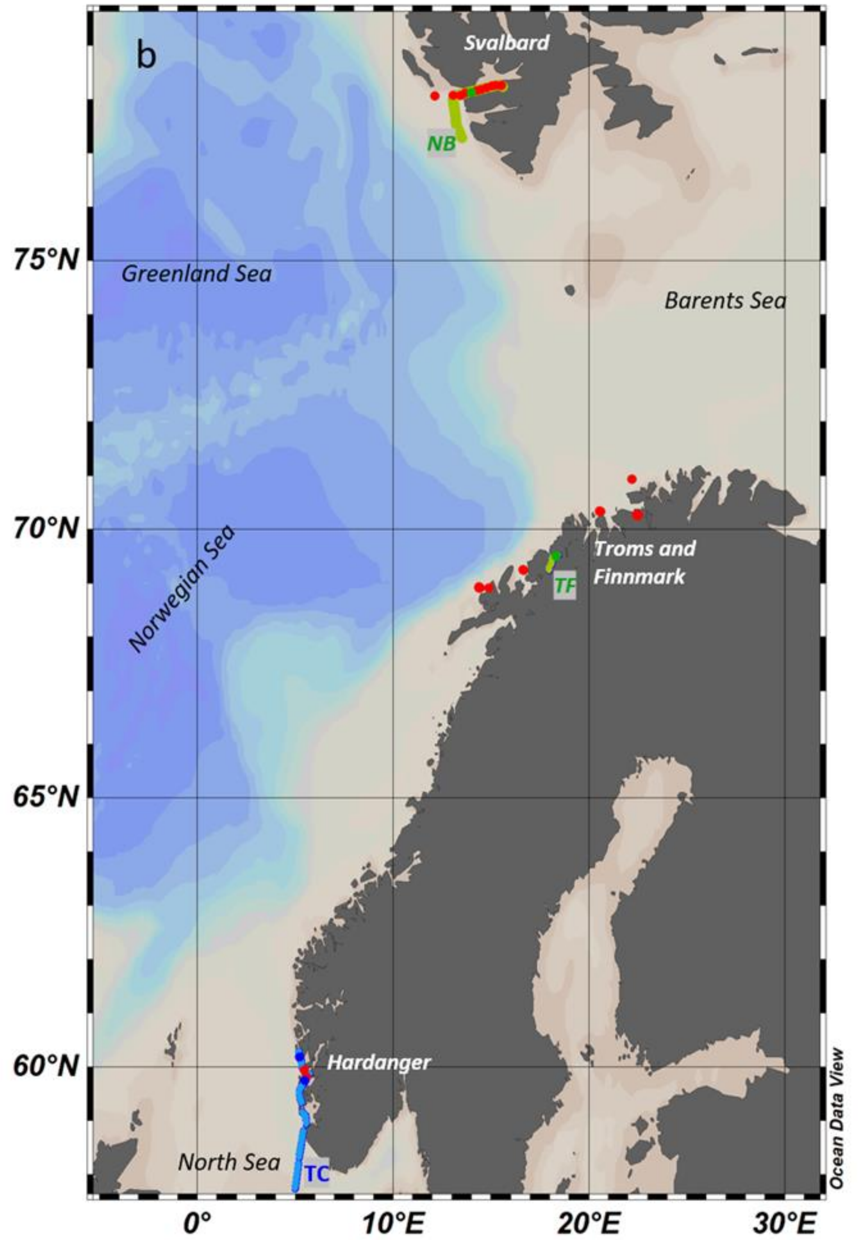

__Figure 1b__. Map showing the stations in the program Ocean Acidification of Coastal Waters in 2019. The three areas of interest were Hardanger, Troms and Finnmark, and Svalbard (__Figure 45__). Red dots show stations where IMR sampled the water column, green dots show stations where NIVA and ApN sampled the water column, and blue dots show where NORCE sampled the water column. Light green line shows NIVA's surface underway carbon measurements; NB=Norbjørn and TF=Trollfjord. Light blue line shows NORCEs surface underway carbon measurement; TC=Tranc Carrier.

__Figur 1b__. Kart over stasjoner som har inngått i programmet Havforsuring i kystsonen i 2019. Programmet har fokusert på tre områder: Hardanger, Troms og Finnmark og Svalbard (__Figur 45__). Røde prikker viser snitt der IMR har tatt prøver fra hele vanndypet, grønne prikker viser NIVA og ApN sine vanndyp-stasjoner, og blå prikker viser der NORCE har samlet inn vann fra hele vanndypet. Lysegrønn linje viser NIVAs underveis karbonmålinger; NB=Norbjørn og TF=Trollfjord, og lyseblå linje viser NORCE sine underveis karbonmålinger; TC=Trans Carrier.

Positions for fixed sections, transects and fixed stations that are part of the measurement program in 2019 are shown in ***Figure 1***. The Institute of Marine Research (IMR) has conducted regular sections in the Skagerrak region of the North Sea/Skagerrak (Torungen-Hirtshals), the Norwegian Sea (Svinøy-NW, Gimsøy-NW), and in the Barents Sea (Fugløya-Bjørnøya) and in the northern Barents Sea. In addition, monthly sampling was carried out at the coastal stations at Arendal and Skrova, which is a collaboration with the ØKOKYST program (Environment Agency). In 2019, the NORCE Norwegian Research Centre (NORCE) and University of Bergen (UiB) conducted continuous and discrete measurements at Station M. NIVA has measured transects in the Barents Sea opening (Longyearbyen-Tromsø), Norwegian coast (Bergen-Kirkenes) and in Skagerrak (Oslo-Kiel).

The Environment Agency has funded the sampling activities presented in this report but the participants in the program have also contributed data and expertise from other projects. The Fram Center Flag Ship for Ocean Acidification program funded parts of the Barents Sea opening cruises on MS *Norbjørn* and during previous years (2012-2015), NIVA's activities related to ocean acidification (OA-SIS) have funded the technology development of the pCO_2 and pH sensors used for underway measurements. For IMR, there are two projects in the Flag Ship for "Ocean acidification and ecosystem effects in Norwegian waters" at the Fram Center and IMR's ecosystem surveys program that provides expertise and infrastructure that is included in the 2019 report.

2.1 Sampling and Variables

This project uses internationally recognized methods and procedures for seawater sampling and instrumentation, as described in Dickson et al. (2007); Guide to Best Practices for Ocean CO_2 Measurements. Following the previous report (Jones et al., 2019), collection of measurements and sampling of hydrography, C_T, A_T, and nutrients in the full water column at fixed sections was performed by IMR aboard the IMR vessels RV *GM Dannevig* in the North Sea/Skagerrak, RV Johan Hjort and RV *Kristine Bonnevie* in the Norwegian Sea, and RV *Johan Hjort* in the Barents Sea. NORCE-UiB collected measurements and samples from the full water column at Station M in the Norwegian Sea using IMR research vessels RV *Johan Hjort and* RV *Kristine Bonnevie*. In addition, NORCE-UiB was responsible for continuous surface and sub-surface measurements at Station M, and the surface measurements covered pCO_2 in sea and atmosphere, as well as dissolved oxygen, and hydrography. In 2019, only continuous hydrography and no carbon measurements were determined in the sub-surface waters. NIVA collected surface water samples manually on Ships of Opportunity equipped with FerryBoxes between Tromsø and Longyearbyen on the cargo ship MS *Norbjørn* and between Oslo and Kiel on the cruise ship MS *Color Fantasy*. The FerryBox system included sensors for chlorophyll *a* fluorescence and colored dissolved organic matter (cDOM) fluorescence (TriOS GmbH MicroFlu). The chlorophyll *a* fluorescence sensor data was corrected for biofouling and calibrated using the chlorophyll *a* measured from water samples. The cDOM sensor was calibrated by the manufacturer using quinine sulphate and checked regularly with solid state standards and arbitrary units are reported here.

The carbonate system in seawater can be described using four measurable variables: total alkalinity (A_T, µmol/kg), total inorganic carbon (C_T, µmol/kg), pH, and the partial pressure of CO_2 (pCO_2, µatm), detailed in ***Table 2***.

Table 2
Seawater ions and variables of the carbon system used in this report

Variable	Name	Explanation
CO_2	Carbon dioxide	Gas in the atmosphere (natural and man-made origin) which is absorbed/emitted by the ocean
HCO_3^-	Hydrogen carbonate	Dissolved inorganic carbon ion in water
CO_3^{2-}	Carbonate	Dissolved inorganic carbon ion in water, plays role in degree of saturation (Ω)
C_T	Total inorganic carbon	The sum of carbonic acid and dissolved CO_2 in water (CO_2*), carbonates and hydrogen carbonates (***Eq. 5, Appendix 6.3***)
A_T	Total alkalinity	Capacity of water to neutralize acid (buffer capacity) and consists of the sum of the bases of the solution formed by weak acids (***Eq. 4, Appendix 6.3***)
pH	pH	Measure of acidity that indicates the concentration of hydrogen ions (H^+) in water (***Eq. 6, Appendix 6.3***)
pCO_2	Partial pressure of CO_2	Pressure of CO_2 if CO_2 gas is the only gas in a volume (***Eq. 7, Appendix 6.3***)
Ω	Saturation degree of calcium carbonate	Amount of carbonate ions in water relative to the saturation concentration, relevance for dissolution of solid calcium carbonate (calcite and aragonite)
Chl *a*	Chlorophyll *a*	The key pigment for photosynthesis and used as a measure of phytoplankton biomass

Throughout the report we have used pCO_2 for the partial pressure of CO_2. In fact, fCO_2, which is the fugacity of CO_2, is measured, which considers the fact that CO_2 does not behave as an ideal gas. The difference between pCO_2 and fCO_2 is around 0.3%. In order to avoid the effects of continued biological activity in the water sample after it is collected, which will shift the balance of organic and inorganic carbon, water samples for C_T and A_T are fixed with saturated mercury chloride solution. In addition, the samples are stored in the dark at approx. 4°C before being analysed. Discrete pH analyses were made immediately after sampling at NIVA, post-cruise at IMR, and a mixture of immediately after sampling and post-cruise at UiB.

2.2 Measurements of Total Alkalinity and Total Inorganic Carbon

Measurements of C_T and A_T were performed on water column samples from the sections Torungen-Hirtshals, Svinøy-NW, Gimsøy-NW, Fugløya-Bjørnøya, northern Barents Sea, Arendal coastal station, Skrova coastal station, from station M, and from the surface water during the crossing Tromsø-Longyearbyen and Oslo-Kiel.

The samples were analysed by IMR with a VINDTA 3D (Marianda, Germany) and CM5017O coulometer (UIC instruments, USA) for C_T and a VINDTA 3S (Marianda, Germany) for A_T. NORCE and UiB used a VINDTA 3D (Marianda, Germany) and CM5011 coulometer (UIC instruments, USA) for C_T and a VINDTA 3S (Marianda, Germany) for A_T. NIVA used a VINDTA 3C (Marianda, Germany) and CM5012 coulometer (UIC instruments, USA). The measured values were calibrated against certified reference material (CRM) for quality assurance and as an accuracy check for all data (Certified Reference Material, CRM, A. Dickson, SIO, USA).

Sodium chloride salt is added to the hydrochloric acid for the A_T titration to be comparable to the ionic strength of natural seawater, about 0.7 M. The pH electrodes used by all groups are adapted to seawater samples with high ionic strength (Metrohm 6.0259.100). The VINDTA instruments at IMR, NORCE-UiB and NIVA use 20 ml and 100 ml sample volume for C_T and A_T, respectively. In the A_T titrations, semi-open titration cells are used at all three institutions. Equivalence points were calculated using a curve fit method recommended by Dickson et al. (2007). The analysis method for determining C_T concentrations is described in Johannessen et al. (2011).

2.3 pH Measurements

NIVA uses the spectrophotometric pH method onboard for determining *in situ* pH on the total scale (pH_T). The measurements were performed on a HACH DR-2800 field spectrophotometer (5 cm cuvette) using (*meta*-cresol purple; *m*-cresol purple) as the indicator dye in two concentrations and measurement from 434, 578 and 730 nm were used in calculations (SOP 6B; Dickson et al., 2007). The pH of the seawater induces a colour change of the mixture and this is detected by a spectrophotometer. pH is calculated based on the detected colour change. Two replicates were measured for each sample. Underway pH measurements were made with a custom-fabricated flow-through spectrophotometric sensor system using thymol blue and *m*-cresol purple, fibre optic LED sources, and an Ocean Optics STS-VIS spectrometer (Reggiani et al. 2016). IMR measured pH_T using a spectrophotometer (Agilent 8453 Diode-array) and *m*-cresol purple indicator in a 1 cm quartz cuvette, following standard procedures as outline above. Two or three replicates were measured for each sample.

NORCE-UiB usually measures *in situ* pH using a spectrophotometric pH sensor from Sunburst Technologies, USA; the Submersible Autonomous Moored Instrument (SAMI2-pH). The *m*-cresol purple indicator is mixed with seawater flowing through a cuvette. This sensor was not available during the deployment in 2019, and thus, pH was calculated from continuous pCO_2 and salinity measurements, where salinity was used to estimate A_T (Nondal *m fl*. 2009). Average difference between measured pH and calculated pH was in general less than 0.02 pH units (***Figure 69***, ***Appendix 6.1***), which is within the so called “weather goals” expressed by GOOS (Global Ocean Observing System) Essential Ocean Variables and GOA-ON (Global Ocean Acidification Observing Network). UiB also measured discrete pH in a few samples using a Jasco V-750 spectrophotometer with 10 cm cell length and *m*-cresol purple as indicator. There samples are used together with measured A_T and C_T to calculate organic alkalinity (see ***Appendix 6.4***). *In situ* pH is also calculated from A_T and pH_T (measured at 25 °C) with *in situ* temperature, salinity and pressure using CO2SYS (Pierrot et al. 2006).

2.4 pCO_2 Measurements

NORCE-UiB measured pCO_2 in surface water and lower atmosphere at Station M using infra-red (IR) technology. Measurements of pCO_2 are made every 3rd hour using an instrument from Battelle Memorial Institute, USA; the MAPCO2 system, which utilizes an air-water bubble equilibrator to extract CO_2 from the surface water (Sutton et al. 2014). The CO_2 is determined by a LI-820 IR detector, which is frequently calibrated by running a span reference gas (NOAA/ESRL) in addition to a zero-reference gas through the system. The MAPCO2 system is compared with a General Oceanic pCO_2 system (Pierrot et al., 2009), which represents the "gold standard" of CO_2 measurement systems and the accuracy of the MAPCO2 system is in general about 2 µatm.

NIVA measured pCO_2 using Franatech/NIVA pCO_2 membrane-equilibrator sensors on three FerryBox lines MS *Trollfjord*, MS *Norbjørn*, and MS *Color Fantasy*. The sensors were updated by the manufacturer in 2017 with new infra-red CO_2 detectors (Gassmitter, Sensors Europe Gmbh, Germany) with a lower volume equilibrium chamber, and new check valves and pressure regulators which have improved water flow. This new sensor has been used on all three ships in 2019. The sensors were under improvement during parts of 2019, so the deployment time has not been 100% on the ships. A new on-board gas calibration system using secondary gas standards and a zero gas was installed on all ships in late 2019. This includes a set of three commercially produced air:CO_2 gases (with nominal CO_2 concentrations approx. 200, 400, 800 ppm) and ultra-high purity (5.0) nitrogen (0 ppm CO_2). The pCO_2 sensors were calibrated with NOAA/ESRL reference gases (297.31, 547.41, 735.97 ppm CO_2) before deployment onboard, and the secondary gas standards were assigned CO_2 concentrations using the NOAA/ESRL references. The onboard calibration was performed 1-2 times per month and experience from the onboard calibration showed low sensor drift and the accuracy will meet the weather standard with < ~5 ppm uncertainty.

2.5 Calculation of pH and the Degree of Saturation of Calcite and Aragonite

If two out of the four measurable variables (C_T, A_T, pH and pCO_2) are known then others can be calculated, which includes the degree of saturation (Ω) of calcium carbonate bio-minerals: calcite (Ω calcite) and aragonite (Ω aragonite). The degree of saturation is an indicator of the concentration of carbonates in the water, where Ω > 1 means the water is over-saturated with respect to carbonate. If Ω < 1 then the seawater is undersaturated with carbonate and the chemical environment is therefore unfavorable to organisms with carbonate shells, such as winged snails or coral reefs.

To calculate all of the carbon variables, the chemical model CO2SYS is used (Pierrot et al. 2006). The primary couple of variables used are A_T and C_T alongside temperature, depth (pressure), salinity, phosphate and silica as input values for CO2SYS and the output includes in situ pH, pCO_2, Ω calcite and Ω aragonite. In these calculations, carbonic acid constants from Mehrbach et al. (1973), modified by Dickson and Millero (1987), were used. In the plots, the pH is given in total scale (pH_T) and at in situ temperature. The constant for HSO_4^- from Dickson (1990) and in situ temperature and pressure are used when pH is calculated from C_T and A_T. Calcium ion concentration ($[Ca_2+]$) was assumed to be proportional to the salinity (Mucci, 1983), and corrected for pressure according to Ingle (1975). NIVA and IMR measure pH directly in addition to using calculated pH derived from A_T and C_T in the CO2SYS program. The discrete pH measurements were performed at 25°C. NORCE-UiB measure pH directly on a few of the coastal samples.

2.6 Dissolved organic carbon

At the Straumsfjorden coastal station (VR54), water samples were taken by NIVA/Akvaplan-niva at 0, 5, 10, 20, 30 m for dissolved organic carbon (DOC; GF/F filtered, rinsed with ~1 L of seawater, samples preserved with 0.04 M H_2SO_4) and analyzed by high-temperature catalytic oxidation using Elementar vario TOC cube (accredited according to NS-EN 1484:1997).

3. Results

3.1 Skagerrak

3.1.1 Spatial variability along Torungen-Hirtshals section

In the Skagerrak region, measurements have been made at six hydrographic stations along the Torungen-Hirtshals section in January 2019 (***Figure 2***). This region is strongly affected by the warm and salty Atlantic water (red) and fresh coastal waters (green, ***Figure 3***) that characterize the oceanic conditions. Position, depth and sampling data are displayed in ***Table 1, Appendix 6.2***.

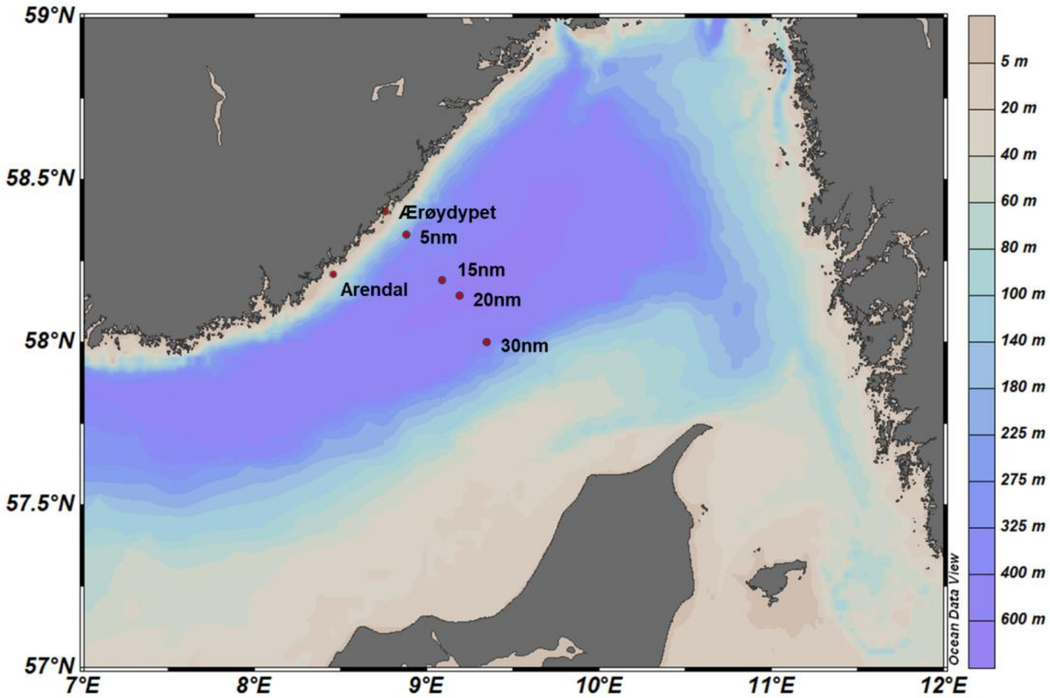

Figure 2. *Stations from the Torungen-Hirtshals section in January 2019 and the Arendal coastal station.*

Figur 2. *Stasjoner fra Torungen-Hirtshals snittet i januar 2019 og fra Arendal kyststasjon.*

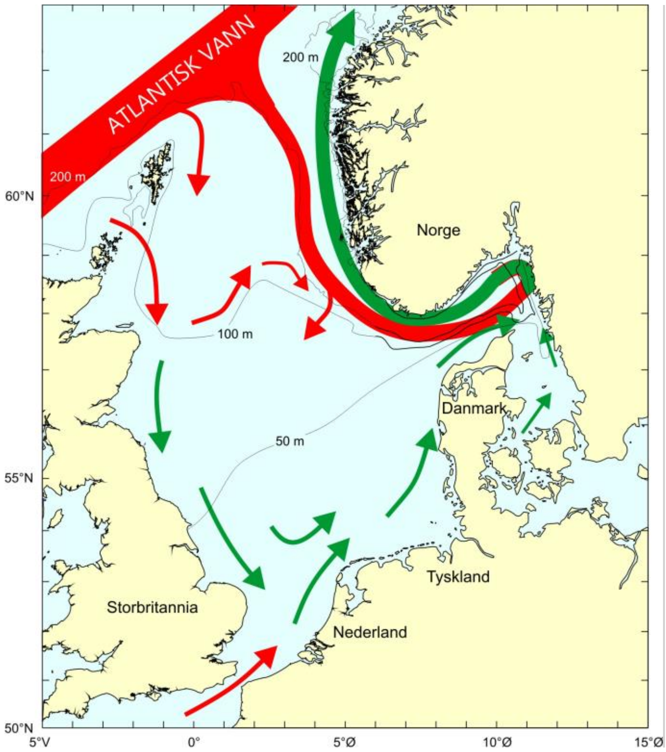

***Figure 3**. Schematic map of the main currents in the North Sea and Skagerrak regions. The red arrows indicate the influx of Atlantic water, mostly at 100-200 m, while the green arrows indicate the main circulation patterns of coastal waters, typically in the top 20m (www.imr.no). The Norwegian coastal current receives inputs from the southern North Sea and the Baltic Sea.*

***Figur 3**. Skjematisk kart over de viktigste transportveiene i Nordsjøen og Skagerrak. De røde pilene indikerer innstrømning av atlantisk vann, for det meste i 100-200 m dyp, mens de grønne pilene angir hovedretningene til sirkulasjon av kystvann, typisk beliggende i de øverste 20m (www.imr.no). Kyststrømmen får tilførsler fra Nordsjøen og Østersjøen.*

Winter data from January 2019 show high pH values in the upper 100 m of the water column that reached maximum of 8.07 in the central part of the section (***Figure 4***). This high pH is due to the low C_T and A_T values in the surface layer, due to the influence of freshwater and likely some CO_2 uptake during photosynthesis, even if it is early in the season (***Figure 71***, ***Appendix 6.1***). The pH decreases with depth with strong vertical gradients between 100-200 m due to the transition from cold, fresh surface waters to the warmer, more saline Atlantic water. Lowest pH of 7.95 occurred in the cold (6.06 °C) and salty (35.14) bottom water at 600 m depth in the central part of the section. This corresponded to moderate A_T (2315-2318 µmol kg^{-1}) and high C_T (2185-2190 µmol kg^{-1}) values, which is likely due to remineralisation of exported organic matter and the presence of an older water mass in the bottom depths that is enriched with CO_2.

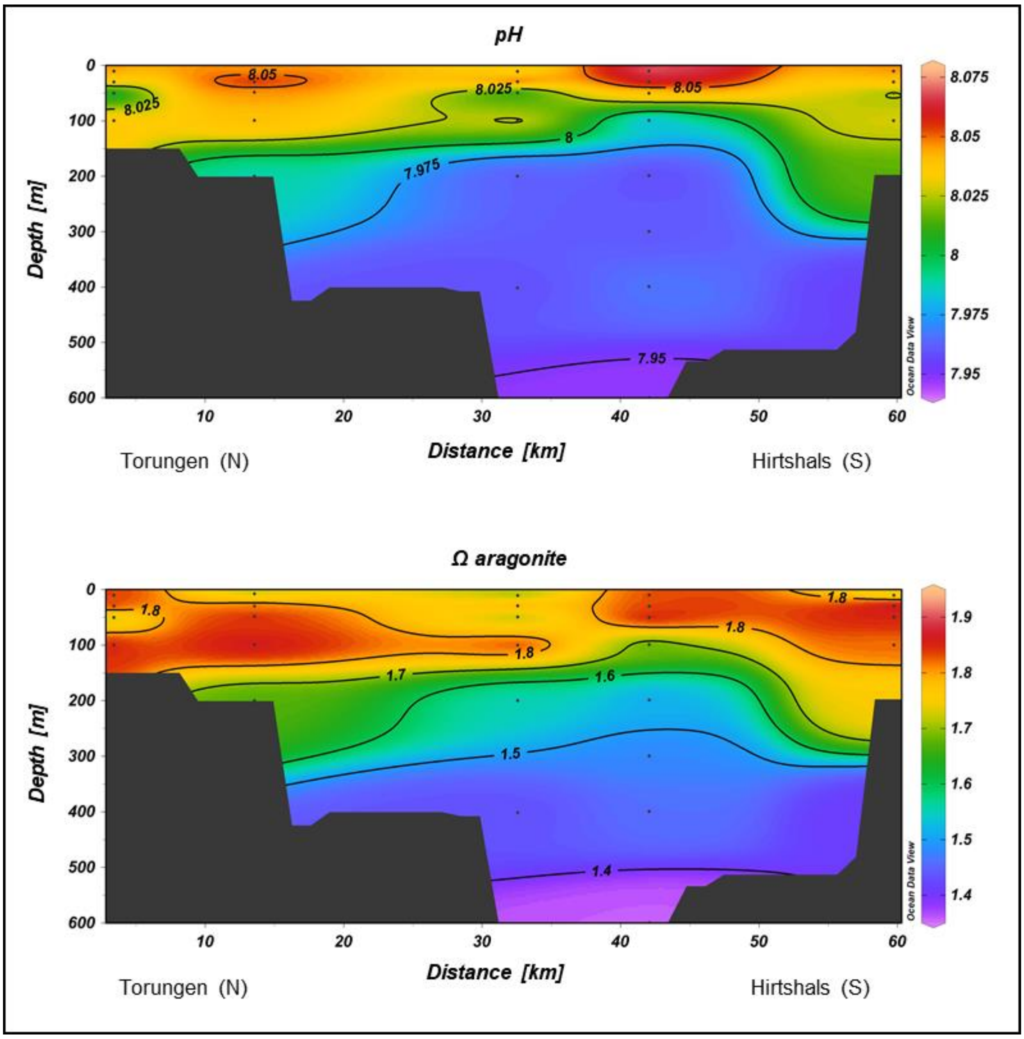

Figure 4. *pH and Ω aragonite along the Torungen-Hirtshals section in January 2019.*

Figur 4. *pH og Ω aragonitt langs snittet Torungen-Hirtshals i januar 2019.*

The distribution of Ω aragonite in 2019 had maximum values up to 1.91 in surface layer close to the coasts at the northern and southern ends of the section, coinciding with high pH. Lowest Ω aragonite of 1.36 were found alongside lowest pH at 600 m depth in the central part of the section. These values compare well with previous years and the time of year.

3.1.2 Seasonal variability at Arendal station

Monthly sampling and measurements were made at Arendal coastal station by IMR from January to November 2019 (***Figure 2*)**. Position, depth and sampling data are displayed in ***Table 2, Appendix 6.2***. This region of the Skagerrak is strongly influenced by the fresh coastal waters in the upper 20 m and the warm and salty Atlantic water at 100-200 m depth offshore (***Figure 72, Appendix 6.1***).

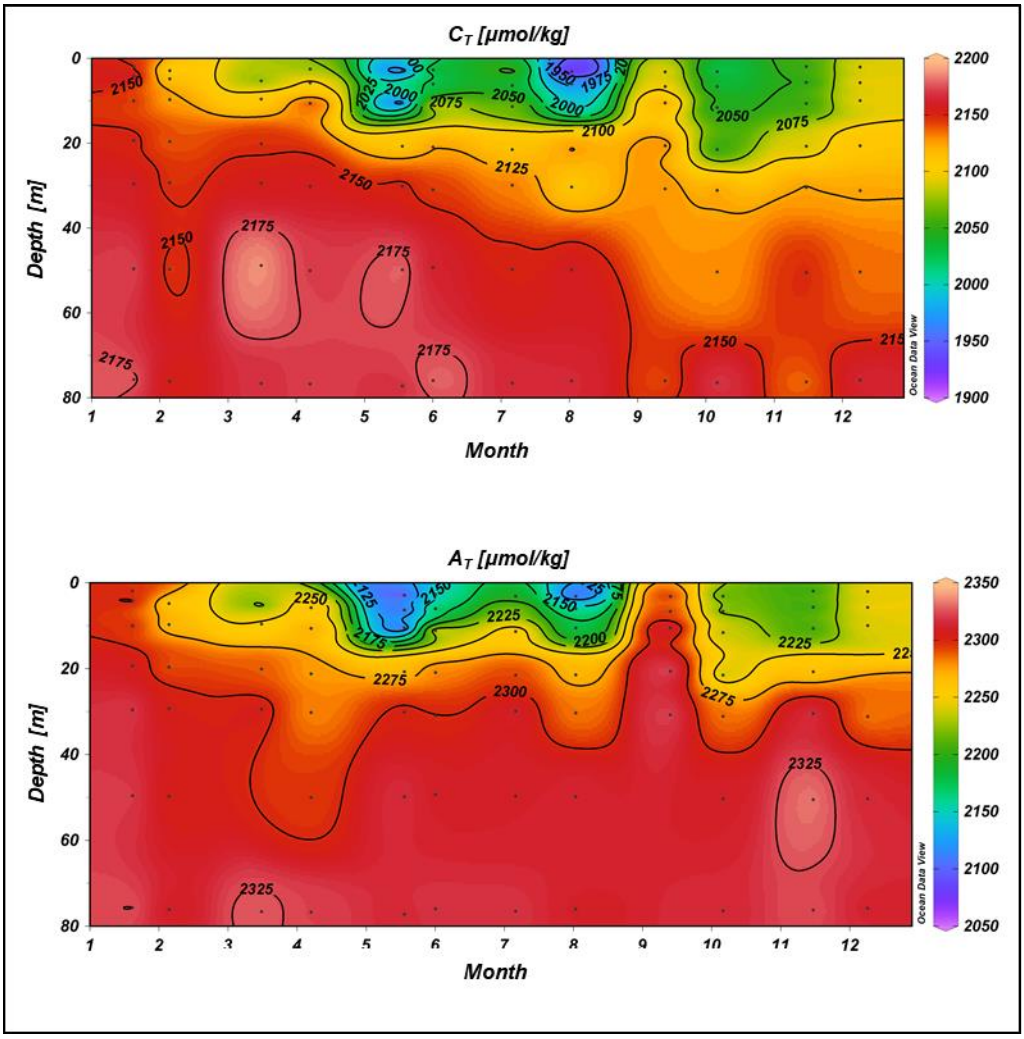

Figure 5. Monthly C_T and A_T in the upper 80 m at Arendal coastal station in 2019. Black dots indicate sample depths.

Figur 5. Månedlig C_T og A_T i de øverste 80 m ved Arendal kyststasjon i 2019. Svarte prikker viser prøvedyp.

Monthly changes in salinity (***Figure 72, Appendix 6.2***) showed strong seasonality in the upper 20 m of the water column. Reductions in salinity to 25.21 from March until September is likely due to enhanced freshwater input from rivers and rainfall and influences of the colder and fresher coastal current. Deep vertical mixing during winter increased salinity up to 34.9 in the whole water column due to mixing of surface waters with the underlying salty Atlantic water. Seasonal warming increased temperatures up to ~18 °C in the surface layer from July to October and stratified the upper water column during spring and summer (***Figure 72***, ***Appendix 6.2***). Biological production in spring and summer reduced C_T to lowest values of 1909 µmol kg^{-1} in the upper 20 m and freshwater dilution reduced A_T to ~2070 µmol kg^{-1} (***Figure 5***).

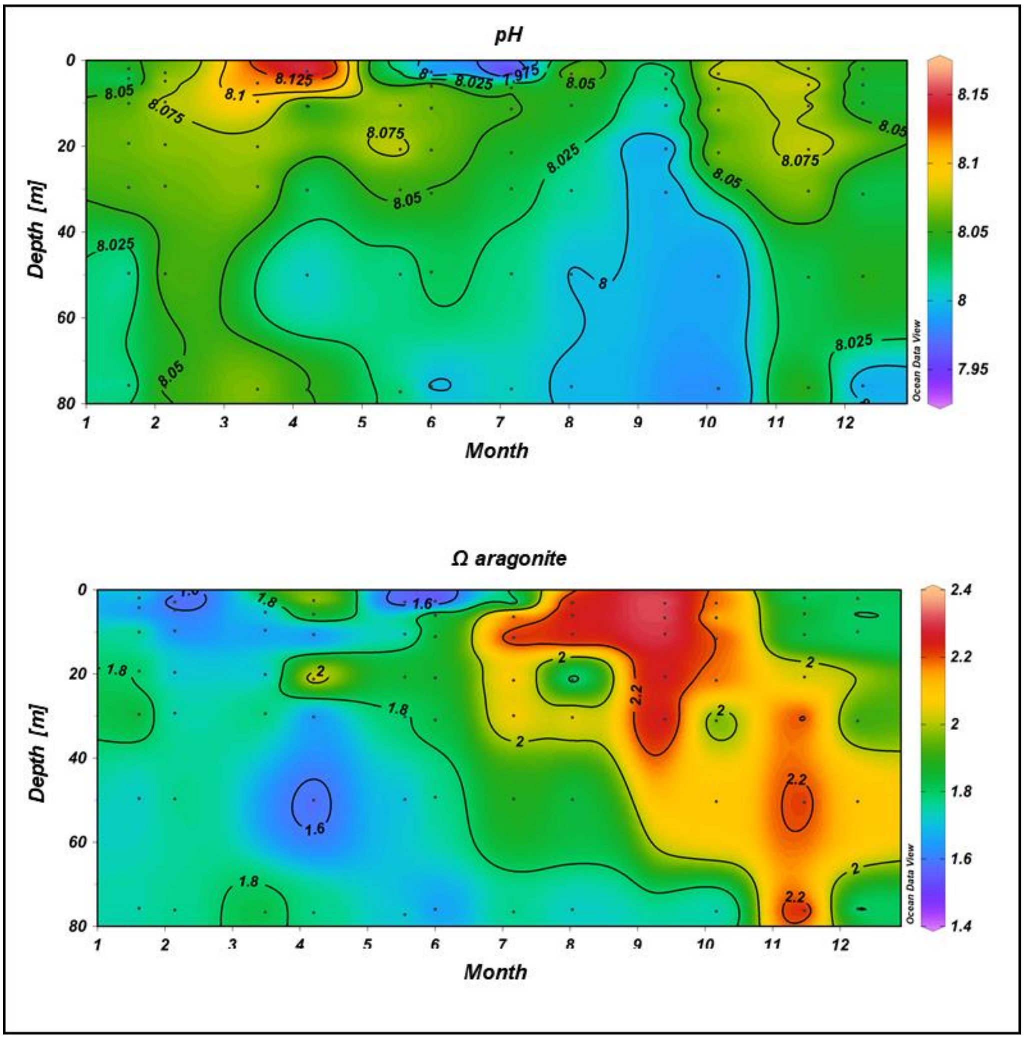

Figure 6. *Monthly pH and Ω aragonite in the upper 80 m at Arendal coastal station in 2019. Black dots indicate sample depths.*

Figur 6. *Månedlig pH og Ω aragonitt i de øverste 80 m ved Arendal kyststasjon i 2019. Svarte prikker viser prøvedyp.*

High pH was found in the upper 20 m with maximum values in spring (***Figure 6***). Lowest pH (7.93) occurred between June-July as fresher water with reduced A_T was present in the surface layer and temperatures were increasing through seasonal warming. Below the surface layer, the influence of Atlantic water could be distinguished by lower pH (< 8) water being projected upwards in the water column. Ω aragonite was highest (2.33) in the surface layer between July and October where biological production had reduced C_T. Elevated Ω aragonite at 2-2.27 in the water column in November, which coincided with warming waters extending deeper into the water column. Lowest Ω aragonite (1.49) was found in June at the surface and lower values (< 1.6) occurred from February to June at varying depths, which corresponded to periods of lower salinity from freshwater inputs and natural variability in the coastal current at this location.

3.1.3 Seasonal variability in surface water

The stations covered using MS *Color Fantasy* going between Oslo and Kiel are shown in ***Figure 7***. Position and sampling data are displayed in ***Table 10***, ***Appendix 6.3***. The Skagerrak region is strongly influenced by freshwater runoff and riverine inputs, Atlantic water and Baltic water. The three northernmost stations cover the Oslofjord, where Oslo is situated at about 60 °N.

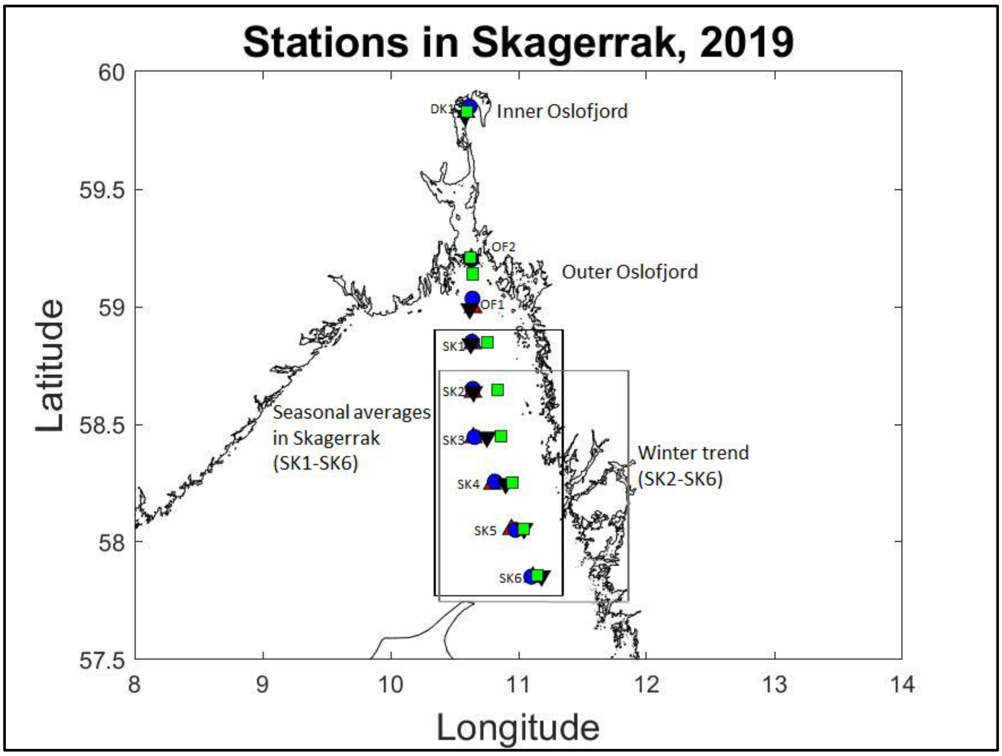

Figure 7. *Stations from Oslo-Kiel in 2019. Samples were taken during 25 February (red ▲); 28 May (blue ●); 22.8 (black ▼); 28 November (green ■).*

Figur 7. *Stasjonskart for snittet Oslo-Kiel. Toktene ble gjort 25 februar (rød ▲), 28mai (blå ●), 22.8 (sort ▼) og 28 november (grønn ■).*

The seasonal variation of temperature and salinity since 2012 is shown in ***Figure 8***. The seasonal averages for Skagerak were calculated on data from stations SK1-SK6. In 2019, the average surface temperature for the Skagerrak reached a minimum of 4.4 °C in February and increased to maximum of 17 °C in August for all stations except the northernmost that was affected by Glomma river. The average salinity was as low as 21.48 in November and as high as 31.73 in February. The variation in salinity in the outer Oslofjord is likely driven by increased freshwater inputs from the river Glomma at about 59.15° N, between OF1 and OF2 in Outer Oslofjord. The low salinities in the Skagerrak in November is likely result from increased freshwater inputs and mixing with fresher water originating in the Baltic Sea.

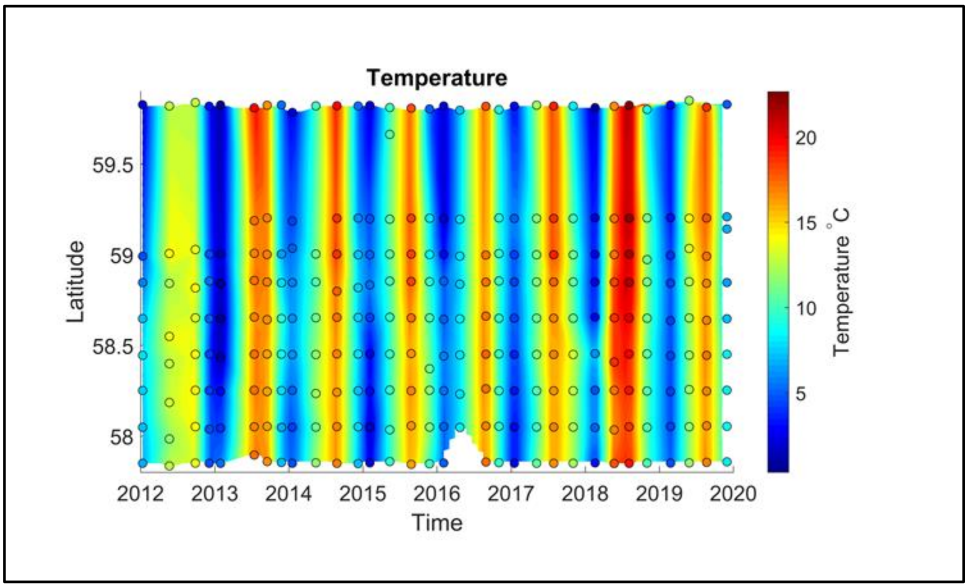

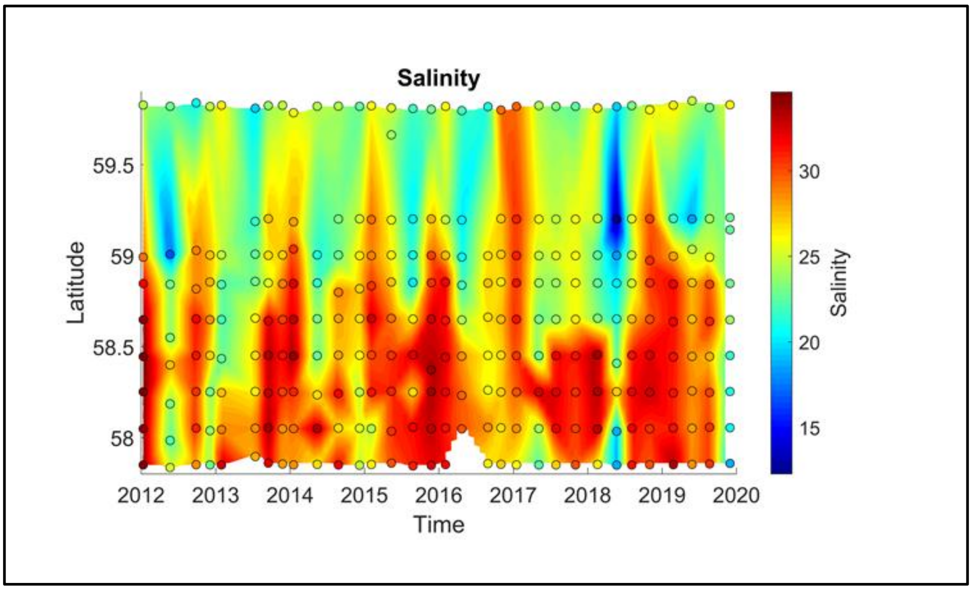

***Figure 8**. Salinity and sea surface temperature in the Oslofjord and Skagerrak. The circles show the measured values, while the interpolated values are shown in the background.*

***Figur 8**. Saltholdighet og temperatur i overflatelaget i Oslofjorden og Skagerrak. Ringene viser målte verdier, mens interpolerte verdier vises i bakgrunnen.*

The seasonal variation of pH and Ω aragonite from 2012-2019 is shown in ***Figure 9***. The pH variability in 2019 followed the same pattern as the previous years, with the higher pH related to increased primary production (May) and the lower pH related to increased freshwater inputs (November) and winter conditions with increased vertical mixing (February in Skagerrak). None of the cruises in 2019 identified the typical winter conditions (cold and relatively high salinity) in the outer Oslofjord, as the stations were already influenced by increased freshwater inputs (rivers, melt water) during the cruise in late February (***Figure 10***). The average pH for the Skagerrak region was as high as 8.07 in May when the primary production was high and reached 7.98 in November during a period of low salinity in the Skagerrak. The Ω aragonite reached as low as 1.13 in November and highest values of 2.22 occurred in August. The Ω aragonite at

58.65° N (SK2; ***Figure 7***) seemed unusually high (3.19) and was regarded an outlier. The inner Oslofjord was undersaturated (Ω aragonite < 1) in November, and likewise the outer Oslofjord in February. Overall, the whole of Oslofjord had a low Ω aragonite during February and November.

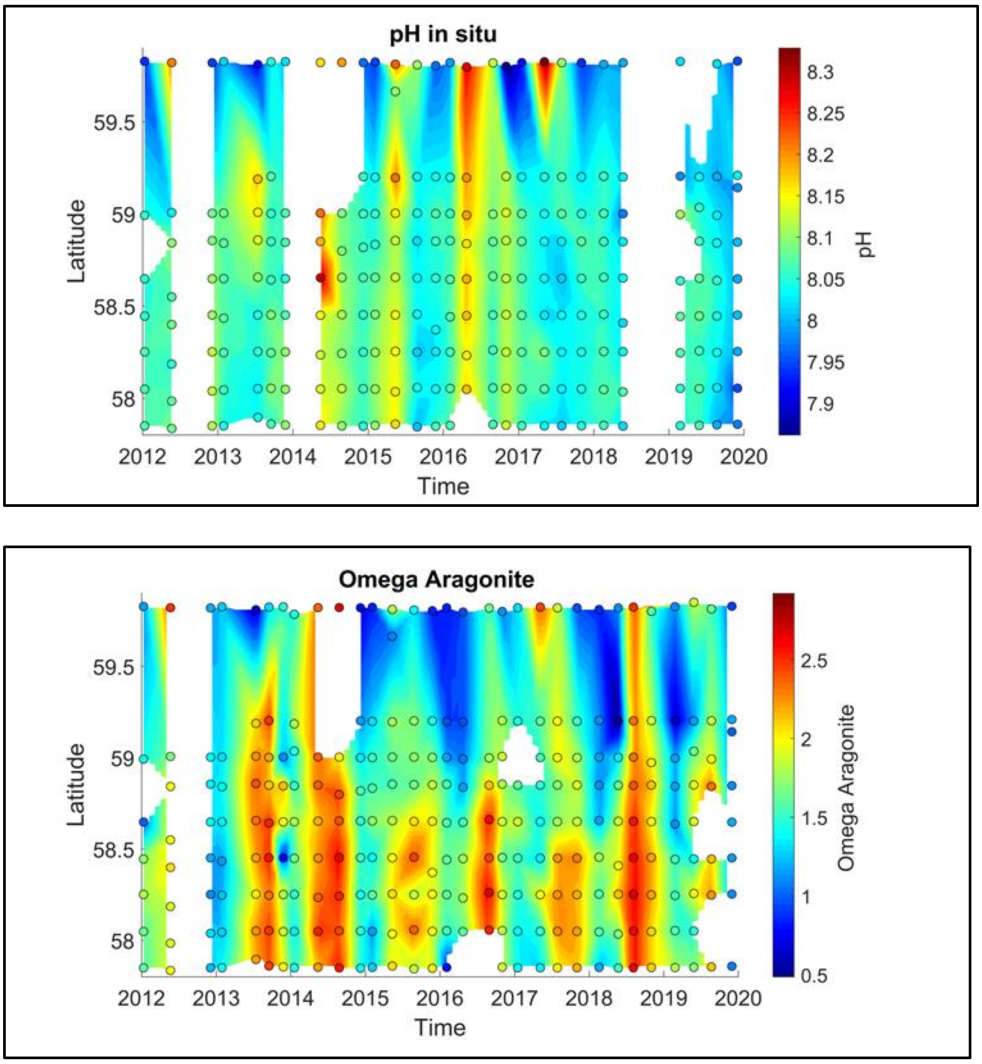

Figure 9. *pH_T and Omega aragonite, calculated from C_T and A_T, in the Oslofjord and Skagerrak. The circles show the measured values, while the interpolated values are shown in the background.*

Figur 9. *pH_T og Omega aragonitt, beregnet fra C_T og A_T) i Oslofjorden og Skagerrak. Ringene viser målte verdier, mens interpolerte verdier vises i bakgrunnen.*

The seasonal and interannual variation of seawater temperature, salinity, pH and Ω aragonite shown in ***Figure 8Figure*** **9** is based upon observations from cruises over 8 years. This time series is starting to reveal the extent of natural variation. The Ω aragonite values continue to be low and sometimes undersaturated during winter in the Oslofjord and Skagerrak surface waters, when the vertical mixing is high and there is less biological production, or else during low salinity events. The low Ω aragonite values in the inner Oslofjord are recurring every winter. The lower salinity and A_T in the Inner Oslofjord, as compared to the more marine waters in the Skagerrak and Outer Oslofjord, seem to cause the Inner Oslofjord to be more susceptible to severe reductions in Ω aragonite. The Oslofjord and northernmost part of Skagerrak seem to show high natural variability mainly driven by river input and biological production.

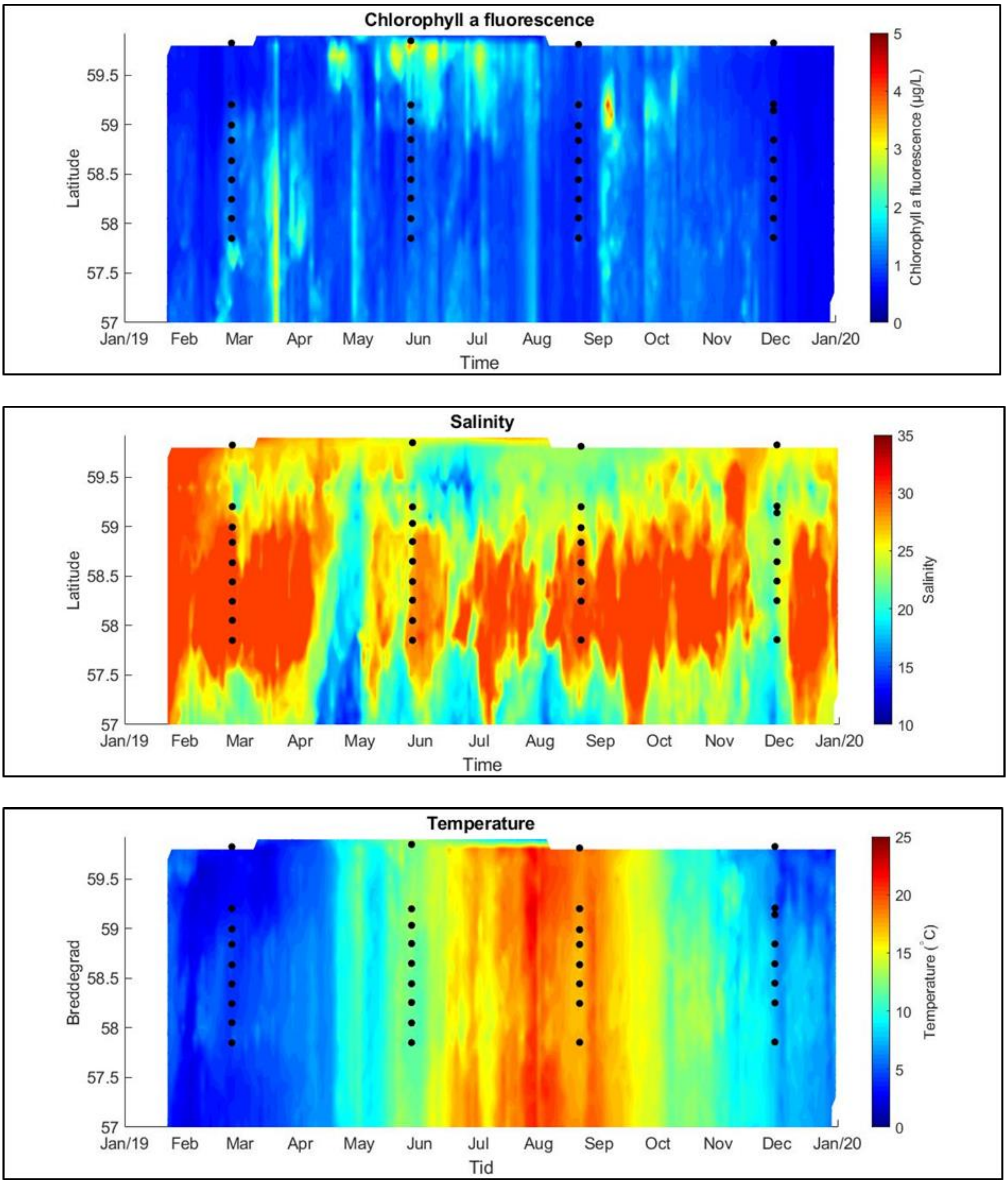

Figure 10*. Stations in the OA monitoring between Oslo and Kiel (circles) overlaid continuous FerryBox data for chlorophyll a fluorescence (top), salinity (middle) and temperature (bottom) during the year. The FerryBox measurements are logged every minute and were gridded (x: 2 days, y: 0.1°) and interpolated.*

Figur 10*. Stasjoner fra havforsuringsprogrammet mellom Oslo Og Kiel (punkt) overlagt kontinuerlige FerryBox-data for klorofyll a fluorescens (topp), saltholdighet (midten) og temperatur (bunn) gjennom året. FerryBoxdataene logges hvert minutt og dataene er griddet (x: 2 dager, y: 0.1°) og interpolert.*

Continuous sensor data collected during the 'ØKOKYST' program, allow for investigating the influence of biological production on pH (chlorophyll *a* fluorescence; ***Figure 10)*** as well as giving a fuller picture for salinity and temperature. The sampling carried out in 2019 did overlap with the onset of the phytoplankton spring bloom during February, and in May during the peak of a bloom in the inner Oslofjord. The onset of the spring bloom in the south of Skagerrak in late February likely caused the slightly higher pH measured there compared to the lower pH in the Oslofjord, where the fluorescence and thus inferred biological production was still low, and the salinity was already decreasing from increased freshwater input. Unfortunately, pH was not measured in May for the Inner Oslofjord, when the cruise overlapped with a phytoplankton bloom there. Although there was little cruise overlap with phytoplankton blooms during the summer months, the low vertical mixing supports higher pH during summer in the surface water.

Underway observations of pCO_2 (µatm) and pH for the entire transect between Oslo-Kiel (i.e., discrete sampling was made as far south as~57.8 °N while sensor observations were made as far south as ~54 °N) are shown in ***Figure 11***. pCO_2 observations were available from January to April and September to December 2019, while pH observations were only available for February and October 2019. The temperature sensor in the pCO_2 instrument was defect between 15-30 April, and in this period, we used the inlet temperature recorded by the FerryBox plus the average difference between inlet temperature and the instrument temperature determined between January-march (2 °C) for calculations of pCO_2. Observations from early in the year show that pCO_2 exhibited little variability from Oslo to Kiel (January to February) and decreased rapidly in mid-February to <~300 µatm and pH_T increased to >~8.1 in the ~54-57.5 °N region. This was followed by another decline in pCO_2 to <~300 µatm in the Skagerrak region (~58-59 °N) in late March to mid-April. In September/October 2019, some low pCO_2/high pH observations were made in in the Skagerrak region while some observations of pCO_2 as high as ~600 µatm and pH as low as ~7.9 were made in the Kattegat region (~54-56 °N). In November/December 2019, pCO_2 continued to increase across the entire study region but was also much higher in the Kattegat region.

The seasonal variability in pCO_2 and pH was likely strongly driven by phytoplankton production, and this was consistent with the chlorophyll *a* fluorescence shown in ***Figure 10***. The spring bloom began in March and peaked in mid-March around 57-58.5 °N in the Skagerrak where pCO_2 was drawn down to <300 µatm. The observed increase in pCO_2 to ~450 µatm in mid-April coincided with a freshening and warming period across most of the Oslo-Kiel transect with salinity <25 and temperatures >10 °C, which suggested a strong physical and/or geochemical influence on the carbonate system. The primary production in the Skagerrak continued until the end of October, observed as decline in chlorophyll *a* fluorescence to <1 µg L^{-1}. pCO_2 began to increase after October likely in part due to lack of biological production (chlorophyll a fluorescence was <1 µg L^{-1}) as well as vertical mixing/transport of high pCO_2/low pH waters. Since the discrete sampling took place on either side of the major decrease in pCO_2, the discrete sampling failed to capture the full carbonate chemistry dynamics during these events (e.g., decrease in pCO_2 observed in late March/early April in the Skagerrak and increase in pCO_2 during the mid-April fresh/warm period were bracketed by the cruises on 25 February and 28 May). Additionally, the southern part of the Oslo-Kiel transect was the most dynamic in terms of carbonate system variability but was outside the domain of the discrete sampling program. Nevertheless, the continuous measurements highlight significant variability over short distances within the domain (0.05 pH units; 50 µatm) highlighting the importance of continuous measurements to realistically catch the heterogeneity of the region.

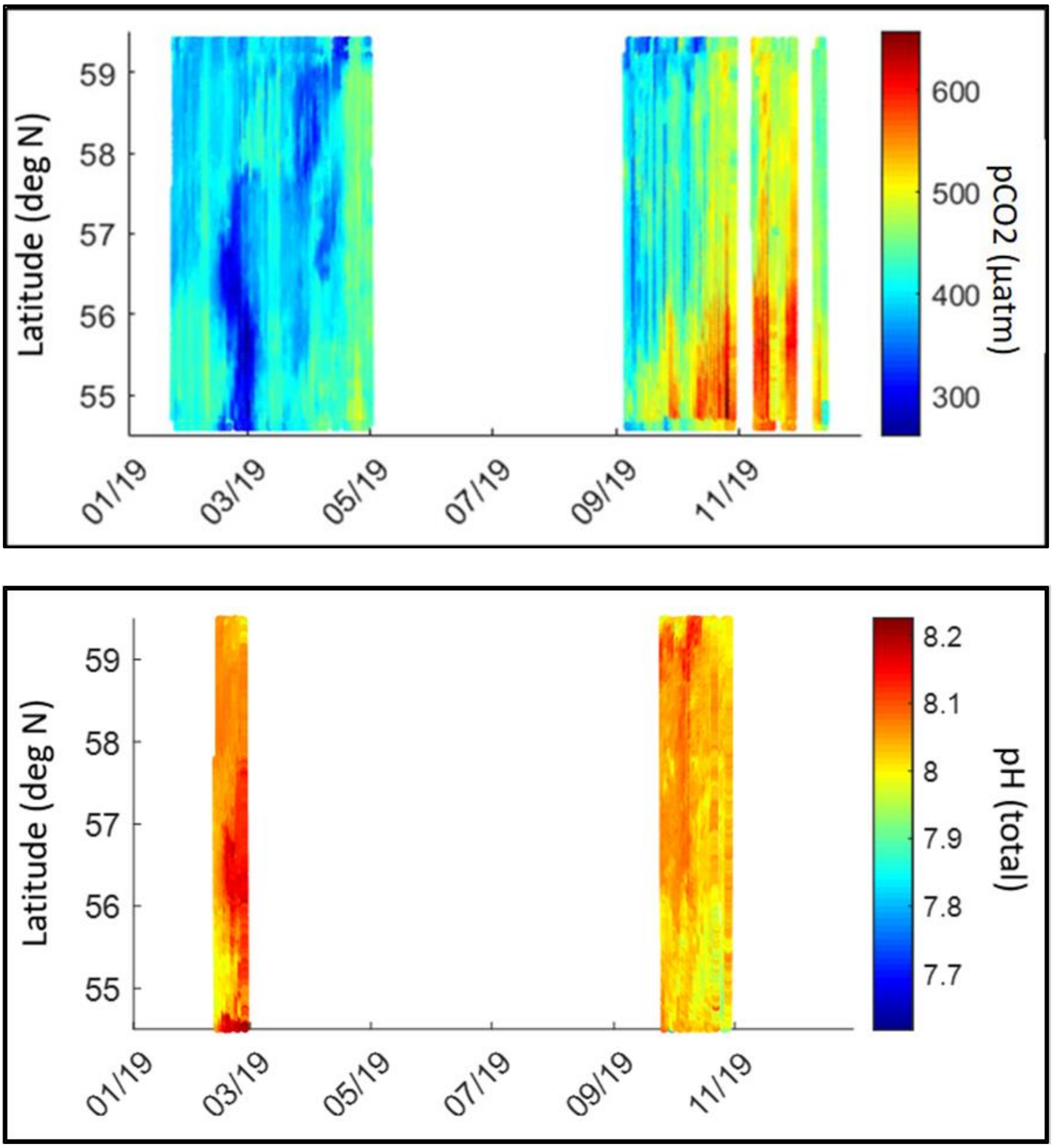

***Figure 11**. pCO_2 (µatm) and pH measured by underway sensors in 2019.*

***Figur 11**. pCO_2 (µatm) og pH målt underveis i 2019.*

3.1.4 Trend analysis at selected stations

3.1.4.1 Trend analysis by linear regression

From the Oslo-Kiel data in the Skagerrak region, trend analyses using linear regression on annual average surface winter data are shown in ***Figure 12***. There are few data points and the temporal changes show no or weak trends in temperature, salinity, pH, or Ω aragonite, and trend lines were therefore not included. Increased temporal coverage by additional years of measurements is needed to enable more robust estimates of a trend for this area.

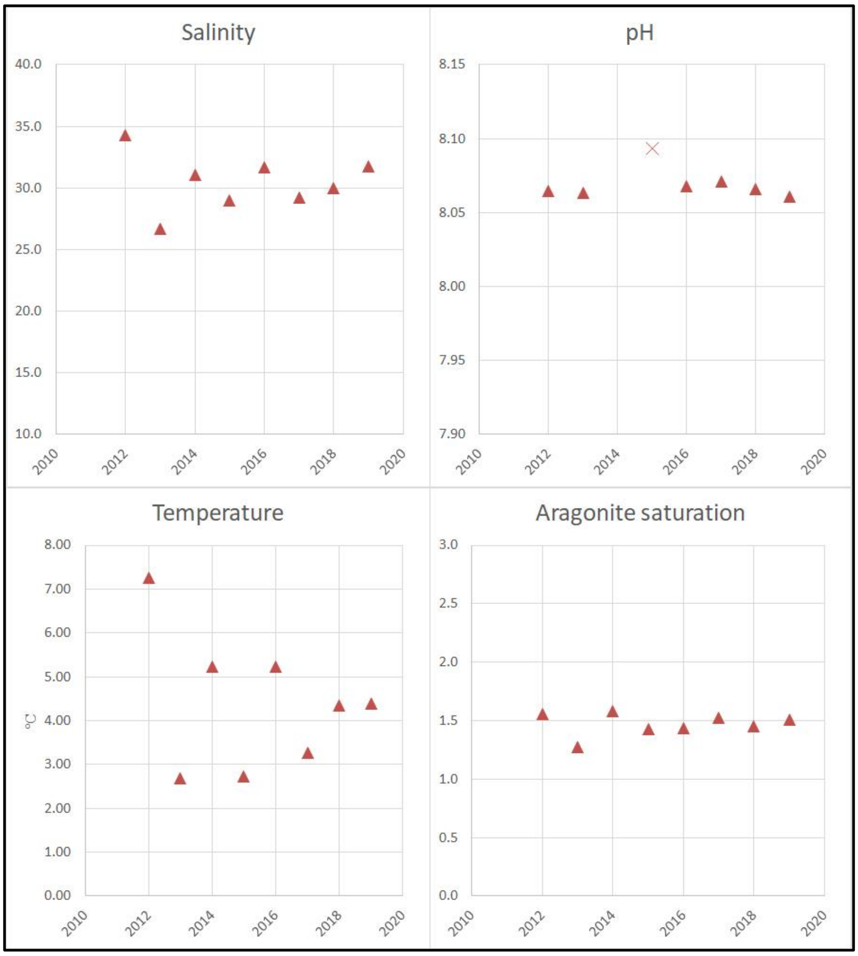

Figure 12. *Trend analyses over 8 years using linear regression showed no trends in temperature, salinity, pH, Ω aragonite in surface (4 m) waters from 2012 to 2019 winter data in the Skagerrak. The data are mean values from the five southernmost stations.*

Figur 12.*Trend analyse over 8 år gjennom linjær regressjon viste ingen trend i temperatur, saltholdighet, pH og Ω aragonitt av midlede overflatedata (4 m) fra vinter 2012 til 2019 i Skagerak. Data er middelverdier fra de 5 sørligste stasjonene.*

Along the Torungen-Hirtshals section, temporal changes in pH and Ω aragonite in the deepest water mass at 600 m depth in the Skagerrak are affected by increased temperature by a rate of 0.22 °C yr^{-1} (***Figure 13***). Year 2010 was unusually cold year, and 2018 was also colder than the other years. This follows a pattern of relative decrease in temperature occurs every 5-8 years, in line with the dominant hydrography of the region where Atlantic and North Sea water overspill into the area and renew the deeper water mass in the Skagerrak. This was accompanied by a general increase in salinity from 2010 to 2017, however measurements in 2018 and 2019 show slightly lower salinity and fresher water compared to the general trend of the preceding years. The variation in pH and Ω aragonite show variability from lower and higher values alternating from year to year. Overall, decreasing time trends are evident, giving an average reduction in pH and Ω aragonite of 0.008 yr^{-1} and 0.01 yr^{-1}, respectively. These trends indicate increased temperatures, and likely increasing amounts of warm, saline Atlantic water entering the deeper parts of the Skagerrak region.

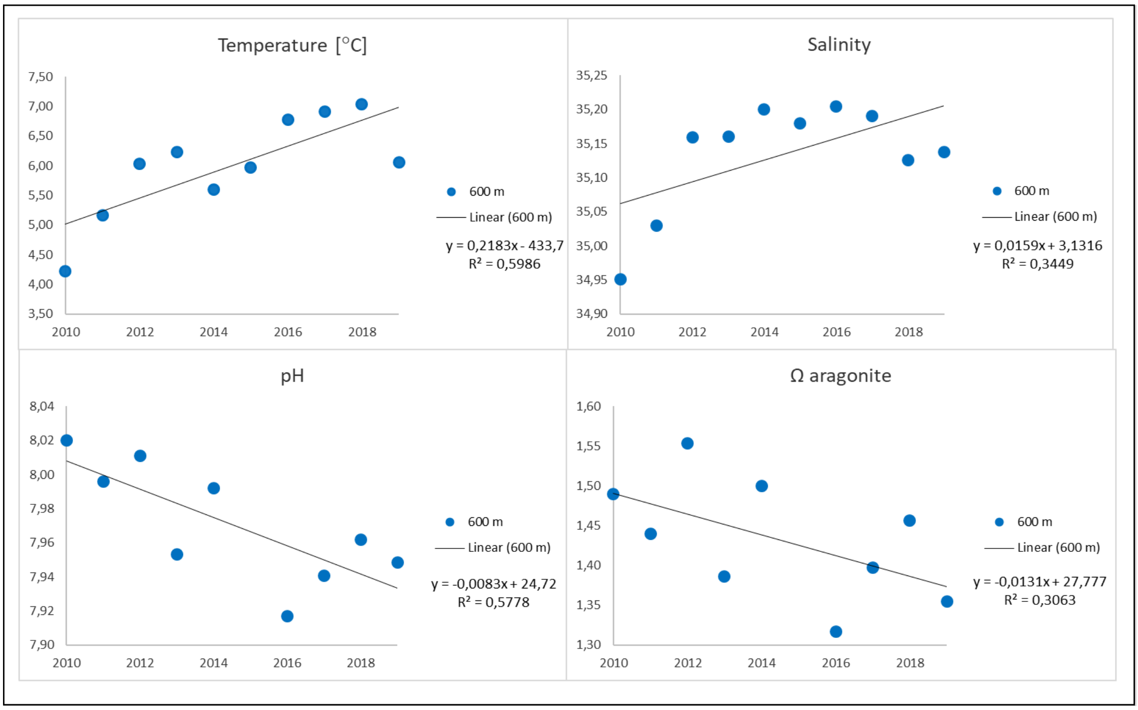

***Figure 13**. Trend analyses over 9 years using linear regression of temperature, salinity, pH and Ω aragonite at 600 m depth from the station in central Skagerrak (20 nm) along the Torungen-Hirtshals section.*

***Figur 13**. 9 års trendanalyse gjennom linjær regressjon av temperatur, saltinnhold, pH og Ω aragonitt ved 600 m dyp på stasjonen i sentrale Skagerrak (20 nm) langs Torungen-Hirtshals snittet.*

3.2 Norwegian Sea

3.2.1 Spatial variability along the Svinøy-NW section

In January 2019, carbonate chemistry measurements were carried out by IMR on water samples from the whole water column at six stations along the hydrographic section between Svinøy and 64.13 °N, 1.26 °E; Svinøy-NW (***Figure 14***). Position, depth and sampling data are displayed in ***Table 3***, ***Appendix 6.2***. The Svinøy-NW section extends from the Norwegian coast with warm and fresh surface water offshore into Atlantic and Arctic water masses in the Norwegian Sea (***Figure 15***). The Svinøy section has completed hydrographic sampling since 1935.

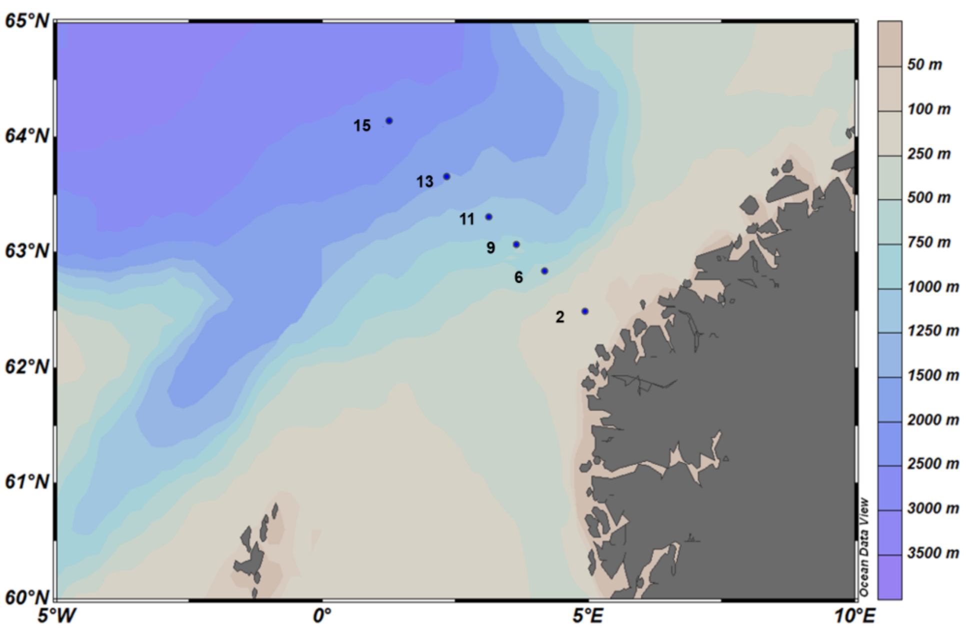

***Figure 14**. Map and stationnumbers from Svinøy-NW in the Norwegian Sea in January 2019.*

***Figur 14**. Kart og stasjonsnummer langs Svinøy-NV i Norskehavet i januar 2019.*

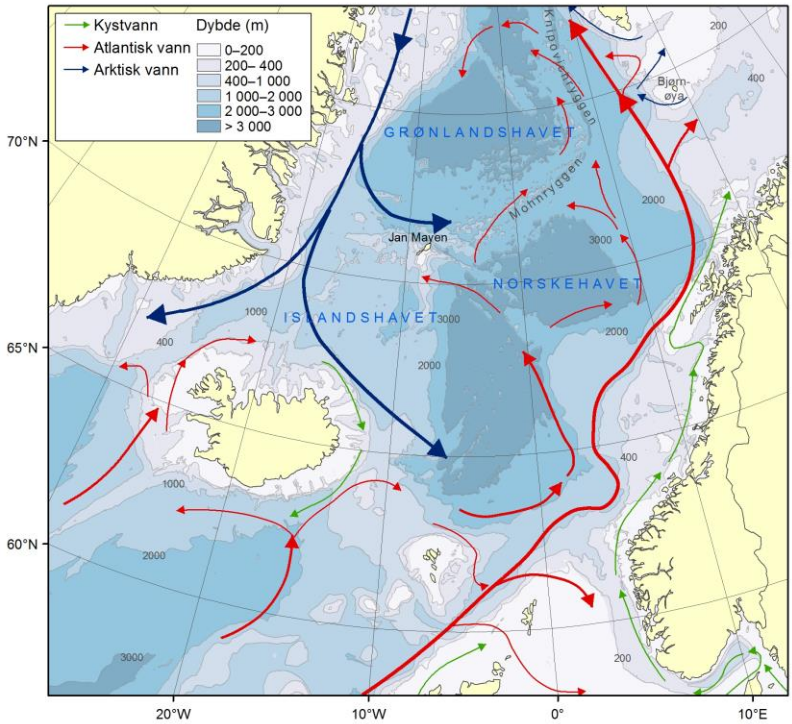

***Figure 15**. Major currents and water masses in Norwegian Sea: Atlantic water (red), polar water (blue) and coastal water (green). www.imr.no.*

***Figur 15**. Strømmer og hovedsakelige tre vannmasser i både Norskehavet og Barentshavet: atlanterhavsvann (rød), arktisk vann (blå) og kystvann (grønn). www.imr.no.*

Warm and salty Atlantic waters enter the Norwegian Sea between Shetland, the Faroe Islands and Iceland and flow northwards following the coastal topography of Norway. The Atlantic water becomes cooler during the passage north and is able to absorb a lot of atmospheric CO_2 in the surface layer. The distribution of pH along the Svinøy section in 2019 shows high values ~8.07 (***Figure 16***) accompanied by low A_T ~2290 µmol kg $^{-1}$ and C_T ~2122 µmol kg $^{-1}$ in the relatively cold surface waters of the Norwegian coastal current (***Figure 73***, ***Appendix 6.1***).

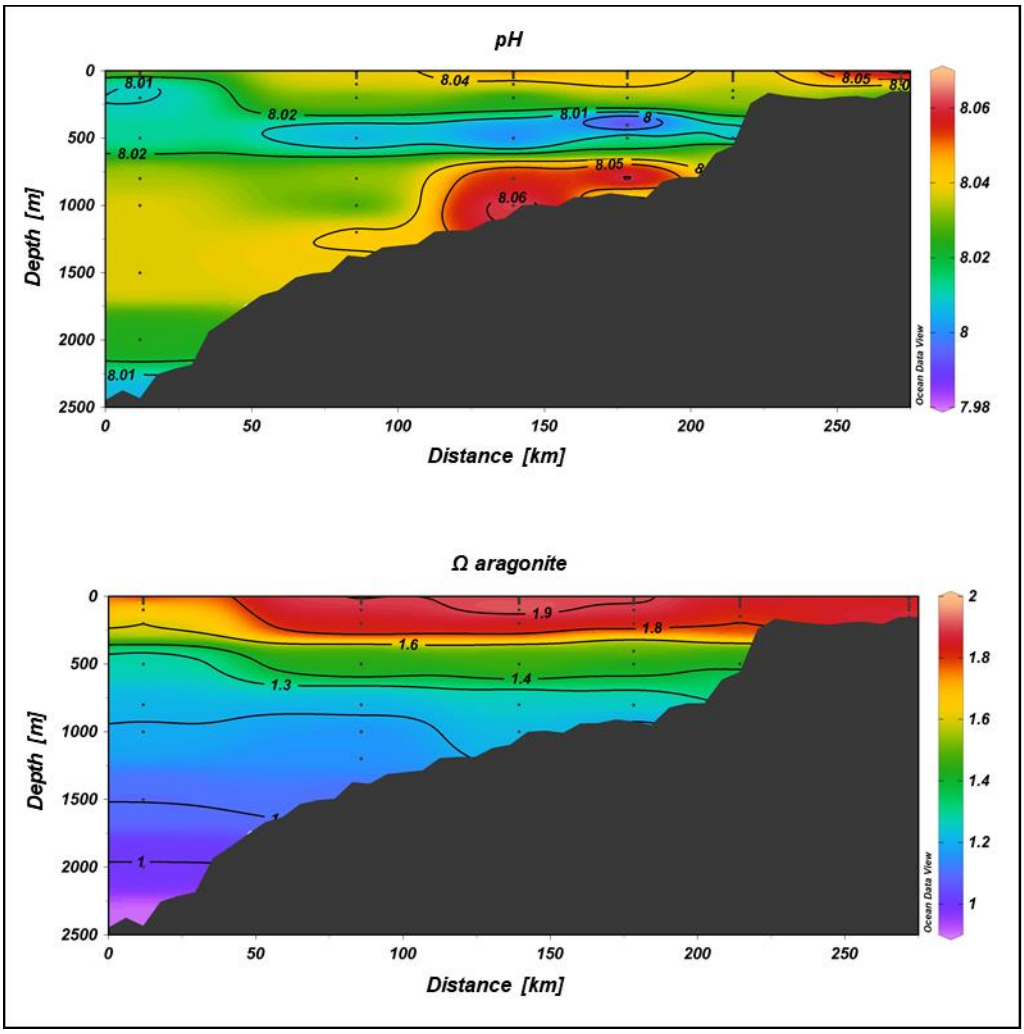

Figure 16. *pH and Ω aragonite along the Svinøy-NW section in January 2019.*

Figur 16. *pH og Ω aragonitt langs Svinøy-NV snittet i januar 2019.*

Strong vertical gradients separate the surface layer with the underlying Atlantic water that is distinguished by lowest pH 7.99-8.01 from about 50 m to 500 m depth. Ω aragonite was highest at 1.93 as a result of seasonal biological C_T uptake in the surface layers, particularly in the central part of the section. Surface water Ω aragonite varied between 1.83 and 1.91 as a result of competing processes such as freshwater inputs, biological production and mixing with sub-surface Atlantic water. Below 500 m depth, steep gradients in pH and Ω aragonite indicate the presence of a thin layer of Arctic Intermediate Water above the cooler and fresher Norwegian Sea Deep Water that naturally has lower A_T, due to lower salinity compared to Atlantic water. The deeper waters are characterised by higher pH of 8.05-8.06 and Ω aragonite between 1.28

and 1.47. Low pH (8.01) and lowest Ω aragonite of 0.90 were found at 2440 m in the deep basin of the Norwegian Sea. The saturation horizon for aragonite was located at around 1900 m.

3.2.2 Spatial variability along the Gimsøy-NW section

In March and May 2019, carbonate chemistry measurements were carried out by IMR on water samples from the whole water column at five stations along the hydrographic section between Gimsøy and 71.08 °N, 6.00 °E; Gimsøy-NW (***Figure 17***). Position, depth and sampling data are displayed in ***Table 5***, ***Appendix 6.2***. Normally, sampling is carried out during the winter months to reduce the impact of biological production (carbon uptake) on the carbonate chemistry in the water column. Due to logistical constraints, sampling along the Gimsøy section in 2019 was carried out also in May and therefore data in the upper 100 m at the outer station (station 21, ***Figure 17***) will reflect the signal of carbon (i.e., CO_2) removal in the spring and early summer.

The Gimsøy-NW section encompasses the upper Norwegian coastal current, Arctic water at intermediate depths and Atlantic water that flow northwards towards the Barents Sea. This region has numerous sites of cold-water coral reefs that are potentially particularly sensitive to low pH water and low calcium carbonate mineral saturation. Together with the Norwegian basin, this area has experienced faster rates of pH decrease in comparison to other parts of the Norwegian Sea (Skjelvan et al. 2014; Jones et al. 2018) and the global ocean average (Takahashi et al. 2014).

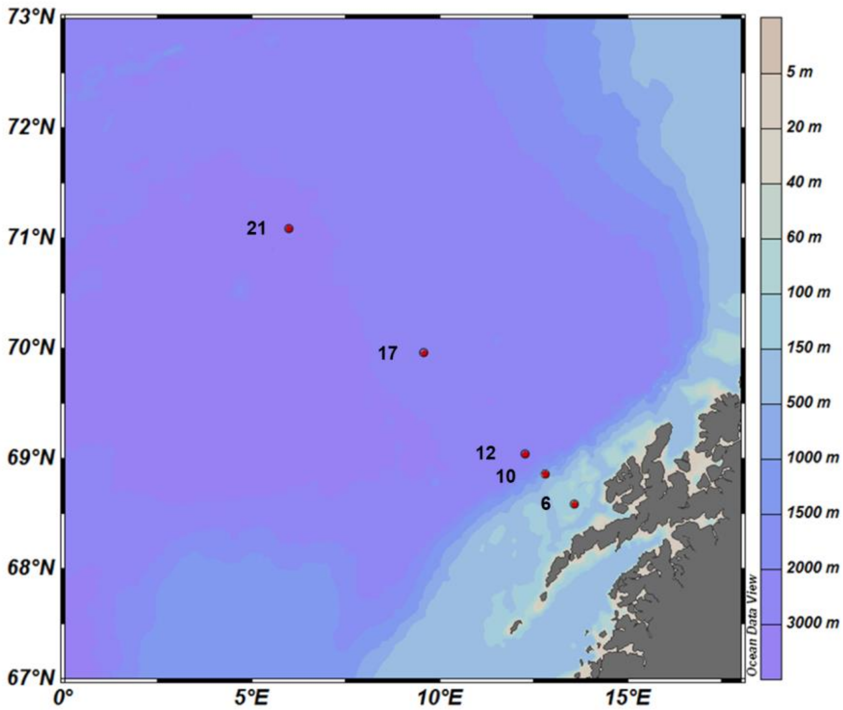

Figure 17. *Map and numbers of the stations along the Gimsøy-NW section in the northern Norwegian Sea in March and May 2019.*

Figur 17. *Kart og nummer over stasjoner langs Gimsøy-NV snittet i nordlige Norskehavet i mars og mai 2019.*

The section is dominated by warm and salty Atlantic water in the upper 500 m with C_T of about 2150-2175 µmol kg^{-1} and high A_T of about 2310-2320 µmol kg^{-1} (***Figure 74*, *Appendix 6.1***). Colder Norwegian Sea Deep Water and Arctic water had slightly higher C_T and lower A_T (approx. 2170-2190 and 2305 µmol kg^{-1}, respectively), compared to the Atlantic water, and both water masses were located below 500 m away from the shelf slope and into the deep basin. Highest pH of 8.07 was found closest to the coast, in the warm waters overlying the shelf where biological production had reduced C_T in the surface layer (***Figure 18***). This was accompanied by high Ω aragonite of 1.75 in the warm and productive surface waters. Highest Ω aragonite of 1.95 occurred at the sea surface as incursions of Atlantic water increased A_T in the upper part of the water column alongside biological C_T uptake. Lowest pH of 7.96 and lowest Ω aragonite was found at 3120 m depth in the deeper parts of the Norwegian Sea occupied by Norwegian Sea Deep Water. The saturation horizon for aragonite was located between 1500 m and 2000 m depth. This was shallower than the saturation horizon depth that fluctuated around 2000 m depth at Station M further offshore and at the Svinøy section to the south.

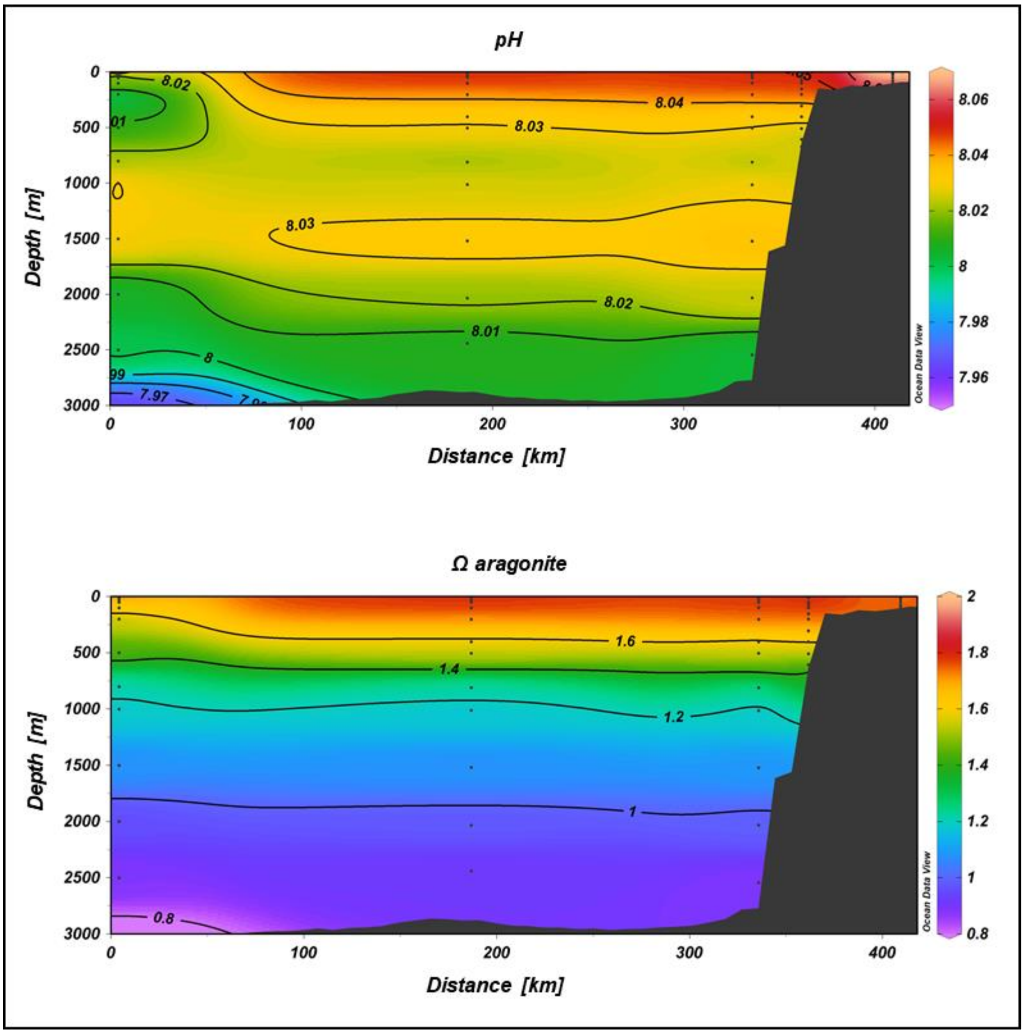

Figure 18. *pH and Ω aragonite along the Gimsøy-NW section in March and May 2019.*

Figur 18. *pH og Ω aragonitt langs Gimsøy-NV snittet i mars og mai 2019.*

3.2.3 Seasonal variability in the open ocean at Station M

Ocean Weather Station M (Station M) is an open ocean fixed station positioned at 66°N 2°E between the Svinøy and Gimsøy section in the Norwegian Sea (***Figure 1***). Hydrography has been monitored at this station since 1948. In 2019, NORCE-UiB sampled the full water column during cruises in January, April, May, June, and November. The samples were analysed for A_T and C_T (***Figure 70 a-b, Appendix 6.1***; ***Table 4, Appendix 6.2***) and the remaining carbonate system variables were calculated (***Figure 19***). Further, from January to April and from June to November 2019, a surface buoy equipped with a pCO_2 system and hydrography sensors was anchored at the station, delivering continuous measurements. ***Figure 20*** shows surface buoy data from the years 2011-2019. A deep mooring was also deployed at Station M to determine the hydrography at different depth layers and here is shown carbon data from the mixed layer depth over the years 2013-2019 (***Figure 21***). The combined sampling strategy used at Station M provides supplementary information, as discrete measurements give information about seasonal and longer term variation of the carbonate system at all depths (***Figure 27***), while continuous measurements provide information about small scale variations over a day, a week, or a year from selected depths. The continuous data also provide information about long term trends, which is shown in ***Figure 28***.

The water column at Station M consists of an upper layer (300-400 m deep) of warm and saline Atlantic Water, and a deep layer (deeper than approximately 1000 m) of cold and less saline Norwegian Sea Deep Water. Between these two layers is the Arctic Intermediate Water with fluctuating thickness (***Figure 19a-b***). The Atlantic Water in the northward flowing Norwegian Atlantic Current becomes shallower further north than Station M, e.g. at the Gimsøy section. The station is frequently influenced by fresher surface water during late summer, and this was confirmed also for 2019 (continuous salinity data, not shown). In 2019, the Station M surface temperature varied from 6.0 °C in March to 13.6 °C in August (***Figure 20a***), which is similar to that of 2018.

In 2019, the spring phytoplankton bloom was initiated in May, with decreasing surface C_T (***Figure 46, Appendix 6.1***) and nutrients (not shown), but the effect on pH is not apparent until June, when the surface pH increases slightly. In August 2019, pH was highest (8.17; ***Figure 20c***), and after this, pH decreased because the effect of increasing temperature (which decreases pH) overrode that of biological production (which increases pH). The surface pH was lowest in February-March (***Figure 20c***), when the temperature was low. Surface Ω aragonite was also lowest in February-March, while the highest surface Ω aragonite value in 2019 (2.87) was reached in August (***Figure 20d***).

The seasonality of the surface water is particularly well illustrated in ***Figure 20***, which also illustrates the large difference between the oceanic and atmospheric seasonal pCO_2 amplitude (***Figure 20a-b***). The lower pCO_2 values in surface seawater, with respect to the atmosphere, create an air-sea gradient and drive oceanic uptake of atmospheric CO_2 throughout the year. Winter surface characteristics in 2019 were for C_T, pH and Ω aragonite 2156±5 µmol kg^{-1}, 8.05±0.04, and 1.80±0.17, respectively.

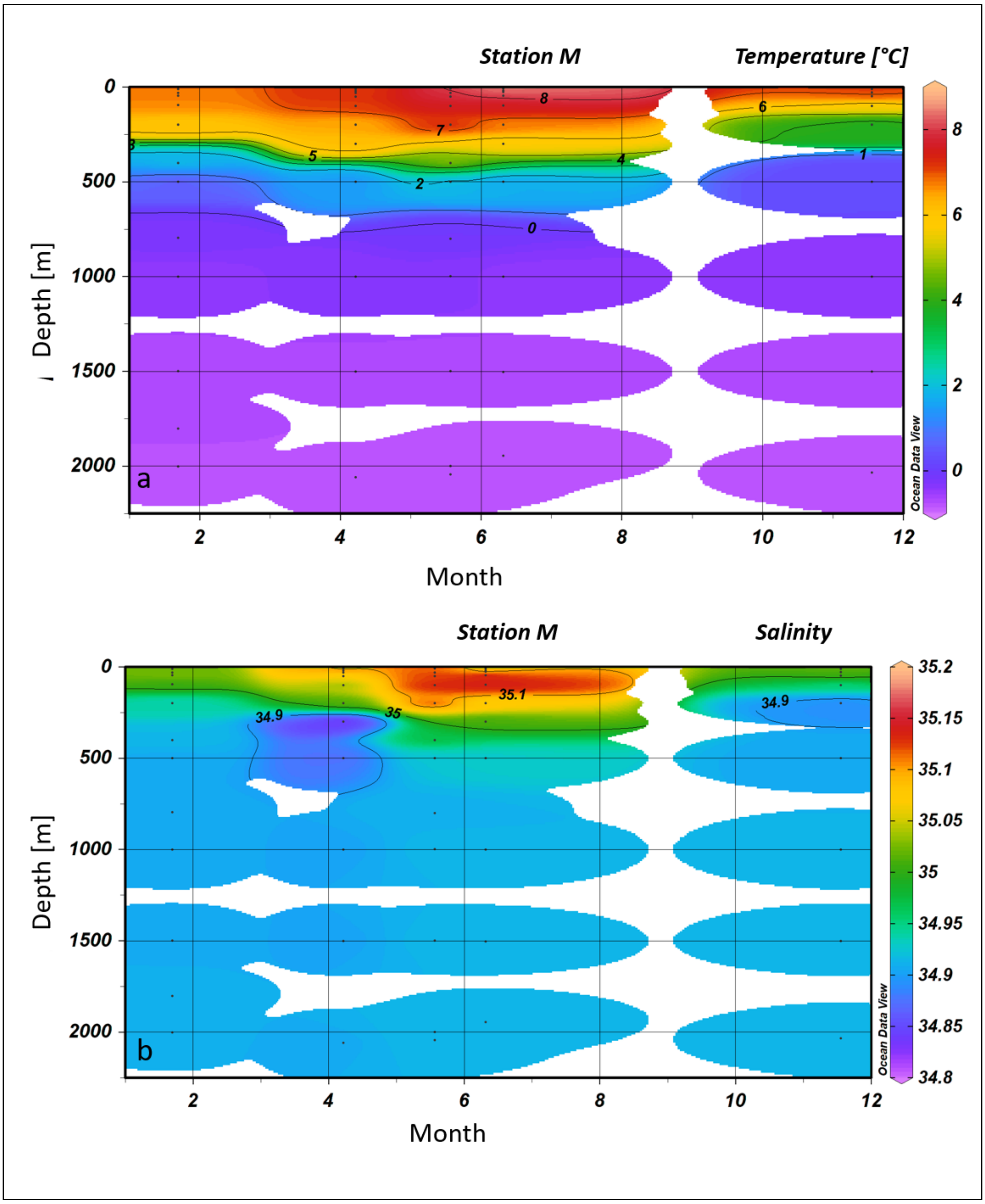
Station M
Temperature [°C]
Depth [m]
Month
a
Station M
Salinity
Depth [m]
Month
b
Ocean Data View

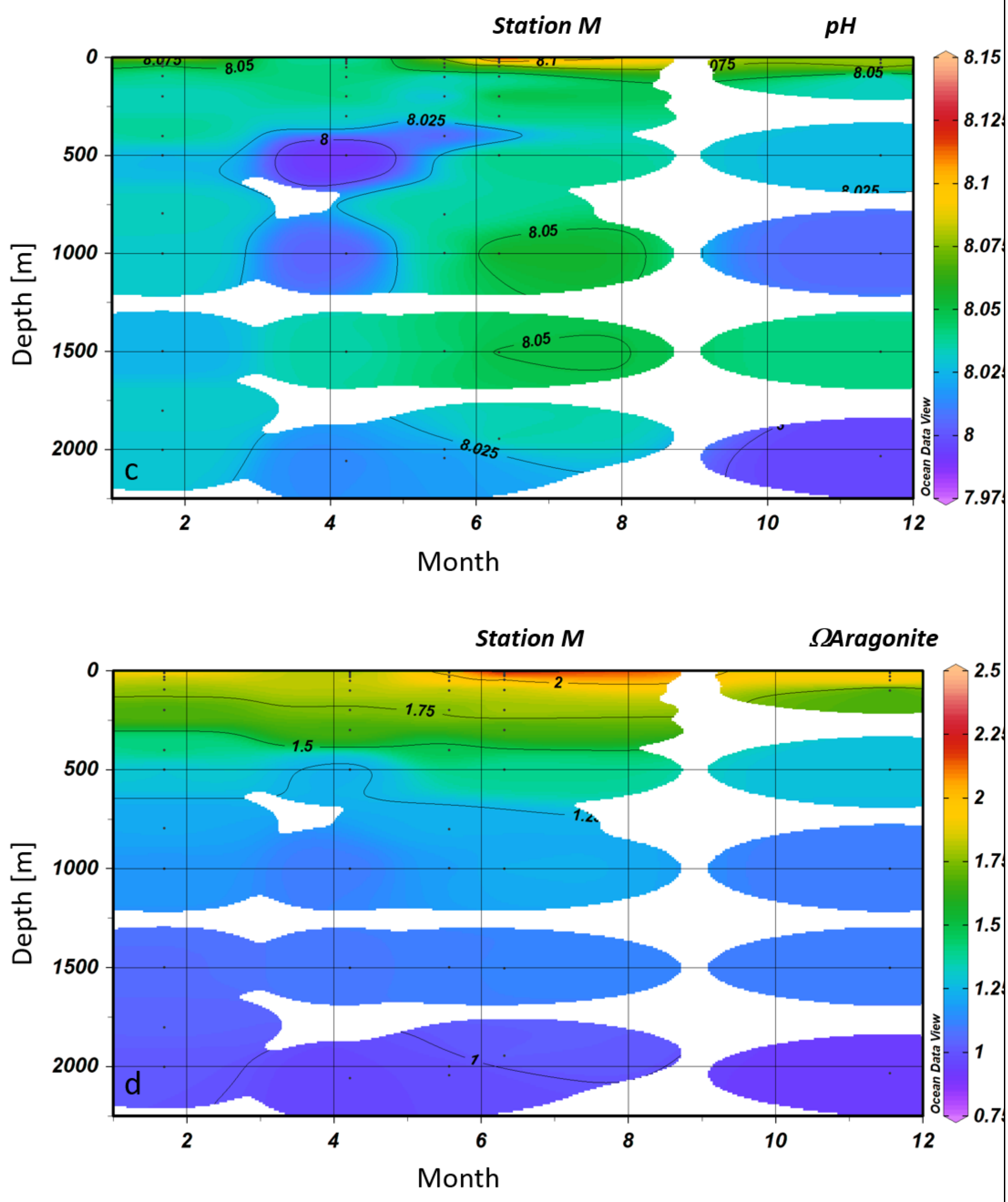

***Figure 19**. a) temperature (°C), b) salinity, c) pH, and d) Ω aragonite at Station M in 2019. Black dots indicate sampling depths.*

***Figur 19**. a) temperatur (°C), b) saltinnhold, c) pH og d) Ω aragonitt fra Stasjon M i 2019. Svarte prikker viser prøvedyp.*

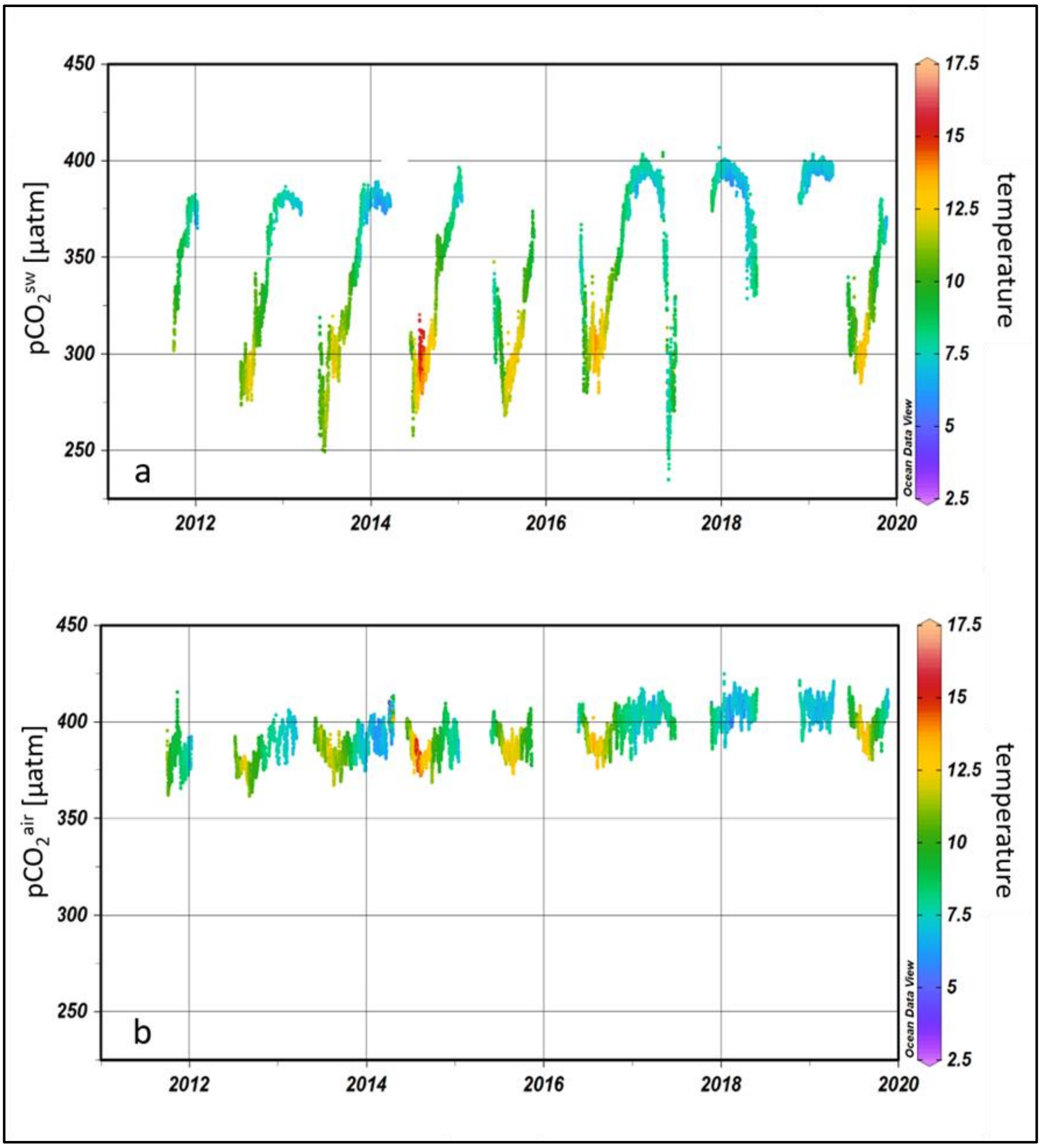
450
400
350
300
250
pCO2sw [µatm]
a
2012
2014
2016
2018
2020
17.5
15
12.5
10
7.5
5
2.5
temperature
Ocean Data View
450
400
350
300
250
pCO2air [µatm]
b
2012
2014
2016
2018
2020
17.5
15
12.5
10
7.5
5
2.5
temperature
Ocean Data View

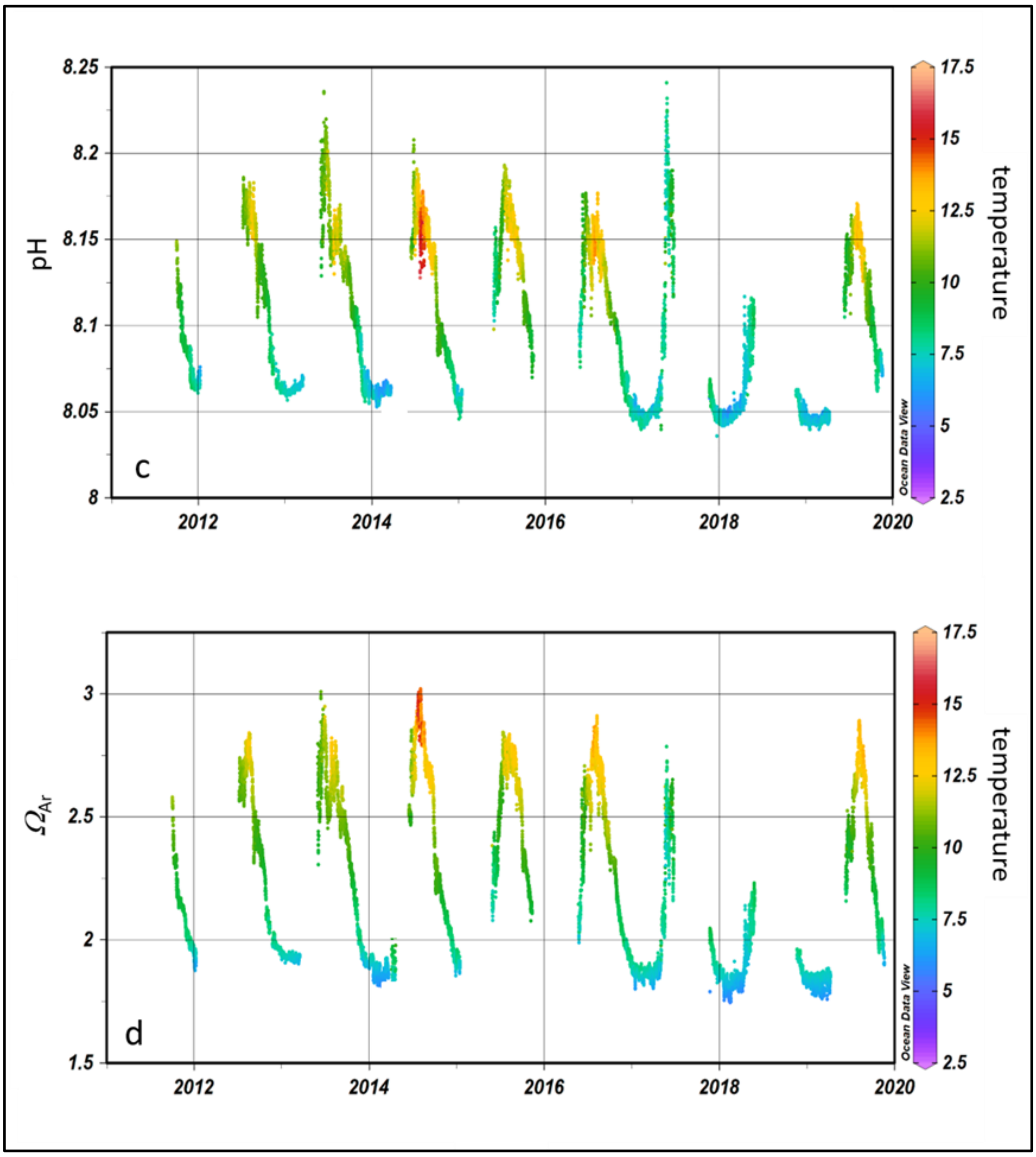

***Figure 20**. a) sea surface pCO_2, b) atmospheric pCO_2, c) sea surface pH, and d) sea surface Ω aragonite at Station M between 2011 and 2019. The colour scale indicates temperature.*

***Figur 20**. a) pCO_2 i havet, b) pCO_2 i atmosfæren, c) pH i overflatevann og d) Ω aragonitt i overflatevann på Stasjon M i perioden 2011 til 2018. Fargeskala viser temperatur.*

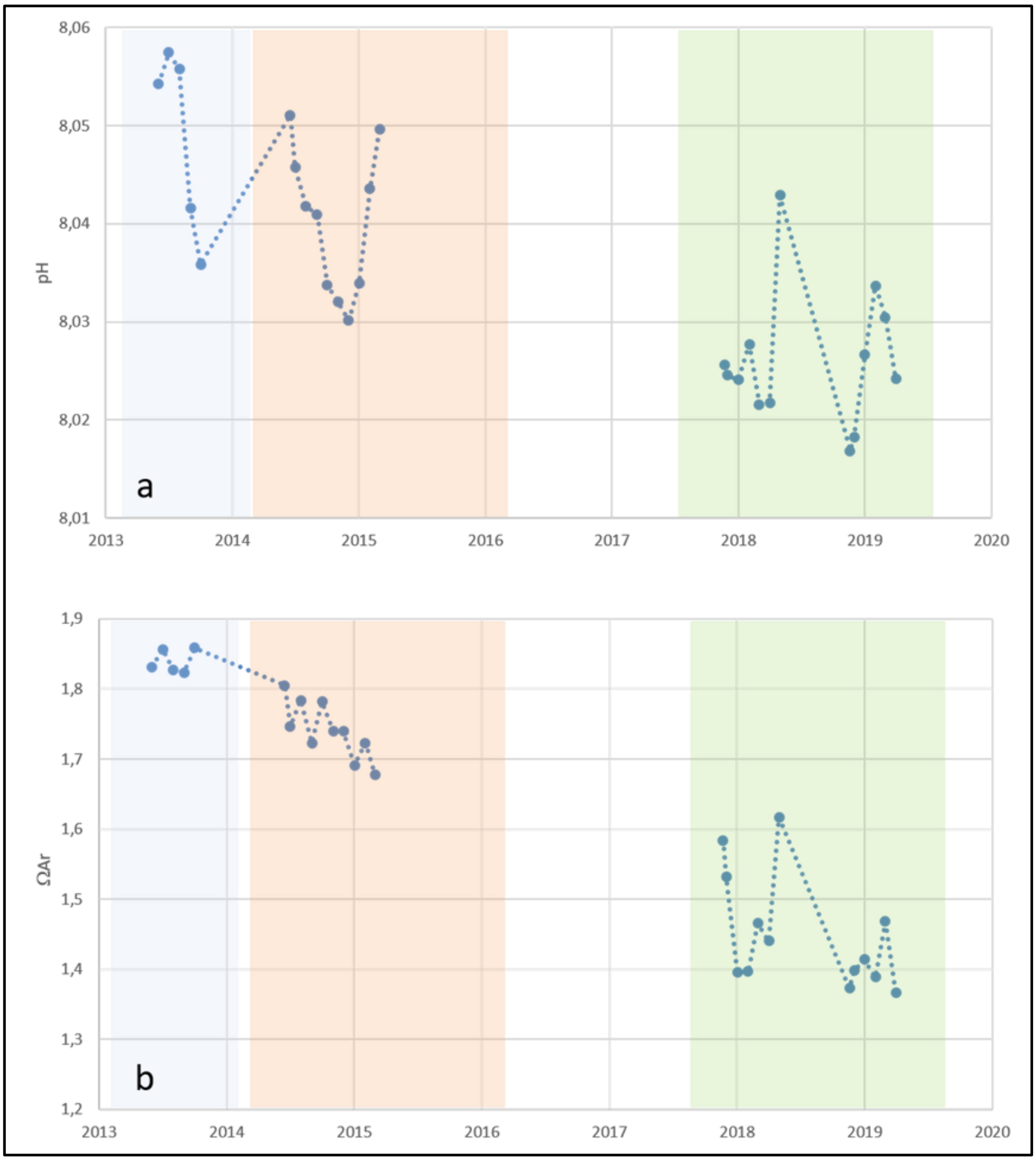

***Figure 21**. Mixed layer monthly averages of a) pH and b) Ω aragonite at Station M between 2011 and 2019. The light blue colour indicates the period when the measurements are from 150 m depth, the orange colour is when the measurements are from 200 m depth, while the green colour is the period with measurements from 400 m.*

***Figur 21**. Månedsmiddel av a) pH og b) Ω aragonitt i blandingslaget ved Stasjon M i perioden 2011 til 2019. Lyseblå farge viser perioden da målingene ble gjort på 150 m dyp, oransje farge er når målinger ble gjort på 200 m dyp, mens den grønne fargen indikerer målinger på 400 m dyp.*

Monthly averages of the mixed layer continuous measurements at Station M is shown in ***Figure 21***, where the different colours represent the depths of measurements. Seasonal variations are seen from the pH data at 150-200 m depth (***Figure 21a***; light blue and orange background), with lowest pH during late autumn, when CO_2-rich water (due to remineralised organic matter) is mixed up from below and temperature is low. What appears to be a decreasing trend is connected to the fact that the measurements are collected at different depths, i.e. the pH and Ω aragonite at 500 m depth is lower than those at 150 -200 m depth. The values are confirmed by the discrete measurements form Station M.

3.2.4 Seasonal variability in coastal water

3.2.4.1 Skrova

Skrova is a coastal station in Vestfjorden at 68.1 ⁰N, 14.5 ⁰E and has been sampled each month for carbonate chemistry by IMR since 2015. Position, depth and sampling data are displayed in ***Table 6***, ***Appendix 6.2***. This time series provides valuable data on seasonal variation of inorganic carbon in the Norwegian Coastal Current, to 300 m depth (***Figure 22***).

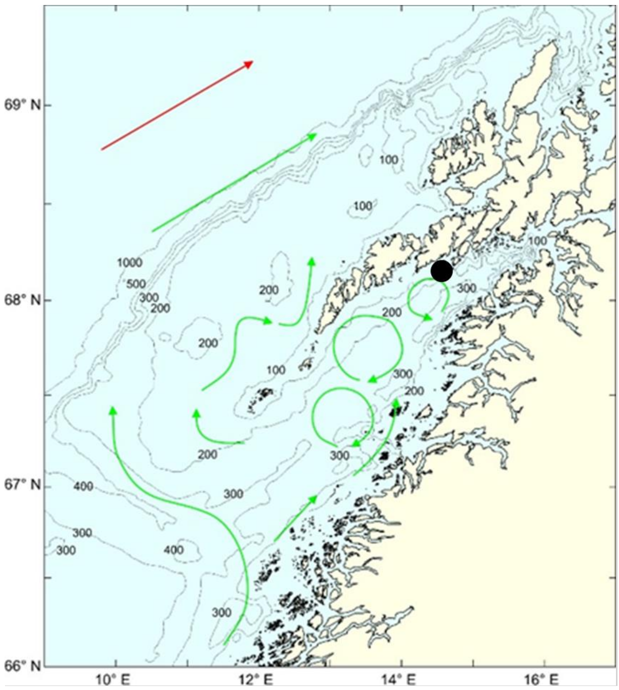

Figure 22*. The location and current patterns in the Lofoten region. Green arrows indicate Coastal Current flow patterns, red arrow indicate the Norwegian Atlantic Current. Skrova station is marked by a black circle.*

Figur 22*. Kart over Lofoten som viser de viktigste strømmene. Grønne piler viser kyststrømmen og rød pil viser den norske Atlanterhavsstrømmen. Svart prikk viser Skrova kyststasjon.*

Observations and modelling show that the exchange of coastal current water in Vestfjorden is high and efficient, and the residence time of the upper 100 m of fjord water in summer is less than a month. Therefore, the variation at the Skrova coastal station reflects the natural variability in the Norwegian current, which fluctuates between the exchanges with Atlantic water. This is reflected in salinity and temperature temporal variations. However, the pattern in the upper mixed layer is repeated every year as a function of the spring bloom of phytoplankton and the productive season of photosynthesis and biological carbon uptake, leading to increases in pH, and elevated levels of Ω aragonite. The 2015 and 2018 data showed similarly high values in pH in the upper layers due to spring and summer photosynthetic consumption of CO_2.

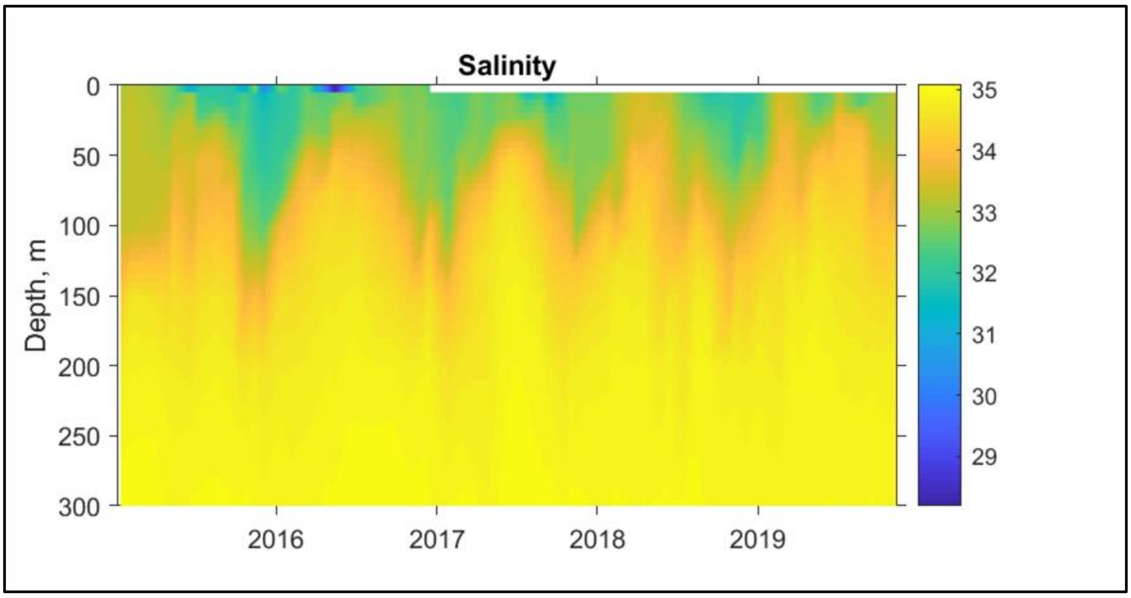

Figure 23. Seasonal and annual variation in salinity in the water column at the coastal station Skrova 2015-2019.

Figur 23. *Års- og mellomårlig variasjon i saltholdighet i hele vannsøylen ved kyststasjon Skrova i 2015-2019.*

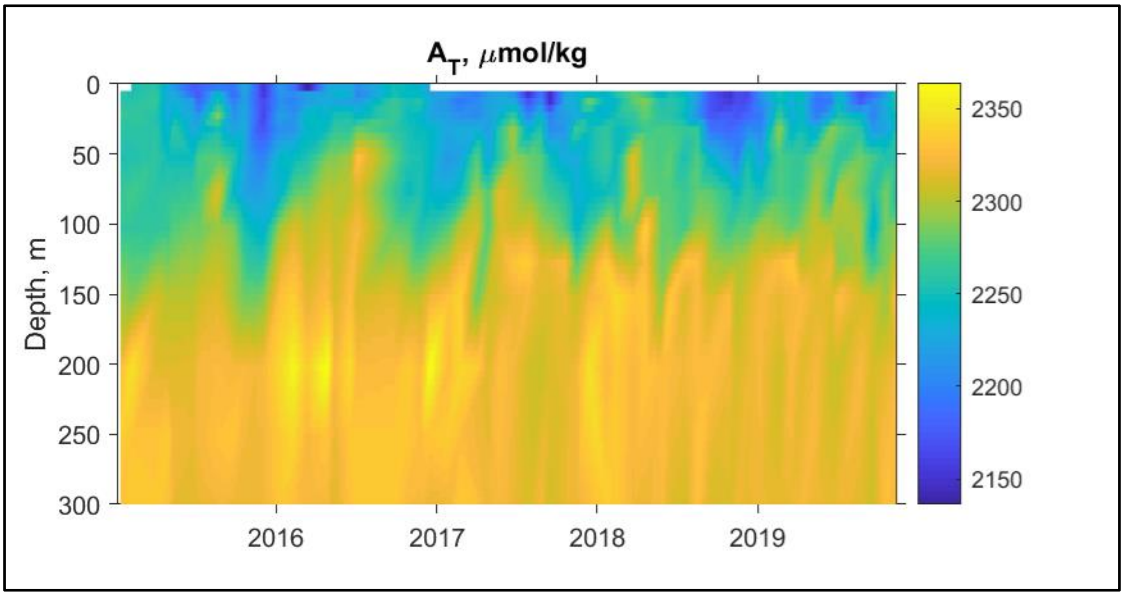

Figure 24. *Seasonal and annual variation in A_T in the water column at the coastal station Skrova 2015-2019.*

Figur 24. *Års- og mellomårlig variasjon i A_T i hele vannsøylen ved kyststasjon Skrova i 2015-2019.*

The variation in salinity (***Figure 24***) shows large seasonal variability in the upper 100 m and that the depth of the mixed layer shallows to about 40-60 m during the summer. Higher salinity subsurface water reaches the upper layers (upper 50 m). The distribution of salinity mainly governs the variation in A_T, with lowest values in the upper 50 m (***Figure 24***).

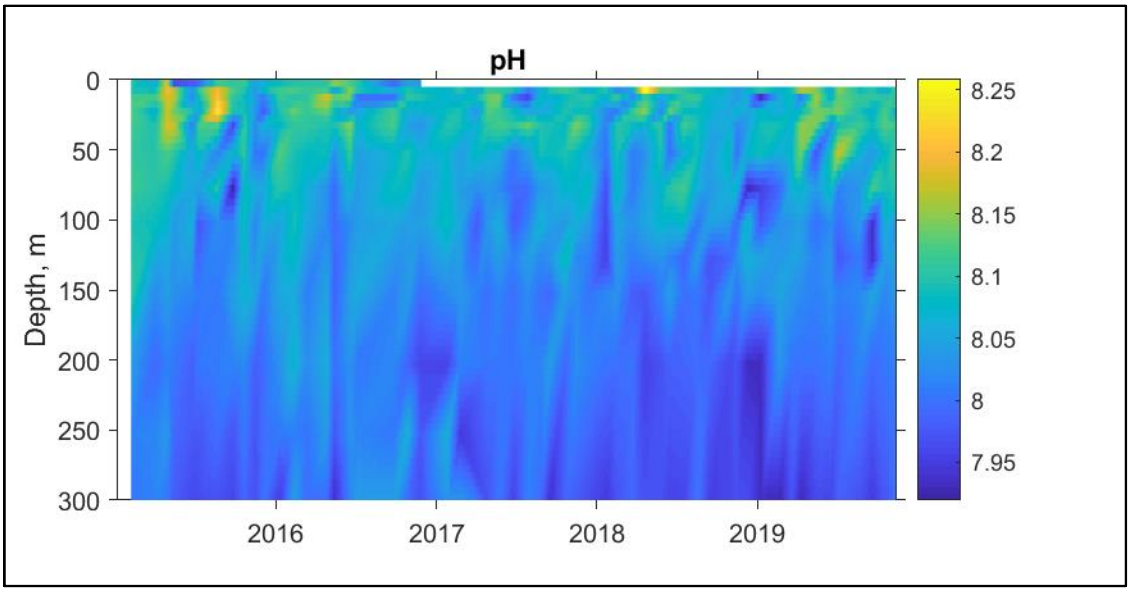

Figure 25. *Seasonal and annual variation in pH in the water column at the coastal station Skrova 2015-2019.*

Figur 25. *Års- og mellomårlig variasjon i pH i hele vannsøylen ved kyststasjon Skrova i 2015-2019.*

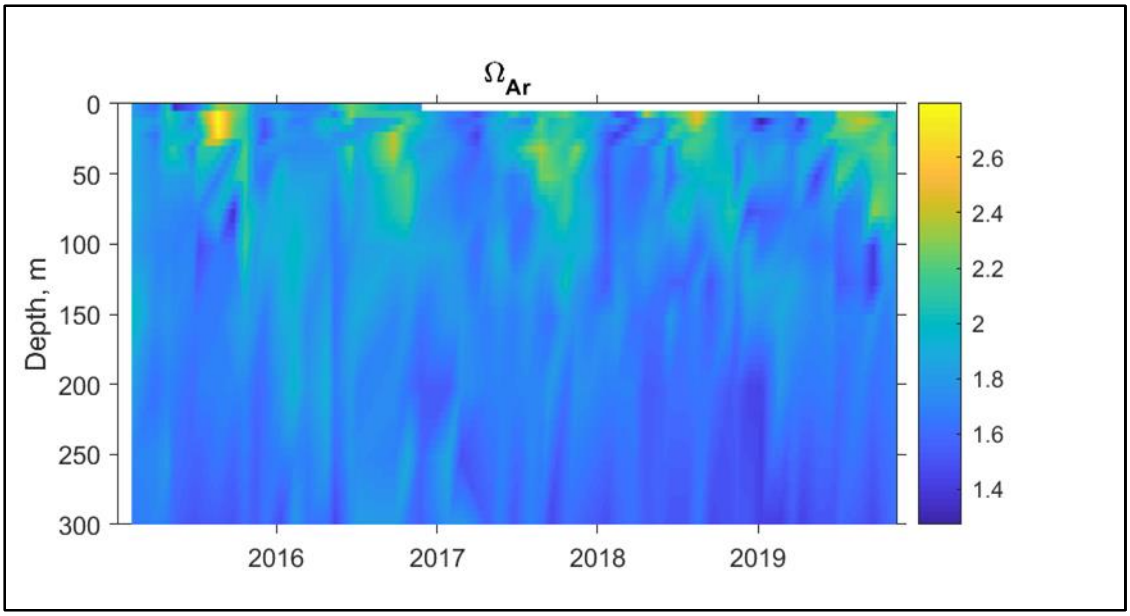

Figure 26. *Seasonal and annual variation in Ω aragonite in the water column at the coastal station Skrova 2015-2019.*

Figur 26. *Års- og mellomårlig variasjon av Ω aragonitt i hele vannsøylen ved kyststasjon Skrova i 2015-2019.*

The variation in pH through the water column (***Figure 25***) shows interannual variability, partly driven by biological production, seawater temperature and inputs of freshwater and mixing with other waters in the coastal area. The Ω aragonite was highest (2.31-2.40) in the upper 10 m from July to September. Higher values occur in the upper 100 m almost every year. By early autumn, Ω aragonite starts to decrease due to reduced biological production, seasonal cooling of the water column and mixing with CO_2-rich sub-surface water (***Figure 26***).

3.2.5 Trend analysis at selected stations

From Station M, the time series of discrete data from the years 2011 to 2019 are presented in ***Figure 27***. Seasonal changes were seen in the upper 200 m or so, and the seasonality is driven by biological activity as well as mixing with deeper waters. Below the Atlantic Water, the variability is disconnected with seasons and are rather a result of mixing of water masses, which occurs with variable frequency and strength. The deepest water mass has relatively stable characteristics; however, changes are seen over years (Østerhus and Gammelsrød, 1999; Skjelvan et. al. 2008; Skjelvan et. al. 2014).

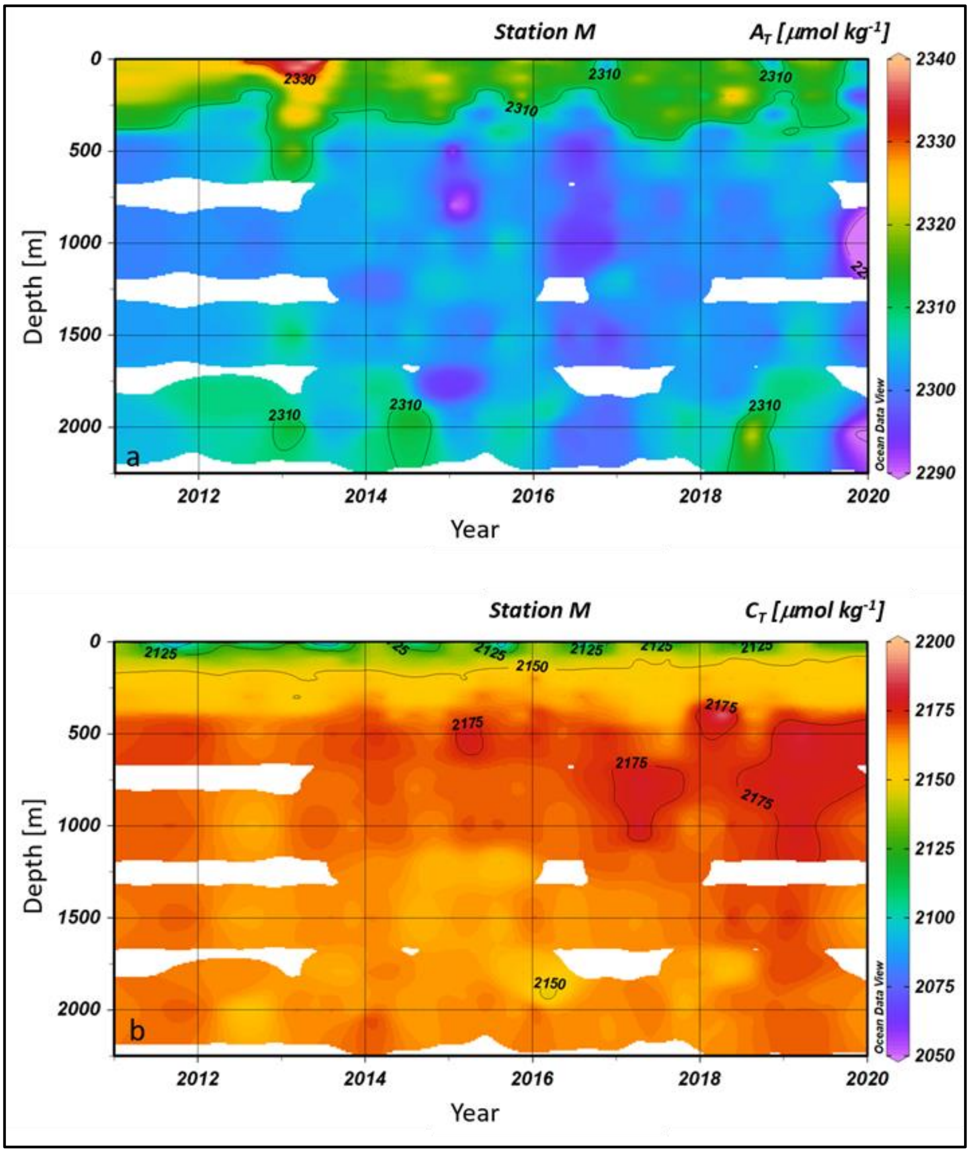

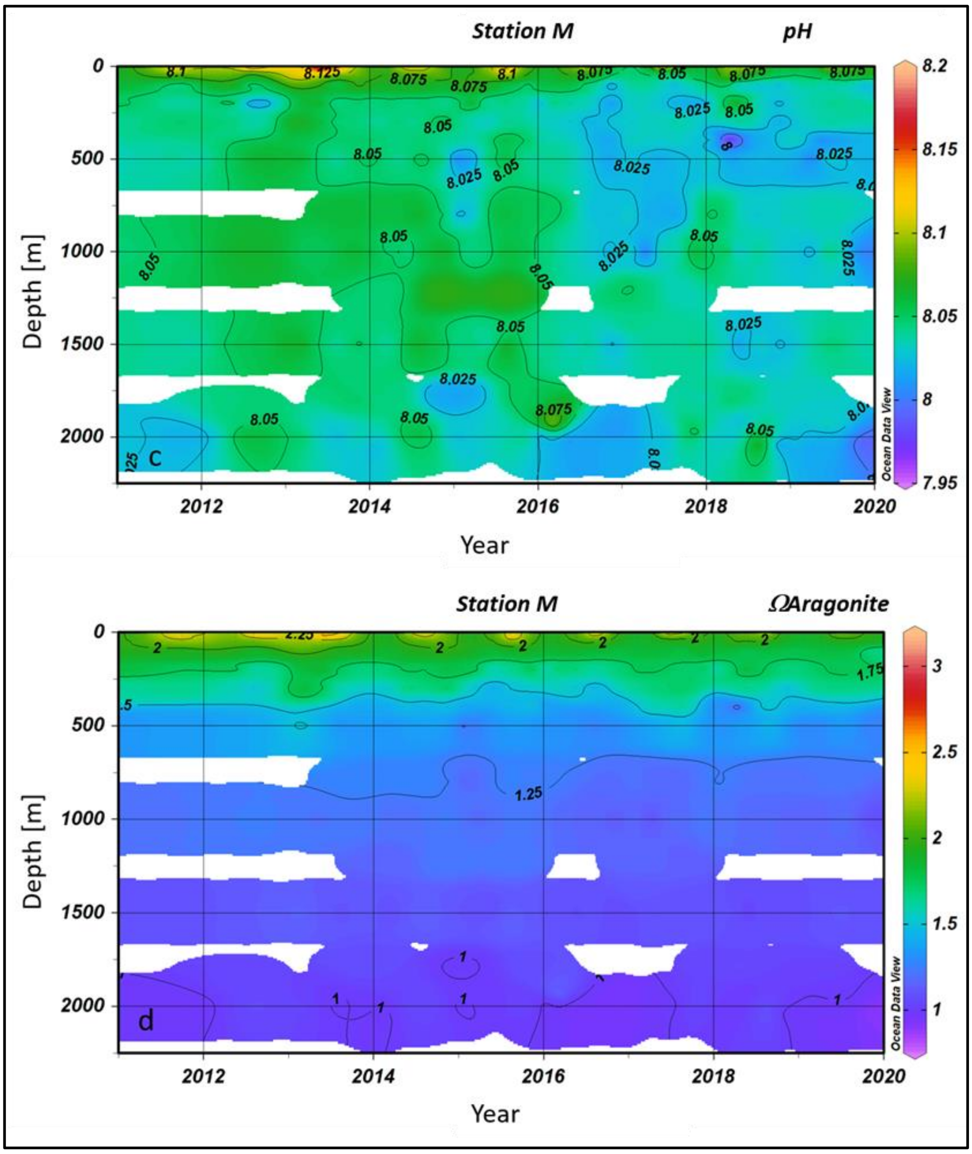

***Figure 27**. a) C_T, b) A_T, c) pH, and d) Ω aragonite at Station M in during the years 2011 to 2019.*

***Figur 27**. a) C_T, b) A_T, c) pH og d) Ω aragonitt fra Stasjon M i årene 2011 til 2019.*

Over the years, the deep water masses have warmed (***Figure 70c-d, Appendix 6.1***), while pH and Ω aragonite have decreased (***Figure 27a-d***), and the saturation horizon (Ω aragonite = 1) has fluctuated around 2000 m depth over the last 9 years. In fact, the C_T over the full water depth has increased since 2011 (***Figure 27b***). The C_T increase is connected to an increasing uptake of CO_2 from the atmosphere, and consequently, an increasing pCO_2 of the surface water over the years. This is shown in ***Figure 20a***, where the winter values of pCO_2 have increased by nearly 20 µatm over the last 9 years. This is similar to the atmospheric growth rate of approximately 2 µatm per year.

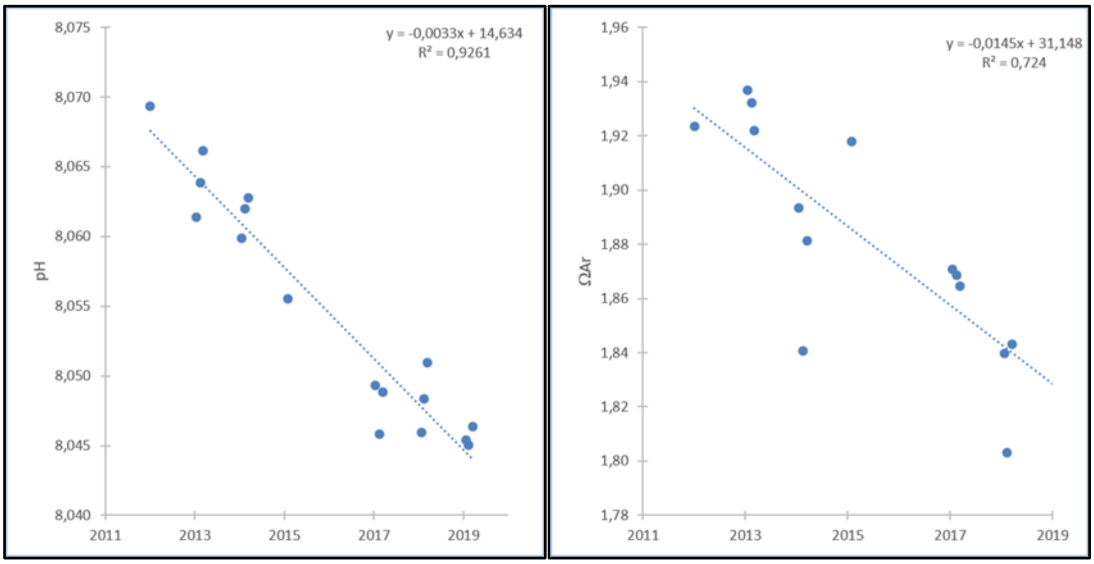

***Figure 28**. Winter surface water trends of pH (left) and Ω aragonite (right) at Station M during the years 2011-2019. The values are monthly averages calculated from continuous measurements at the station. Winter is defined as January to March.*

***Figur 28**. Vintertrend i overflate pH (til venstre) og Ω aragonitt (til høyre) fra Stasjon M i årene 2011 til 2019. Punktene viser månedsmiddel beregnet fra kontinuerlige målinger fra stasjonen, og vinter er definert som januar til mars.*

Based on the continuous winter data (January to March) from Station M, the surface trends over the years 2011 to 2019 have been examined (***Figure 28***). Monthly pH and Ω aragonite are decreasing significantly over these 9 years: 0.0033 yr^{-1} and 0.015 yr^{-1}, respectively. These trends are comparable to the negative trends estimated for the Norwegian Basin by Skjelvan et al. (2014) of -0.0041 and -0.012 for pH and Ω aragonite, respectively. Furthermore, the pH trends are stronger than those of Bates et al. (2014), who presented surface trends from the Iceland Sea and Irminger Sea, amongst others.

Further analysis of temporal changes in the Norwegian Sea can be identified from the hydrographic station located at ~1.3 °E along the Svinøy-NW section. The temperature, C_T, A_T and Ω aragonite at 1000, 1500, 2000 and 2400 m show temporal trends and interannual variability related to the variations in water masses at this location (***Figure 29***).

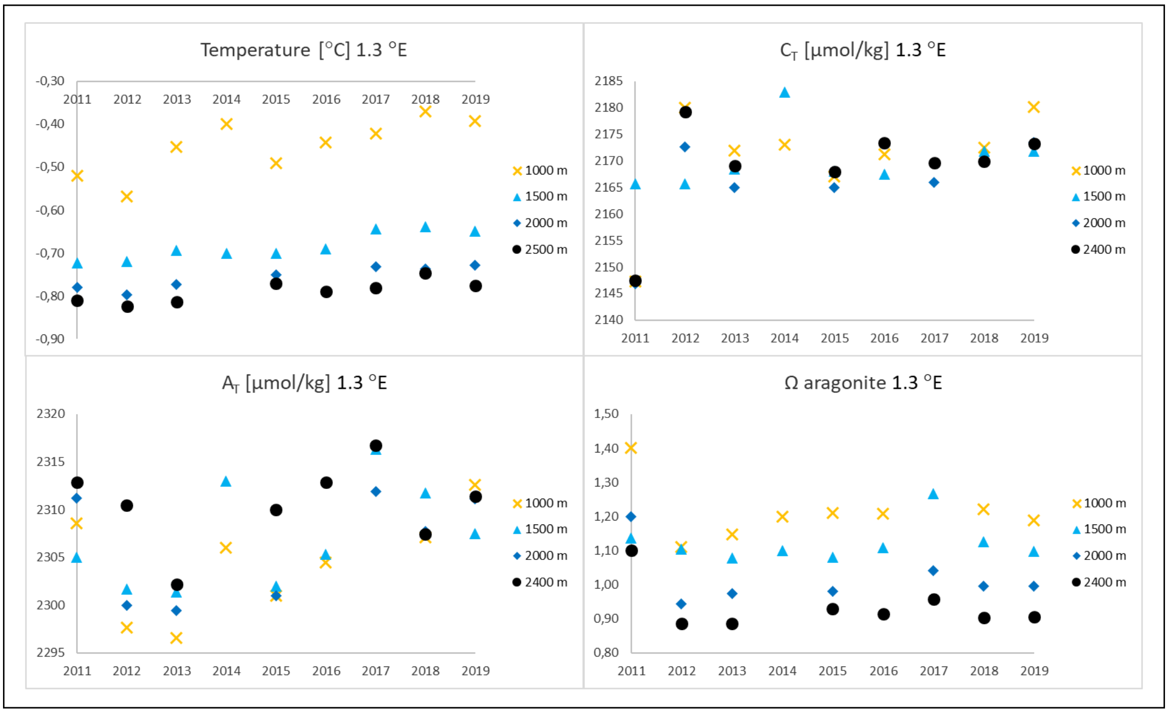

Figure 29*. Trend analysis based on the years 2011 to 2019 in temperature and Ω aragonite at 1000, 1500, 2000, 2500 m depth from the 1.3°E station along the Svinøy-NW section.*

Figur 29*. Trendanalyse basert på årene 2011 til 2019 av temperatur og Ω aragonitt ved 1000, 1500, 2000 2500 m dyp på stasjonen 1.3 °E langs Svinøy-NV snittet.*

The temperature at 1000 m is higher and more variable compared to those from deeper waters, likely due to mixing between Norwegian Sea Deep Water and Arctic water. C_T and A_T had relatively little variation at 2169 ± 9 µmol kg^{-1} and 2307 ± 6 µmol kg^{-1} across the 1000-2400 m depth range in all years. This was accompanied by variable Ω aragonite of 1.07 ± 0.13, especially at 1000 and 1500 m. The depth of the saturation horizon for aragonite varied between 1550 m and 2000 m depth during the time series, following observations at Station M further north in the Norwegian Sea.

Along the Gimsøy-NW section in the northern the Norwegian Sea, interannual variability can be identified at 1500 m depth at ~12.3 °E (***Figure 30***). The temperature and salinity showed increasing trends between 2011 and 2019, likely due to variability in mixing between the cold Arctic water with the overlying warm and salty Atlantic water. Analogous to the Svinøy data, C_T showed some variability and no distinct trend, although higher in 2019, with concentrations of 2169 ± 7 µmol kg^{-1} as an indication of Atlantic water. This was accompanied by variable pH with an average value of 8.053 ± 0.032 during the whole time series.

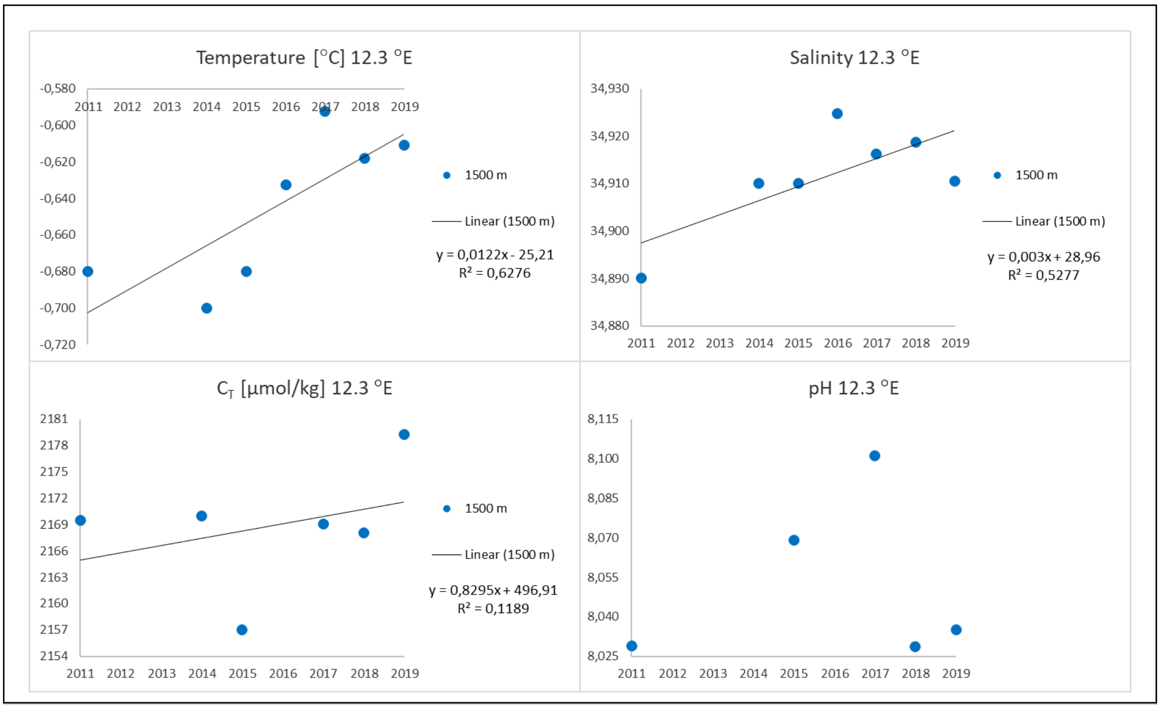

***Figure 30**. Yearly trend analysis in temperature, salinity, C_T and pH at 1500 m depth at station 12.3 °E along the Gimsøy-NW section*

***Figur 30**. Årlig trendanalyse av temperatur, saltholdighet, C_T og pH ved 1500 m dyp på stasjonen 12.3 °E langs Gimsøy-NV snittet.*

At the coastal station Skrova, the large seasonal variation in the surface water is driven by biological processes in spring as phytoplankton production consumes CO_2 and consequently increases seawater pH (***Figure 31***). In the autumn, mixing with subsurface carbon-rich water and degradation of organic material releases CO_2 and pH decreases to reach minimum pH and Ω aragonite in the winter. It is not yet possible to determine a yearly trend in the data, however, the seasonal amplitude (winter-summer) is greater compared to any slight long-term trend, which for surface waters of the global ocean is estimated at -0.002 pH units yr^{-1} (Takahashi et al. 2014) and shown to be -0.0033 pH units yr^{-1} at Station M in the Norwegian Sea (***Figure 28***).

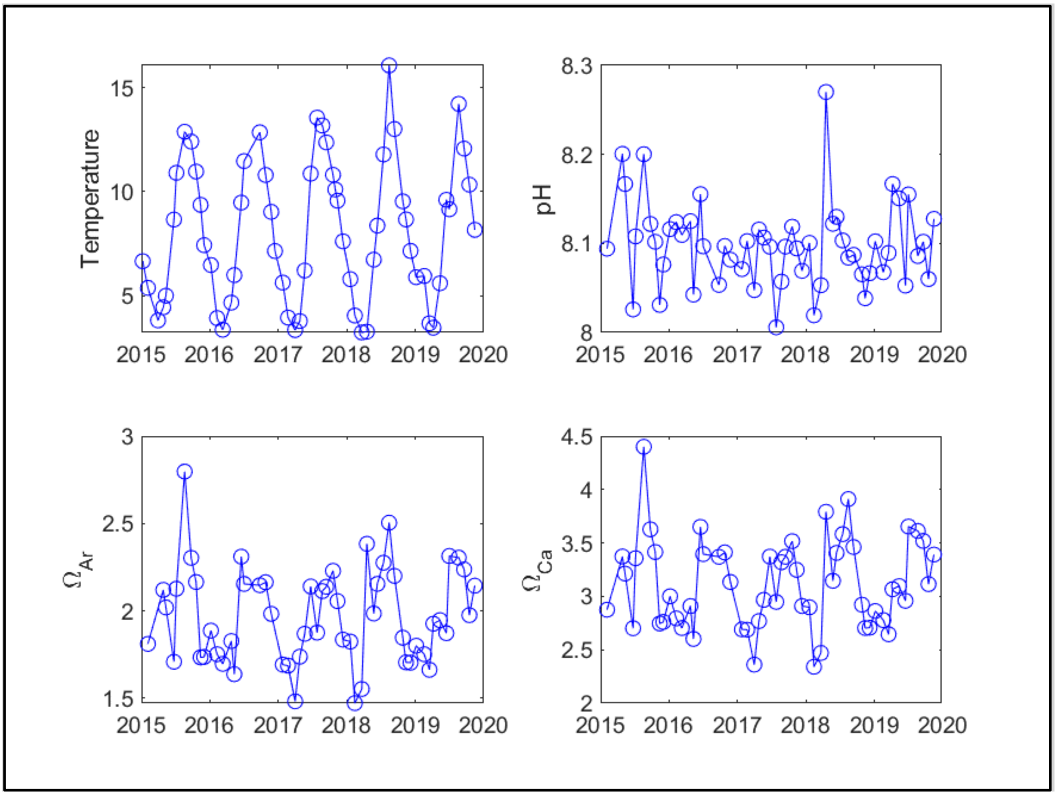

Figure 31. *Seasonal variation in temperature, pH and Ω aragonite and Ω calcite in surface water at Skrova.*

Figur 31. *Årsvariasjon i temperatur, pH og Ω aragonitt og Ω kalsitt i overflaten ved Skrova.*

3.3 Barents Sea

3.3.1 Spatial variability along the Fugløya-Bjørnøya section

In January 2019, carbonate chemistry measurements were carried out by IMR in the whole water column at five fixed stations along the hydrographic section between Fugløya and Bjørnøya in the south western Barents Sea (***Figure 32***). Position, depth and sampling data are displayed in ***Table 7, Appendix 6.2***.

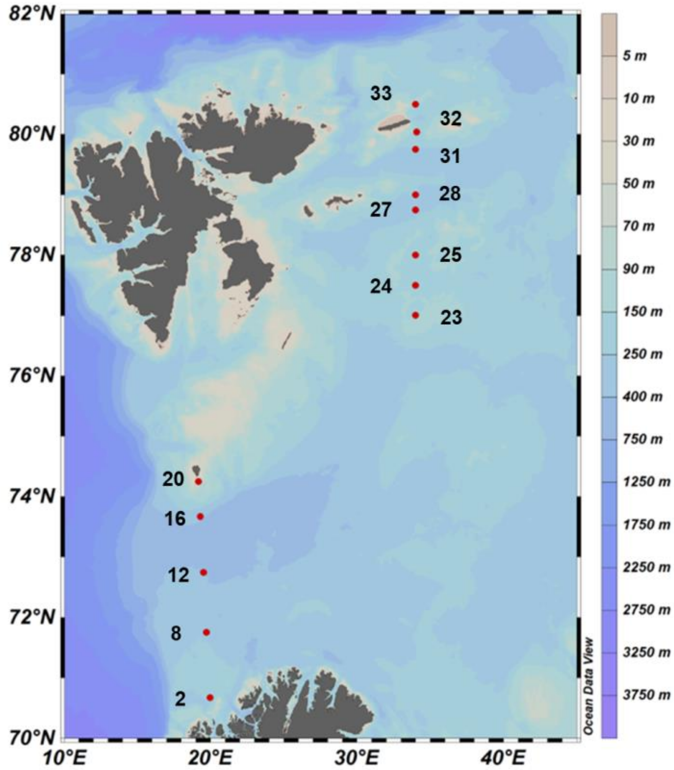

***Figure 32**. Map and station numbers from stations along the Fugløya-Bjørnøya section in January 2019 and in the northern Barents Sea in September 2019.*

***Figur 32**. Kart og nummer over stasjoner langs Fugløya-Bjørnøya snittet i januar 2019 og i nordøstlige Barentshavet i september 2019.*

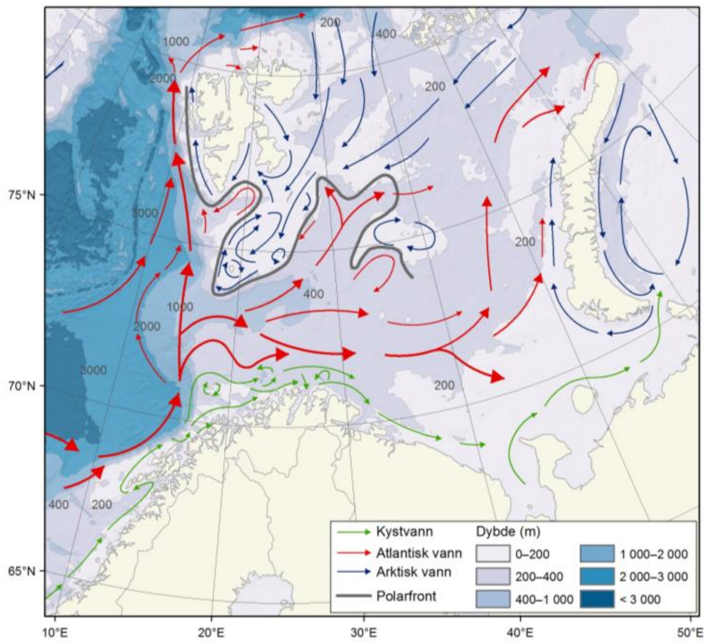

***Figure 33**. Map showing major currents in the Barents Sea. Red arrows show Atlantic water, green coastal current and blue arrows show the Arctic water. Grey line shows the position of the polar front. Map from www.imr.no.*

***Figur 33**. Kart som viser hovedstrømmene i Barentshavet. Røde piler viser atlantisk vann, grønne piler er kyststrømmen og blå piler viser arktisk vann. Grå linje viser omtrentlig posisjon til polarfronten. Kart fra www.imr.no.*

The Barents Sea is a relatively shallow marine basin with maximum depths around 400 m. The Fugløya-Bjørnøya section extends from the Norwegian coastal current in the south and passes through the area of the Atlantic water inflow into the Barents Sea (***Figure 33***). The entire water column from the coast to approximately 72 °N is influenced by the Norwegian coastal water of relatively low salinity (< 34.8) and temperatures in the range of 5-7 °C (***Figure 75, Appendix 6.1***). The central part of the section is deepest (around 500 m depth) at 73.5 °N in the Barents Sea. In 2019, Atlantic water with salinity > 35.1 and temperature 5-6 °C occupied nearly the whole water column between 71.5 and 73.5 °N. At the northern end of the section, strong horizontal gradients in salinity and temperatures characterised the transition to colder and fresher Arctic waters.

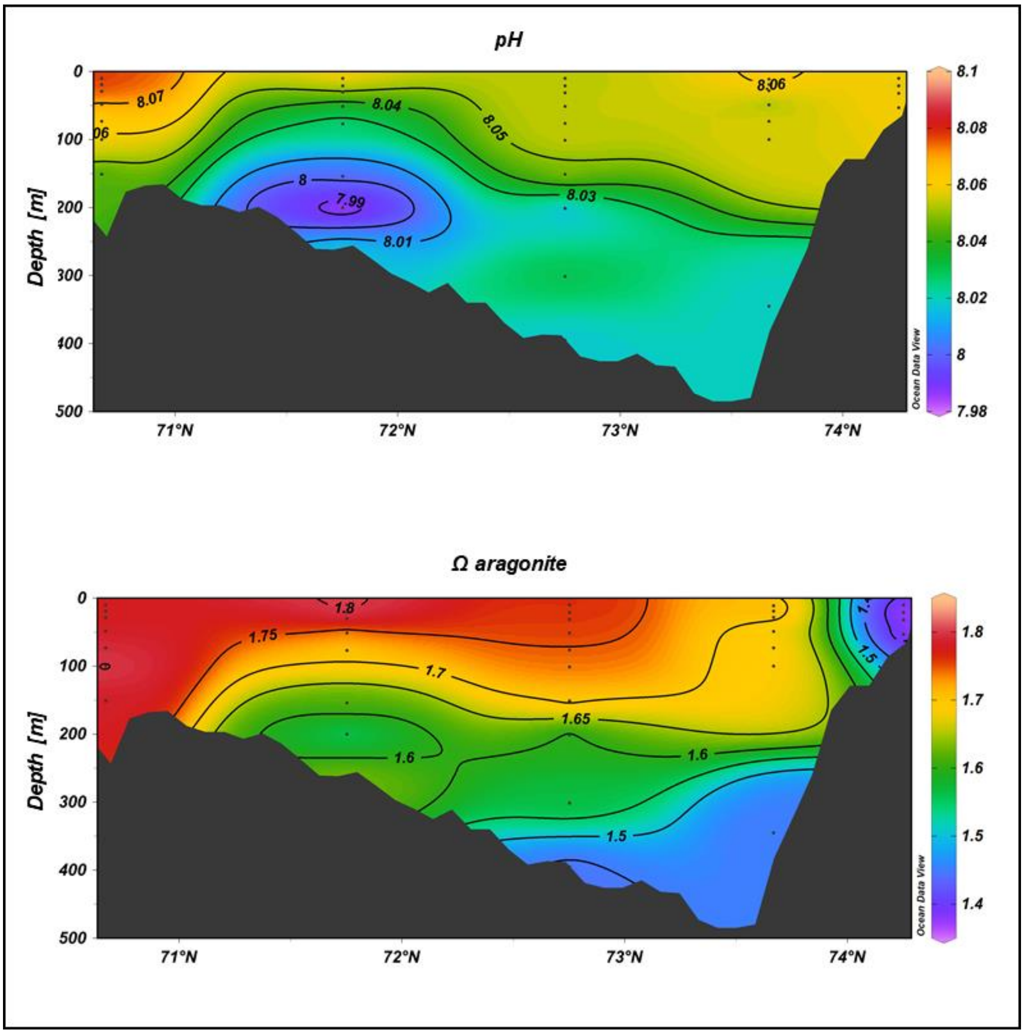

Figure 34. pH and Ω aragonite along the Fugløya-Bjørnøya section in January 2019.

Figur 34. pH og Ω aragonitt langs Fugløya-Bjørnøya snittet i januar 2019.

The inflow of Arctic water travelling southwards from north east Svalbard creates strong horizontal gradients with the Atlantic Water at the Polar Front close to Bjørnøya at around 74 °N. The Arctic water at the northern extent of the section was distinguished by lower salinity (< 34.7) and lower temperatures (< 1 °C). The distribution of A_T reflects the variations in salinity with lowest values in the coastal water and Arctic water and higher values in Atlantic water.

The Atlantic water has higher A_T of 2280-2295 µmol kg^{-1}, relative to lowest A_T around 2244 µmol kg^{-1} and 2254 µmol kg^{-1} in the coastal water and Arctic water, respectively. The concentration of C_T was lowest (~2115 µmol kg^{-1}) in the coastal waters at the southern end of the section and increased to 2160-2180 µmol kg^{-1} in the Atlantic water in the central part of the section. Highest pH of 8.08 and high Ω aragonite of 1.75-1.80 reflect the biological carbon uptake that occurred in the coastal waters at the southern part of the section. Lowest pH of 7.98 was found in the bottom water at 200 m depth at 71.75 °N (***Figure 34***). The lowest Ω aragonite of 1.34-1.36 occurred in the cold and fresh Arctic water.

3.3.2 Spatial variability along the northern Barents Sea section

In September 2019, carbon chemistry measurements were carried out by IMR on water samples collected throughout the water column at eight fixed stations in the northern Barents Sea (***Figure 32***). This dynamic region is influenced by Atlantic water from Fram Strait in the south and Arctic water from the north, as well impacted by seasonal sea ice processes. Position, depth and sampling data are displayed in ***Table 8***, ***Appendix 6.2***.

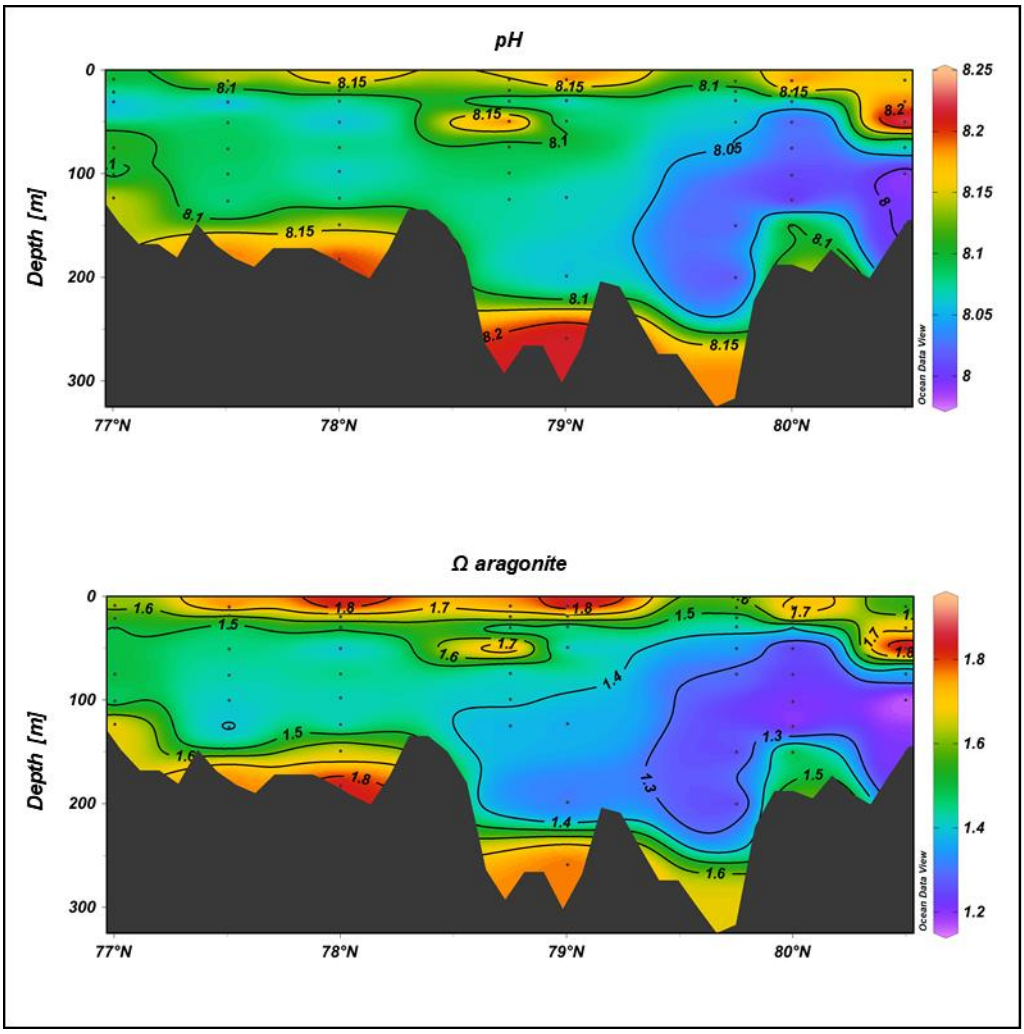

Figure 35. *pH and Ω aragonite along the northern Barents Sea section in September 2019.*

Figur 35. *pH og Ω aragonitt fra nordlige Barentshavet i september 2019.*

Salinity in the upper 50 m decreased northwards along the section to lowest values (< 33.75) in the fresh Arctic water north of 79.5 ºN (***Figure 76, Appendix 6.1***). Temperatures in the upper layer were warmest at 1.5-1.8 °C in the Atlantic water influenced southern part of the section. Between 50 and 100 m, the cold (< 0 °C) Arctic water spread across most of the section, with incursions of Atlantic water warming the water column at 78 ºN. The whole region is affected by seasonal ice cover and recent ice melt.

In the surface water, C_T and A_T are low and decrease northwards to lowest values north of ~2073 µmol kg^{-1} and ~2222 µmol kg^{-1}, respectively, at 80ºN. This characterises the fresh polar water in the upper 50 m with influence of recent inputs of sea ice meltwater and strong biological carbon uptake. Surface layer pH was highest at 8.23 and Ω aragonite was high at 1.88 in the Arctic water in the north (***Figure 35***). The highest Ω aragonite of 1.91 was found in the central part of the section, as biological production had reduced C_T and impacts of A_T dilution from sea ice meltwater were reduced. The highest A_T around 2304 µmol kg^{-1} was found in bottom water overlying the seafloor at several locations, accompanied by highest C_T of 2216 µmol kg^{-1} in the Atlantic water in the southern part of the section. Lowest pH and lowest Ω aragonite of 7.99 and 1.15-1.21, respectively, was found below 100 m depth in the cold and fresher waters in the north. This is probably due to increased CO_2 resulting from microbial degradation of organic matter and the release of high CO_2 brines from sea ice and not from anthropogenic ocean acidification.

3.3.3 Seasonal variability in surface water

The stations covered by MS *Norbjørn* between Tromsø and Longyearbyen are shown in ***Figure 36***. Position and sampling data are displayed in ***Table 9, Appendix 6.2***. Surface water from 4 m depth was sampled on four cruises in March, June, August and November 2019. The ship's route varies depending on weather and ice conditions as well as different port calls for cargo deliveries between cruises.

The Barents Sea opening is influenced by Atlantic water, Norwegian coastal water and Arctic water. Atlantic Water is the dominant water mass in the open sea between Tromsø and Svalbard, but it is heavily mixed with meltwater from sea ice and coastal water from Norway and Svalbard during the summer. Along the coast of Svalbard, the Atlantic water mixes with Arctic water and meltwater from glaciers and rivers during summer. The Norwegian Coastal Current flows along the coast of Norway, and this is mixed with Atlantic water towards the north into the Barents Sea. For calculating the seasonal averages of the different variabless, the transect between the coast of Norway to Isfjord in Svalbard was divided into sections of 69-72 ˚N (Norwegian coast), 72-74 ˚N (Open Sea South of Bjørnøya), 75-76 ˚N (Open Sea North of Bjørnøya) and 76-78 ˚N (Svalbard Coast).

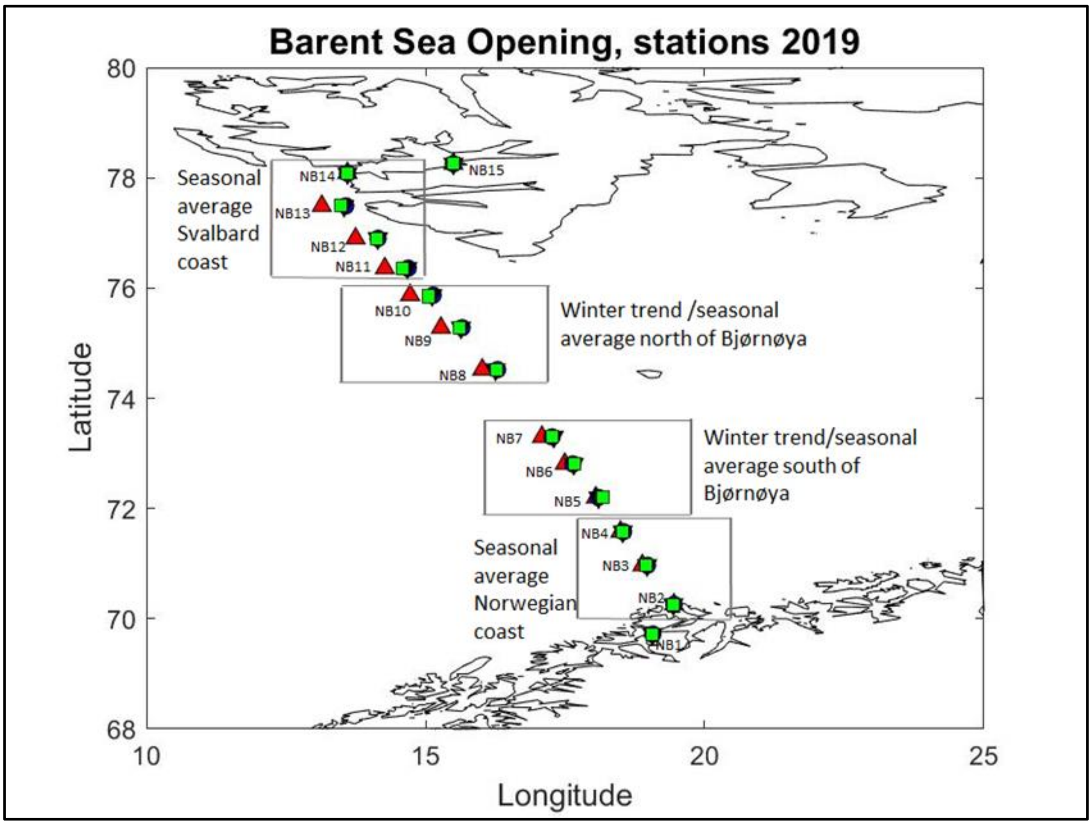

Figure 36*. Station map for the Barents Sea opening in 2019. Samples were taken during 12-14 March (red ▲), 7-9 June (blue ●), 30 August-1 September- (black ▼) and 22-24 November (green ■). The stations locations varied because of weather or ice conditions.*

Figur 36*. Stasjoner langs Barentshavsåpningen i 2019. Toktene ble gjort 12-14 februar (rød ▲), 7-9 juni (blå ●), 30 august-1 september (sort ▼) og 22-24 november (grønn ■). Stasjonene er noe væravhengig som man kan se av spredningen i lengdegrader.*

Temperature and salinity since 2010 are shown in ***Figure 37***. As seen in previous years there was increased freshwater input along the Svalbard coast in August, when the temperatures were highest (5.7°C on average), which is likely originated from glacial meltwater and river input. This reduced salinities along the coast of Svalbard to 33.23 on average, with the lowest salinity of 32.59 at 78.08 °N. The temperature along the coast of Svalbard in late November indicate mixing of cold polar water (minimum -1.55°C at 77.49 °N), likely coming from the South-East of Svalbard with the coastal current. The polar water affected the three northernmost coastal stations temperatures to an average of -1.16 °C.

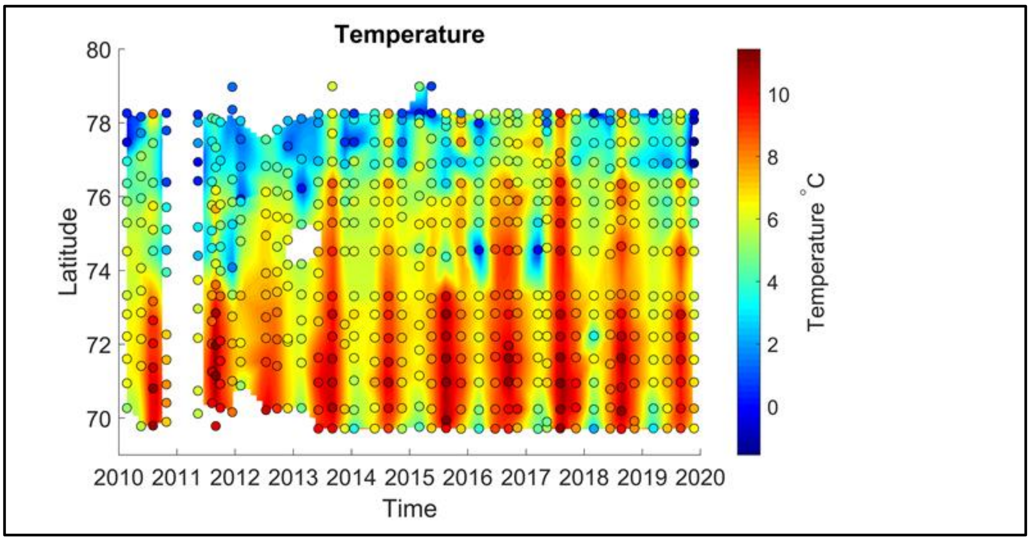

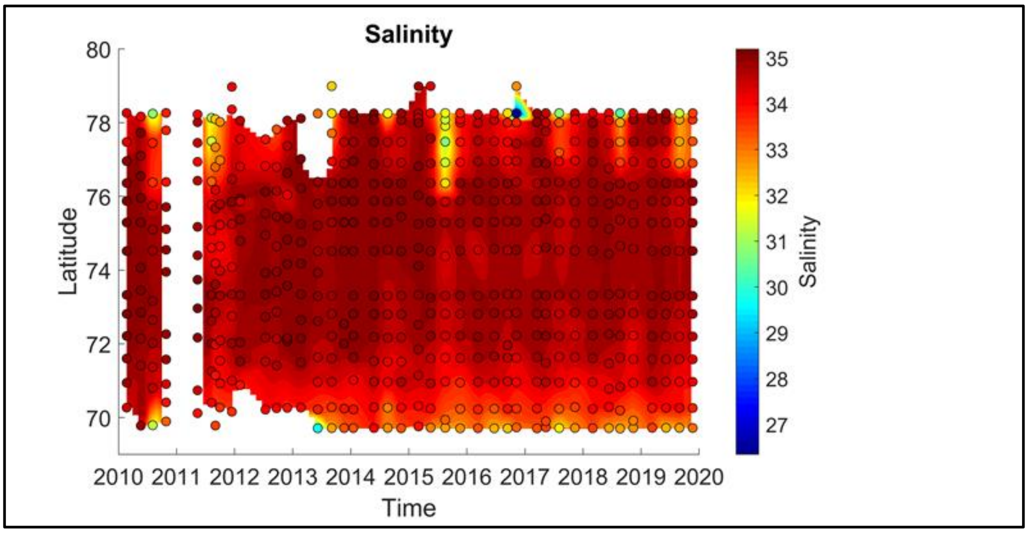

Figure 37*. Ten years of temperature and salinity measurements from the Barents Sea entrance as part of the Tilførselprogrammet and the Ocean Acidification monitoring program. The circles show the measured values, while the interpolated values are shown in the background.*

Figur 37*. Ti års målinger i Barentshavsåpningen av temperatur og saltholdighet målt under Tilførselsprogrammet og Havforsuringsovervåkningen. Ringene viser målte verdier, mens interpolerte verdier vises i bakgrunnen.*

Near the Norwegian coast, salinities were highest in March during periods of cold winter temperatures (4.08 °C at 70.26 °N) and low freshwater inputs, with salinities as high as 34.8 as far south as 70.96 °N. The freshwater inputs increased during summer and autumn, causing lower salinities that extended further north and heavily influenced the salinities in open water. The open waters had less variation in temperature and salinity, with temperature minimum of 4.09 °C in November at 75.87 °N and 10.24 °C at the highest in August at 72.81°N. The salinities for open water during winter were consistent with the North Atlantic water type >35, which during summer and autumn were more mixed with fresh water inputs, down to a minimum 34.5 in August.

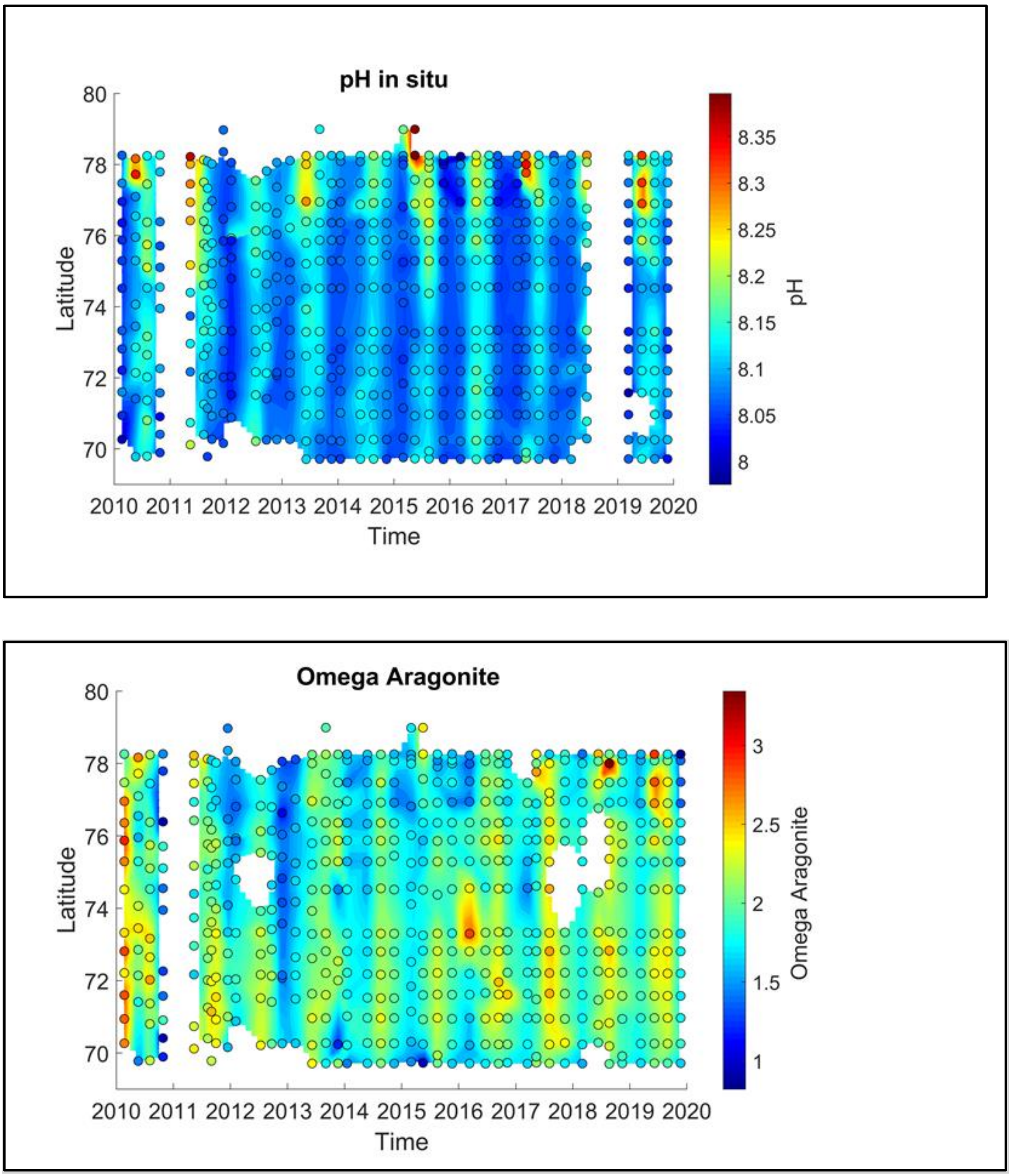

***Figure 38**. Ten years of measurements in the Barents Sea Opening of in situ pH_T and Ω aragonite. The circles show the measured and calculated values, while the interpolated values are shown in the background.*

***Figur 38**. Ti års målinger i Barentshavsåpningen av In situ pH_T og Ω aragonitt. Ringene viser målte og beregnede verdier, mens interpolerte verdier vises i bakgrunnen.*

The pH and Ω aragonite since 2010 are shown in ***Figure 38***. The pH and Ω aragonite were relatively high along the coast of Svalbard in June (maximum of 8.32 at 77.49 °N), indicating an ongoing phytoplankton bloom utilizing CO_2 and thereby increasing the pH. The pH was also relatively higher during summer both north and south of the station at about 74.5 °N. This is approximately the location of the Bjørnøya and the Bjørnøya current, and it seem to divide the blooms north and south of Bjørnøya. This could also show the northern extent of the influence of the Norwegian coastal current and the southern extent of the influence of the Svalbard coastal water during the summer. pH and Ω aragonite were lower during winter, with the lowest pH at 7.99 at 71.58 °N near the Norwegian coast in March and the lowest Ω aragonite at 1.37 at 76.90 °N near the Svalbard coast in November, during the event with polar water along the coast of Svalbard. On average the water affected by the polar water in November had a pH of 8.09 and Ω aragonite of 1.38.

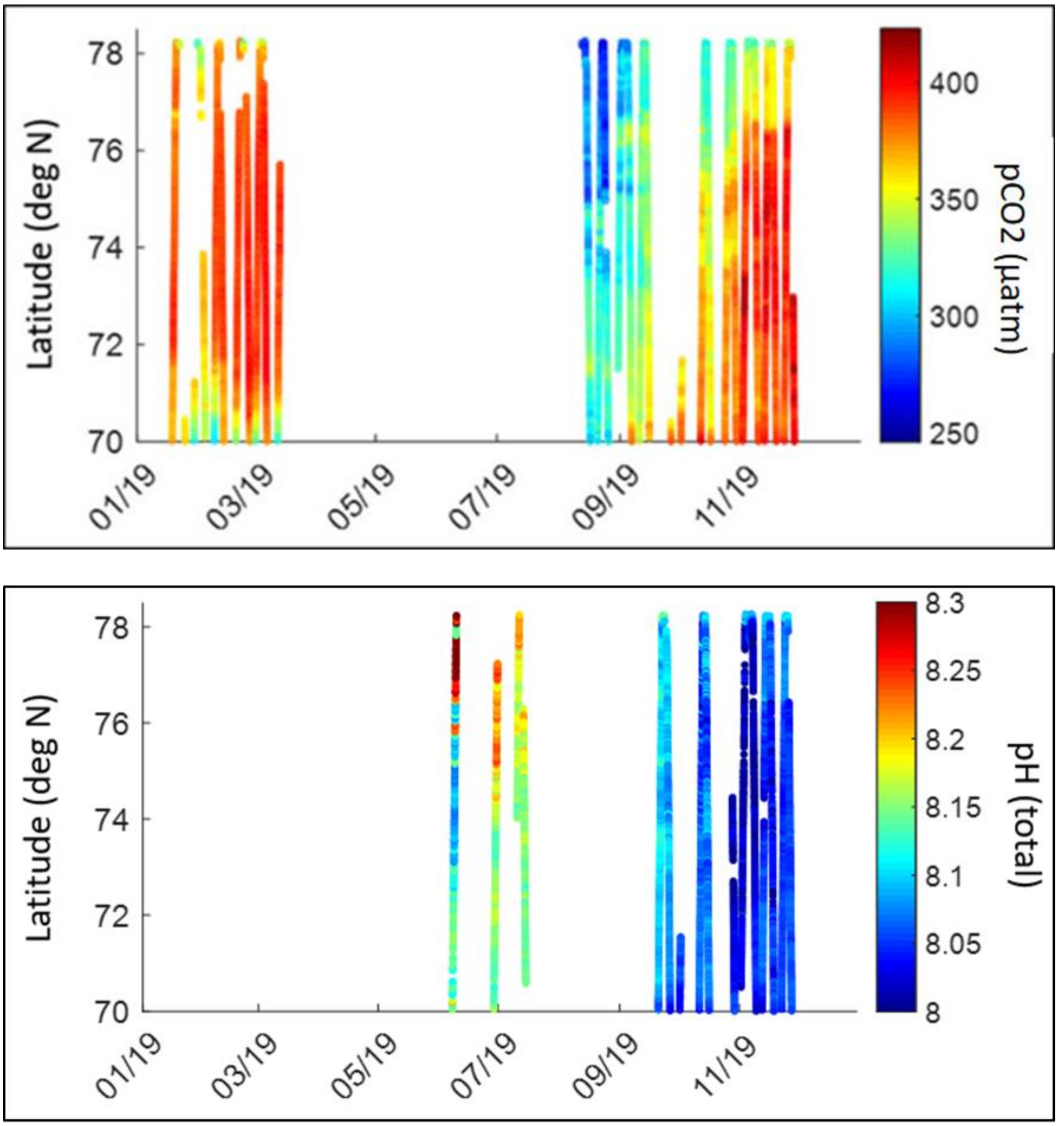

***Figure 39**. pCO₂ (µatm) and pH (total scale) measured with underway sensors on MS Norbjørn in 2019.*

***Figur 39**. pCO₂ og pH målt med underveissensorer på Norbjørn i 2019.*

Underway observations of pCO_2 (µatm) and pH (total scale) between Tromsø and Longyearbyen are presented in ***Figure 39***. pCO_2 observations were available from January to February and mid-August to November 2019, while pH observations were available for a few transects in June/July and from mid-September to November 2019. Observations from early in the year show that pCO_2 was relatively high (up to ~405 µatm) in the central part of the transect in the Atlantic water mass, and relatively lower in the Norwegian coastal and Arctic water masses (as low as ~330 µatm). The relatively few summer sensor data show that pH was relatively high near Svalbard (up to ~8.3) and lower in the central and southern part of the transect. The lowest pCO_2 observations were made in the summer period with observations of <~300 µatm near Svalbard and <~350 µatm in the central and southern part of the transect. By autumn/winter, pCO_2 began to increase to >~350 µatm and pH began to decline to ~8.0-8.1 across the study region.

The observed regional variability agrees well with the seasonal cycle in discretely-measured pH shown in ***Figure 38***. In the early and late part of the year, pCO_2/pH appears to be strongly connected to salinity-temperature-water mass influences. The summertime (June-August) observations of high pH and low pCO_2 near Svalbard are likely to also be linked to increased primary production and inorganic carbon uptake, and possibly reduced buffering capacity of the carbonate system due to the influence of freshwater input.

3.3.4 Trend analysis at selected stations

3.3.4.1 Trend by linear regression

Shown in ***Figure 40-Figure* 41** below are the trend analyses using linear regression on average yearly surface winter data from the sections 72-74 °N and 74-76 °N, with Atlantic or near Atlantic water (S > 35 and T > 4 °C) from the Barents Sea opening. There was not enough data to do trend analysis of polar water (T< 0°C) from this transect. Although the dataset was limited to winter data only and sectioned by latitudes, the trends are uncertain.

The seawater salinity and temperature in surface waters of the Barents Sea opening at 72 to 74 °N showed a freshening of 0.016 yr^{-1} and cooling of 0.068 °C yr^{-1}. Changes in pH and Ω aragonite were variable and any trends over time were weak, thus the trend lines were not included. The measurements must be continued to extend the time series for a more robust trend analysis to be made.

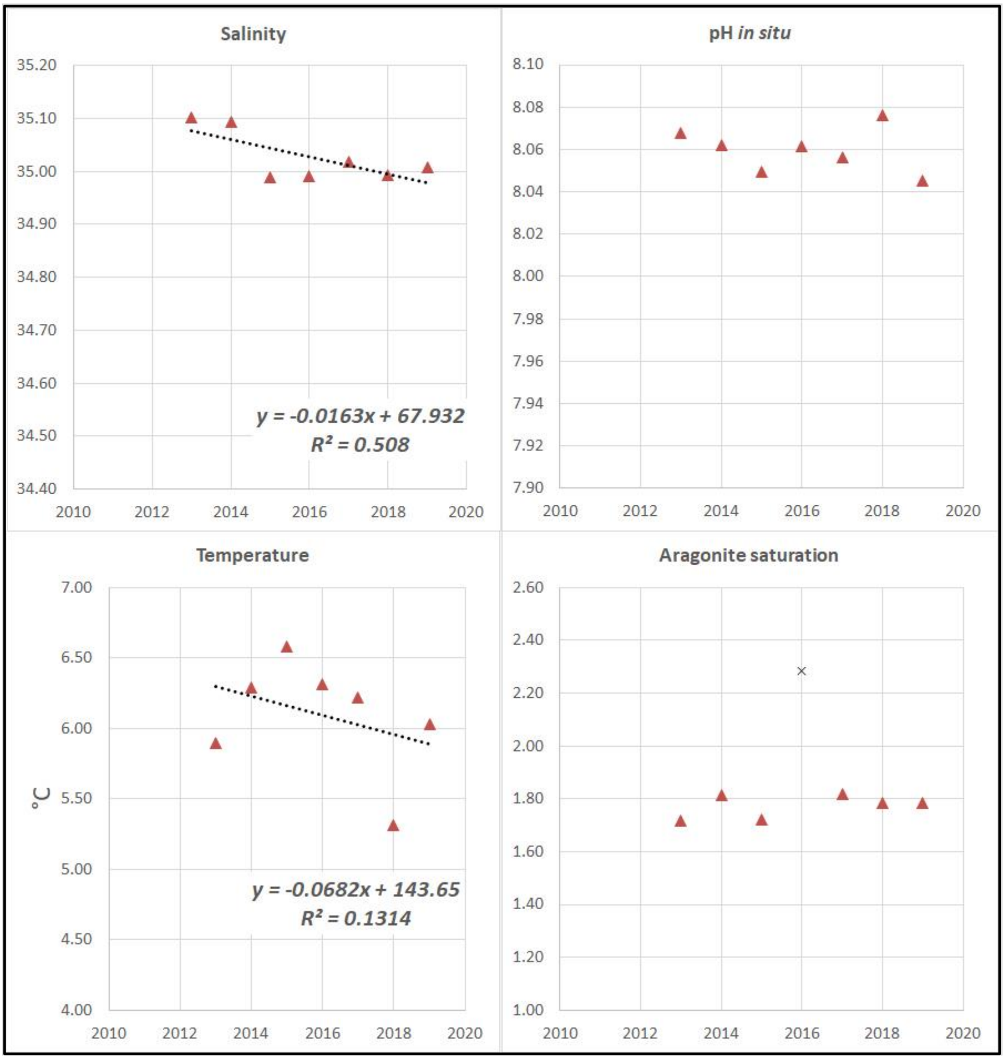

***Figure 40**. Linear regression trends in temperature, salinity, pH and Ω aragonite of winter data in the surface (4 m) at 72-74 °N in the Barents Sea Opening.*

***Figur 40**. Lineær regresjon av temperatur, saltholdighet, pH og Ω aragonitt av midlede vinterdata fra overflata (4 m) fra 72-74°N i Barentshavsåpningen.*

The trend of seawater salinity and temperature in surface waters of the Barents Sea opening at 74-76 °N showed a freshening of 0.028 yr^{-1}, accompanied by a decrease in pH of 0.002 yr^{-1} (***Figure 41***). It is hard to detect any trend in temperature and Ω aragonite in this area, and measurements must be continued for further years to able a more robust trend analysis. We see a clearer trend of decreasing pH in the surface water in the 74-76° N section than further south (72-74° N), which may be due to the lower buffering capacity of the northern waters that are more influenced by fresher Arctic water.

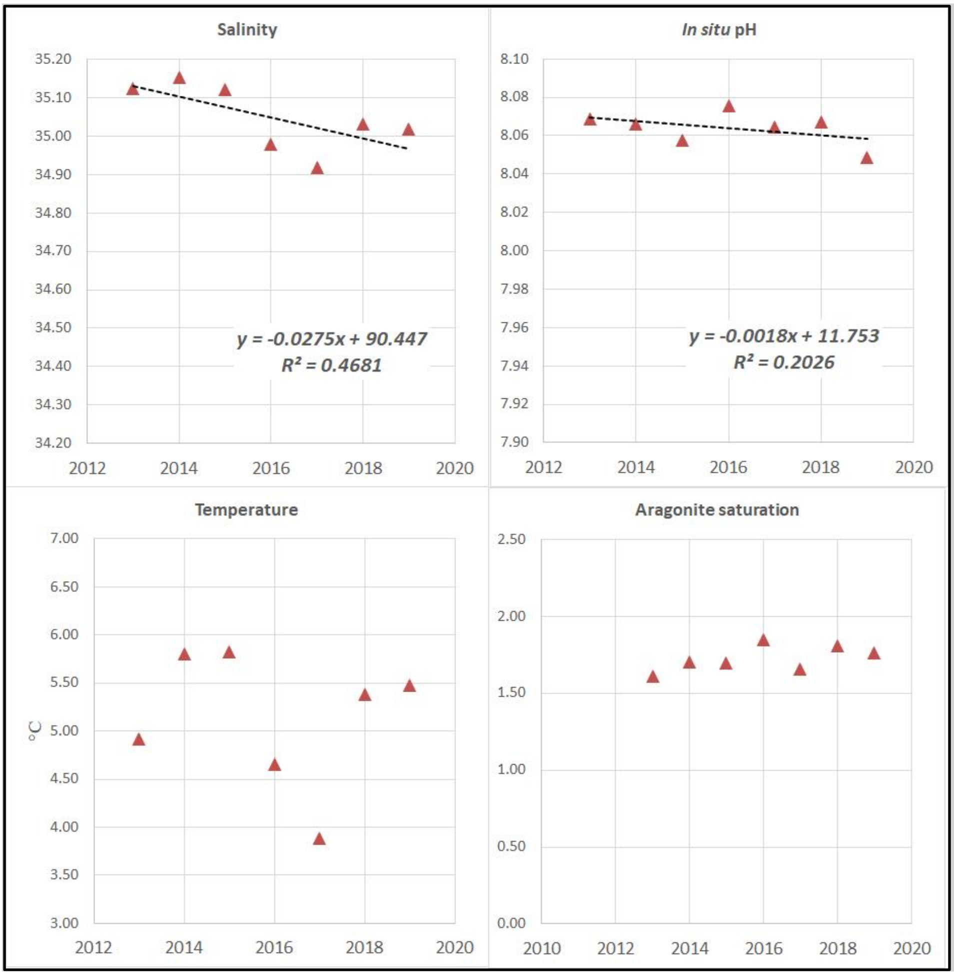

***Figure 41**. Linear regression trends in temperature, salinity, pH and Ω aragonite of winter data in the surface (4 m) at 74-76 °N in the Barents Sea opening.*

***Figur 41**. Lineær regresjon av temperatur, saltholdighet, pH og Ω aragonitt av midlede vinterdata fra overflata (4 m) fra 74-76°N i Barentshavsåpningen.*

Along the Fugløya-Bjørnøya section, the distribution of pH and Ω aragonite at 2 sampling depths at 300-400 m depth (deepest station) from 2012 to 2019 at ~72.8 °N showed variability associated with the variations in Atlantic water to the south and Arctic water to the north present at the time of sampling (***Figure 42***). Cooler waters were generally associated with higher C_T concentrations and indicated larger volumes of the colder, carbon-rich Arctic water in 2019. Salinity changes revealed the waters at 300-400 m tended to become fresher over time, which further supports the increase in low salinity Arctic water at this location. Since 2016, the cooling and freshening trend is more consistent and was accompanied by a reduction in the Ω aragonite to lowest values of 1.44-1.57 in 2019.

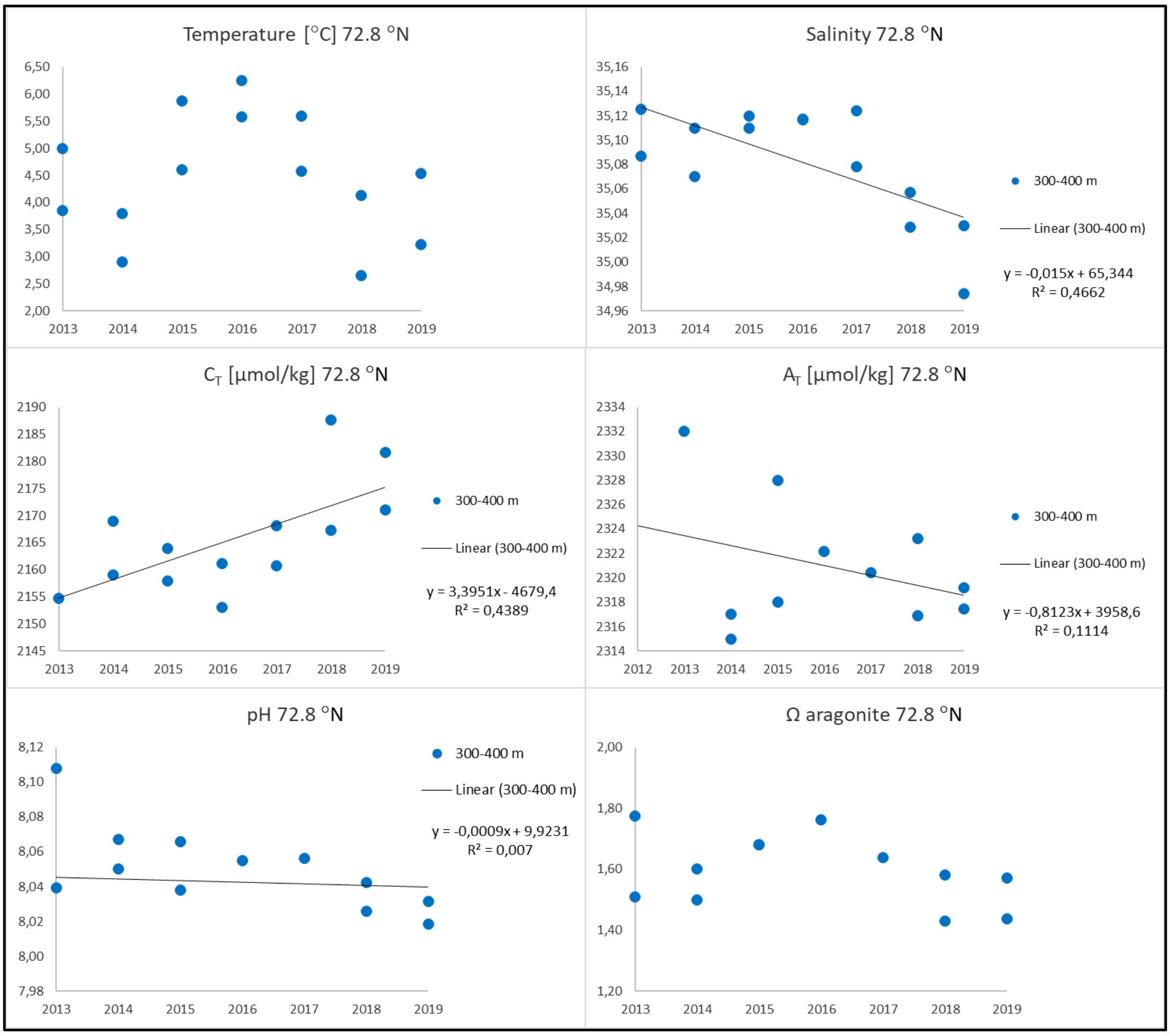

***Figure 42**. Trend analysis of temperature, salinity, C_T, A_T, pH and Ω aragonite at 300-400 m depth station 72.8 °N along the Fugløya-Blørnøya section.*

***Figur 42**. Trendanalyse av temperatur, saltholdighet, C_T, A_T, pH og Ω aragonitt ved 300-400 m dyp på stasjonen 72.8 °N langs Fugløya-Bjørnøya snittet.*

Along the northern Barents Sea section, the distribution of seawater temperature and salinity at 2 sampling depths in the 250-300 m depth range at 79.5-79.75 °N shows changes of -0.38 °C yr^{-1} and -0.018, respectively, from 2012 to 2019 (***Figure 43***). Alongside the general freshening and cooling trend, A_T decreased by 1.1 µmol kg^{-1} yr^{-1} and changes in C_T didn't reveal any distinct trend over time. pH exhibits an increase of 0.004 yr^{-1} and Ω aragonite varied from year to year throughout the time series and showed no observable trend with an average value of 1.31 ± 0.13. Similar to the trends along the Fugløya-Bjørnøya section, increased Arctic water with lower A_T induces a lot of variability in pH and Ω aragonite in the region.

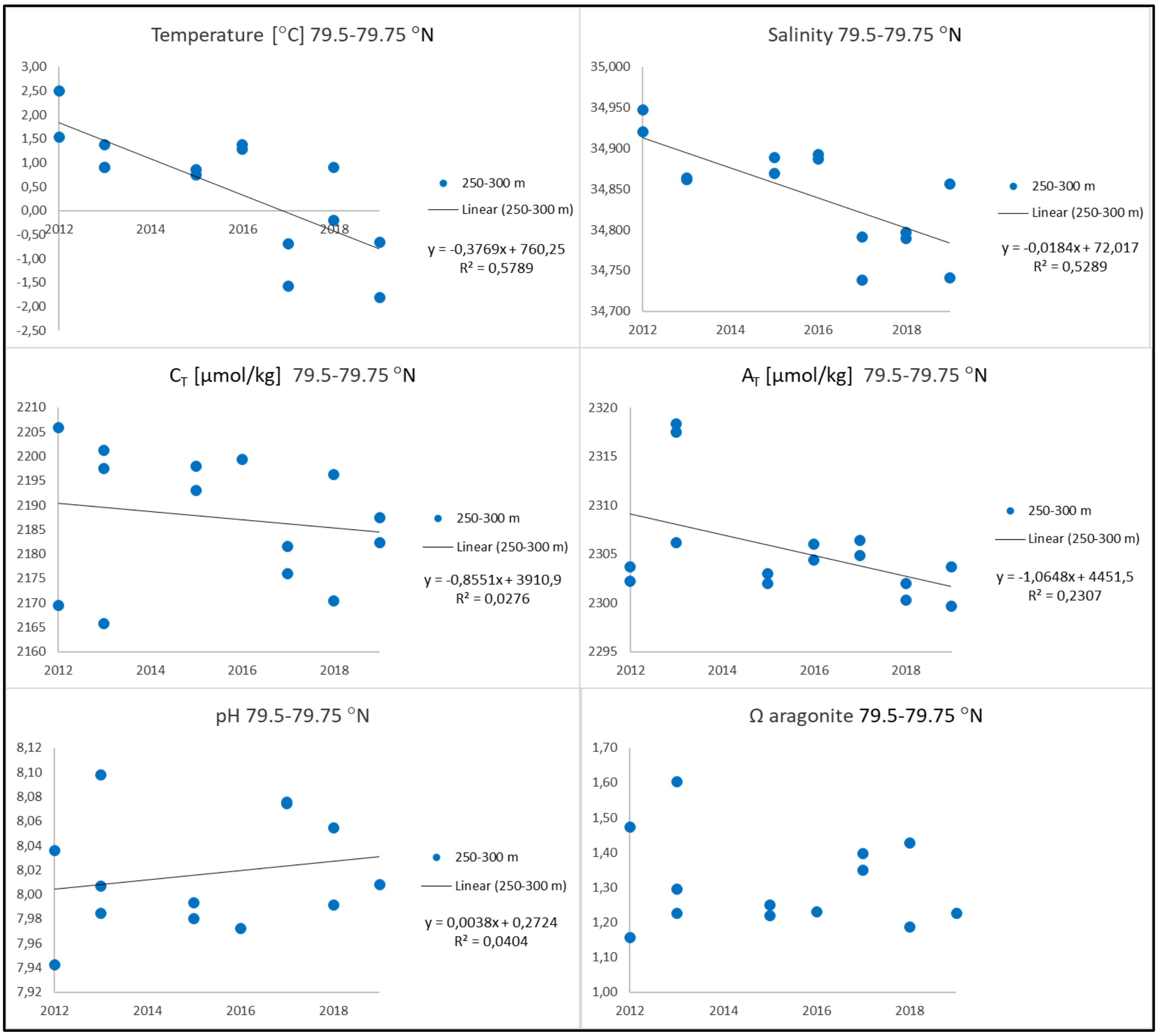

Figure 43*. Trend analysis of temperature, salinity, C_T, A_T, pH and Ω aragonite at 250-300 m depth from the stations 79.5-79.75 °N along the section in the northern Barents Sea.*

Figur 43*. Trendanalyse av temperatur, saltholdighet, C_T, A_T, pH og Ω aragonitt på 250-300 m dyp på stasjonen 79.5-79.75 °N langs snittet i nordlige Barentshavet.*

3.4 Norwegian Coast

3.4.1. Underway data from Bergen - Kirkenes

The FerryBox line between Bergen and Kirkenes on MS *Trollfjord* was equipped with salinity, temperature, chlorophyll *a* fluorescence, and a membrane equilibrator-based pCO_2 sensor (

). Salinity and temperature exhibited a seasonal cycle in which summertime was low in salinity and warm, as well as a large dynamic range in salinity and temperature. The coastal regions near Kirkenes were low in salinity year-round, due to riverine inputs, and coastal regions just south of Tromsø (Malangen), Trondheimsfjord, and southern Norway were low in salinity during spring, summer, and early autumn. Surface temperatures were low during winter and began to warm in May/June. Phytoplankton chlorophyll *a* was elevated in April (spring bloom) in southern/mid-coastal Norway, and in northern Norway spring bloom occurred in May-July.

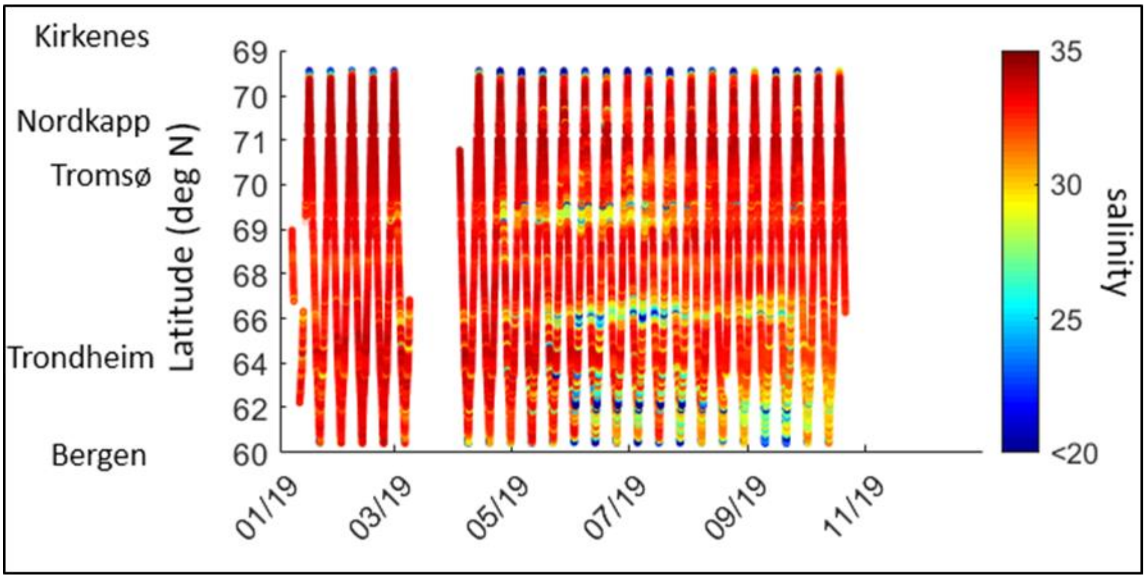

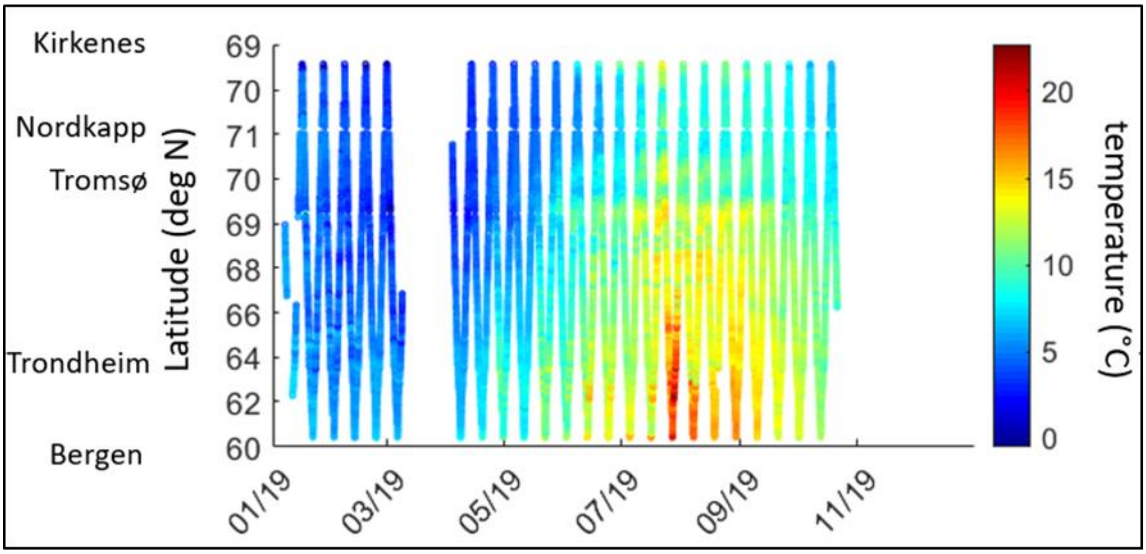

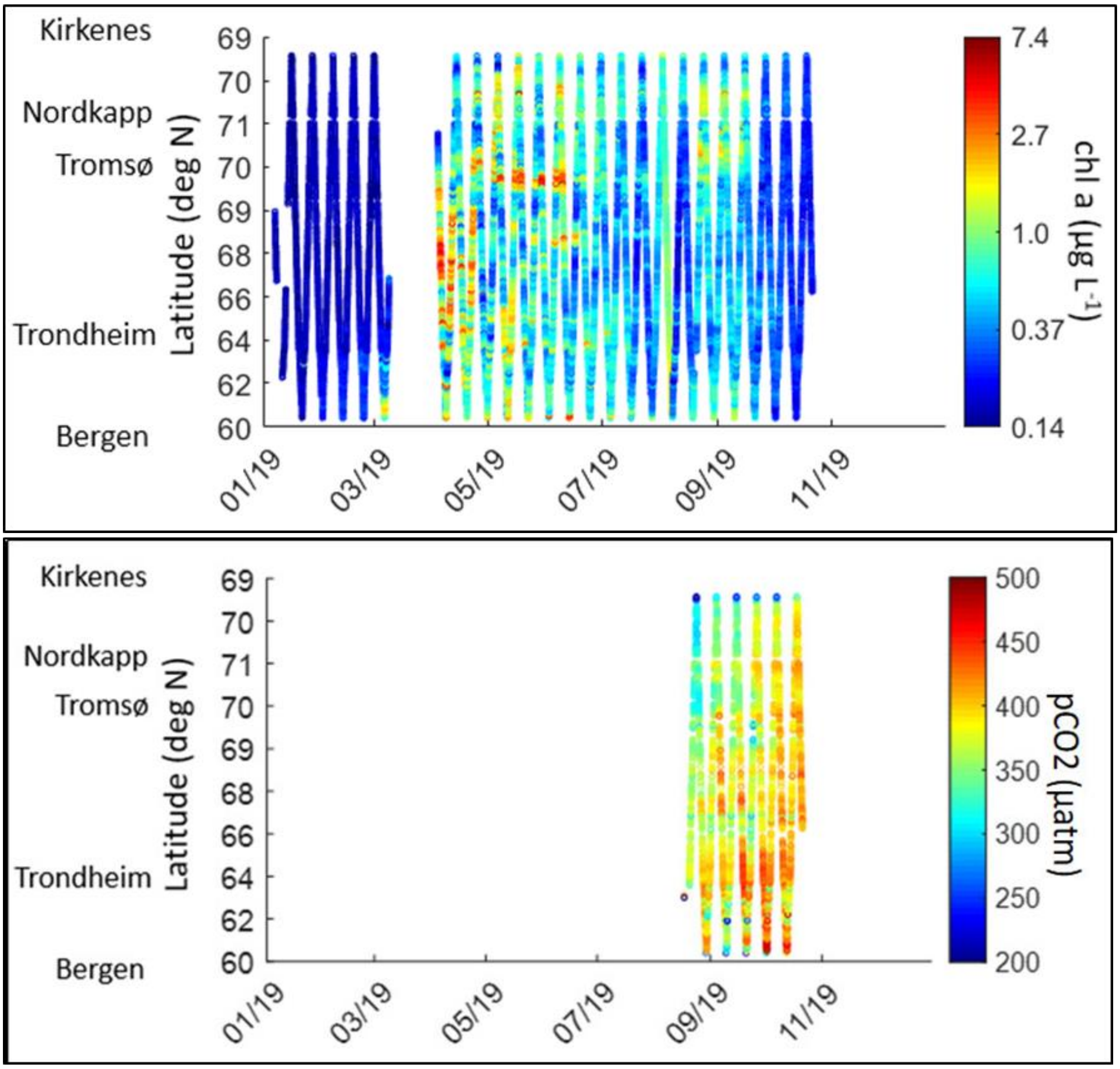

***Figure 44**. Coastal variation in salinity, temperature (°C), chlorophyll a (µg L^{-1}) and pCO$_2$ (µatm) along the Norwegian coast measured with underway sensors on MS Trollfjord in 2019.*

***Figur 44**. Variasjon i pCO$_2$ (µatm) målt med underveissensorer langs norskekysten målt fra FerryBox på MS Trollfjord i 2019.*

pCO$_2$ sensor measurements were only available from mid-August to late-October and exhibited large regional variability with generally low pCO$_2$ (~300-400 µatm) in the northern regions (>~70 °N) and higher pCO$_2$ (~350-450 µatm) in the mid/southern regions (<70 °N), and a general increasing trend of +~100 µatm from August to October. The mid-August to late-October period had relatively low phytoplankton biomass and the start of the cooling in the coastal zone. Therefore, salinity (input of freshwater and lower buffering capacity) and temperature were likely the dominant influences on carbonate system. The lowest pCO$_2$ was found in the Kirkenes coastal region (~69 °N), as low as ~200 µatm during August-October. The low pCO$_2$ observations were likely related to the low salinity (<~10-15) and low temperature influence on carbonate system. Another coastal region that exhibited lower pCO$_2$ and salinity signatures was the Sandnessjøen area (~66 °N) where pCO$_2$ was ~350 µatm and salinity <~25 in mid-August to the end of September.

3.5 Monitoring of ocean acidification in the coastal zone

The project 'Monitoring of ocean acidification in the coastal zone' is performed by the partners NIVA, IMR, NORCE and Akvaplan-niva (ApN) on behalf of the Norwegian Environment agency. The aim of the project is to increase the knowledge on the status, natural variability and trends (on a longer perspective) of ocean acidification in the coastal zone in Norway. The project period is from July 2019 to 2020 (period could be extended), and in total the monitoring program includes five fixed water column station, four lines with underway surface measurements (discrete and/or continuous) and seven cold-water coral reefs. There are three study regions in the project (***Figure 45***; ***Table 3*** for more information on stations): Hardanger (***Section 3.5.1***), Troms and Finnmark (***Section 3.5.2***) and Svalbard (***Section 3.5.3***).

The project follows the methods and procedures for sampling and analyses of the ocean carbonate system, as outlined in ***Chapter 2***. The stations and transect sampled in 2019 are summarized in ***Table 3*** and ***Figure 45***, and the data from all stations are given in ***Table 11-17***, ***Appendix 6.2***.

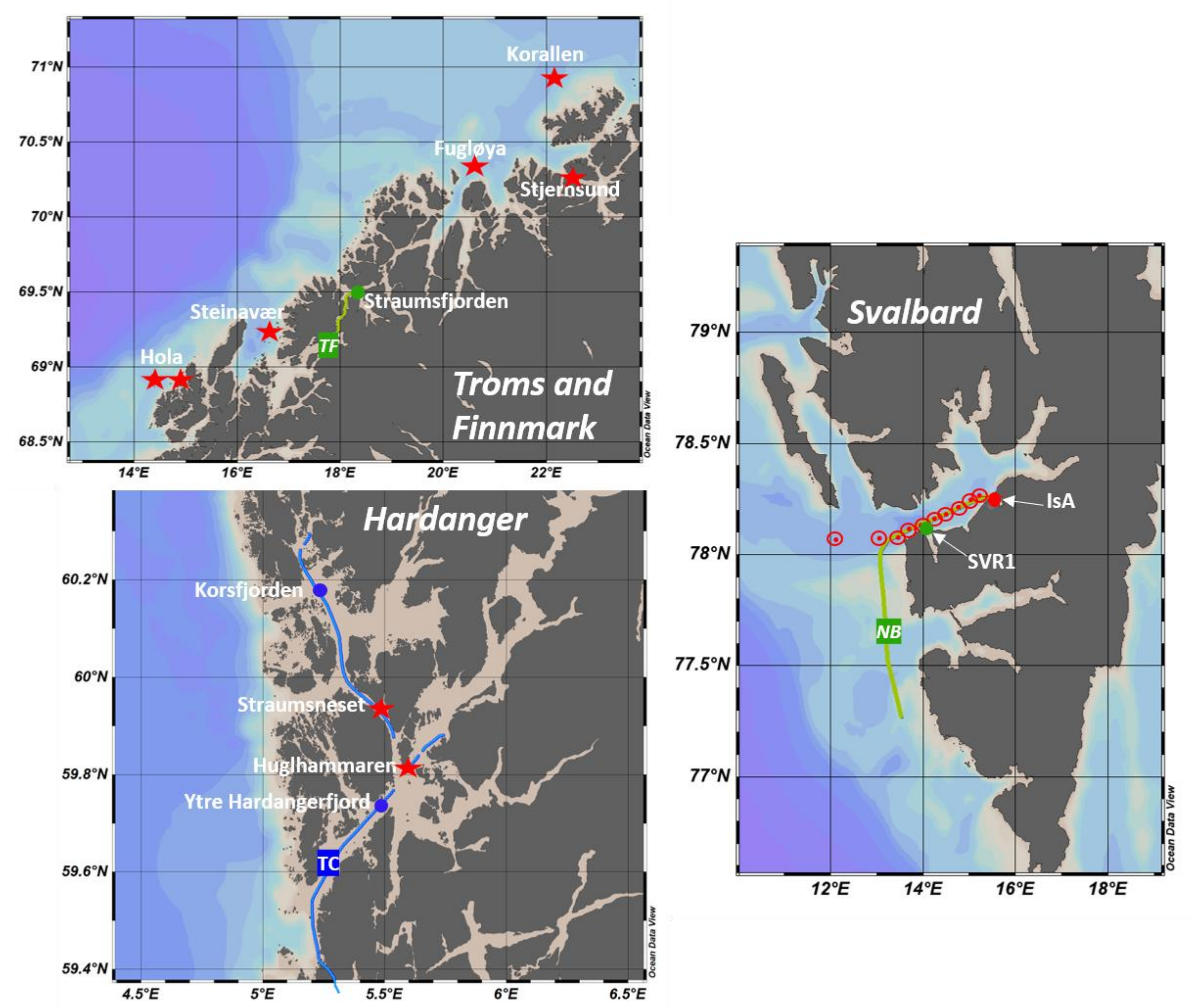

Figure 45. *Map showing the stations in the program Monitoring of ocean acidification in the coastal zone in 2019. The three areas of interest were Hardanger, Troms and Finnmark and Svalbard. Red, green, and blue colors refer to the responsibilities of IMR, NIVA/ApN, and NORCE, respectively (see* ***Table 3*** *for more info). Stars show the coral stations, dots represent the water column stations, circles with dots show surface stations, and lines show continuous measurement. NB = MS Norbjørn, TF = MS Trollfjord, TC = MS Tranc Carrier*

Figur 45. *Kart over stasjoner som har inngått i programmet Overvåkning av havforsuring i kystsonen i 2019. Programmet har fokusert på tre områder: Hardanger, Troms og Finnmark og Svalbard. Rød, grønn og blå farge viser til ansvarsområder for henholdsvis IMR, NIVA/ApN og NORCE. Stjerner viser korallstasjoner, prikker viser vannkolonnestasjoner, ringer med prikker i viser overflatemålinger og linjer viser kontinuerlige målinger. NB = MS Norbjørn, TF = MS Trollfjord, TC = MS Trans Carrier.*

Table 3
A summary of transects and cruises where sampling was performed in 2019. The stations are arranged according to study regions, Hardanger (yellow), Troms and Finnmark (green) and Svalbard (white). Temperature and salinity are measured on all stations.

Section/station (sample type)	Sampling month	Depth	Variables	Institution	Financing
Ytre Hardangerfjord station - VT69 (discrete)	July, Aug, Oct, Nov	Water column	A_T, C_T, nutrients	NORCE*	Environment Agency
Korsfjorden station - H7 (discrete)	July, Aug/Sept, Oct, Nov	Water column	A_T, C_T, nutrients	NORCE*	Environment Agency
Trans Carrier (continuous)**	July - September	Surface	pCO_2	NORCE	RCN
Huglhammaren coral reef (discrete)	June, October	Water column	A_T, C_T, nutrients	IMR	Environment Agency
Straumsneset coral reef (discrete)	June, October	Water column	A_T, C_T, nutrients	IMR	Environment Agency
Straumsfjorden station - VR54 (discrete)	February - November	Water column	A_T, C_T, nutrients, Chl *a*	NIVA/ApN	Environment Agency, NIVA
Trollfjord: Tromsø - Finnsnes (continous)*	October	Surface	pH, pCO_2, Chl *a*	NIVA	Environment Agency, RCN, NIVA
Hola coral reefs (discrete)	July, October	Deep water	A_T, C_T, nutrients	IMR	Environment Agency
Steinavær coral reef (discrete)	July	Deep water	A_T, C_T, nutrients	IMR	Environment Agency
Fugløya coral reef (discrete)	July	Deep water	A_T, C_T, nutrients	IMR	Environment Agency
Korallen coral reef (discrete)	July	Deep water	A_T, C_T, nutrients	IMR	Environment Agency
Stjernsund coral reef (discrete)	July, September	Water column	A_T, C_T, nutrients	IMR	Environment Agency
IsA station (discrete)	May, August, September, October, November	Water column	A_T, C_T, nutrients	IMR	Environment Agency
Underway surface stations in Isfjorden - ISF1-10 (discrete)	November	Surface	A_T, C_T, nutrients	IMR	Environment Agency
Isfjorden/Grønfjorden station -SVR1 (discrete)	August, September	Water column	A_T, C_T, nutrients, Chl *a*	NIVA/ApN	Environment Agency
Norbjørn: Isfjorden (continuous) *	January-March and August-November (pH and pCO_2), June (pH only)	Surface	pH, pCO_2, Chl *a*	NIVA	Environment Agency, RCN, European Commission, NIVA

A_T = total alkalinity, C_T = dissolved inorganic carbon, pCO_2 = partial pressure of CO_2, Chl *a* = chlorophyll *a*
* NORCE uses UiB (University of Bergen) as subcontractor.
** Data from Trans Carrier will be reported in 2021.
*** Excerpts of full FerryBox transects (***Table 1***).

3.5.1. Hardanger

3.5.1.1. Coastal water column stations in Hardanger

NORCE have examined the marine carbon cycle in the Hardanger area between 2007 and 2010, and from 2015 and onwards. Here we show time series of the water column between 2015 and 2019 from two stations: ytre Hardanger (H7) and Korsfjorden (VT69) (***Figure 46***), in addition to deep water trends at Korsfjorden station between 2007 and 2019. Depth and sampling data for 2019 are displayed in ***Table 11*** and ***Table 12*** (***Appendix 6.2***).

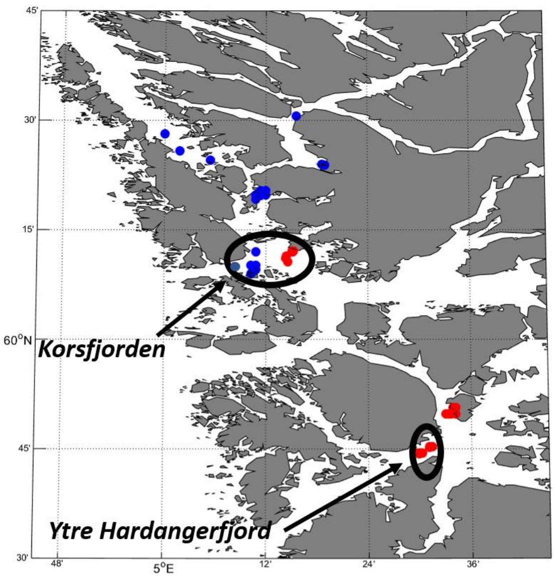

Figure 46. *A map showing the Bergen - Hardanger area, where NORCE and UiB have taken samples for the marine carbon cycle in the period 2007 to 2010 (blue dots) and from 2015 and onwards (red dots). The black circles show the two locations for the 2019 sampling: Korsfjorden and ytre Hardangerfjord.*

Figur 46. *Kart over området Bergen - Hardanger der NORCE og UiB har samlet vannprøver i perioden 2007-2010 (blå prikker) og fra 2015 og videre (røde prikker). De svarte sirklene viser hvor 2019-innsamlinga av data ble gjort; Korsfjorden og ytre Hardangerfjord.*

The seasonal variability of temperature, salinity, pH, and Ω aragonite is shown in ***Figure 47***, and the variability in the upper 100 m or so is far above that seen in the deeper layers of the water column. The surface water at the station ytre Hardangerfjord reaches temperatures of more than 17 ℃ in August 2018 and 2019, while in Korsfjorden, the surface was colder in summer 2019 (14.5 ℃), compared to that of the extraordinarily warm summer of 2018 (>17 ℃). The coldest surface water appears in February-March (4-5 ℃). The surface salinity is closely connected to precipitation and run-off from land and is generally low during autumn (27-30). The northern station is slightly more saline than the southern, which most likely is connected to the fact that the northernmost area (Korsfjorden) is more open to the ocean than the southernmost part, and thus more exposed to the northwards flowing Norwegian coastal current. The deep water at both locations has an Atlantic character, with salinities above 35 and relatively high temperatures (5-7 ℃).

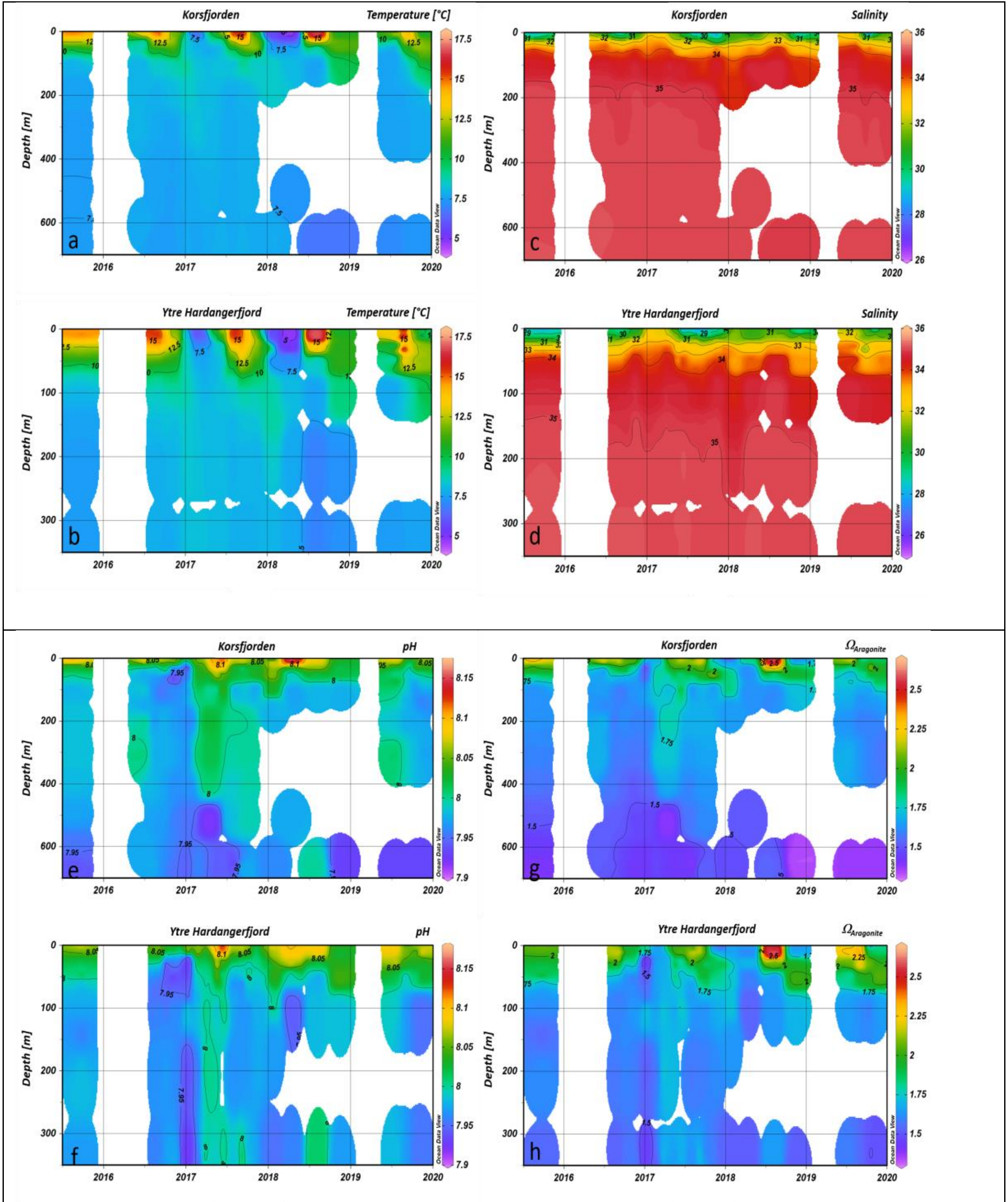

Figure 47*. Timeseries from Korsfjorden of a) temperature, c) salinity, e) pH, and g) Ω aragonite, and from ytre Hardangerfjord of b) temperature, d) salinity, f) pH, and h) Ω aragonite*

Figur 47*. Timeseries from Korsfjorden of a) temperatur, c) saltholdighet, e) pH, og g) Ω aragonitt, og fra ytre Hardangerfjord of b) temperatur, d) saltholdighet, f) pH, og h) Ω aragonitt*

Surface pH and Ω aragonite are low during winter, but the degree of saturation is never below 1 (***Figure 47***). pH increases with increasing biological production, which is also the case for Ω aragonite, but the latter responds later than pH due to the low temperature in late winter/early spring. pH decreases and Ω aragonite increases with increasing temperature, and the largest Ω aragonite values are seen in late summer, when the production has come to an end, the water is warm, and pH has started to decrease. The situation is fairly similar at the two stations, however, lower pH and Ω aragonite values are seen in the deeper Korsfjorden compared to the shallower ytre Hardangerfjord.

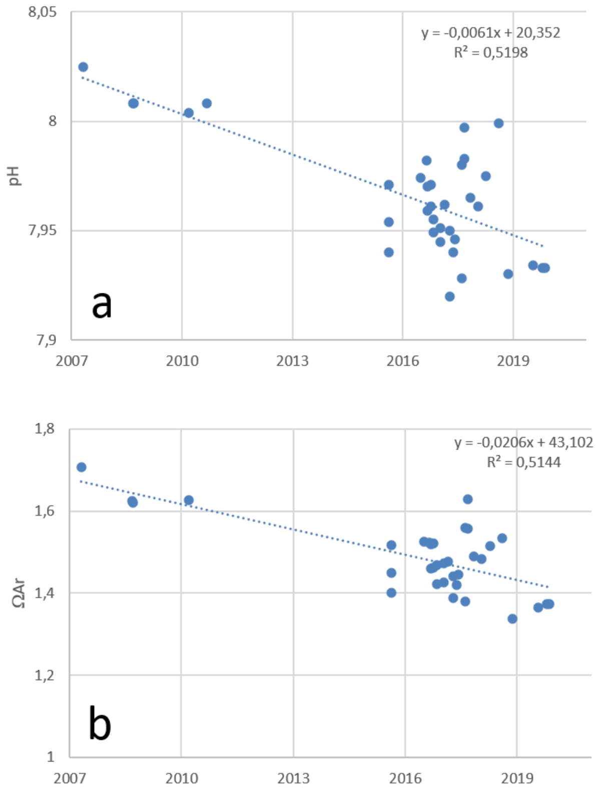

Figure 48. *Deep water (>500 m) trends from Korsfjorden of a) pH and b) Ω aragonite.*

Figur 48. *Trender i dypvannet (>500 m) i Korsfjorden; a) pH og b) Ω aragonitt.*

Figure 48 shows trends in pH and Ω aragonite of the deep (>500 m) waters of Korsfjorden in the period 2007 to 2019. As shown in ***Figure 46***, the data are from slightly different areas in Korsfjorden (black upper circle), so the results must be taken with care. However, the plots show that over a period of 13 years, the pH of the deep Korsfjorden water has decreased by 0.006 pH units per year, while the Ω aragonite has decreased by 0.021 units per year. These amounts are similar to those from Jones et al. (2018) but with a stronger correlation.

3.5.1.2. Coral reefs in Hardanger

Cold-water coral reefs: sensitivity of ocean acidification and monitoring of reef health

In 2019, a total of 7 *Lophelia pertusa* reefs were included in the ocean acidification monitoring campaign from IMR. The aim was to continue the studies from 2018 on the natural variation in physical and chemical processes around cold water coral reefs to better understand how these ecosystems respond and adapt to warmer seas and ocean acidification. The monitoring in 2019 included 2 wall reefs in Hardanger and 5 sill or hill reefs in northern Norway (***Chapter 3.5.2.2***).

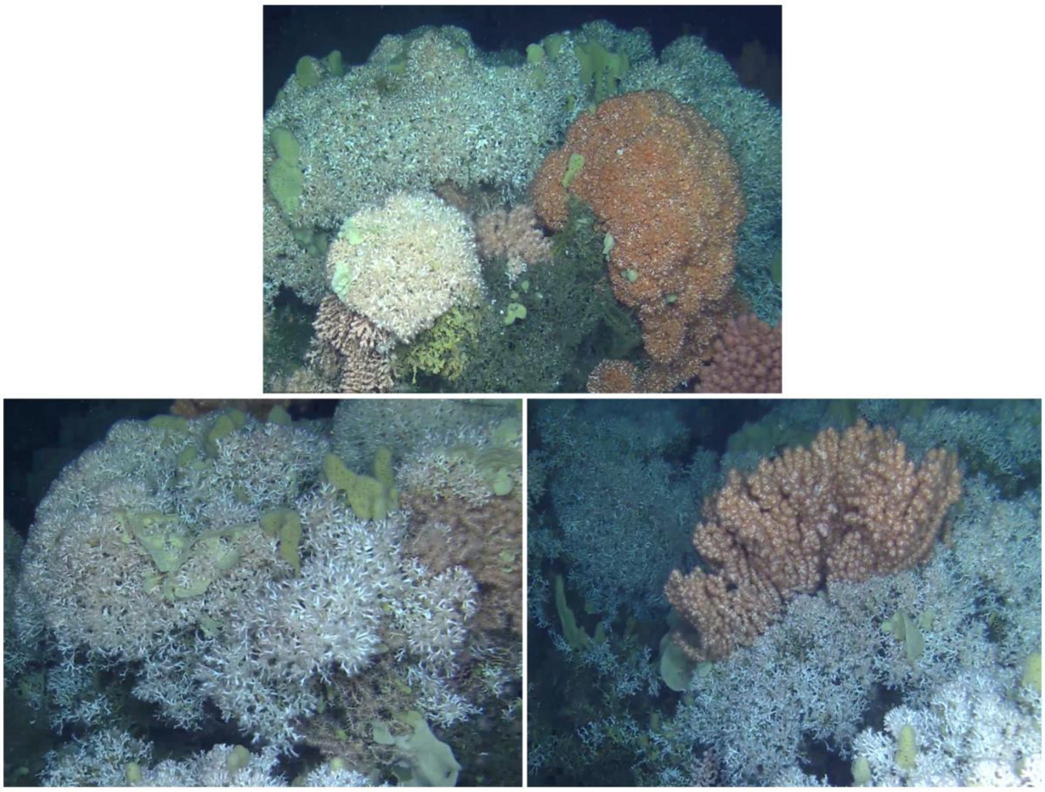

***Figure 49**. Cold water coral reefs found at the Norwegian coast, with the scleractinian coral Lophelia pertusa (white and red), gorgonian corals (Paragorgea arborea and Anthothela) and sponges (Phakellia and Mycale).*

***Figur 49**. Kaldtvannskoraller langs norskekysten, med Lophelia pertusa (hvit og rød), gorgonier (Paragorgea arborea og Anthothela) og svampdyr ((Phakellia and Mycale).*

Along the Norwegian coast, cold-water coral reefs are built mainly by the scleractinian coral *Lophelia pertusa* with minor contributions of the scleractinian coral *Madrepora oculata* to the reef framework in some locations (

Figure 49). The images from Stjernsund show both white and orange *Lophelia pertusa* lobes which are forming the structure of the reef and associated gorgonian corals (*Paragorgea arborea* and *Anthothela*) and sponges *(Phakellia* and *Mycale*). No *Madrepora oculata* colonies are present on these images. The reefs form three dimensional highly complex habitats on the otherwise relatively flat continental shelf and act as biodiversity and productivity hotspots (Catchalot et al. 2015, Freiwald et al. 2012). The reefs can vary in size and shape with some reefs extending for several km in width and length while others are just a few hundred meters in diameter. In height, the reefs normally reach up to 15 meters. Living corals is found mainly in the upper 20-40 cm of the reef while the remainder of the mound is composed of old and dead coral skeleton. The outer edge of the reefs is composed of a mixture of dead coral skeleton, coral rubble and sand. All these microhabitats are vital parts of the reef ecosystem. In total, more than 1300 benthic invertebrate species, including foraminiferans, sponges, hydroids, bryozoans, bivalves, anemones and polychaetes live, on or in-between the coral branches (Freiwald et al. 2012) with the dead coral skeleton arising as the most species rich of reef microhabitats (Freiwald et al. 2004, Johnsson et al. 2004, Mortensen and Fosså 2006, Buhl-Mortensen 2017, De Clippele et al. 2019).

The global distribution of cold-water coral reefs is strongly limited by the depth of the aragonite saturation horizon (Guinotte et al. 2006). Below the saturation horizon water is under-saturated with respect to aragonite, Ω aragonite < 1.0, and in general devoid of cold-water corals. In waters with a Ω aragonite < 1.0 corals experience elevated costs of calcification (Allemand et al. 2011), reduced calcification rates and breaking strength of the skeleton of living *Lophelia pertusa* (Hennige et al. 2015) and very importantly increased dissolution rates of the dead coral skeleton, which is a major component of the reef ecosystem. While the living coral can compensate for aragonite undersaturation by manipulating their internal calcifying fluid and raise their internal pH by 0.3-0.6 units (McCulloch et al. 2012, Allison et al. 2014) and hence continue to calcify in waters undersaturated with respect to aragonite, the dead coral skeleton will slowly dissolve, inevitably. There are only very few published studies reporting on carbonate chemistry data from areas with *Lophelia pertusa* reefs and only one field study, from the Gulf of Mexico, that has mapped skeletal characteristics of *Lophelia pertusa* in populations growing in waters near the aragonite saturation horizon. In that study no correlations between pH and Ω aragonite and skeletal densities were found (Lunden et al. 2013). This resilience could be due to local adaptation or acclimation aided by the dissolution of dead coral skeleton from the reefs that may increase the Ω aragonite of the water in the immediate vicinity of the corals (Farfan et al. 2018). Such very localized elevations in Ω aragonite would go undetected in a water sampling campaign using Niskin bottles mounted on a CTD rosette that is normally not brought closer to the seabed than 3-5 m due to swell and the topographic complexity of the reef habitat. Alternatively, the biomineralization processes in cold-water corals may not be as susceptible to changes in carbonate chemistry variables as predicted.

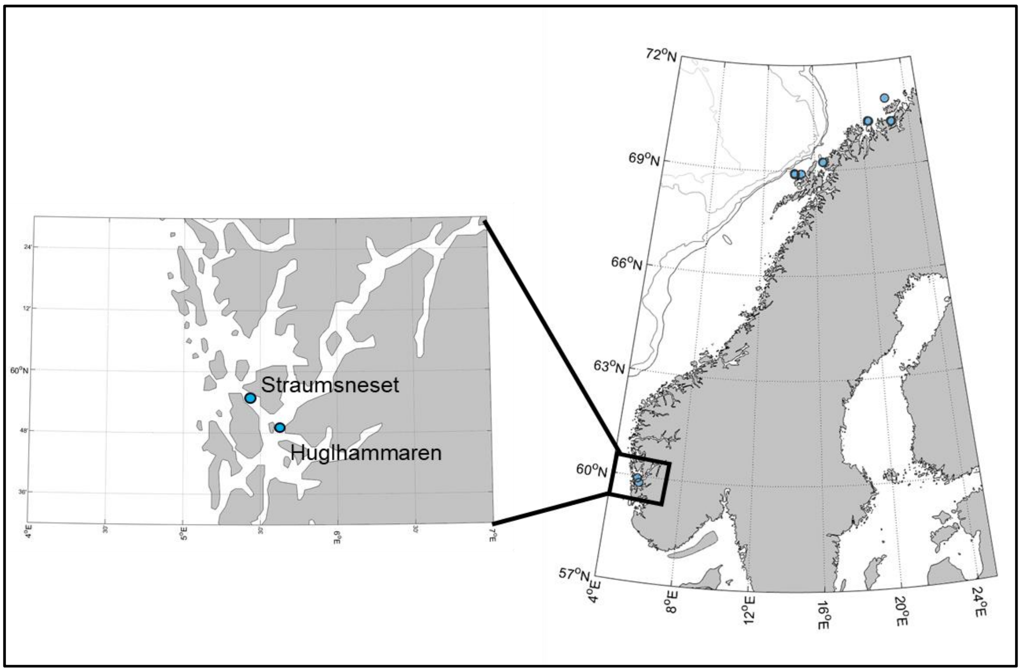

Figure 50. *Maps showing the locations of cold water coral wall reefs in Hardanger*

Figur 50. *Kart som viser beliggenhet av kaldtvannskoraller i veggrev i Hardanger*

Straumsneset and Huglhammaren are wall reefs in the interconnected Langenuen Straight and Hardangerfjord (***Figure 50***). Carbonate chemistry variables were sampled here two times as a part of the seasonal study of OA variables. Depth and sampling data are displayed in ***Table 13, Appendix 6.2***. Data will be used to get an idea of how the carbonate chemistry at the sites varies over time and in space and to study to what extent the carbonate chemistry affects where different deep-water coral species can grow.

Both locations compose of steep and overhanging fjord walls densely colonised by *Lophelia pertusa* and *Madrepora oculata* at depths between 240 and 80 m. The largest single coral lobes observed on the wall measure 3*7 m. The wall reefs are densely colonized by gorgonian corals, sponges, anthozoans, hydroids, sabellid polychaetes and bivalves of *Acesta excavata* and are therefore sometimes also named coral and sponge gardens. The June and October field campaign sampled water at 6 and 5 different depths respectively, just in front of the two wall reefs at Straumsneset and Huglhammaren from the surface layers and down below the depth of cold-water coral occurrence. At the wall reefs in Straumsneset and Huglhammaren ROV dives were performed in June 2019 to visually document the health status of the reefs but no physical samples of the reefs were collected. This is because these reefs have been physically sampled in the last years and since there was no obvious change it was considered unnecessary to re-sample these reefs again already now. *Lophelia pertusa* is slow growing and long-lived and we therefore evaluate closely each time if physical samples are needed or not. The visual examination revealed high biodiversity, representation of coral from a wide range of size classes (including several small and recently settled colonies), and a high proportion of live versus dead coral framework indicating that both Straumsneset and Huglhammaren wall reefs are in good health state.

The June and October field campaign in the Langenuen straight and Hardangerfjorden sampled water just in front of the two wall reefs at Straumsneset and Huglhammaren, from the surface layers and down below the depth of cold-water coral occurrence (i.e. 80-200 m). Both in May and October the three replicate water samples at each depth were collected three hours apart to better display the range of carbonate chemistry conditions at the reefs at the two different seasons. The sampling campaign showed that the temporal variability in carbonate chemistry variables was high (both seasonally and within the day) in the surface water and down to 80 m but comparatively stable in deeper waters, excluding pH.

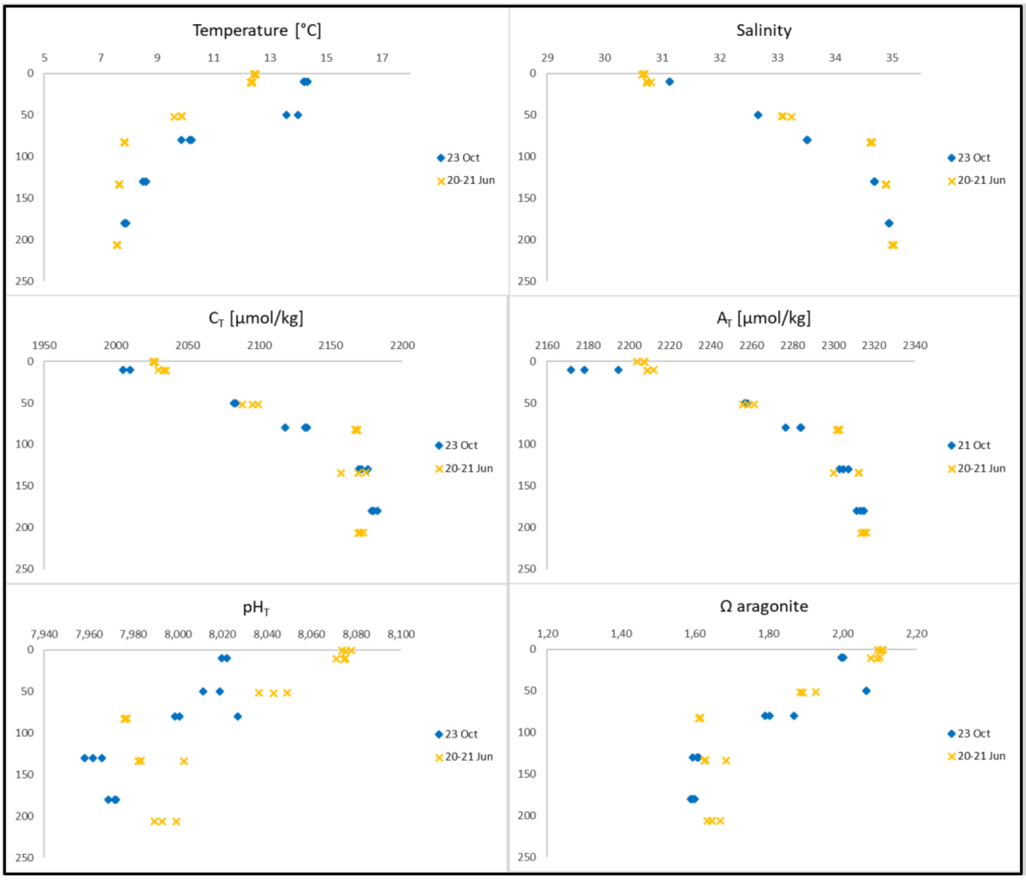

Figure 51. *Temperature, salinity, C_T, A_T, pH and Ω aragonite in the water column at Straumsneset in 2019.*

Figur 51. *Temperatur, saltholdighet, C_T, A_T, pH og Ω aragonitt i vannsøylen ved Straumsneset i 2019.*

At the wall reef in Straumsneset (i.e. in water samples collected at 80, 130 and 200 m depth) Ω aragonite ranged between 1.68 and 1.61, A_T between 2316 and 2300 µmol kg^{-1}, C_T between 2175 and 2157 µmol kg^{-1} and pH between 8.00 and 7.97 within one day in June (***Figure 51***). At the same depths, within one day in October, Ω aragonite ranged between 1.87 and 1.59, A_T between 2315 and 2277 µmol kg^{-1}, C_T between 2183 and 2118 µmol kg^{-1} and pH between 8.03 and 7.96. Hence at this wall reef carbonate chemistry varied more within a single day than between seasons and with October being the more variable time point sampled.

At Huglhammaren (***Figure 52***), we found that during one day in June Ω aragonite varied between 1.63 and 1.54, A_T between 2312 and 2289 µmol kg^{-1}, C_T between 2182 and 2170 µmol kg^{-1} and pH between 7.99 and 7.95 at the depths where cold-water corals grow (i.e. between 80 and 200 m). At the same depths, during one day in October, Ω aragonite varied between 1.74 and 1.54, A_T between 2315 and 2299 µmol kg^{-1}, C_T between 2188 and 2153 µmol kg^{-1} and pH between 7.91 and 7.97. Similar to Straumsneset the Huglhammaren wall reef carbonate chemistry varied more within a single day than between seasons and with October being the more variable time point sampled.

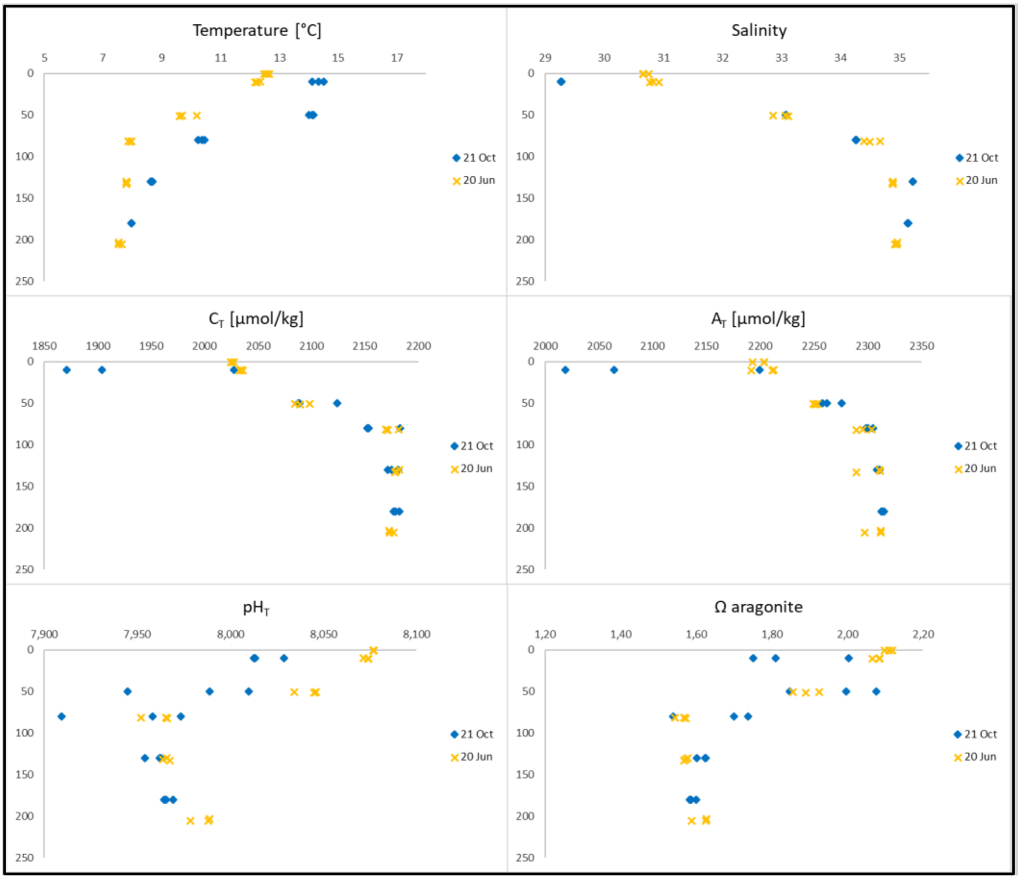

***Figure 52**. Temperature, salinity, C_T, A_T, pH and Ω aragonite in the water column at Huglhammaren in 2019.*

***Figur 52**. Temperatur, saltholdighet, C_T, A_T, pH or Ω aragonitt i vannsøylen ved Huglhammaren i 2019.*

The seasonal study confirmed observations from previous years (Skjelvan et al. 2016, Jones et al. 2019) with slightly higher Ω aragonite in Straumsneset as compared to Huglhammaren and with aragonite saturation at the depths of the wall reefs generally ranging between 1.58 and 1.68. A_T between 2300 and 2320 µmol kg^{-1}, C_T between 2160 and 2180 µmol kg^{-1} and pH between 7.96 and 8.03. The values measured at the depths where cold-water corals grow are in the higher range of Ω aragonite, A_T, and pH and in the lower range of C_T measured from *Lophelia pertusa* reefs in the Gulf of Mexico (Lunden et al. 2013). In an extensive study Findlay et al. (2014) mapped carbonate chemistry around 5 deep cold-water coral locations off the British Isles (i.e. Mingulay area, Banana Reef, Logachev, Pisces, Herbrides Terrace Seamount) and found that Ω aragonite ranged from 1.35 to 2.44, C_T between 2088 and 2186 µmol kg^{-1} and A_T between 2299 and 2346 µmol kg^{-1}. All our measurements from the wall reefs in Hardanger are well within these ranges. Noticeably, these two, apparently very healthy vertical wall reefs exist in C_T levels between 2160 and 2180 µmol kg^{-1}, disproving that healthy cold-water coral reefs in the NE Atlantic Ocean are generally found in C_T levels below 2170 µmol kg^{-1} (Flögel et al. 2014). That shows the importance of monitoring the A_T levels to get a complete understanding of the carbonate chemistry.

3.5.2. Troms and Finnmark

3.5.2.1. Coastal waters in Malangen

Malangen is a large and open fjord system in the northern Norwegian Sea with a deep sill, and the Straumsfjord coastal water column station (VR54) is located mid-fjord at around 150 m depth (***Figure 54***). At the Straumsfjorden station, NIVA has had extended monitoring since 2017, including carbon chemistry between 0-30 m (5 depths) since February 2019. Since September 2019, the full water column (10 depths) has been sampled as part of the program "Monitoring of ocean acidification in the coastal zone". The underway observations in this region were made by MS *Trollfjord*, crossing the Straumsfjorden station along an approximately southwest-northeast direction (see transect in ***Figure 53***). Due to operational and technical issues, including a dry dock maintenance of the ship in October/November 2019 followed by a new FerryBox system installation, only five transects of underway pCO_2 observations were available during the project period from July to December 2019.

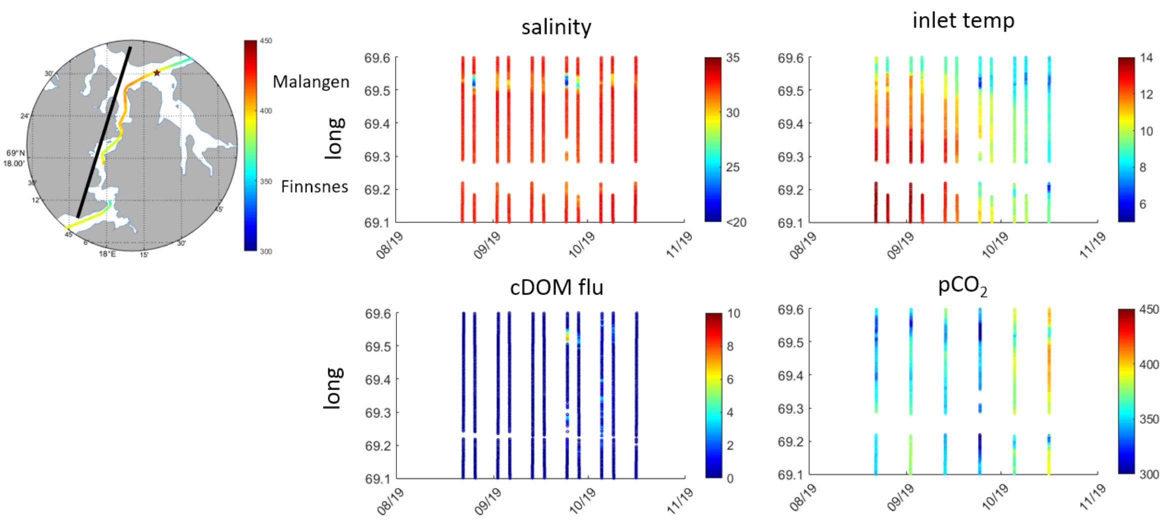

Figure 53. *Timeseries from MS Trollfjord in Malangen of surface salinity, temperature (℃), cDOM fluorescence (arbitrary units) and pCO_2 (µatm).*

Figur 53. *Dataserier fra MS Trollfjord i Malangen av saltholdighet, temperatur (℃), cDOM fluoresence (vilkårlig enhet) og pCO_2 (µatm) i overflaten.*

The underway measurements from MS *Trollfjord* of salinity, temperature (℃), cDOM fluorescence (arbitrary units), and pCO_2 (µatm) are shown in ***Figure 53***. The period between August and October 2019 included some low salinity input events near Malangen (S <25), which also at times coincided with reduced temperature and cDOM fluorescence, especially in late September and early October. pCO_2 also showed variability ranging from ~300-400 µatm which is typical for the region, which also included some variability driven by freshwater input (reduced pCO_2 near Malangen associated with low salinity and high cDOM) and water mass cooling that began at the end of September and continued to cool through October.

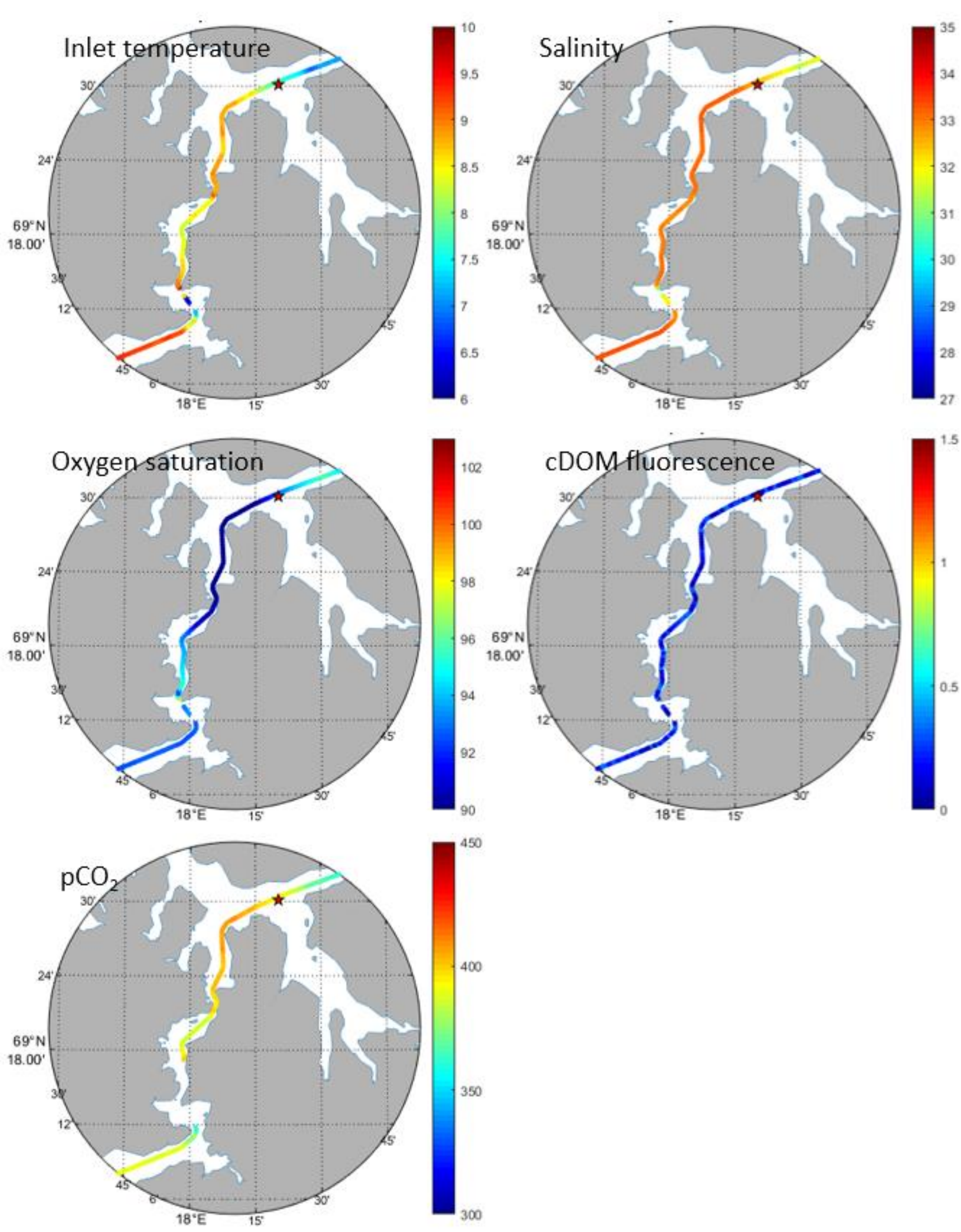

Figure 54. *Continuous surface measurements from MS Trollfjord in the Malangen region (between Finnsnes and Tromsø) on 15 October 2019 for temperature (°C), salinity, O_2 saturation (%), cDOM fluorescence (arbitrary units) and pCO_2 (μatm). Red star marks the position of the Straumsfjorden (VR54) station.*

Figur 54. *Kontinuerlige overflatemålinger fra MS Trollfjord i Malangen (mellom Finnsnes og Tromsø) den 15 oktober 2019 for temperatur (°C), saltholdighet, O_2 metning (%), cDOM fluoresence (vilkårlig enhet) og pCO_2 (μatm). Rød stjerne viser posisjonen til Straumsfjorden (VR54) stasjonen.*

The spatial variability in the Malangen region (between Finnsnes and Tromsø) for temperature (℃), salinity, oxygen saturation (%), cDOM fluorescence (arbitrary units), and pCO_2 (µatm) on 15 October 2019 is shown in ***Figure 54***. Salinity varied between 31and 35 over the transect and temperature between 6 and 10 ℃, with a noticeable freshening and cooling near the Straumsfjorden coastal station. Oxygen was undersaturated throughout the transect, cDOM fluorescence was low and relatively unvaried, and pCO_2 ranged from 330 to 400 µatm. Based on the oxygen undersaturation, time of year (large blooms are not likely), and the magnitude of change in sea temperature, the variability in pCO_2 was likely due to temperature effects on the inorganic carbonate system during this period.

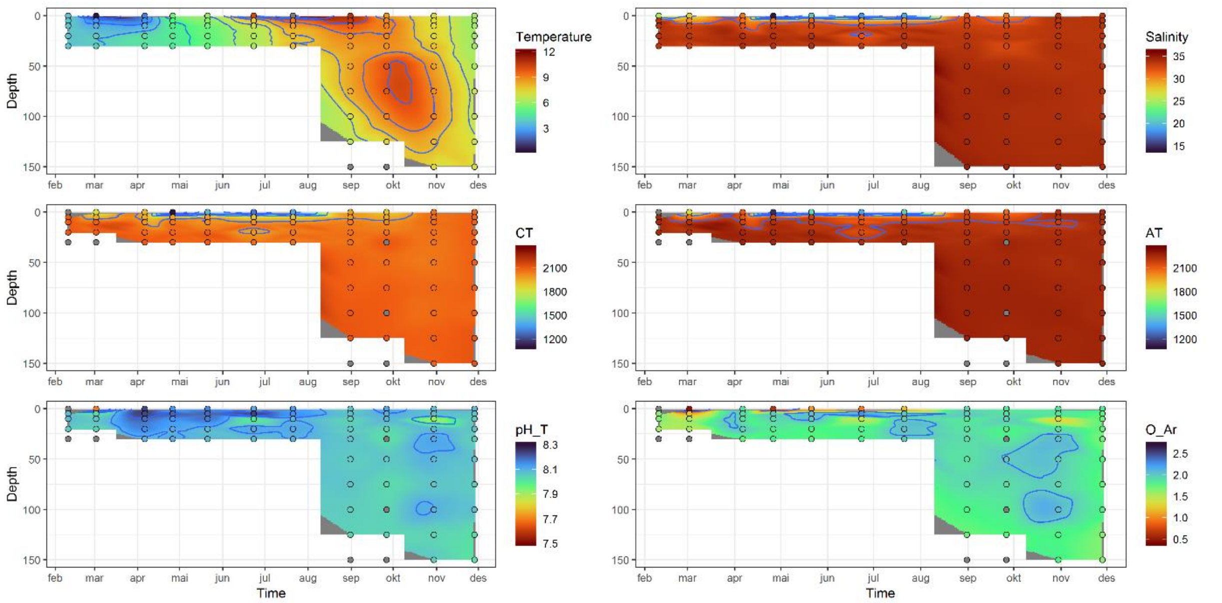

Figure 55*. Timeseries from Straumsfjorden (VR54) of temperature (℃), salinity, C_T (µmol kg^{-1}), A_T (µmol kg^{-1}), pH and Ω aragonite in 2019*

Figur 55*. Dataserier fra Straumsfjorden (VR54) for temperatur (℃), saltholdighet, C_T (µmol kg^{-1}), A_T (µmol kg^{-1}), pH and Ω aragonitt i 2019.*

The seasonal variation in temperature, salinity, C_T, A_T, pH and Ω aragonite at the Straumsfjorden coastal station (VR54) is shown in ***Figure 55***. Depth and sampling data are displayed in ***Table 14, Appendix 6.2***. The coolest surface waters were found between March and April 2019 (<0.5 ℃), with the warmest surface waters in July (12 ℃) and warming extending to deeper waters during late summer and autumn. There was pronounced variability in surface salinity, with low values (14-25) in the surface period from February to July. In a recent study, this freshening was shown to be connected to freshwater discharge in the nearby river Målselv, which has a pronounced spring flood in May/June most years (Frigstad et al. In Press). The spring flood in Målselv creates a freshwater lens in the surface layer in the Malangen region, with high concentrations of dissolved organic carbon (DOC of 200 µmol kg^{-1}; ***Figure 54***) and inorganic nutrients (especially NO_3 and $Si(OH)_4$, data not shown). Below this layer (5-30 m) the salinity was higher (30-33) with less seasonal variation. The deeper water between 50 and 150 m was monitored since August 2019, and generally shows less variation in salinity with a more Atlantic-water character (34-35) and higher concentrations of PO_4 and NO_3 (data not shown).

There was pronounced seasonal variability in C_T and A_T in surface waters (0 m), with low values (minimum values 1103 μmol kg^{-1} for C_T and 1156 μmol kg^{-1} for A_T) during the period from April to July, corresponding with the period of river-influenced low salinity surface waters as explained above. The Ω aragonite in this period was mostly at or below saturation (0.5 - 1.9), meaning that these surface waters could be corrosive to organisms with calcium carbonate shells. The lowest pH (7.69) occurred during March at the surface, followed by an increase in pH in surface waters in the period April to August 2019. Photosynthesis will act to increase pH (due to drawdown in C_T), and this period also had higher chlorophyll *a* (2-5 μg L^{-1}; ***Figure 56***) and depleted nutrient concentrations (PO_4 and NO_3, data not shown).

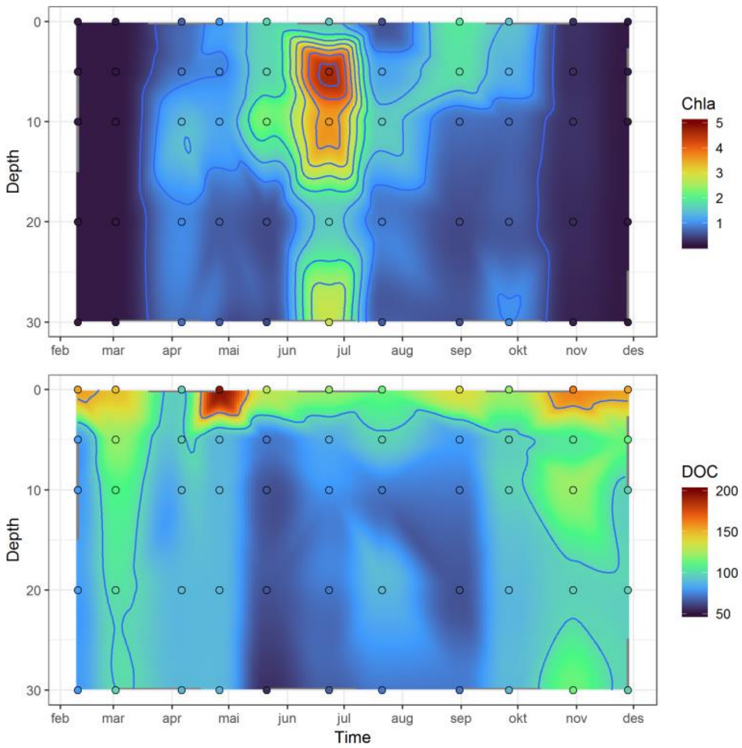

Figure 56*. Timeseries from Straumsfjorden (VR54) of chlorophyll a (μg L^{-1}) and DOC (μmol kg^{-1}) in 2019.*

Figur 56*. Dataserier fra Straumsfjorden (VR54) for Klorofyll a (μg L^{-1}) og DOC (μmol kg^{-1}) i 2019.*

It has been shown that undersaturated waters with respect to Ω aragonite can be related to mixing with freshwater, which depending on the pH and buffering capacity of the freshwater source can have large effects on coastal Ω aragonite (Rheuban et al., 2019, Carstensen et al., 2018). The Målselv river is monitored through the national River Monitoring program, and the pH in 2018 varied between 7.0 - 7.5 with moderate levels of calcium (used as proxy for buffer capacity; Gundersen et al., 2019). Generally, most riverine discharges have lower pH (higher CO_2) compared to marine waters, related to low buffering capacity and/or respiration of terrestrial organic matter, which can significantly affect the carbonate chemistry in river-influenced coastal areas (Salisbury et al., 2008). However, the river chemistry will depend on the mineral composition of the catchment area, and carbonate-mineral rocks have been observed to buffer part of the freshening effect on the carbonate chemistry (Fransson et al., 2015). The relationship between carbonate chemistry at the Straumsfjorden station and the river discharge and catchment properties in the Målselv river needs to be examined more closely, especially in terms of links between river and coastal water chemistry and the representativity of Malangen for other northern Norwegian river-influenced fjords.

3.5.2.2. Coral reefs in coastal areas of northern Norway

A general trend is that ocean acidification is proceeding at higher rates at high latitudes than at lower latitudes resulting in a more rapidly shoaling of the aragonite saturation horizon there as compared to other regions. Monitoring carbonate chemistry and cold-water coral state in the northern regions of Norway is therefore considered particularly interesting with respect to the ongoing ocean acidification (AMAP, 2013).

In 2019, a total of 5 *Lophelia pertusa* reefs were included in the OA monitoring in Nordland (Hola) and Troms and Finnmark (Steinavær, Fugløya, Stjernsund, Korallen), see ***Figure 57***. Depth and sampling data are displayed in ***Table 13, Appendix 6.2***. Carbonate chemistry variables around 4 of the reefs, i.e. Korallen, Fugløyrevene, Steinavær and Hola were only measured once (in July) while Stjernsund was sampled two times as a part of the seasonal study of OA variables. Data will be used to get an idea of how the carbonate chemistry at the sites varies over time and in space and to study to what extent the carbonate chemistry affects where different deep-water coral species can grow.

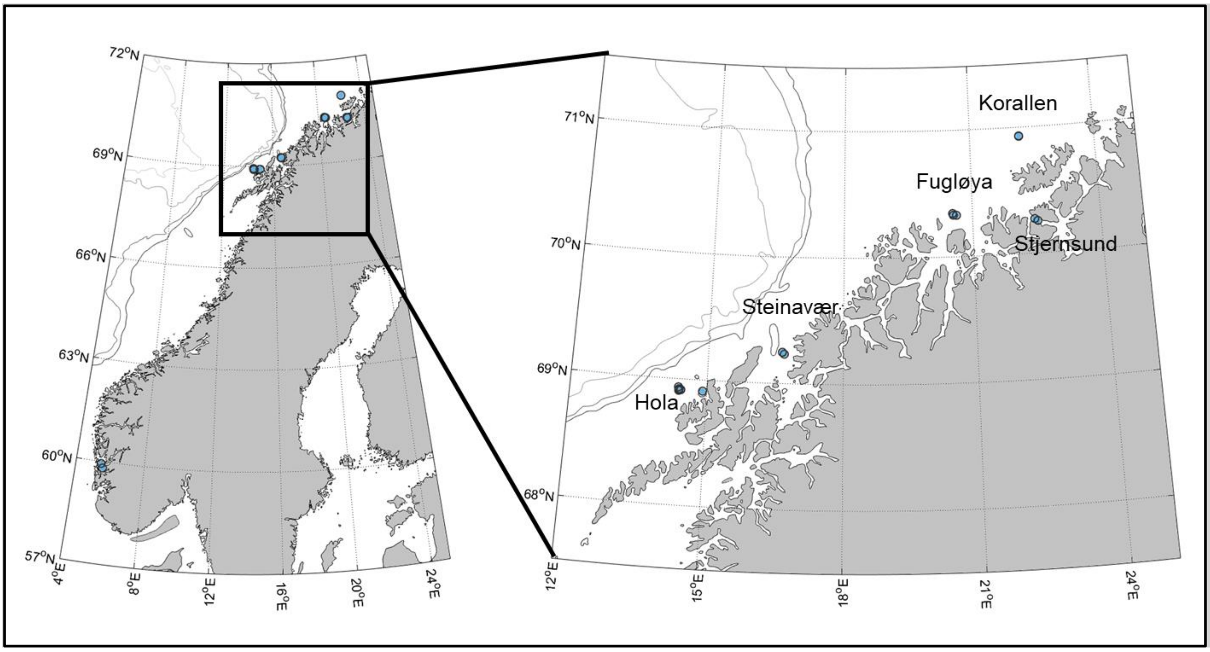

Figure 57. *Maps showing the locations of cold water coral reefs in Troms and Finnmark.*

Figur 57. *Kart som viser beliggenheten til kaldtvannskorallene i Troms og Finnmark.*

The northernmost known cold-water coral reefs in the world is the Korallen reef (70°55N, 22°11E) west of Sørøya in Troms and Finnmark. Korallen reef is located on a small topographic elevation at 260 to 280 m depth on the edge of a deep trench. The reef composes a series of densely packed large coral lobes forming a more or less continuous cover on the main part of the reef that measures approximately 1000 m in length and 500 m in width (Fosså et al. 2015). The Stjernsund reef (70°16N, 22°28E) is located on the sill in Stjernsund. It is a topographically complex reef with a dense cover of large coral lobes on 300 to 250 m depth on both the eastern and western side of the sill. The reef is highly productive and has a high number of associated large megafauna, such as gorgonian corals and sponges. The reef has been well described by Rüggenberg et al. (2011) and Rovelli et al. (2015).

The Fugløya reef (70°20N, 20°37E) composes several small isolated circular coral mounds of approximately 80 to 400 m in diameter (Lindberg et al. 2017, Fosså et al. 2015). The coral mounds grow from 220 to 160 m depth and are between 10 and 50 m high and therefore the tallest *Lophelia pertusa* mounds known from the Norwegian shelf and fjords. The large lobes of *L. pertusa* are associated with a rich fauna of associated megafauna such as gorgonian corals and sponges. The Steinavær reef (69°15N, 16°38E) is a well-developed, large coastal hill reef (700*1500 m) growing in steep terrain on top of a northwesterly/south-southeasterly directed topographical elevation between Selfjorden and Andfjorden (Fosså et al. 2015). It is a topographically complex reef with several ridges and crests and is rich in associated gorgonian corals and sponges. The Hola reef aggregation (68°55N, 14°24E) is located at roughly 300 m depth in the Hola Trough, approximately 25 km from the shelf break and 20 km from the archipelago of Vesterålen, Northern Norway. The reef aggregation composes 414 isolated elongated coral reefs that are 100-200 m long (Fosså et al. 2015, Boe et al. 2009). All 5 reefs studied in the 2019 field campaign are protected, to some degree, from human impact. Korallen, Stjernsund, Fugløyrevene, and Hola are protected through the fisheries legislations that ban bottom trawling and other fishing activity that might damage the reef. Steinaværrevet is part of the Andfjorden marine protected area.

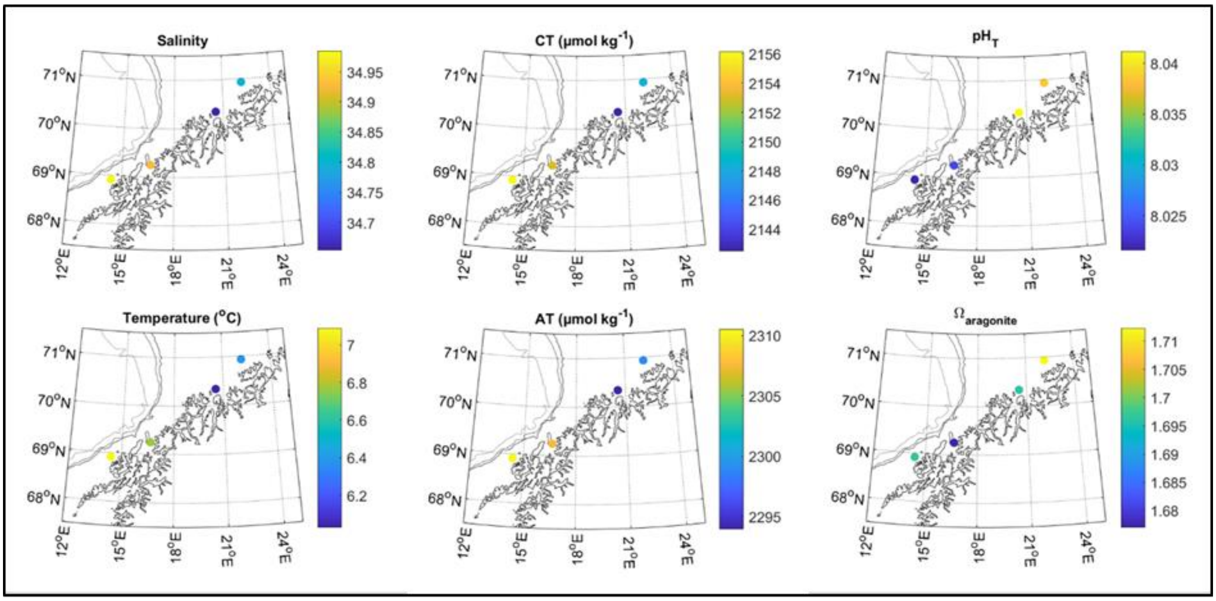

***Figure 58**. Average temperature, salinity, C_T, A_T, pH and Ω aragonite (from 3 bottom water samples per site) over the seafloor at four cold water coral sites (Korallen, Fugløy, Steinavær and Hola) in July.*

***Figur 58**. Gjennomsnittlig temperatur, saltholdighet C_T, A_T, pH og Ω aragonitt (fra 3 bunnvannsprøver pr sted) ved sjøbunnen på fire lokaliteter for kaldtvannskoraller (Korallen, Fugløy, Steinavær og Hola) i juli.*

The July field campaign sampled bottom water at 4 sites, Korallen, Fugløyrevene, Steinaværrevet and Hola reefs at three different locations within each reef at a distance of 3-5 m from the sea bed (***Figure 58***). All water samples were taken with a few hours apart and in-between the water sampling casts ROV dives were conducted to assess the health status of the reefs. The sampling pattern allowed us to assess spatiotemporal variability in water characteristics. Regional variability can be seen in the colder and fresher bottom waters for the 2 northern reef sites compared to the southern reef sites. This is also reflected din the carbonate chemistry as the colder, fresher waters are characterized by lower C_T and A_T compared to the more Atlantic Water influenced southern sites, with higher C_T and $A_{T.}$ As a result, higher pH was found in bottom waters in the north and Ω was more variable. At the Stjernsund reef water samples were taken at 8 different depths: near the seabed, at 310, 275, 235, 100, 50, 30 and 10 m for carbonate chemistry variables. The near sea-bed sample was taken at 425 m at the station located east of the sill and at 345 m at the station located west of the sill. This sampling design allowed us to assess variability between water upstream and down-stream of the reef. Two ROV dives were conducted at Stjernsund.

In Korallen, Fugløya, Steinavær and the Hola reefs Ω aragonite ranged from 1.64 to 1.74, C_T between 2156 and 2132 μmol kg^{-1} and A_T between 2312 and 2288 μmol kg^{-1} at the depths where *L. pertusa* is occurring. This corroborates the findings that high-quality cold-water coral reefs in the north-eastern Atlantic Ocean are generally associated with waters of a C_T concentration below 2170 μmol kg^{-1} (Flögel et al. 2014). Ω aragonite measured in the northern Norwegian reefs were higher than that documented for 8 different *L. pertusa* ecosystems at 300 to 600 m depth in the Gulf of Mexico that had a Ω aragonite of 1.25-1.69, A_T between 2388 and 2254 μmol kg^{-1} and pH ranging from 8.03 to 7.85 (Lunden et al. 2013). pH in the 5 northern Norwegian reefs sampled in this study never reached below 8.015 and was 8.050 at the most. All 5 northern Norwegian reefs were well within the ranges of environmental conditions found around five reefs off the British Isles where Ω aragonite ranged from 1.35 to 2.44, C_T between 2088 and 2186 μmol kg^{-1} and A_T between 2299 and 2346 μmol kg^{-1} (Findlay et al. 2014).

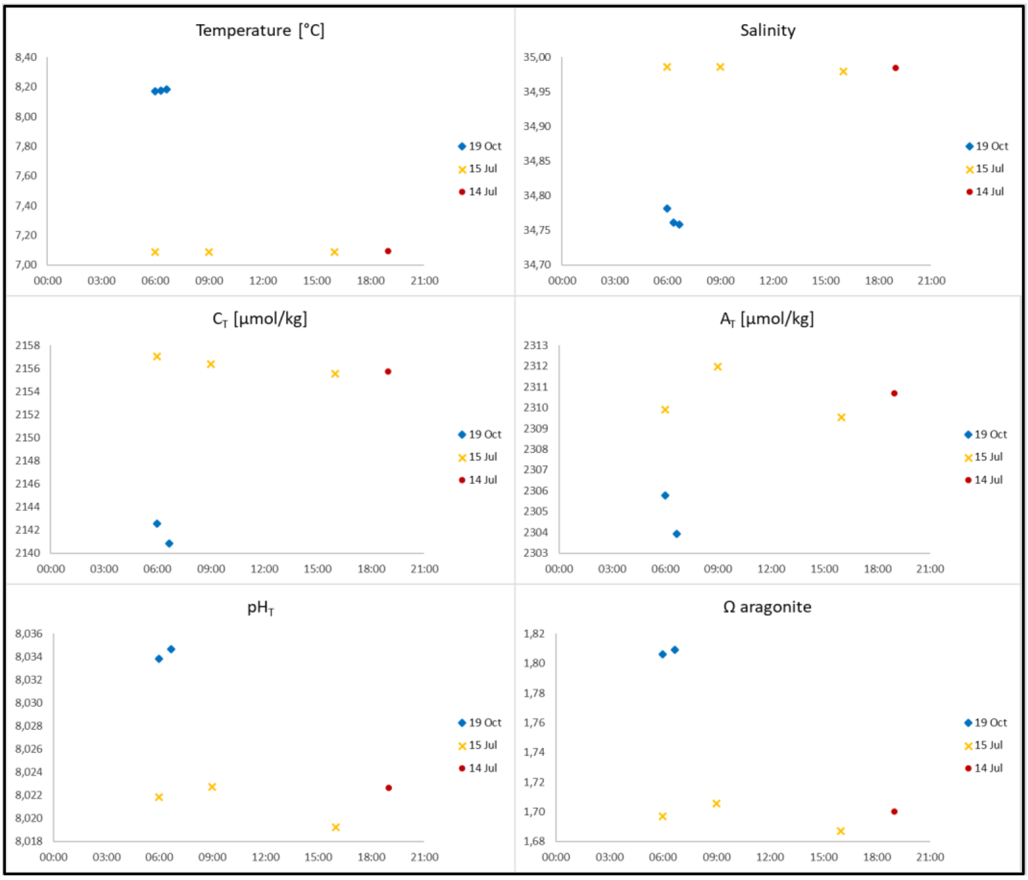

Figure 59. *Temperature, salinity, C_T, A_T, pH and Ω aragonite over the seafloor at Hola reef revealed from October 2018 and July 2019 measurements.*

Figur 59. *Temperatur, saltholdighet, C_T, A_T, pH og Ω aragonitt sjøbunnen ved Holarevet vist ved målinger fra oktober 2018 og juli 2019.*

At the Hola reefs clear (but small) difference in water characteristics were observed with warmer and less saline waters around the reefs in October 2018 as compared to July 2019. Average values of Ω aragonite was 1.8 in October as compared 1.7 in July, A_T was 2305 as compared to 2311 µmol kg^{-1}, C_T was 2142 µmol kg^{-1} as compared to 2155 µmol kg^{-1} and pH was 8.03 as compared to 8.02 (***Figure 59***).

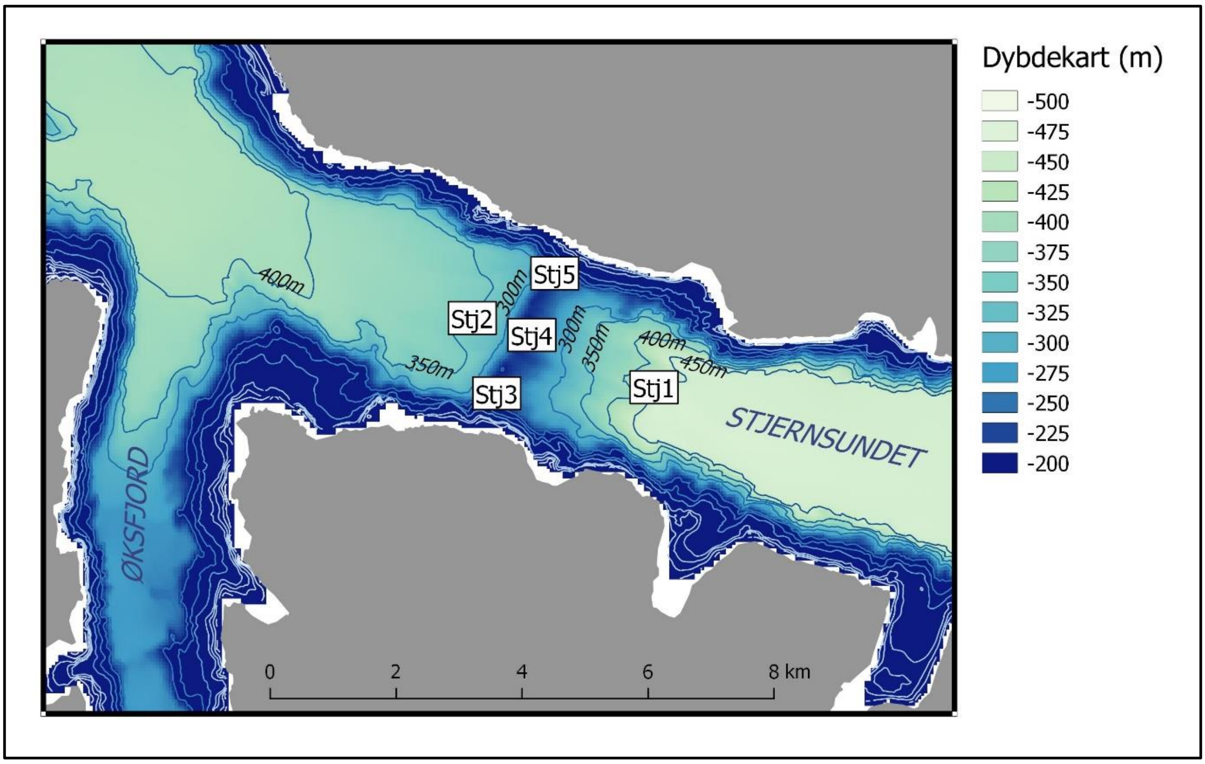

Figure 60. *Map of Stjernsund and the sampling locations.*

Figur 60. *Kart over Stjernsund og prøvelokaliteter*

In Stjernsund (***Figure 60***), carbonate chemistry variables were sampled two times throughout the year as a part of the seasonal study of ocean acidification variables. At the depths of the Stjernsund sill (approximately 200-350 m) we found that all measured variables, i.e. temperature, salinity, Ω aragonite, C_T, A_T and pH (***Figure 61***), were well within the range of that documented in other healthy cold-water coral settings in the Atlantic Ocean (Lunden et al. 2013; Findlay et al. 2014). Some seasonal differences were evident including warmer water masses and lower pH in September as compared to July, throughout the water column (***Figure 62***). In the deeper waters, below 200 m, C_T was lower in July as compared to September and Ω aragonite was slightly higher. For the deeper waters no clear seasonal trends were documented for A_T and C_T.

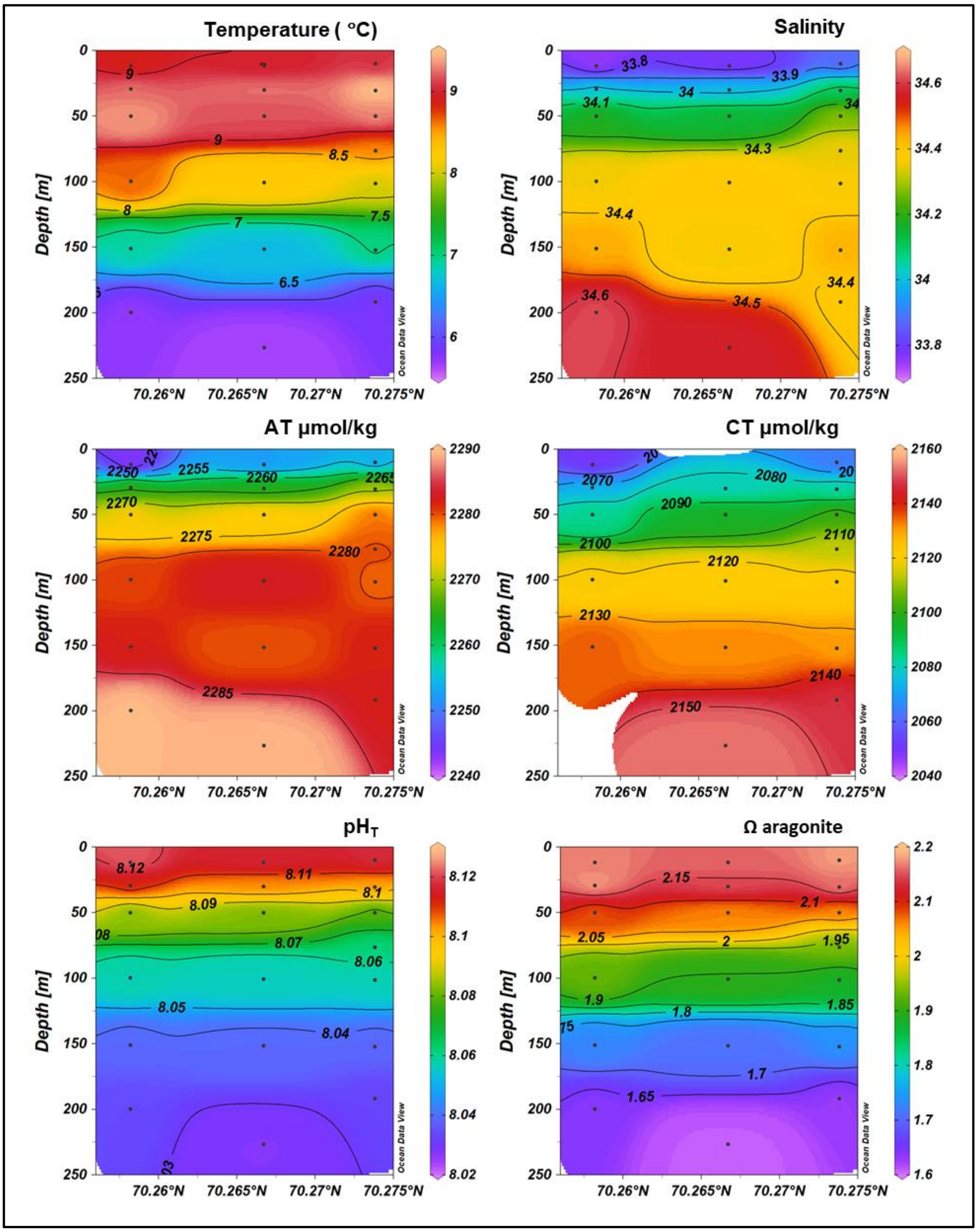

***Figure 61**. Temperature, salinity, C_T, A_T, pH and Ω aragonite in the water column across Stjernsund (Stj3-Stj5) on 22 September 2019.*

***Figur 61**. Temperatur, saltholdighet, C_T, A_T, pH og Ω aragonitt i vannsøylen over Stjernsund (Stj3-Stj5) den 22 september 2019.*

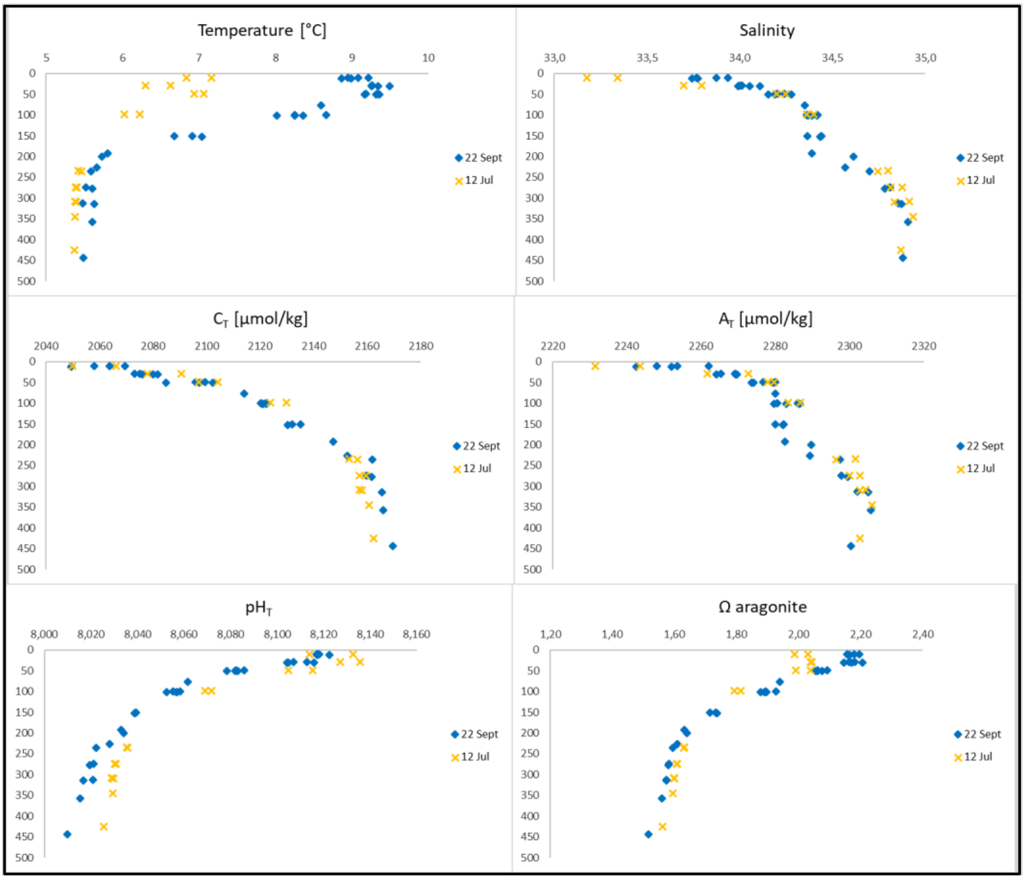

Figure 62*. Variations in temperature, salinity, C_T, A_T, pH and Ω aragonite in the water column at Stjernsund from 2 stations on 12 July and 5 stations on 22 September 2019.*

Figur 62*. Variasjon i temperatur, saltholdighet, C_T, A_T, pH og Ω aragonitt i vannsøylen ved Stjernsund fra to stasjoner den 12 juli og 5 stasjoner den 22 september 2019.*

At all northern Norwegian reefs, i.e. Korallen, Stjernsund, Fugløyrevene, Steinaværrevet and Hola reefs ROV video investigations were performed in July 2019 to visually assess the health status of the reefs and to sample *Lophelia pertusa* fragments for measurements of physiological and biological health indicators. The visual examination of Korallen, Stjernsund, Fugløyrevene and Steinaværrevet revealed high diversity of associated megafauna and a very high proportion of live versus dead coral framework indicating good health state of the reefs (Vad et al. 2017). The visual examinations of reefs in Hola revealed a high diversity of associated megafauna in some reefs but not others and a variable proportion of live versus dead coral framework between different reefs. It should, however, be noted that the reefs at Hola are of the elongated type that grow toward the current (Fosså et al. 2015) and are expected to have a higher proportion of exposed dead framework as compared to circular reefs. At the same cruise the health state of *Lophelia pertusa* corals were assessed. Coral metabolism, standardized to ash free dry weight, was within the range considered normal for *L. pertusa* at these temperatures; 3.6±0.1 µmol O_2 g^{-1} h^{-1} at Fugløya, 3.3±0.6 µmol O_2 g^{-1} h^{-1} at Korallen, 3.9±0.2 µmol O_2 g^{-1} h^{-1} at Stjernsund, 3.4±0.3 µmol O_2 g^{-1} h^{-1} at Steinavær and 5.9±0.7 µmol O_2 g^{-1} h^{-1} at Hola. Energy reserves in the coral fragments (measured as loss on ignition, LOI) were in the upper range of that normally found, indicating a good health state of the reefs. LOI was 9.4% at Hola, 7.0% at Fugløya, 6.7% at Korallen, 8.2% at Stjernsund and 5.8% at Steinavær.

3.5.3. Svalbard

3.5.3.1. Coastal water column stations in Isfjorden

The IsA station is located in the outer part of Adventfjorden, a small branch of the larger Isfjorden, on the west Spitsbergen coast. The IsG (SVR1) station is located in the outer part of Isfjorden. The Isfjorden system is mainly influenced by two external source waters. The Coastal Current (CC) brings relatively cold Arctic Water (ArW), originating from Barents Sea (e.g., Cottier et al. 2005; Nilsen et al. 2008). The West Spitsbergen Current (WSC) transports warmer and more saline Atlantic water (AW) off the continental shelf, which, enters occasionally into the fjords (e.g., Cottier et al. 2005; Nilsen et al. 2008; Nilsen et al. 2016). AW is to some extent mixed with ArW on the shelf, and forms Transformed Atlantic Water (TAW) when it enters the fjords. The water masses circulate counterclockwise around the fjord boundaries. Glacial meltwater is probably the most important freshwater source to the Isfjorden system (Nilsen et al. 2008). Moreover, the surrounding watershed of Adventfjorden brings a combination of snow and glacial runoff that reaches peak discharge during the summer season. This water has rather low concentrations of A_T and C_T. Measured and calculated values of 294 ± 3 and 339 ± 7 μmol kg^{-1} for A_T and C_T, respectively, were observed in the Adventdalen (Advent valley) riverbed in 2015 (Ericson et al. 2018).

Large seasonal variability is observed in the hydrography as well as in the carbonate chemistry at the IsA station (***Figure 63***). Depth and sampling data are displayed in ***Table 15, Appendix 6.2***. The lowest pH and Ω aragonite values were observed in May and November. Largest seasonal variability is observed in the upper 50 meters where Ω aragonite values range from 2.3 in July, likely as a consequence of CO_2 uptake through primary production to reach lowest values of near 1.4 at the end of November. The low pH and Ω aragonite values at the end of November is most likely caused by addition of CO_2 from below caused by increased upwelling in autumn, possibly induced by storms. This is supported by the homogenous C_T concentrations throughout the water column at this time. Highest values of A_T and C_T are observed in May and suggest influence of AW in the Isfjorden. This is supported by the high salinity and relatively warm water observed in May. Ericson et al. (2019) confirms the influence on the carbonate chemistry by regular intrusions of AW to the IsA station. This is the first year of ocean acidification monitoring in Isfjorden so no trend analysis can be performed.

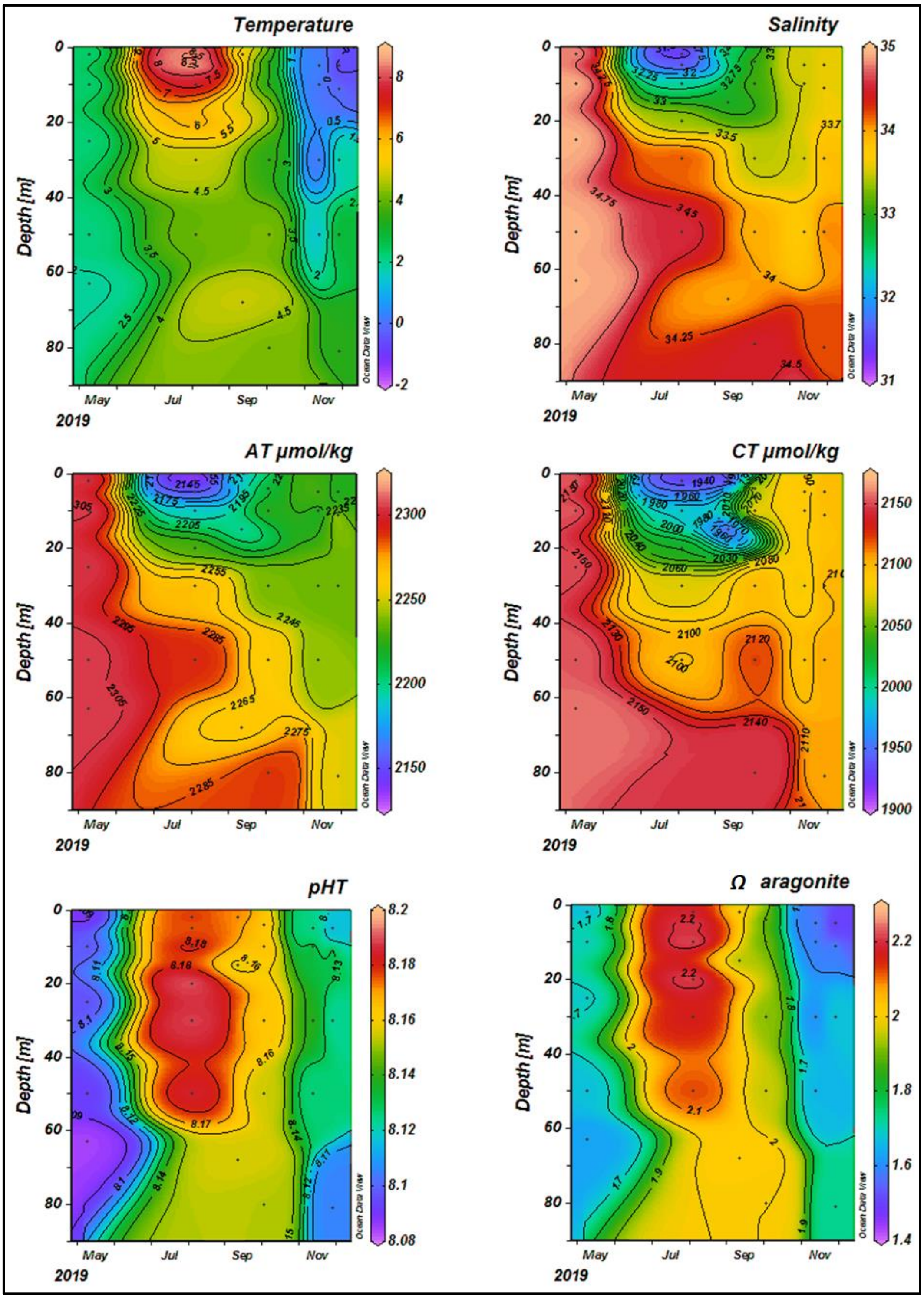

Figure 63*. Seasonal variability from May to November (x-axis) in the water column at IsA (y-axis, depth, m) of: salinity (upper left panel), temperature (upper right, °C), A_T (µmol kg^{-1}, mid left panel), C_T (µmol kg^{-1}, mid right panel), pH (pHT, lower left panel), and Ω aragonite (right panel).The black dots show the samples that were taken.*

Figur 63*. Sesongvariasjon fra mai til november (x-akse) i vannsøylen ved IsA (y-akse, dyp, m) av: saltholdighet (øvre venstre panel), temperatur (øvre høyre, °C), A_T (µmol kg^{-1}, midtre venstre panel), C_T (µmol kg^{-1}, midtre høyre panel), pH (nedre venstre panel), og Ω aragonitt (nedre høyre panel). Sorte prikker viser hvor prøver blitt tatt.*

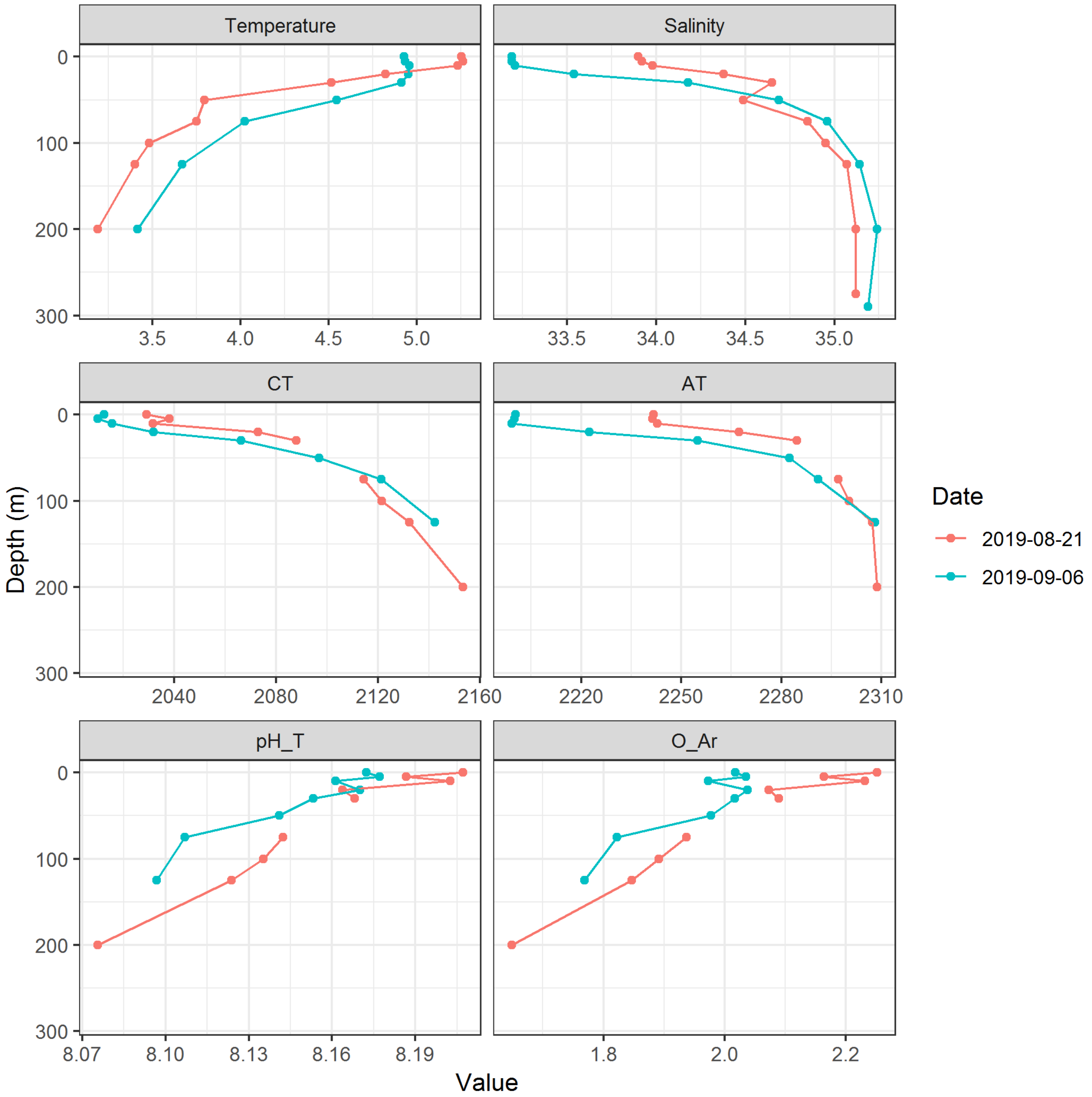

Figure 64. *Timeseries from Isfjorden/Grønnfjorden (SVR1) of temperature (°C), salinity, C_T (µmol kg^{-1}), A_T (µmol kg^{-1}), pH and Ω aragonite.*

Figur 64. *Dataserier fra Isfjorden/Grønnfjorden (SVR1) temperatur (°C), saltholdighet, C_T (µmol kg^{-1}), A_T (µmol kg^{-1}), pH og Ω aragonitt.*

The SVR1 station (Isfjorden/Grønnfjorden, IsG), was sampled twice in 2019 (August and September) and it is therefore not possible to describe the seasonal variation (***Figure 64***). Depth and sampling data are displayed in ***Table 16***, ***Appendix 6.2***. The station is located towards the mouth of Isfjorden, at a depth of approximately 270 m. The lowest pH (8.07) and Ω aragonite (1.65) values were found in the deeper waters (below 50 m) in higher salinity waters more characteristic of Atlantic Water (values missing for two deepest depths in September). There was a decrease in surface pH and Ω aragonite over the two-month period, related to a cooling and freshening of surface waters, even though there was a slight increase in chlorophyll *a* over the same period (***Figure 65***). The values at SVR1 were comparable to IsA during the same time period, however with slightly higher salinities, especially in the deeper waters (>35 below 125 m). This decrease in salinity inwards in Isfjorden is also seen in the surface (***Section 3.5.3.2***) and continuous (***Section 3.5.3.3***) measurements in Isfjorden.

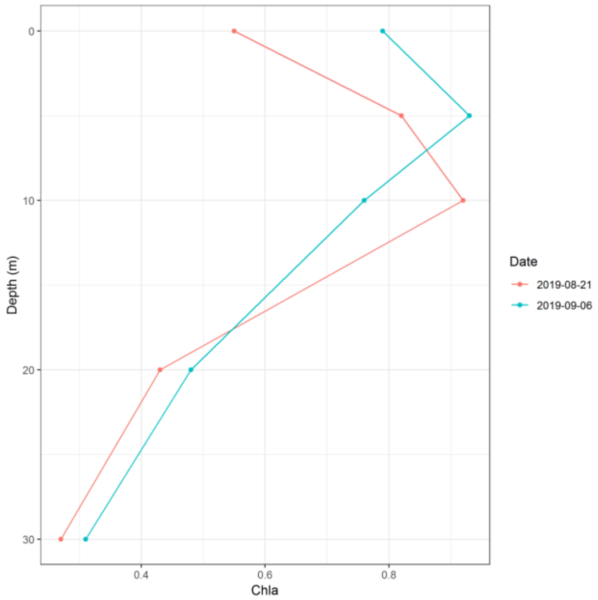

Figure 65*. Timeseries from Isfjorden/Grønnfjorden (SVR1) of chlorophyll a (µg L*$^{-1}$*).*

Figur 65*. Dataserier fra Isfjorden/Grønnfjorden (SVR1) for Klorofyll a (µg L*$^{-1}$*).*

3.5.3.2. Surface measurements in Isfjorden with RV Kronprins Haakon

In 2019, IMR conducted surveys in the Isfjorden, focusing on describing the carbonate chemistry in the surface water (***Figure 66***). Depth and sampling data are displayed in ***Table 17***, ***Appendix 6.2***. Two surveys were conducted in November onboard the RV *Kronprins Haakon* by taking water samples from the seawater intake for onboard analysis of A_T, C_T and pH. In November, pH ranged between 8.09 and 8.15 with highest values in the inner fjord, decreasing towards the outer part of Isfjorden and increased again at the Isfjorden entrance station. The Ω aragonite showed a similar trend and ranged between 1.65 and 1.45. The inner fjord showed a 0.1 Ω aragonite decrease, and a 0.02 pH decrease within the two weeks between the sampling periods. During this time salinity increased while the surface water cooled and C_T increased. The changes in surface water A_T were more variable, decreases in the inner fjord in contrast to increases in the central part. Since pH and Ω aragonite decreased it is likely a result of increased CO_2 through upwelling of subsurface water. Another possible explanation is the horizontal transport of high CO_2 in the Svalbard coastal current, bringing in cold and fresh Arctic water from the Barents Sea.

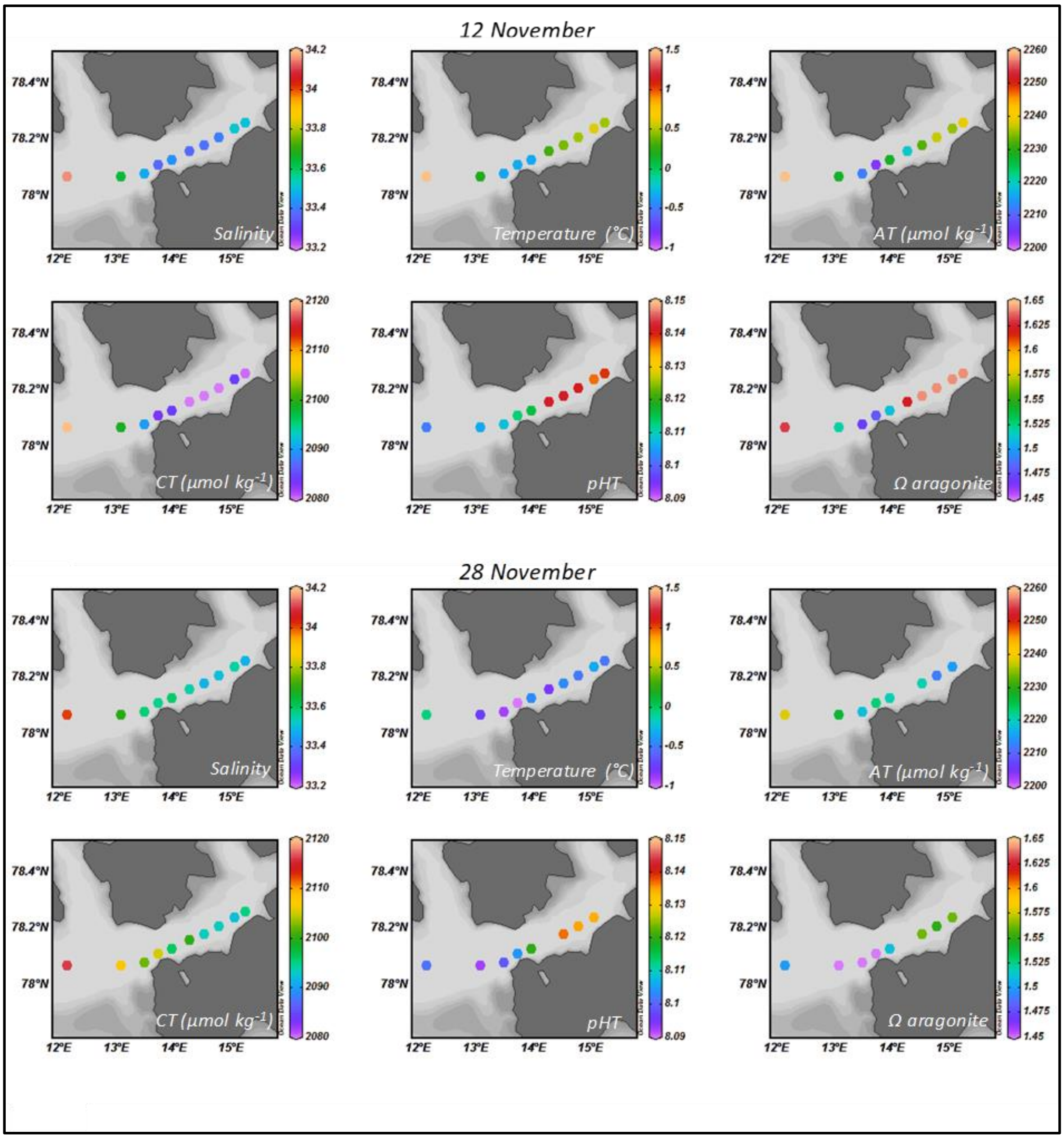

Figure 66. *Surface water data in Isfjorden on 12 November 2019 (upper six panels) and 28 November (lower six panels).*

Figur 66. *Data I overflaten i Isfjorden den 12 november (øvre seks paneler) og den 28 november (nedre seks paneler).*

3.5.3.3. Continuous measurements in Isfjorden with MS Norbjørn

The underway measurements by MS *Norbjørn* FerryBox in the Isfjorden vicinity were made approximately twice per month during trips between Tromsø and Longyearbyen. Seasonal variability in salinity, temperature, oxygen saturation (%), pH (total scale), and pCO_2 (µatm) are shown in ***Figure 67***. Surface waters were relatively saline and cold from January to June

2019 (~35 and <4 °C), and gradually became less saline (as low as 20 near Adventfjorden) and warmer (up to 10 °C) from July to October 2019, which was followed by a cooling period (<4 deg °C) after October 2019. Oxygen saturation was relatively low (<100 %) except for the period between June and August 2019 when phytoplankton biomass and productivity were higher, and this was somewhat reflected in the pH and pCO_2 observations (high pH and low pCO_2 in the summer/early autumn. By winter (November 2019), pH was relatively low (<8.1) and pCO_2 was relatively high (>300 µatm) and nearly 400 µatm in the outer Isfjorden region in November 2019.

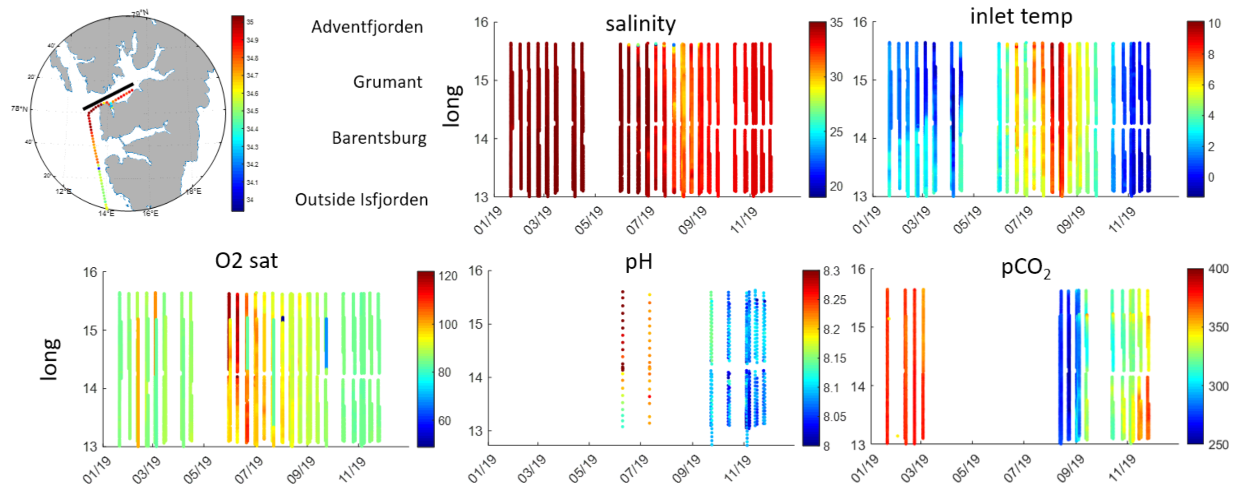

Figure 67. Timeseries from MS Norbjørn in Isfjorden of surface salinity, temperature (°C), oxygen saturation (%), pH, and pCO_2 (µatm).

Figur 67. Dataserier fra MS Norbjørn i Isfjorden for saltholdighet, temperatur (°C), oksygen metning (%), pH, og pCO_2 (µatm) i overflaten.

In terms of spatial variability in the Isfjorden region, three map plots of salinity, temperature, pH, and pCO_2 are shown from 7 June (top), 22 September (middle), and 24 November (bottom) 2019 in ***Figure 68***. In June 2019, strong gradients in salinity, temperature, and pH suggest that different water masses (and possibly as many as three) were captured in the transect from 77 °N to 78.2 °N. From the south, salinity of ~34.5 and temperature of 2-3°C were representative of an Arctic water mass, which was then followed by a salinity of ~35 and a temperature of ~4 °C that was representative of a North Atlantic water mass. Finally, in Isfjorden the salinity and temperature were 34.7-34.8 and ~5°C, respectively, which was representative of a fjord water mass. Variability in pH was also reflected in these three water masses with high pH (>8.3) in the Arctic water mass, pH between 8.05-8.2 in the North Atlantic water mass, and higher pH (>8.25) in the fjord water mass. Discrete C_T, A_T, and pH measurements made on the same 7 June cruise (***Section 3.3.3***) also confirm this spatial variability. Salinity, temperature, pH, and pCO_2 were less pronounced in the 22 September and 24 November observations, although temperature was ~2 °C warmer in Isfjorden compared to the coastal Svalbard part of the transect. This was likely due to less dynamic biological activity and land inputs during this time of the year. pH and pCO_2 observations on 24 November 2019 also agree well with Kronprins Haakon observations that were also made in November (***Figure 66***).

7 June 2019

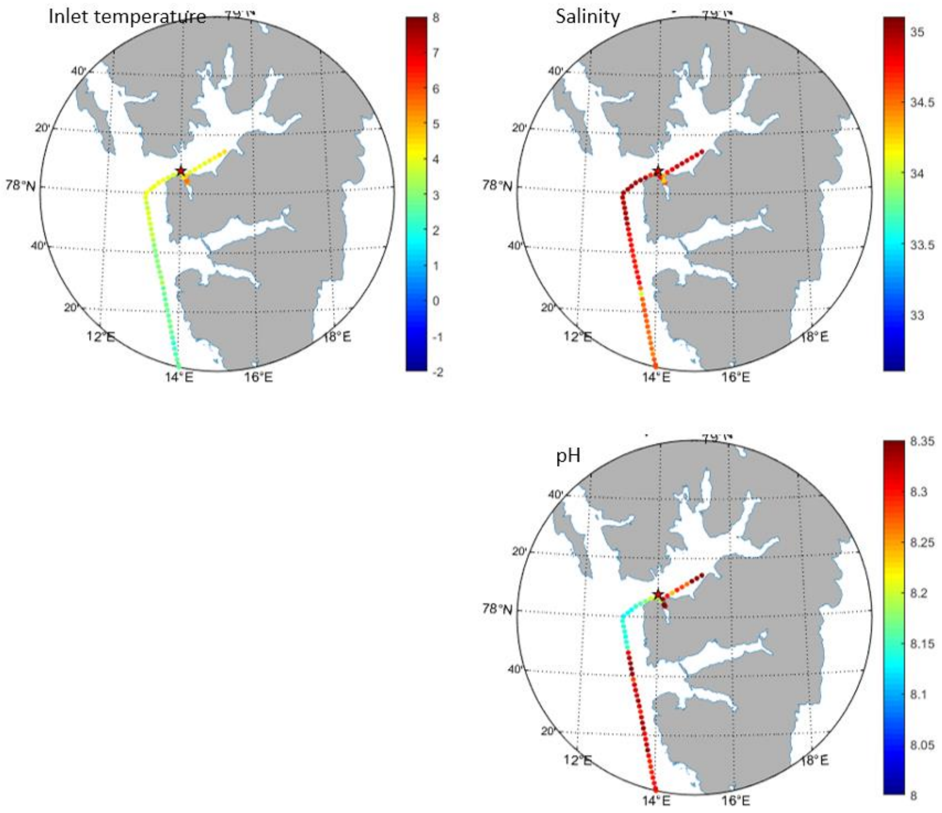

22 September 2019

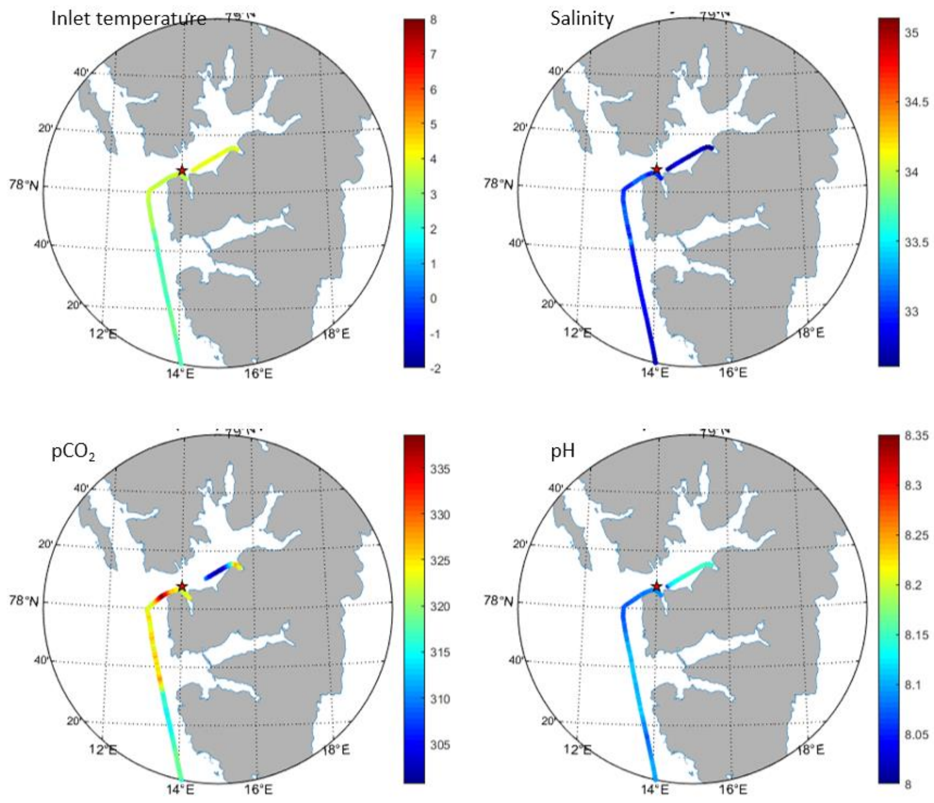

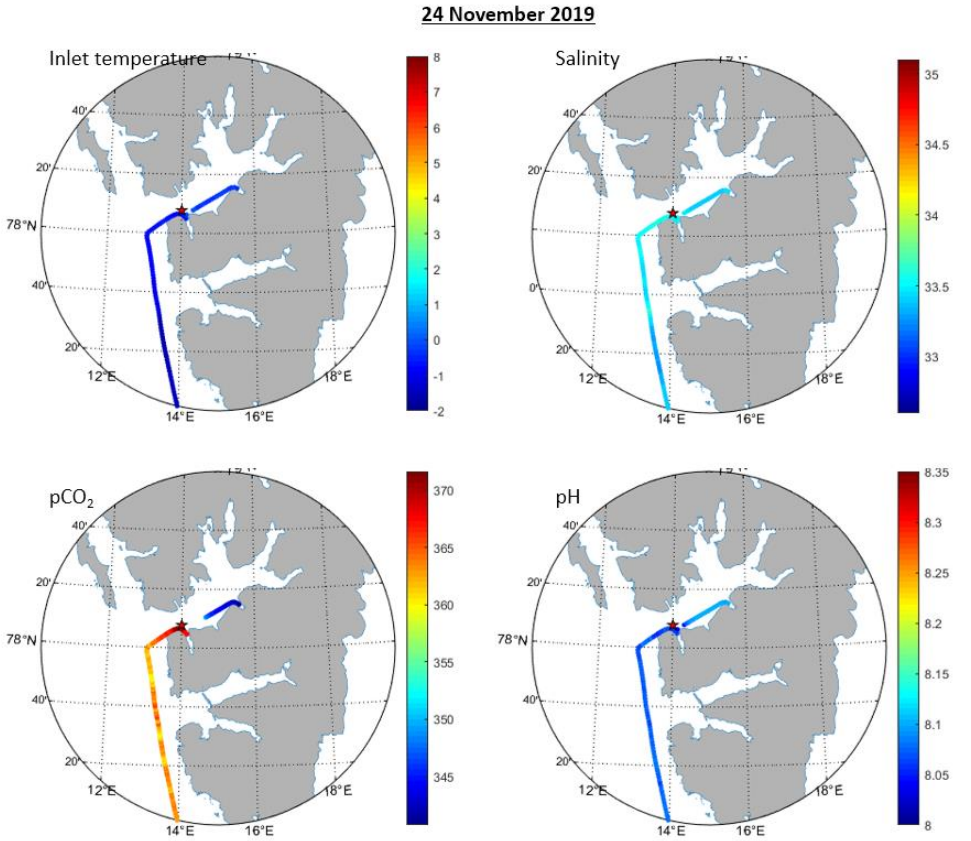

***Figure 68**. Continuous surface measurements from MS Norbjørn in Isfjorden (Svalbard) for temperature (°C), salinity, pH and pCO_2 (µatm) for June (top), September (middle) and November (bottom). Note that the temperature, salinity, and pH data for September 2019 were from 22 September, while the pCO_2 data were from 12 September.*

***Figur 68**. Kontinuerlige overflatemålinger fra MS Norbjørn i Isfjorden (Svalbard) for temperatur, saltholdighet, pH og pCO_2 (µatm) for juni (øverst), september (midt) og november (nederst). Merk at data for temperatur, saltholdighet og pH for september 2019 er fra 22 september, mens pCO_2 er fra 12 september.*

4. Conclusion and Recommendations

The Ocean Acidification monitoring program aims to get an overview of the state of ocean acidification in Norwegian waters and to better understand the variations from season to season and between years. The program started in 2013, and 2019 is the seventh consecutive year of measurements. This report also includes previous acidification data, e.g. from the Tilførselsprogrammet (2010-2012). The project "Monitoring of ocean acidification in the coastal zone" started in July 2019, and the first results from this monitoring program are descriped in ***Chapter 3.5***. There are three study regions in the project: Hardanger, Troms and Finnmark and Svalbard, and the results for 2019 demonstrate the large seasonal and regional variability in ocean acidification variables in Norwegian coastal waters, especially in the surface waters.

In the Skagerrak, the deepest parts of the water column have become warmer (0.22 °C yr^{-1}) and more saline (0.02 yr^{-1}) since 2010, which was an unusually cold year with consequences for the trend analysis. The warming and increased salinity at depths were attributed to increased volumes of Atlantic water entering the Skagerrak and the changes influenced pH and Ω aragonite, which over time decreased by 0.008 yr^{-1} and 0.01 yr^{-1}, respectively. As ocean temperatures are generally increasing, it will be interesting to monitor this region to investigate whether the trends persist or whether other circulation and mixing processes become important.

In the open oceanic surface waters of the Norwegian Sea, the time series data from Station M from 2011 to 2019 show decreasing trends in pH and Ω aragonite of 0.0033 yr^{-1} and 0.015 yr^{-1}, respectively. This is comparable to previous pH trend estimates of -0.0041 yr^{-1} in the Norwegian Basin surface water (Skjelvan et al., 2014; Jones et al., 2019). The C_T in the full water depth at Station M has increased over the last decade, which is connected to an increasing uptake of CO_2 from the atmosphere and, as a result, winter sea surface pCO_2 has increased by nearly 20 µatm over the last decade. The location of the saturation horizon (Ω aragonite = 1) in the Norwegian Sea was at ~1900 m depth at the Svinøy-NW section, around 2000 m at Station M, and between 1500 m and 2000 m at the Gimsøy-NW section. The seawater temperature and Ω aragonite in the Arctic water at 1000 and 1500 m depth at 1°E along the Svinøy-NW section shows interannual variability related to the variations in the mixing with Norwegian Sea Deep Water and Arctic water. Variations in Ω aragonite in the deep Norwegian Sea from 2011 to 2019 show interannual variability related to the presence of cold and fresh Arctic water and warmer Atlantic water mass.

Surface waters across the Barents Sea opening at 69-78 °N have freshened and cooled since 2013, which was accompanied by a decrease in pH by 0.002 per yr^{-1} in the northern part of the transect and Ω aragonite increase of 0.018 yr^{-1} in the southern part of the transect. For the northern Barents Sea, trends at 250-300 m depth at the 79.5 °N in the northern region showed a cooling of ~0.38 °C yr^{-1} and freshening of ~0.02 salinity units per year in the same period. This is likely due to increased sea ice melt in the Arctic domain that would result in cooler and fresher water being transported southwards. Trends in pH and Ω aragonite had large variability between years.

Water column data from seasonal time series provides information that can be used to develop scenarios for future CO_2 emissions, the ocean's absorption of anthropogenic CO_2, and how the depth of the calcium carbonate saturation horizon changes. Even though we begin to get more of an overview of geographic and temporal variation in the ocean acidification variables (Jones et al. 2019), and some of the seasonal drivers, it is too early to fully determine the individual dominant processes of ocean acidification and their regional, seasonal and intermediate variability. This requires further monitoring in a comprehensive manner, i.e. integrated measurements and studies of primary production, ocean physics, and land-sea interactions and exchanges. This may be conducted by dedicated process research cruises as well as using autonomous sensors on moorings measuring a set of biogeochemical variables in addition to pCO_2 and pH, such as dissolved oxygen, dissolved organic matter, chlorophyll *a* and particulate organic matter.

The trends show that variations from year to year result from both natural fluctuations in the oceanographic conditions and anthropogenic inputs. Additional data and expansion of the time series capture the longer-term variability as well as making more robust trend estimates. The rate of change in pH in surface waters of the Norwegian Sea (-0.0033 yr^{-1}) is faster than that reported for surface pH in the Iceland Sea during winter, which changes at a rate of -0.0024 yr^{-1} (Olafsson et al. 2009) for the period 1985–2008. However, the time series here is relatively short and extension of the time series in the Norwegian Sea is required, possibly to include 20 years of monitoring that has been carried out in the Icelandic Sea (Olafsson et al. 2009), to enable the determination of the relationship between anthropogenic influence and natural variation. However, the Norwegian monitoring program provides insight into how the trend may project to certain marine areas. For example, measurements show that the pH in the Norwegian and Lofoten basins decreases rapidly (Skjelvan et al., 2014), and in view of the abundant amounts of cold-water corals and spawning grounds for commercially important fish species in the area, it is very important to continue monitoring the ocean acidification trends. The monthly time series data at several coastal sites in this program have provided important insight into the seasonal dynamics and large natural variability along the coast, which has been very useful when trying to understand the changes in Norwegian inshore waters. The carbonate system measurements made in the Norwegian Sea and the Barents Sea in this program provide unique data from an area where there is a great deal of change related to climate, transport of warming Atlantic waters, decreasing sea ice cover and increased freshwater inputs. The program also contributes data and knowledge to the International Surface Surveillance Network (Global Network for the Ocean Acidification Observation GOA-ON and OSPAR study Group of Ocean Acidification-SGOA), IOC Intersessional carbonate chemistry forum, IGC-OA, and to recent IPCC report.

5. References

Agnalt, A-L, E.S. Grefsrud, E. Farestveit, M. Larsen, F. Keulder. 2013. Deformities in larvae and juvenile European lobster (*Homarus gammarus*) exposed to lower pH at two different temperatures, Biogeosciences 10 (12): 7883-7895.

Allemand D., É. Tambutté, D. Zoccola, S. Tambutté. Coral Calcification, Cells to Reefs. In: Dubinsky Z., Stambler N. (eds) Coral Reefs: An Ecosystem in Transition. Springer, Dordrecht, 2011.

Allison N., I. Cohen, A. Finch, J. Erez, A. W. Tudhope. Corals concentrate dissolved inorganic carbon to facilitate calcification. Nature Communications 5, 5741, 2014.

AMAP, 2013. AMAP Assessment 2013: Arctic Ocean Acidification. Arctic Monitoring and Assessment Programme (AMAP), Oslo, Norway. viii + 99 pp.

Andersen, S., E.S. Grefsrud, T. Harboe. 2013. Effect of increased pCO_2 level on early shell development in great scallop (*Pecten maximus* Lamarck) larvae. Biogeosciences, 10: 6161-6184.

Boe R., V. K. Bellec, M. F. J. Dolan, P. Buhl-Mortensen, L. Buhl-Mortensen, D. Slagstad, L. Rise. Giant sandwaves in the Hola glacial trough off Vesteralen, North Norway. Marine Geology 267:36-54, 2019.

Buhl-Mortensen P., Coral reefs in the Southern Barents Sea: habitat description and the effects of bottom fishing, Marine Biology Research, 2017.

Carstensen, J., M. Chierici, B. G. Gustafsson, and E. Gustafsson. Long-term and seasonal trends in estuarine and coastal carbonate systems. Global Biogeochemical Cycles, 32: 497–513, 2018.

Cathalot C., D. Van Oevelen, T. Cox, T. Kutti, M. Lavaleye, G. Duineveld, F. J. R. Meysman. Cold-water coral reefs: hotspots of benthic carbon cycling in the deep-sea. Frontiers in Marine Science 2:37, 2015.

De Clippele L. H., V. A. I. Huvenne, T. N. Molodtsova and J. M. Roberts JM. The Diversity and Ecological Role of Non-scleractinian Corals (Antipatharia and Alcyonacea) on Scleractinian Cold-Water Coral Mounds Frontiers in Marine Science 6:184, 2019.

Chierici, M., A. Fransson, Nojiri,Y. 2006. Biogeochemical processes as drivers of surface fCO_2 in contrasting provinces in the subarctic North Pacific, GBC, 20, doi:10.1029/2004GB002356.

Chierici, M., I. Skjelvan, M. Norli, K.Y. Børsheim, S. K. Lauvset, H.H. Lødemel, K. Sørensen, A.L. King, T. Johannessen. 2017. Overvåking av havforsuring i norske farvann i 2016, Report (in Norwegian), Miljødirektoratet, M-776|2017.

Chierici, M., I. Skjelvan, M. Norli, E. Jones, K.Y. Børsheim, S. K. Lauvset, H.H. Lødemel, K. Sørensen, A.L. King, T. Kutti, A. Renner, A. Omar, T. Johannessen. 2016. Overvåking av havforsuring i norske farvann i 2015, Report (in Norwegian), Miljødirektoratet, M-573|2016.

Dickson, A. G. & F. J. Millero. 1987. A comparison of the equilibrium constants for the dissociation of carbonic acid in seawater media. Deep-Sea Res. 34, 1733-1743.

Dickson, A.G. 1990. Standard potential of the reaction: AgCl(s) + ½H2(g) = Ag(s) + HCl(aq), and the standard acidity constant of the ion HSO4 – in synthetic sea water from 273.15 to 318.15 K. *J. Chem. Thermodyn.* 22: 113–127.

Dickson, A.G., C.L. Sabine, J.R. Christian (eds.). Guide to Best Practices for Ocean CO_2 Measurements. PICES Special Publication 3, IOCCP Report 8, 191 pp, 2007.

Dupont, S., H. Pörtner. 2013. A snapshot of ocean acidification research. *Marine Biology*,160:1765–1771. doi:10.1007/s00227-013-2282-9.

Farfan G. A., E. E. Cordes, R. G. Waller, T. M. DeCarlo and C. M. Hansel CM. Mineralogy of Deep-Sea Coral Aragonites as a Function of Aragonite Saturation State. Frontiers in Marine Science 5:473, 2018.

Findlay H. S., S. J. Hennige. Fine-scale nutrient and carbonate system dynamics around cold-water coral reefs in the northeast Atlantic. Scientific Reports. 4: 3671, 2014.

Flögel S., C. W. Dullo. Geochemical and physical constraints for the occurrence of living cold-water corals. Deep Sea Research Part II: Topical Studies in Oceanography 99(0): 19-26, 2014.

Fosså J. H., T. Kutti, P. Buhl-Mortensen, H. R. Skjoldal. Vurdering av Norske korallrev. Rapport fra Havforskningen 8-2015, 2015.

Fransson, A., M. Chierici., D. Nomura, M. A. Granskog, S. Kristiansen, T. Martma, G. Nehrke. 2015. Effect of glacial drainage water on the CO2 system and ocean acidification state in an Arctic tidewater-glacier fjord during two contrasting years, Journal of Geophysical Research: Oceans DOI 10.1002/2014JC010320.

Freiwald A., J. H. Fosså, A. Grehan, T. Koslow, J. M. Roberts. Cold-water coral reefs. Out of sight no longer out of mind. UNEP-WCMC. Page 84, Cambridge, UK, 2004.

Friedlingstein et al. Global carbon budget 2019, Earth Syst. Sci. Data, 11, 1783–1838, https://doi.org/10.5194/essd-11-1783-20192019, 2019.

Freiwald A., L. Beuck, M. Wisshak. Korallenriffe im kalten Wasser des Nordatlantiks - Entstehung, Artenvielfalt und Gefährdung. In: Beck E (ed) Die Vielfalt des Lebens. Wiley-VCH, Weinheim, pp 89-96, 2012.

Frigstad, H., Ø. Kaste, A. Deininger, K. Kvalsund, G. Christensen, R.G.J. Bellerby, K. Sørensen, M. Norli, A. L. King. Influence of riverine input on Norwegian coastal systems. Frontiers in Marine Science, In Press

Guinotte J. M., J. Orr, S. Cairns, A. Freiwald, L. Morgan, R. George R. Will human induced changes in seawater chemistry alter the distribution of deep-sea scleractinian corals? Front Ecol Environ 4: 141-146, 2016.

Gundersen C. B., Ø. Kaste, J. Sample, H. F. Veiteberg Braaten, J. R. Selvik, D. H. Hjermann, M. D. Norling, J. L. Guerrero Calidonio. The Norwegian river monitoring programme – water quality status and trends in 2018. Norwegian Environment Agency report M-1508, 2019.

Hennige S. J., L. C. Wicks, N. A. Kamenos, G. Perna, H. S. Findlay, J. M. Roberts. Hidden impacts of ocean acidification to live and dead coral framework. Proc. R. Soc. B 282: 20150990, 2015.

Ingle, S.E. 1975. Solubility of calcite in the ocean. *Mar. Chem.*, 3.

Järnegren, J., T. Kutti. 2014. Lophelia pertusa in Norwegian waters. What have we learned since 2008? - NINA Report 1028. 40 pp. ISSN: 1504-3312. ISBN: 978-82-426-2640-0.

Johannessen, T., K. Sørensen, K.Y. Børsheim, A. Olsen, E. Yakushev, A. Omar & T.A. Blakseth. Tilførselsprogrammet 2010. Overvåking av forsuring av norske farvann med spesiell fokus på Nordsjøen. Report (in Norwegian), KLIF, TA 2809-2011, 2011.

Jonsson L. G., P. G. Nilsson, F. Floruta, T. Lundälv. Distributional patterns of macro- and megafauna associated with a reef of the cold-water coral Lophelia pertusa on the Swedish west coast. Marine Ecology Progress Series 284: 163-171, 2004.

Jones, E., M. Chierici, I. Skjelvan, M. Norli, K.Y. Børsheim, H.H. Lødemel, T. Kutti, K. Sørensen, A.L. King, K. Jackson & T. de Lange, Monitoring of the ocean acidification in Norwegian seas in 2017, Report, Miljødirektoratet, M-1072, 2018.

Jones, E., M. Chierici, I. Skjelvan, M. Norli, K.Y. Børsheim, H.H. Lødemel, K. Sørensen, A.L. King, S. Lauvset, K. Jackson, T. de Lange, T. Johannsessen & C. Mourgues. Monitoring ocean acidification in Norwegian seas in 2018, Rapport, Miljødirektoratet, M-1417|2019, 2019.

Le Quéré, C. et al. 2016. Global carbon budget 2016, *Earth Syst. Sci. Data* 8, 405-448.

Le Quéré, C. et al. 2018. Global carbon budget 2017, *Earth Syst. Sci. Data* 10, 605-649.

Lindberg B., C. Berndt, J. Mienert J. The Fugløy reefs on the Norwegian-Barents continental margin: cold-water corals at 70 N, their acoustic signature, geologic, geomorphologic and oceanographic setting. International Journal of Earth Sciences 96 (1). pp. 201-213, 2007.

Lunden J. J., S. E. Georgian, E. E. Cordes. Aragonite saturation states at cold-water coral reefs structured by Lophelia pertusa in the northern Gulf of Mexico. Limnology and Oceanography 58:354-362, 2013.

McCulloch M., J. Trotter, P. Montagna, J. Falter, R. Dunbar, A. Freiwald, G. Försterra, M. López Correa, C. Maier, A. Rüggeberg, M. Taviani, R. Thresher. Boron Isotope Systematics of Cold-water Scleractinian Corals: Internal pH Up-regulation and Response to Ocean Acidification. Geochimica et Cosmochimica Acta 87: 21-34, 2012

Mehrbach, C., C.H. Culberson, E.J. Hawley, R M. Pytkowicz. 1973. Measurements of the apparent dissociation constants of carbonic acid in seawater at atmospheric pressure. *Limnol. Oceanogr*. 18, 897-907.

Mortensen, P.B., M.T. Hovland, J.H. Fosså, D.M. Furevik. 2001. Distribution, abundance and size of Lopheliapertusa coral reefs in mid-Norway in relation to seabed characteristics. *J. Mar. Biol. Asso*. U.K 81, 581-597.

Mortensen P. B., J. H. Fosså. Species diversity and spatial distribution of invertebrates on Lophelia reefs in Norway. In: Suzuki Y, Nakamori T, Hidaka M, Kayanne H, Casareto BE, Nadaoka K, Yamano H, Tsuchiya M (eds) Proc 10th Int Coral Reef Symp. Okinawa, p 1849-1868, 20016

Mucci, A. 1983. The solubility of calcite and aragonite in seawater at various salinities, temperatures and at one atmosphere pressure, *Am. J. Sci.*, 283, 780–799, doi:10.2475/ajs.283.7.780.

Nilsen F., F. Cottier, R. Skogseth, S. Mattsson. Fjord–shelf exchanges controlled by ice and brine production: the interannual variation of Atlantic Water in Isfjorden, Svalbard. Cont. Shelf Res., 28, 1838–1853, 2008.

Nilsen F., R. Skogseth, J. Vaardal-Lunde. A Simple Shelf Circulation Model: Intrusion of Atlantic Water on the West Spitsbergen Shelf. J. of Phys. Oceanogr., 15, 2016.

Olafsson, J., S.R. Olafsdottir, A. Benoit-Cattin, M. Danielsen, T.S. Arnarson, T. Takahashi. 2009. Rate of Iceland Sea acidification from time series measurements, Biogeosciences, 6, 2661-2668, doi:10.5194/bg-6-2661-2009.

Orr, J. C., V. J. Fabry, O. Aumont et al. 2005. Anthropogenic ocean acidification over the twenty-first century and its impact on calcifying organisms. *Nature* 437, 681-686.

Pierrot, D., E. Lewis, D.W.R. Wallace. MS Excel Program Developed for CO2 System Calculations. ORNL/CDIAC-105a. Carbon Dioxide Information Analysis Center, Oak Ridge National Laboratory, U.S. Department of Energy, Oak Ridge, Tennessee. doi: 10.3334/CDIAC/otg.CO2SYS_XLS_CDIAC105a, 2006.

Pierrot Pierrot, D., C. Neill, K. Sullivan, R. Castle, R. Wanninkhof, H. Lüger, T. Johannessen, A. Olsen, R.A. Feely, C.E. Cosca. 2009. Recommendation for autonomous underway pCO_2 measuring systems and data-reduction routines, Deep-Sea Res. II, 56, 512-522, doi:10.1016/j.dsr2.2008.12.005.

Rheuban, J. E., S. C. Doney, D. C. McCorkle, R. W. Jakuba. Quantifying the effects of nutrient enrichment and freshwater mixing on coastal ocean acidification. Journal of Geophysical Research: Oceans, 124, 2019.

Rovelli L., K. M. Attard, L. D. Bryant, S. Flögel. Benthic O2 uptake of two cold-water coral communities estimated with the non-invasive eddy correlation technique. Mar Ecol Prog Ser 525:97-104, 2015.

Rüggeberg A., S. Flögel, W. C. Dullo, K. Hissmann, A. Freiwald. Water mass characteristics and sill dynamics in a subpolar cold-water coral reef setting at Stjernsund, northern Norway. Marine Geology 282: 5-12, 2011.

Salisbury J., M. Green, C. Hunt, J. Campbell. Coastal acidification by rivers: A new threat to shellfish? Eos, Transactions, American Geophysical Union 89(50):513, 2008.

Skjelvan, I., E. Falck, F. Rey, S.B. Kringstad. 2008. Inorganic carbon time series at Ocean Weather Station M in the Norwegian Sea, *Biogeosci.*, 5, 549-560.

Skjelvan, I., E. Jeansson, M. Chierici, A. Omar, A. Olsen, S. Lauvset, T. Johannessen. 2014. Ocean acidification and uptake of anthropogenic carbon in the Nordic Seas, 1981-2013, Report (in Norwegian), Norwegian Environment Agency, M244-2014.

Skjelvan, I., A. M. Omar. 2015. Status of knowledge about ocean acidification in fjords at the west coast of Norway, Report (in Norwegian), Norwegian Environment Agency, M426-2015.

Skjelvan, I., M. Chierici, K. Sørensen, K. Jackson, T. Kutti, H. L. Lødemel, A. King, E. Reggiani, M. Norli, R. Bellerby, E. Yakushev, A. M. Omar. 2016. Ocean acidification in western Norwegian fjords and CO_2 variability in Lofoten, Report (in Norwegian), Norwegian Environment Agency, M642-2016.

Steinacher, M., F. Joos, T.L. Frölicher, G.-K. Plattner, S.C. Doney. 2009. Imminent ocean acidification in the Arctic projected with the NCAR global coupled carbon cycle-climate model. *Biogeosciences* 6, 515-533.

Sutton, A.J., C.L. Sabine, S. Maenner-Jones, N. Lawrence-Slavas, C. Meinig, R.A. Feely, J.T. Mathis, S. Musielewicz, R. Bott, P.D. McLain, H.J. Fought, A. Kozyr. 2014. A high-frequency atmospheric and seawater pCO2 data set from 14 open-oceansites using a moored autonomous system, *Earth Syst. Sci. Data*, 6, 353-366.

Takahashi, T, S.C. Sutherland, R. Wanninkhof et al. 2009. Climatological mean and decadal change in the surface ocean pCO_2 and net sea-air CO_2 flux over the global oceans. *Deep-Sea Res. II* 56, 554-577.

Takahashi, T, S.C. Sutherland, D.W. Chapman, J.G. Goddard, C. Ho, T. Newberger, C. Sweeney, D.R. Munro. 2014. Climatological distributions of pH, pCO_2, total CO_2, alkalinity, and $CaCO_3$ saturation in the global surface ocean, and temporal changes at selected locations. *Marine Chemistry* 164, 95-125.

Talmange, S. C., C. J. Gobler. 2009. The effects of elevated carbon dioxide concentrations on the metamorphosis, size, and survival of larval hard clams (Mercenariamercenaria), bay scallops (Argopectenirradians) and Eastern oysters (Crassostreavirginia). *Limnol. Oceanogr*. 54, 2072-2080.

Turley, C.M., J.M. Roberts, J.M. Guinotte. 2007. Corals in deep-water: will the unseen hand of ocean acidification destroy cold-water ecosystems? Coral Reefs 26, 445-448.

Vad J., C. Orejas, J. Moreno-Navas, H. S. Findlay, J. M. Roberts. (2017), Assessing the living and dead proportions of cold-water coral colonies: implications for deepwater Marine Protected Area monitoring in a changing ocean. PeerJ 5:e3705, 2017

Østerhus, S., T. Gammelsrød. 1999. The abyss of the Nordic Seas is warming, *Jour. of Climate*, 2(11), 3297-3304.

6. Appendix

6.1 Plots

Station M.

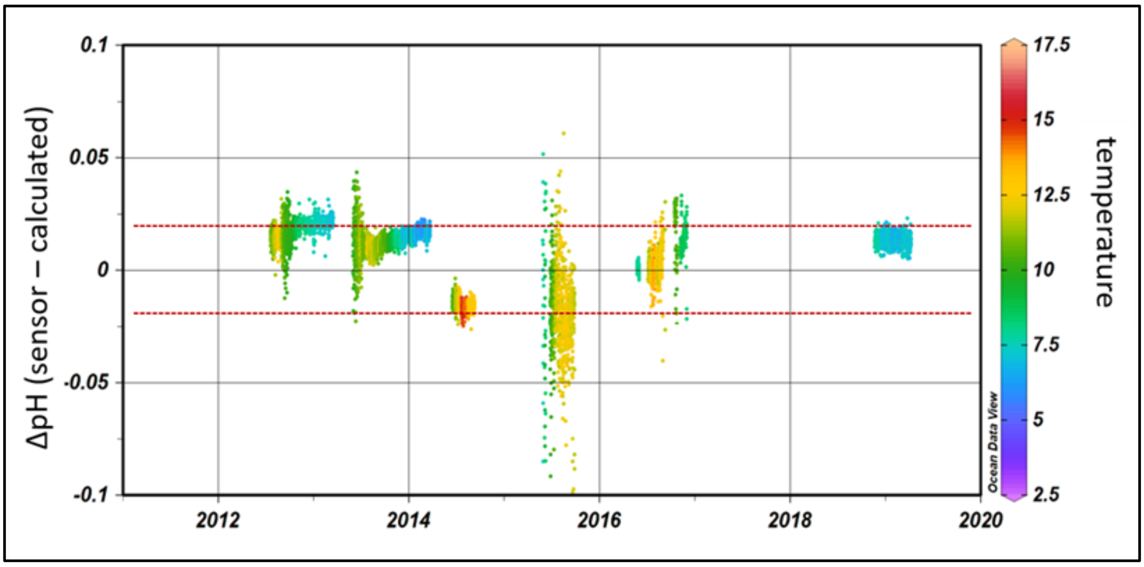

Figure 69. *Difference between measured and calculated pH. The red dashed lines represent the weather goal accuracy for pH of 0.02. Data from Station M.*

Figur 69. *Forskjell mellom målt og beregnet pH. De stiplede røde linjene representerer pH-nøyaktighet 0,02 ("weather goal"). Data fra Stasjon M.*

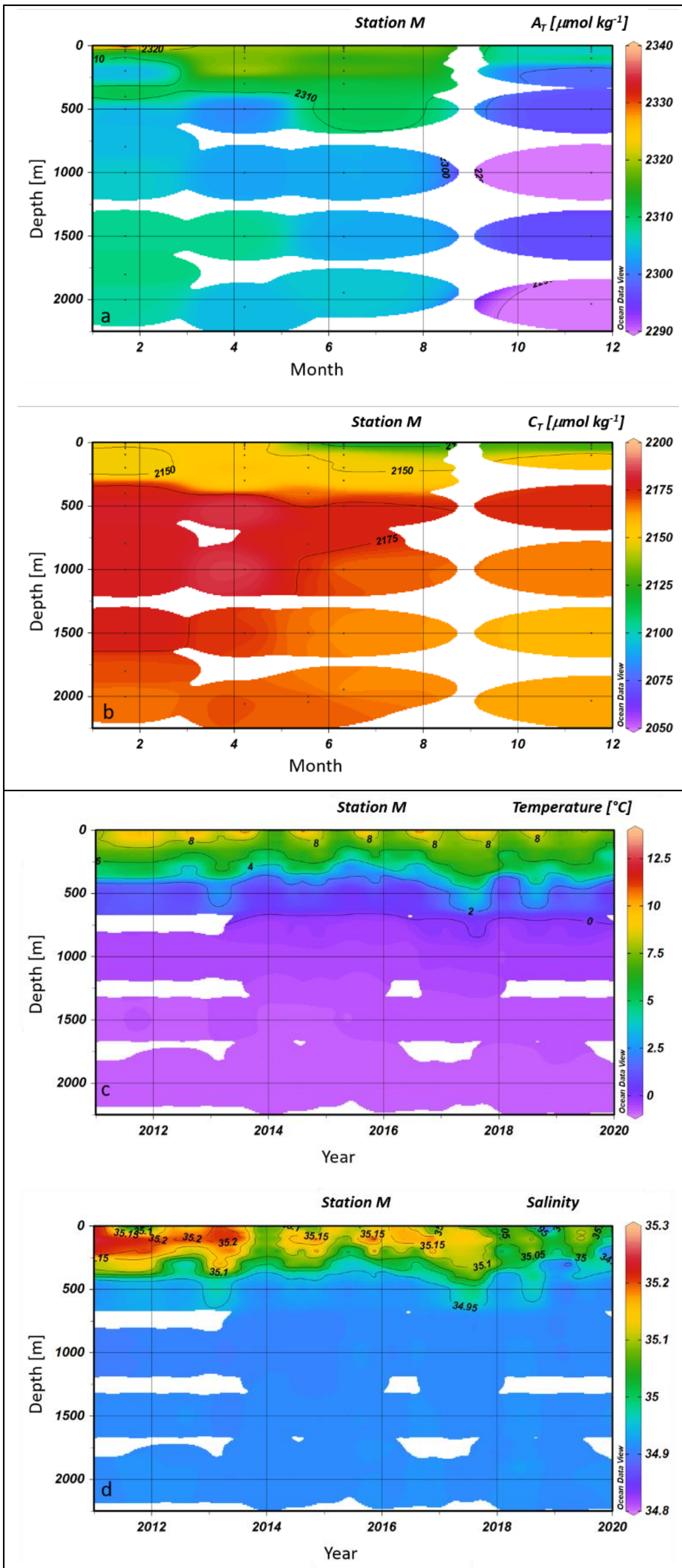

***Figure 70**. a) A_T and b) C_T from Station M in 2019, where black dots indicate sample depths, and c) temperature and d) salinity at the station during the years 2011-2019.*

***Figur 70**. a) A_T og b) C_T fra stasjon M i 2019, der svarte prikker viser prøvedyp, og c) temperatur og d) saltholdighet fra stasjonen i årene 2011-2019.*

Water column data from Torungen-Hirtshals section.

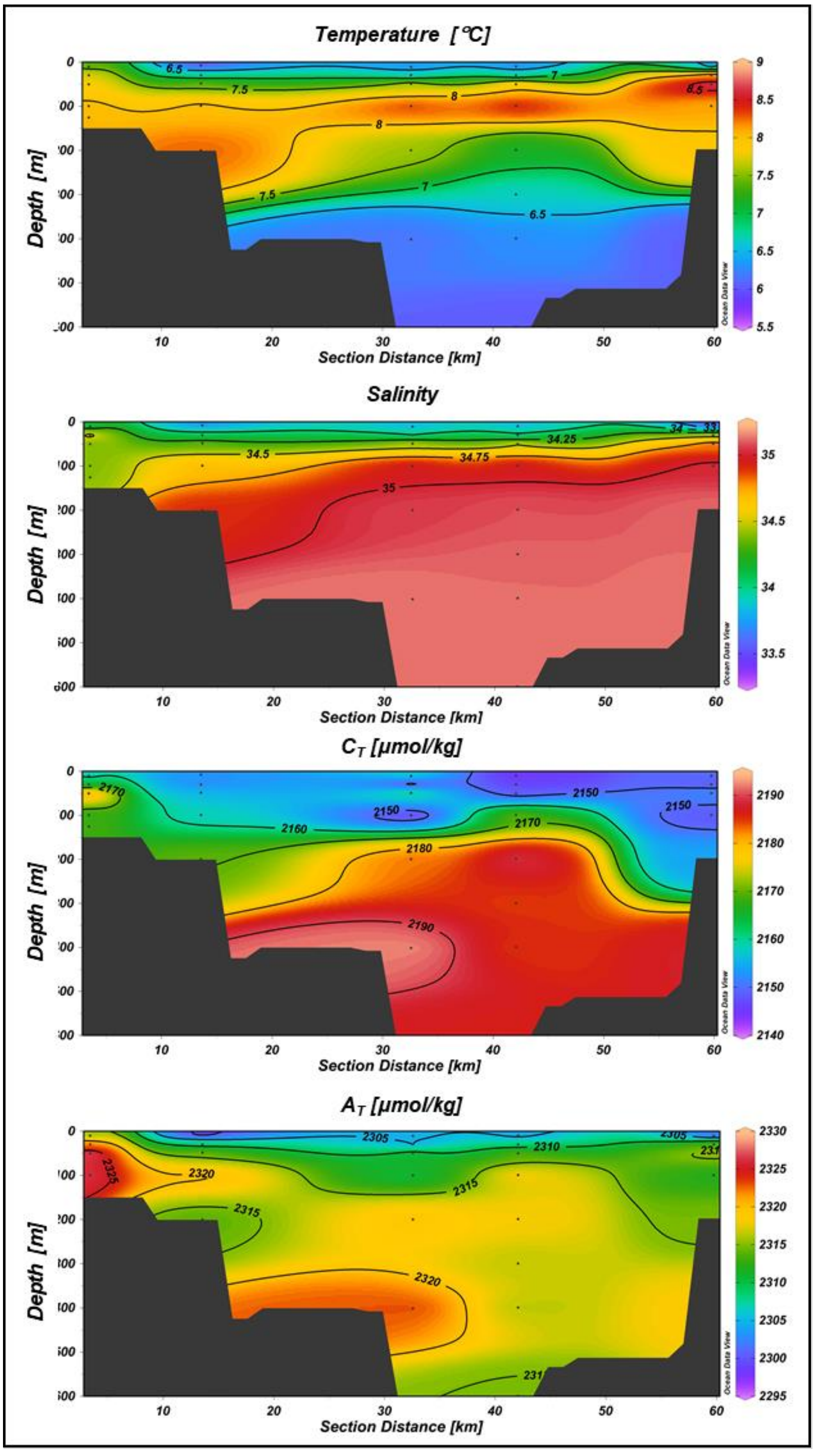

Figure 71. *Temperature, salinity, C_T and A_T from Torungen-Hirtshals in January 2019. Black dots indicate sample depths.*

Figur 71. *Temperatur, saltholdighet, C_T and A_T langs Torungen-Hirtshals snittet i januari 2019. Svarte prikker viser prøvedyp.*

Water column data from Arendal coastal station.

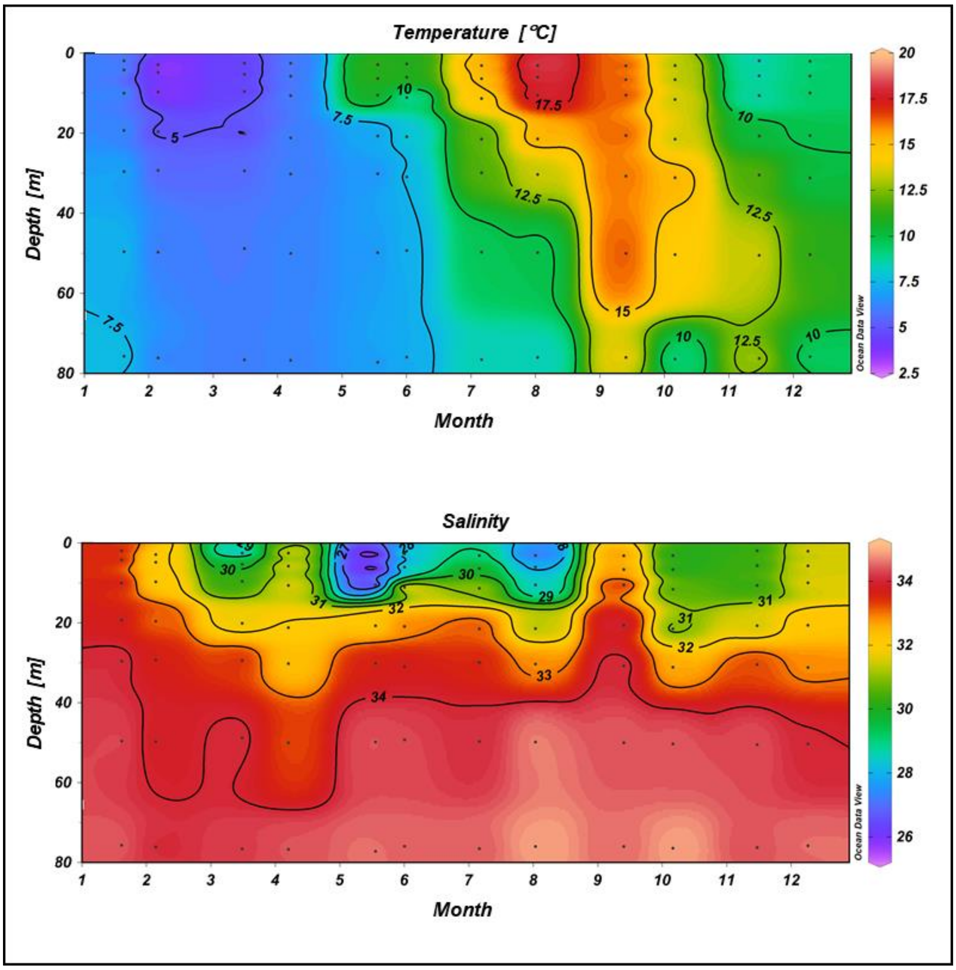

Figure 72. Monthly temperature and salinity in the upper 80 m at Arendal coastal station in 2019. Black dots indicate sample depths.

Figur 72. Månedlig temperatur og saltholdighet i de øverste 80 m ved Arendal kyststasjon i 2019. Svarte prikker viser prøvedyp.

Water column data from Svinøy-NW section.

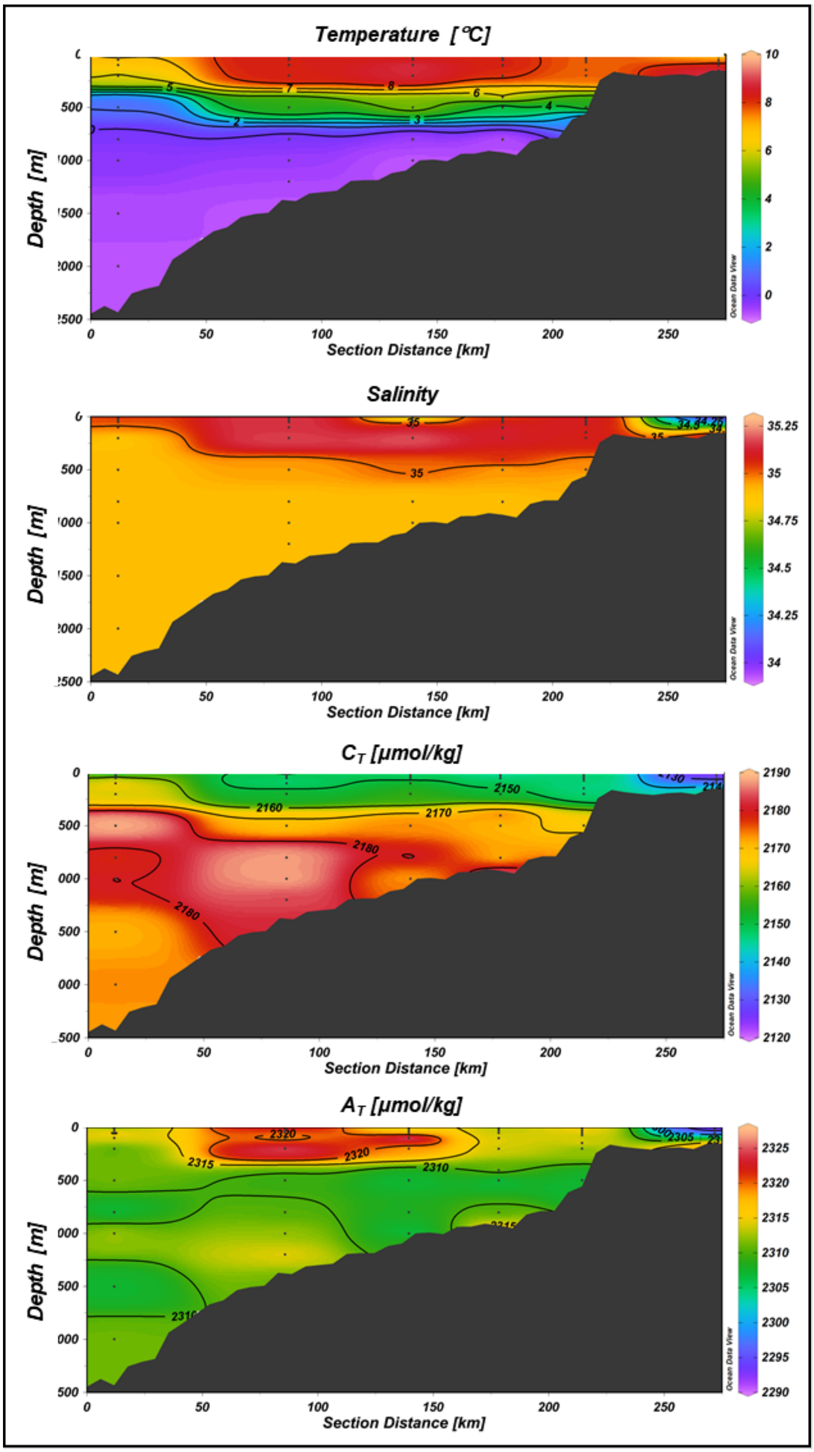

***Figure 73**. Temperature, salinity, C_T and A_T from Svinøy-NW in January 2019. Black dots indicate sample depths.*

***Figur 73**. Temperatur, saltholdighet, C_T and A_T langs Svinøy-NV snittet i januari 2019. Svarte prikker viser prøvedyp.*

Water column data from Gimsøy-NW section.

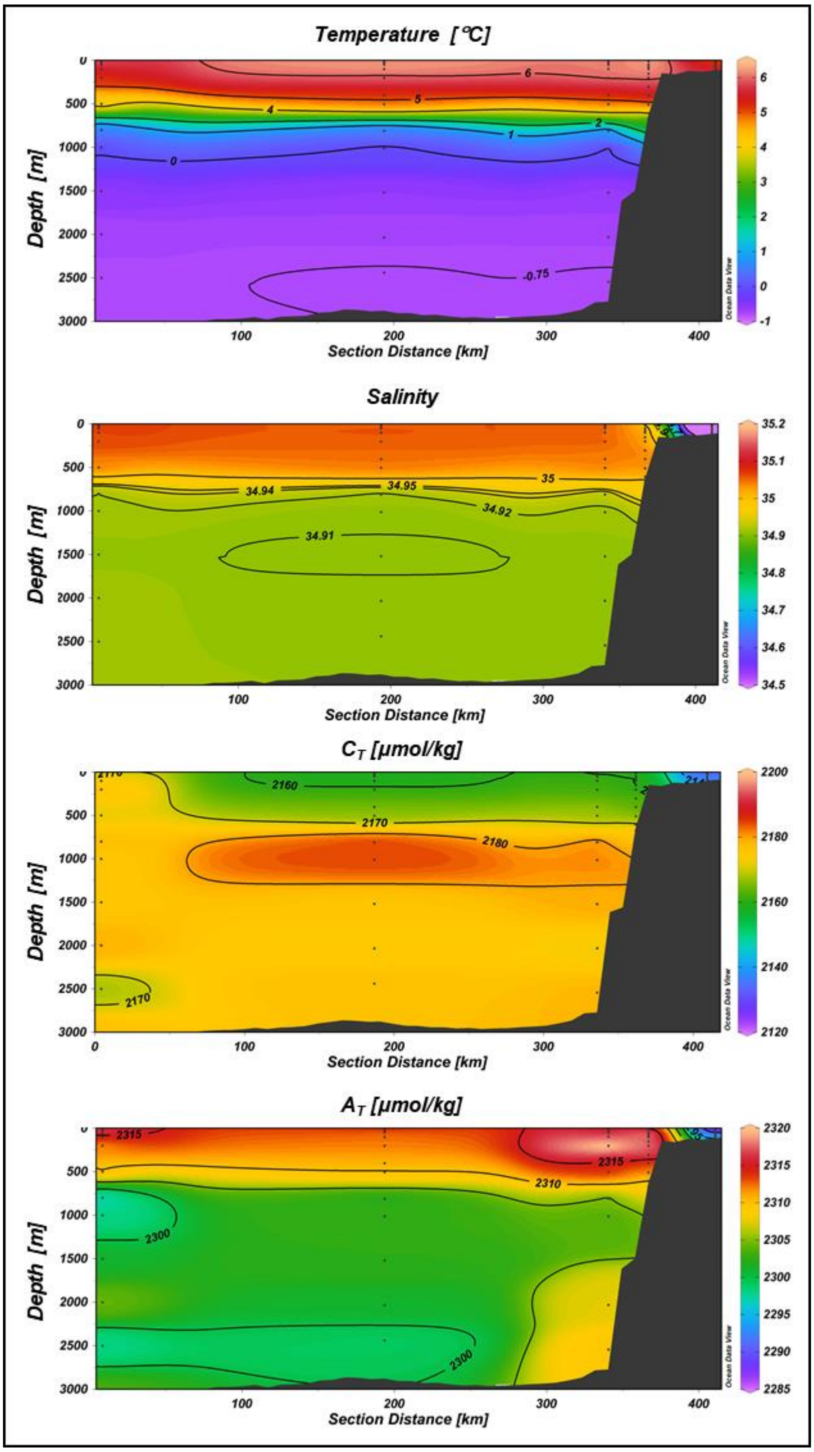

***Figure 74**. Temperature, salinity, C_T and A_T from Gimsøy-NW in January 2019. Black dots indicate sample depths.*

***Figur 74**. Temperatur, saltholdighet, C_T and A_T langs Gimsøy-NV snittet i januari 2019. Svarte prikker viser prøvedyp.*

Water column data from Fugløya-Bjørnøya section.

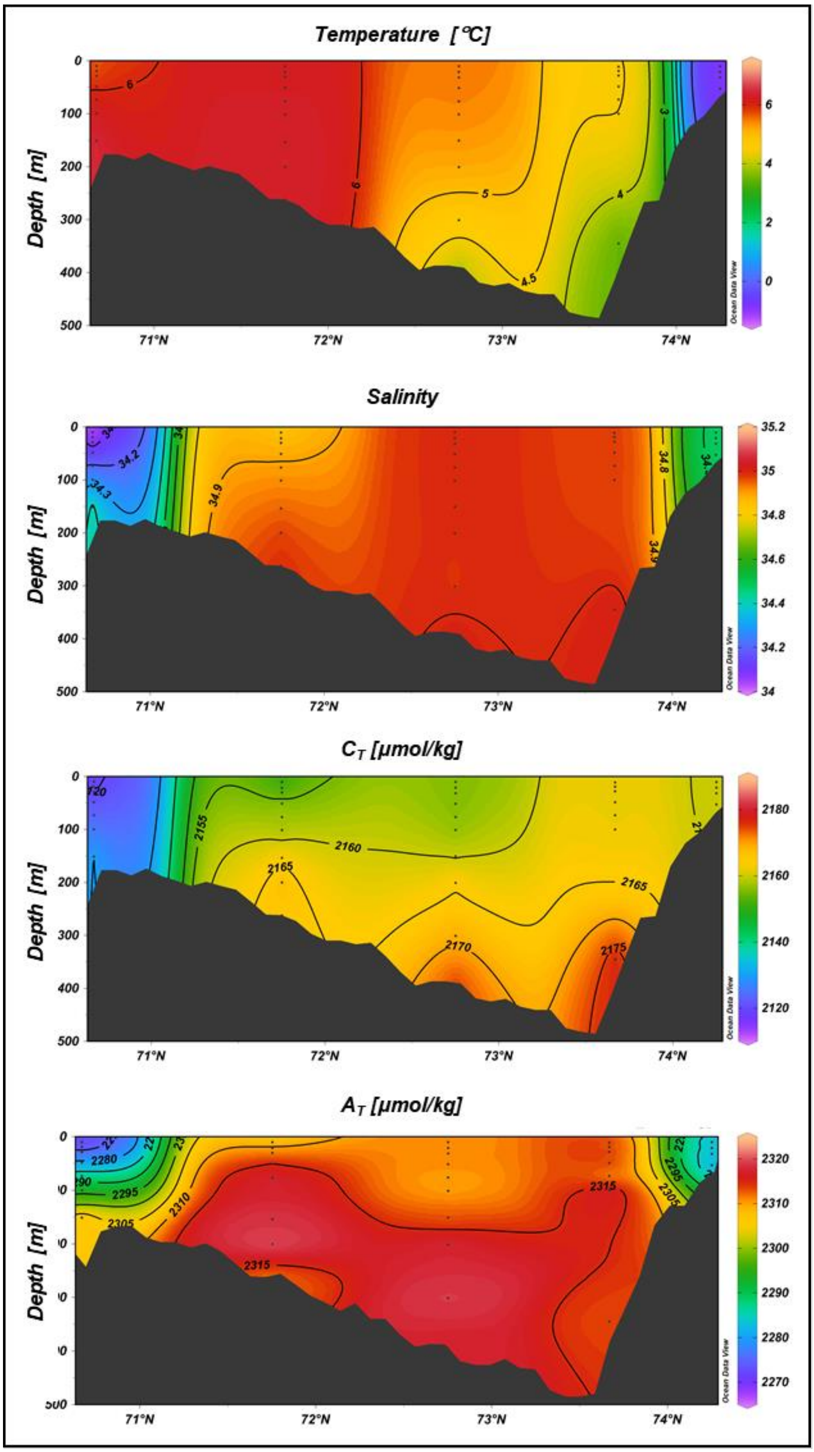

***Figure 75**. Temperature, salinity, C_T and A_T from Fugløya-Bjørnøya in January 2019. Black dots indicate sample depths.*

***Figur 75**. Temperatur, saltholdighet, C_T and A_T langs Fugløya-Bjørnøya snittet i januar 2019. Svarte prikker viser prøvedyp.*

Water column data from Barents Sea section.

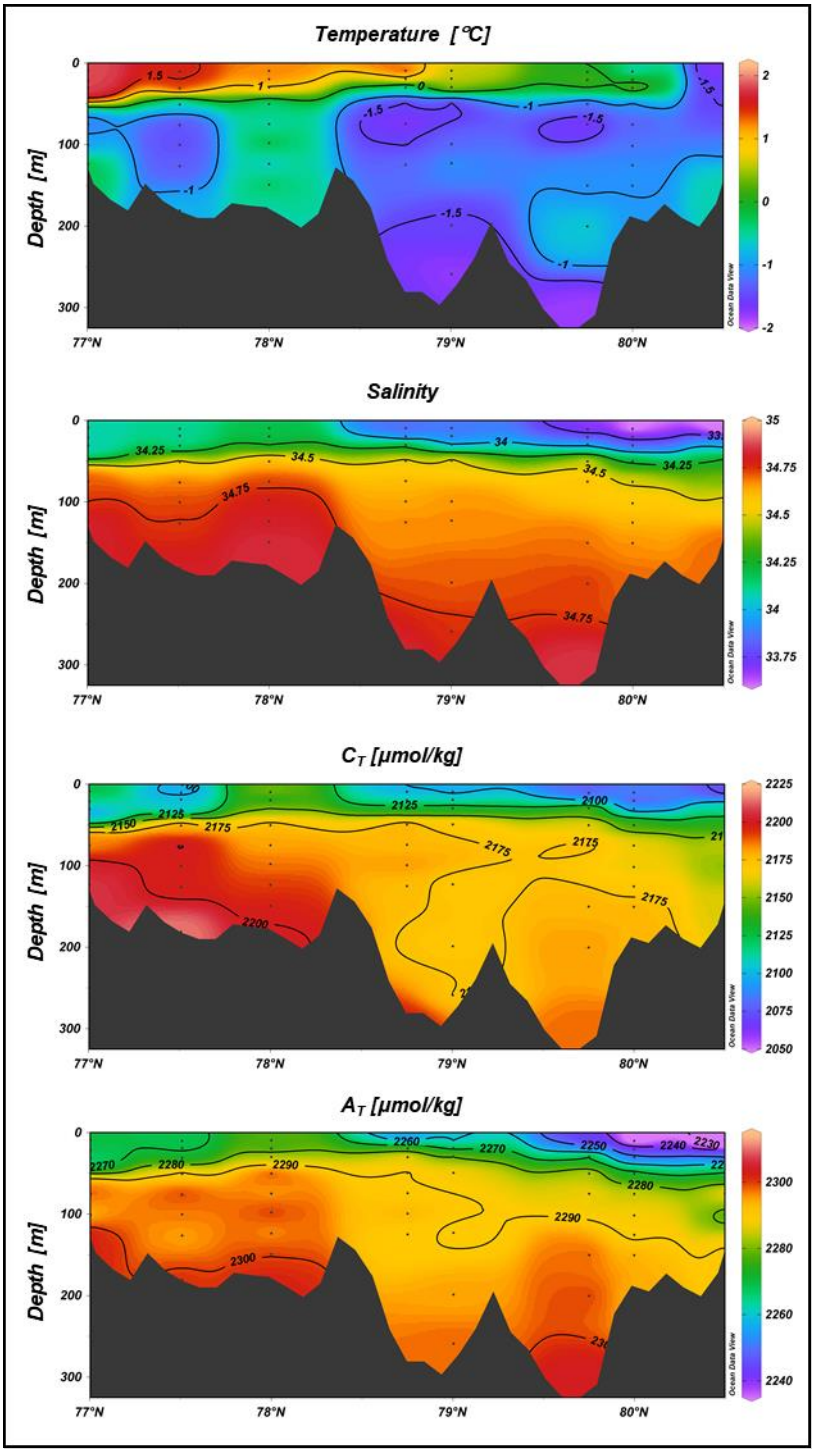

***Figure 76**. Temperature, salinity, C_T and A_T along the section in the northeast Barents Sea in September 2019. Black dots indicate sample depths.*

***Figur 76**. Temperatur, saltholdighet, C_T and A_T langs snittet i nordlige Barentshav i september 2019. Svarte prikker viser prøvedyp.*

6.2 Data Tables

***Table 1**. Torungen-Hirtshals; January 2019.*

Stn	Date	Lat	Lon	Depth	S	T	A_T	C_T	pH_T	Ω_{Ca}	Ω_{Ar}	NO_3	PO_4	$SiOH_4$
		°N	°E	m		˚C	µmol/kg	µmol/kg				µmol/kg	µmol/kg	µmol/kg
Ærydypet	20.01	58.40	8.77	10.2	33.98	7.31	2314	2157	8.049	2.91	1.84	4.09	0.40	3.17
Ærydypet	20.01	58.40	8.77	29.7	34.75	7.79	2323	2160	8.043	2.95	1.87	3.77	0.41	3.03
Ærydypet	20.01	58.40	8.77	50.3	34.34	7.91	2329	2190	7.989	2.65	1.68	3.84	0.39	3.02
Ærydypet	20.01	58.40	8.77	99.5	34.40	8.05	2326	2167	8.040	2.93	1.86	3.93	0.40	3.07
Ærydypet	20.01	58.40	8.77	125.2	34.41	8.05	-	2169	-	-	-	3.93	0.41	3.22
5nm	20.01	58.33	8.88	7.7	33.61	5.78	2295	2153	8.045	2.69	1.70	3.96	0.38	2.60
5nm	20.01	58.33	8.88	29.6	34.02	6.62	2309	2151	8.061	2.89	1.83	4.17	0.40	2.55
5nm	20.01	58.33	8.88	48.4	34.46	7.71	2316	2157	8.045	2.93	1.86	3.99	0.41	2.76
5nm	20.01	58.33	8.88	99.0	34.73	8.09	2321	2158	8.041	2.94	1.87	3.49	0.42	2.86
5nm	20.01	58.33	8.88	199.6	34.92	8.27	2314	2170	7.988	2.63	1.67	4.04	0.42	2.50
15nm	20.01	58.20	9.08	10.6	33.78	6.18	2305	2162	8.025	2.64	1.67	3.99	0.35	2.21
15nm	20.01	58.20	9.08	29.1	33.82	6.33	2302	2142	8.069	2.89	1.83	4.15	0.36	2.25
15nm	20.01	58.20	9.08	49.2	34.64	8.06	2313	2166	7.989	2.65	1.68	6.57	0.51	2.51
15nm	20.01	58.20	9.08	99.8	35.03	8.40	2310	2144	8.031	2.91	1.85	7.10	0.54	2.71
15nm	20.01	58.20	9.08	199.4	35.06	7.59	2320	2183	7.961	2.44	1.55	9.19	0.73	4.33
15nm	20.01	58.20	9.08	401.1	35.14	6.17	2323	2193	7.959	2.25	1.43	11.00	0.87	5.43
20nm	20.01	58.13	9.18	9.6	33.79	6.15	2302	2144	8.074	2.91	1.84	3.70	0.35	2.18
20nm	20.01	58.13	9.18	29.8	33.84	6.28	2308	2146	8.072	2.91	1.84	3.94	0.35	2.21
20nm	20.01	58.13	9.18	49.9	34.71	8.58	2316	2147	8.034	2.97	1.88	4.97	0.44	2.40
20nm	20.01	58.13	9.18	99.2	35.02	8.49	2319	2173	7.974	2.62	1.66	8.03	0.63	3.55
20nm	20.01	58.13	9.18	198.7	35.09	7.12	2318	2190	7.958	2.38	1.51	10.15	0.80	4.52
20nm	20.01	58.13	9.18	299.2	35.11	6.65	2317	2185	7.961	2.32	1.48	10.39	0.80	4.29
20nm	20.01	58.13	9.18	399.0	35.12	6.29	2316	2185	7.967	2.29	1.46	10.17	0.80	4.03
20nm	20.01	58.13	9.18	599.1	35.14	6.06	2315	2187	7.948	2.13	1.36	11.03	0.88	5.47
30nm	20.01	58.00	9.35	10.0	33.27	5.72	2297	2150	8.049	2.70	1.70	3.57	0.34	2.28
30nm	20.01	58.00	9.35	29.7	34.56	8.53	2317	2147	8.043	3.02	1.91	4.39	0.41	2.24
30nm	20.01	58.00	9.35	49.5	34.97	8.89	2317	2153	8.017	2.91	1.85	6.25	0.52	2.76
30nm	20.01	58.00	9.35	99.5	35.04	8.07	2312	2148	8.029	2.87	1.82	8.10	0.61	2.86
30nm	20.01	58.00	9.35	200.1	35.12	7.95	2315	2154	8.016	2.76	1.75	8.72	0.65	3.12
30nm	20.01	58.00	9.35	402.9	35.14	6.06	2318	2188	7.956	2.22	1.41	11.09	0.89	5.93

Table 2. Arendal coastal station; January-December 2019.

Date	Lat	Lon	Depth	S	T	A_T	C_T	pH_T	Ω_{Ca}	Ω_{Ar}	NO_3	PO_4	$SiOH_4$
	°N	°E	m		C°	µmol/kg	µmol/kg				µmol/kg	µmol/kg	µmol/kg
20.1.	58.23	8.50	1.9	33.59	6.11	2299	2153	8.047	2.74	1.73	4.08	0.39	3.49
20.1.	58.23	8.50	4.2	33.68	6.35	2306	2170	8.013	2.59	1.64	4.15	0.42	3.43
20.1.	58.23	8.50	10.0	33.70	6.38	2301	2147	8.058	2.84	1.79	4.07	0.41	3.41
20.1.	58.23	8.50	19.3	33.74	6.36	2309	2153	8.063	2.87	1.81	3.99	0.39	3.19
20.1.	58.23	8.50	29.6	34.14	7.10	2322	2161	8.058	2.94	1.86	3.68	0.39	3.02
20.1.	58.23	8.50	49.6	34.32	7.54	2322	2175	8.010	2.72	1.72	3.66	0.39	2.99
20.1.	58.23	8.50	75.7	34.45	7.83	2327	2179	8.014	2.77	1.75	3.72	0.40	3.03
5.2.	58.23	8.50	2.9	31.94	3.53	-	2097	8.069	2.47	1.55	4.72	0.40	3.51
5.2.	58.23	8.50	4.8	31.95	3.54	2255	2113	8.082	2.56	1.60	4.75	0.39	3.51
5.2.	58.23	8.50	9.7	32.05	3.64	2265	2124	8.081	2.58	1.61	4.90	0.39	3.50
5.2.	58.23	8.50	19.6	33.11	4.80	2290	2138	8.071	2.71	1.70	5.13	0.40	3.35
5.2.	58.23	8.50	29.3	33.63	5.44	2302	2146	8.064	2.77	1.74	4.98	0.39	2.84
5.2.	58.23	8.50	49.7	33.84	6.04	2302	2144	8.060	2.80	1.77	4.93	0.40	2.95
5.2.	58.23	8.50	76.1	34.07	6.22	2308	2151	8.056	2.80	1.77	5.22	0.41	2.89
16.3	58.23	8.50	2.5	28.22	4.43	-	-	-	-	-	3.48	0.18	4.67
16.3	58.23	8.50	5.3	29.75	4.45	2216	2071	8.118	2.69	1.68	2.89	0.20	2.74
16.3	58.23	8.50	9.6	30.23	4.47	2251	2108	8.097	2.65	1.65	3.31	0.23	2.83
16.3	58.23	8.50	20.1	31.72	4.92	2290	2148	8.075	2.68	1.68	4.06	0.31	2.63
16.3	58.23	8.50	29.4	33.50	5.59	2309	2155	8.074	2.84	1.79	4.29	0.36	2.55
16.3	58.23	8.50	48.8	34.12	5.98	-	2191	-	-	-	4.26	0.39	2.44
16.3	58.23	8.50	76.6	34.25	6.08	2328	2168	8.069	2.90	1.83	4.22	0.40	2.40
7.4.	58.23	8.50	2.5	31.56	6.01	-	2076	8.157	3.22	2.02	0.24	0.06	1.45
7.4.	58.23	8.50	5.8	31.60	6.02	2272	2108	8.119	3.02	1.90	0.36	0.05	1.45
7.4.	58.23	8.50	10.6	31.64	6.03	2278	2146	8.038	2.58	1.62	0.13	0.07	1.32
7.4.	58.23	8.50	21.2	32.01	6.15	2276	-	-	3.36	2.11	0.17	0.06	1.25
7.4.	58.23	8.50	30.2	32.32	6.14	2279	2156	8.024	2.54	1.60	0.17	0.08	1.20
7.4.	58.23	8.50	50.0	33.29	6.26	2296	2171	8.005	2.50	1.58	0.94	0.20	2.24
7.4.	58.23	8.50	76.7	34.40	6.28	2322	2172	8.049	2.80	1.77	3.84	0.41	3.28
18.5.	58.23	8.50	2.9	25.21	11.26	2077	1941	8.034	2.51	1.55	0.12	0.09	3.17
18.5.	58.23	8.50	6.3	25.22	11.26	2082	-	-	-	-	0.14	0.08	3.16
18.5.	58.23	8.50	10.5	25.60	11.18	2070	1930	8.075	2.72	1.69	0.15	0.12	2.91
18.5.	58.23	8.50	20.7	32.13	6.95	2263	2106	8.088	2.94	1.85	2.04	0.20	2.24
18.5.	58.23	8.50	30.1	33.66	6.52	2306	2157	8.055	2.83	1.78	3.60	0.32	2.77
18.5.	58.23	8.50	49.8	34.41	6.67	2319	2185	8.014	2.65	1.68	5.40	0.46	3.15
18.5.	58.23	8.50	77.2	34.59	6.79	2316	2165	8.029	2.74	1.73	5.94	0.48	3.29
1.6.	58.23	8.50	2.7	28.92	10.93	2168	2055	7.959	2.38	1.49	0.08	0.04	0.54
1.6.	58.23	8.50	6.0	29.03	10.87	2192	2032	8.077	3.05	1.91	0.10	0.13	0.65
1.6.	58.23	8.50	11.1	32.52	8.51	2278	2119	8.061	2.99	1.89	1.79	0.20	1.78
1.6.	58.23	8.50	20.9	32.98	8.07	2285	2128	8.058	2.95	1.86	2.23	0.24	2.05
1.6.	58.23	8.50	30.9	33.76	7.72	2300	2144	8.048	2.90	1.84	3.07	0.32	2.55
1.6.	58.23	8.50	49.3	34.30	7.49	2309	2159	8.030	2.80	1.78	4.38	0.41	3.06
1.6.	58.23	8.50	75.9	34.50	7.36	2319	2183	7.992	2.59	1.64	5.22	0.46	3.36
6.7.	58.23	8.50	3.1	29.08	15.33	2194	2062	7.931	2.67	1.69	0.10	0.02	0.49
6.7.	58.23	8.50	6.4	29.91	15.09	2230	2038	8.065	3.55	2.25	0.11	0.09	0.58
6.7.	58.23	8.50	11.3	31.04	14.62	2266	2071	8.051	3.52	2.24	0.16	0.11	0.98
6.7.	58.23	8.50	21.5	33.18	11.98	2293	2113	8.042	3.29	2.09	0.80	0.16	1.66
6.7.	58.23	8.50	29.9	33.60	11.87	2313	2134	8.032	3.26	2.08	0.62	0.11	1.65
6.7.	58.23	8.50	49.7	34.13	9.69	2312	2153	8.019	2.96	1.88	2.22	0.28	2.41
6.7.	58.23	8.50	76.5	34.49	8.48	2319	2166	8.009	2.79	1.77	3.47	0.39	3.08
2.8.	58.23	8.50	3.1	27.23	18.33	2092	1909	8.067	3.57	2.26	0.14	0.10	0.38

2.8.	58.23	8.50	6.0	27.87	18.13	2159	1972	8.049	3.57	2.27	0.13	0.10	0.41
2.8.	58.23	8.50	10.5	28.43	17.88	2173	1989	8.041	3.54	2.25	0.14	0.12	0.47
2.8.	58.23	8.50	21.4	31.26	15.52	2267	2128	-	2.73	1.74	0.67	0.11	1.36
2.8.	58.23	8.50	30.3	32.90	13.37	2283	2109	8.014	3.24	2.07	1.44	0.15	1.86
2.8.	58.23	8.50	49.8	34.70	9.81	2316	2159	7.998	2.88	1.83	3.72	0.34	2.40
2.8.	58.23	8.50	76.0	34.90	8.41	2311	2165	7.996	2.72	1.73	4.69	0.48	3.04
13.9.	58.23	8.50	3.2	32.80	16.47	2301	2098	8.015	3.63	2.33	0.18	0.10	2.31
13.9.	58.23	8.50	6.6	32.80	16.48	2299	2104	8.015	3.63	2.33	0.18	0.08	2.30
13.9.	58.23	8.50	10.5	33.41	16.57	2322	2130	7.998	3.59	2.31	0.28	0.12	2.09
13.9.	58.23	8.50	20.6	33.99	16.36	2328	2134	7.988	3.52	2.27	0.30	0.13	1.83
13.9.	58.23	8.50	30.7	34.15	16.15	2325	2130	7.994	3.54	2.28	0.19	0.12	1.69
13.9.	58.23	8.50	50.0	34.45	16.47	-	-	-	-	-	0.05	0.09	1.38
13.9.	58.23	8.50	76.0	34.56	13.99	-	2143	-	-	-	1.26	0.25	3.35
6.10.	58.23	8.50	3.1	30.03	13.11	2211	2022	8.088	3.45	2.18	0.20	0.12	0.76
6.10.	58.23	8.50	6.6	30.03	13.12	2214	2029	8.075	3.37	2.13	0.16	0.12	0.76
6.10.	58.23	8.50	11.6	30.57	13.46	2233	2041	8.075	3.47	2.20	0.18	0.13	0.95
6.10.	58.23	8.50	21.5	30.77	13.49	2233	2044	8.071	3.45	2.19	0.33	0.13	1.27
6.10.	58.23	8.50	31.1	32.62	15.27	2285	2128	-	3.01	1.92	0.54	0.16	2.36
6.10.	58.23	8.50	50.3	34.45	14.32	2312	2129	7.988	3.28	2.10	2.29	0.29	2.78
6.10.	58.23	8.50	76.4	34.90	9.18	2316	2170	7.983	2.73	1.74	4.74	0.50	3.29
15.11.	58.23	8.50	1.9	30.23	8.56	2203	2051	8.076	2.88	1.81	2.61	0.29	2.97
15.11.	58.23	8.50	5.7	30.24	8.58	2201	2044	8.090	2.96	1.86	2.64	0.30	2.99
15.11.	58.23	8.50	10.6	30.29	8.64	2205	2051	8.080	2.91	1.83	2.60	0.28	2.97
15.11.	58.23	8.50	20.7	31.50	10.19	2261	2088	8.081	3.21	2.03	1.49	0.28	1.95
15.11.	58.23	8.50	30.4	33.30	11.89	2322	2127	8.071	3.52	2.24	0.78	0.28	1.53
15.11.	58.23	8.50	50.5	34.41	13.49	2335	2151	8.029	3.49	2.23	0.54	0.28	1.32
15.11.	58.23	8.50	76.2	34.42	12.87	2326	2136	8.052	3.55	2.27	1.06	0.29	1.56
9.12.	58.23	8.50	2.0	31.56	9.39	2250	2095	8.042	2.89	1.82	3.91	0.38	3.52
9.12.	58.23	8.50	5.7	31.61	9.42	2252	2101	8.032	2.84	1.79	3.96	0.39	3.55
9.12.	58.23	8.50	9.9	31.66	9.46	2246	2098	8.035	2.85	1.80	4.11	0.38	3.54
9.12.	58.23	8.50	20.6	32.27	9.82	-	2113	-	-	-	4.29	0.39	3.49
9.12.	58.23	8.50	31.2	32.87	10.04	2282	2124	8.028	2.97	1.88	4.38	0.40	3.53
9.12.	58.23	8.50	50.3	34.03	11.17	2315	2136	8.048	3.30	2.10	2.98	0.33	2.00
9.12.	58.23	8.50	75.8	34.57	9.48	2312	2165	7.988	2.77	1.76	7.06	0.58	4.50

Table 3*. Svinøy-NW; January 2019.*

Stn	Date	Lat	Lon	Depth	S	T	A_T	C_T	pH_T	Ω_{Ca}	Ω_{Ar}	NO_3	PO_4	$SiOH_4$
		°N	°E	m		C °	µmol/kg	µmol/kg				µmol/kg	µmol/kg	µmol/kg
2	20.01	62.49	4.95	195.0	35.21	8.82	2320	2148	8.024	2.90	1.85	9.88	0.65	3.45
2	20.01	62.49	4.95	151.6	35.19	9.04	2324	2149	8.025	2.95	1.88	10.25	0.65	3.43
2	20.01	62.49	4.95	100.8	34.93	8.89	2312	2136	8.035	2.99	1.90	7.95	0.53	2.50
2	20.01	62.49	4.95	75.7	34.44	7.96	2300	2131	8.044	2.92	1.85	-	-	-
2	20.01	62.49	4.95	51.3	34.06	6.94	2291	2127	8.059	2.88	1.82	5.91	0.41	2.32
2	20.01	62.49	4.95	20.1	33.98	6.84	2293	2124	8.066	2.92	1.85	6.00	0.39	2.37
2	20.01	62.49	4.95	10.3	33.98	6.84	2291	2122	8.064	2.91	1.84	5.98	0.40	2.38
6	20.01	62.85	4.16	605.5	34.92	0.56	2307	2173	8.041	2.07	1.31	13.97	0.93	8.96
6	20.01	62.85	4.16	498.2	34.98	5.07	2307	2166	8.002	2.30	1.46	13.70	0.88	6.33
6	20.01	62.85	4.16	199.7	35.09	7.68	2311	2148	8.032	2.81	1.79	11.23	0.71	4.26
6	20.01	62.85	4.16	146.4	35.10	7.74	2315	2146	8.033	2.85	1.81	11.24	0.71	4.20
6	20.01	62.85	4.16	73.6	35.10	7.70	2312	2147	8.037	2.89	1.83	10.55	0.71	4.23
6	20.01	62.85	4.16	49.3	35.11	7.78	2317	2149	8.038	2.92	1.85	10.76	0.71	4.21
6	20.01	62.85	4.16	29.2	35.11	7.75	2313	2145	8.039	2.93	1.86	11.02	0.72	4.21
6	20.01	62.85	4.16	8.8	35.12	7.77	2315	2150	8.039	2.94	1.87	11.19	0.71	4.23
9	20.01	63.07	3.66	970.8	34.91	-0.76	2317	2188	8.032	1.83	1.17	13.97	0.98	12.25
9	20.01	63.07	3.66	801.2	34.91	-0.75	2310	2171	8.065	2.00	1.27	13.69	0.97	11.78
9	20.01	63.07	3.66	499.5	34.94	3.22	2306	2171	8.019	2.22	1.41	12.45	0.88	6.61
9	20.01	63.07	3.66	402.2	35.08	6.52	2312	2174	7.985	2.39	1.52	11.00	0.84	5.70
9	20.01	63.07	3.66	201.0	35.11	8.09	2314	2152	8.032	2.86	1.82	10.02	0.69	3.89
9	20.01	63.07	3.66	100.9	35.13	8.26	2314	2150	8.041	2.97	1.89	9.36	0.65	3.50
9	20.01	63.07	3.66	51.6	35.13	8.31	2314	2148	8.042	2.99	1.90	10.05	0.64	3.43
9	20.01	63.07	3.66	29.9	35.08	8.21	2314	2146	8.044	3.00	1.91	10.01	0.64	3.35
9	20.01	63.07	3.66	10.0	34.98	8.00	2312	2144	8.049	3.02	1.91	9.72	0.61	3.25
11	21.01	63.31	3.13	1074.1	34.91	-0.76	2310	2175	8.061	1.91	1.21	14.36	0.97	12.33
11	21.01	63.31	3.13	999.2	34.91	-0.75	2305	2171	8.063	1.93	1.23	14.49	0.96	12.02
11	21.01	63.31	3.13	799.6	34.91	-0.54	2308	2181	8.056	1.99	1.26	14.19	0.93	10.38
11	21.01	63.31	3.13	499.4	35.01	5.31	2307	2174	8.000	2.31	1.47	12.94	0.85	6.35
11	21.01	63.31	3.13	198.4	35.20	8.75	2318	2156	8.022	2.88	1.83	9.85	0.66	3.57
11	21.01	63.31	3.13	98.9	35.21	9.03	2330	2156	8.035	3.04	1.93	9.67	0.62	3.20
11	21.01	63.31	3.13	50.3	35.12	8.99	2319	2146	8.035	3.03	1.93	9.15	0.60	2.77
11	21.01	63.31	3.13	30.3	34.77	7.84	2315	2149	8.052	3.00	1.90	8.04	0.53	2.66
11	21.01	63.31	3.13	12.3	34.73	7.71	2313	2148	8.053	3.00	1.90	7.93	0.52	2.74
13	21.01	63.66	2.34	1449.3	34.91	-0.75	2311	2182	8.039	1.73	1.10	14.55	0.98	12.41
13	21.01	63.66	2.34	1198.4	34.91	-0.61	2315	2184	8.042	1.82	1.16	13.89	0.93	9.88
13	21.01	63.66	2.34	999.7	34.91	-0.45	2312	2189	8.026	1.82	1.16	13.70	0.91	8.91
13	21.01	63.66	2.34	799.0	34.91	-0.21	2310	2188	8.033	1.92	1.22	13.54	0.90	7.70
13	21.01	63.66	2.34	500.2	34.95	4.55	2309	2170	8.006	2.28	1.45	13.22	0.84	6.05
13	21.01	63.66	2.34	199.1	35.17	8.27	2325	2153	8.029	2.88	1.83	10.71	0.67	3.71
13	21.01	63.66	2.34	98.5	35.16	8.28	2318	2147	8.036	2.95	1.87	10.30	0.65	3.63
13	21.01	63.66	2.34	50.5	35.16	8.29	2318	2146	8.039	2.98	1.89	10.32	0.65	3.55
13	21.01	63.66	2.34	28.6	35.16	8.30	2321	2149	8.038	2.99	1.90	10.35	0.65	3.55
13	21.01	63.66	2.34	10.8	35.16	8.29	2326	2153	8.039	3.01	1.91	10.19	0.65	3.55
15	21.01	64.13	1.26	2443.2	34.91	-0.78	2311	2173	8.006	1.40	0.90	16.04	1.02	13.31
15	21.01	64.13	1.26	1997.1	34.91	-0.73	2311	2174	8.024	1.55	1.00	15.24	0.96	11.19
15	21.01	64.13	1.26	1499.6	34.91	-0.65	2307	2172	8.038	1.71	1.10	15.03	0.94	10.10
15	21.01	64.13	1.26	999.8	34.91	-0.39	2313	2180	8.038	1.87	1.19	14.27	0.91	7.84
15	21.01	64.13	1.26	799.6	34.91	-0.16	2307	2179	8.034	1.93	1.22	13.95	0.90	7.02
15	21.01	64.13	1.26	498.9	34.91	1.02	2311	2189	8.012	2.02	1.28	14.02	0.90	5.71
15	21.01	64.13	1.26	200.7	34.88	5.85	2310	2165	8.010	2.51	1.59	11.24	0.71	4.53

15	21.01	64.13	1.26	99.5	34.98	6.56	2314	2168	8.004	2.59	1.64	11.64	0.74	4.57
15	21.01	64.13	1.26	49.7	35.01	6.89	2319	2173	7.997	2.61	1.65	11.50	0.73	4.44
15	21.01	64.13	1.26	29.0	35.04	7.09	2312	2149	8.040	2.86	1.81	11.37	0.73	4.39
15	21.01	64.13	1.26	10.2	35.05	7.15	2311	2147	8.043	2.89	1.83	11.10	0.72	4.41

Table 4. *Station M; January, April, May, June, November 2019.*

Stn	Date	Lat °N	Lon °E	Depth m	S	T C°	A_T µmol/kg	C_T µmol/kg	pH_T	Ω_{Ca}	Ω_{Ar}	NO_3 µmol/kg	PO_4 µmol/kg	$SiOH_4$ µmol/kg
18	22.01	65.84	2.17	1973	34.91	-0.76	2307.8	2167.9	8.030	1.56	1.01	14.7	1.0	12.0
18	22.01	65.84	2.17	1776	34.91	-0.71	2309.0	2171.1	8.032	1.62	1.04	14.5	0.9	11.1
18	22.01	65.84	2.17	1479	34.91	-0.65	2308.6	2177.6	8.025	1.67	1.07	14.2	0.9	10.2
18	22.01	65.84	2.17	988	34.91	-0.42	2306.0	2178.5	8.032	1.84	1.17	13.7	0.9	8.7
18	22.01	65.84	2.17	787	34.91	-0.22	2304.8	2178.9	8.033	1.92	1.22	13.1	0.9	7.3
18	22.01	65.84	2.17	493	34.91	0.54	2304.0	2180.7	8.025	2.03	1.28	13.3	0.9	6.1
18	22.01	65.84	2.17	396	34.92	1.94	2311.6	2176.0	8.039	2.24	1.42	13.4	0.9	5.9
18	22.01	65.84	2.17	197	34.94	6.12	2304.5	2148.3	8.034	2.66	1.68	11.1	0.7	4.5
18	22.01	65.84	2.17	95	35.00	6.64	2308.9	2149.1	8.037	2.77	1.76	10.7	0.7	4.3
18	22.01	65.84	2.17	46	35.02	6.80	2311.5	2148.7	8.043	2.84	1.80	10.8	0.7	4.3
18	22.01	65.84	2.17	30	35.03	6.81	2312.8	2150.0	8.043	2.85	1.81	10.9	0.7	4.4
18	22.01	65.84	2.17	11	35.02	6.75	2341.3	2153.2	8.101	3.24	2.05	11.0	0.7	4.4
467	07.04	65.84	2.15	2029	34.91	-0.78	2304.6	2170.0	8.014	1.50	0.96	14.7	1.0	12.5
467	07.04	65.84	2.15	1480	34.90	-0.64	2308.4	2173.2	8.036	1.71	1.10	14.2	0.9	10.6
467	07.04	65.84	2.15	988	34.90	-0.31	2302.9	2185.6	8.003	1.74	1.11	12.1	0.8	7.3
467	07.04	65.84	2.15	493	34.87	1.46	2301.2	2184.9	7.991	1.96	1.24	13.3	0.9	5.9
467	07.04	65.84	2.15	297	34.84	6.21	2311.6	2153.6	8.033	2.63	1.67	11.6	0.8	5.4
467	07.04	65.84	2.15	197	35.02	6.45	2319.6	2157.1	8.041	2.75	1.75	10.6	0.7	4.6
467	07.04	65.84	2.15	99	35.03	7.06	2318.2	2153.3	8.041	2.85	1.80	10.7	0.7	4.6
467	07.04	65.84	2.15	50	35.04	7.21	2317.2	2150.9	8.044	2.90	1.84	10.1	0.7	4.4
467	07.04	65.84	2.15	30	35.10	7.20	2319.0	2155.0	8.038	2.88	1.82	10.8	0.7	4.6
467	07.04	65.84	2.15	20	35.10	7.20	2322.4	2154.1	8.049	2.94	1.87	10.8	0.7	4.6
467	07.04	65.84	2.15	10	35.11	7.20	2313.9	2162.1	8.010	2.72	1.72	10.8	0.7	4.6
467	07.04	65.84	2.15	3	35.10	7.20	2324.2	2153.2	8.056	2.99	1.90	10.8	0.7	4.6
498	18.05	66.00	2.00	2013	34.92	-0.76	2305.1	2169.4	8.018	1.51	0.97	12.6	0.9	12.2
498	18.05	66.00	2.00	1971	34.92	-0.77	2305.1	2169.0	8.020	1.53	0.99	14.7	1.0	12.4
498	18.05	66.00	2.00	1479	34.92	-0.64	2305.1	2168.0	8.041	1.73	1.11	14.1	0.9	11.0
498	18.05	66.00	2.00	987	34.92	-0.31	2305.1	2175.5	8.036	1.87	1.19	13.6	0.9	7.8
498	18.05	66.00	2.00	791	34.91	-0.09	2304.9	2176.7	8.037	1.94	1.23	13.6	0.9	7.0
498	18.05	66.00	2.00	396	34.97	4.88	2308.0	2167.6	8.004	2.33	1.48	13.5	0.9	6.2
498	18.05	66.00	2.00	197	35.12	7.35	2315.3	2153.4	8.025	2.75	1.74	11.5	0.7	4.6
498	18.05	66.00	2.00	99	35.14	7.56	2316.0	2153.4	8.026	2.82	1.79	11.1	0.7	4.3
498	18.05	66.00	2.00	50	35.13	7.80	2315.7	2142.8	8.050	2.99	1.90	7.8	0.6	3.7
498	18.05	66.00	2.00	29	35.13	7.83	2315.5	2142.0	8.052	3.02	1.91	7.4	0.6	3.7
498	18.05	66.00	2.00	9	35.13	7.98	2315.4	2133.0	8.071	3.16	2.00	6.6	0.5	3.7
623	10.06	66.00	2.00	1917	34.91	-0.78	2305.6	2165.1	8.038	1.60	1.03	-	-	-
623	10.06	66.00	2.00	1483	34.91	-0.68	2303.6	2164.1	8.052	1.76	1.13	-	-	-
623	10.06	66.00	2.00	989	34.91	-0.42	2303.7	2167.4	8.059	1.95	1.24	-	-	-
623	10.06	66.00	2.00	494	34.93	1.61	2310.7	2176.1	8.041	2.19	1.39	-	-	-
623	10.06	66.00	2.00	296	35.01	5.73	2311.5	2153.0	8.042	2.64	1.67	-	-	-
623	10.06	66.00	2.00	196	35.07	6.69	2316.6	2148.0	8.054	2.84	1.80	-	-	-
623	10.06	66.00	2.00	97	35.14	7.48	2314.4	2149.7	8.035	2.86	1.81	-	-	-
623	10.06	66.00	2.00	46	35.18	7.89	2315.5	2147.1	8.039	2.94	1.87	-	-	-
623	10.06	66.00	2.00	26	35.08	8.46	2318.7	2124.7	8.090	3.33	2.11	-	-	-
623	10.06	66.00	2.00	18	35.08	8.47	2321.7	2112.9	8.122	3.55	2.25	-	-	-
623	10.06	66.00	2.00	8	35.09	8.47	2317.1	2109.9	8.119	3.53	2.24	-	-	-
623	10.06	66.00	2.00	5	35.09	8.47	2317.4	2105.1	8.130	3.61	2.29	-	-	-
964	17.11	66.00	2.00	10	35.02	7.23	2308.9	2129.4	8.079	3.10	1.97	7.9	0.6	2.8
964	17.11	66.00	2.00	29	35.01	7.09	2304.6	2126.2	8.078	3.07	1.95	7.7	0.6	2.6
964	17.11	66.00	2.00	49	35.00	6.95	2306.5	2129.0	8.078	3.05	1.93	7.5	0.6	2.6

964	17.11	66.00	2.00	99	34.95	5.47	2309.5	2161.5	8.027	2.60	1.64	12.8	0.8	5.7
964	17.11	66.00	2.00	197	34.89	3.86	2298.6	2219.1	7.856	1.69	1.07	12.7	0.8	5.8
964	17.11	66.00	2.00	494	34.91	0.30	2297.1	2174.5	8.027	2.02	1.28	13.8	0.9	6.7
964	17.11	66.00	2.00	988	34.91	-0.42	2284.2	2166.4	8.006	1.74	1.10	13.8	0.9	8.9
964	17.11	66.00	2.00	1480	34.91	-0.70	2296.7	2159.9	8.041	1.73	1.10	14.1	0.9	11.4
964	17.11	66.00	2.00	2004	34.91	-0.80	2289.2	2161.9	7.996	1.44	0.93	15.0	1.0	13.7

***Table 5**. Gimsøy-NW; March and May 2019.*

Stn	Date	Lat	Lon	Depth	S	T	A_T	C_T	pH_T	Ω_{Ca}	Ω_{Ar}	NO_3	PO_4	$SiOH_4$
		°N	°E	m		C°	µmol/kg	µmol/kg				µmol/kg	µmol/kg	µmol/kg
6	20.03	68.58	13.59	119.7	34.54	6.07	2298	2143	8.053	2.76	1.75	-	-	-
6	20.03	68.58	13.59	100.4	34.54	6.07	2300	2145	8.054	2.78	1.76	6.69	0.51	3.24
6	20.03	68.58	13.59	77.4	34.40	5.59	2296	2141	8.062	2.77	1.75	7.00	0.55	3.36
6	20.03	68.58	13.59	50.8	34.19	5.04	2286	2132	8.072	2.76	1.74	6.04	0.47	3.21
6	20.03	68.58	13.59	25.8	34.15	4.95	2284	2124	8.072	2.76	1.74	6.00	0.47	2.99
6	20.03	68.58	13.59	20.7	34.15	4.96	2284	2133	8.074	2.77	1.75	6.14	0.48	3.24
6	20.03	68.58	13.59	11.0	34.15	4.96	2284	2132	8.074	2.78	1.75	5.92	0.47	3.17
6	20.03	68.58	13.59	4.2	34.15	4.96	2285	2133	8.074	2.78	1.75	-	-	-
10	20.03	68.85	12.80	672.0	34.94	1.36	2307	2184	8.027	2.05	1.30	12.21	0.90	7.71
10	20.03	68.85	12.80	607.0	35.04	4.84	2310	2167	8.021	2.34	1.49	10.65	0.81	5.71
10	20.03	68.85	12.80	507.9	35.05	5.30	2312	2164	8.026	2.45	1.55	10.40	0.79	5.50
10	20.03	68.85	12.80	403.0	35.05	5.52	2313	2162	8.031	2.53	1.60	10.21	0.76	4.96
10	20.03	68.85	12.80	304.1	35.06	5.79	2319	2165	8.037	2.63	1.67	10.24	0.75	4.95
10	20.03	68.85	12.80	200.1	35.06	6.10	2320	2160	8.043	2.73	1.73	9.79	0.73	4.69
10	20.03	68.85	12.80	152.0	35.06	6.20	2319	2161	8.047	2.77	1.76	9.61	0.72	4.65
10	20.03	68.85	12.80	100.3	35.06	6.29	2319	2160	8.048	2.81	1.78	9.61	0.72	4.46
10	20.03	68.85	12.80	76.0	35.06	6.29	2321	2164	8.049	2.83	1.79	9.61	0.72	4.62
10	20.03	68.85	12.80	49.4	35.06	6.36	2320	2161	8.050	2.85	1.80	9.67	0.72	4.70
10	20.03	68.85	12.80	11.9	35.05	6.50	2314	2156	8.050	2.87	1.82	8.97	0.71	4.46
12	20.03	69.03	12.29	2543.7	34.91	-0.76	2309	2178	8.004	1.37	0.89	15.05	0.99	13.15
12	20.03	69.03	12.29	2030.4	34.91	-0.72	2308	2173	8.025	1.54	0.99	14.68	0.97	12.02
12	20.03	69.03	12.29	1520.5	34.91	-0.61	-	2179	-	-	-	14.22	0.95	10.08
12	20.03	69.03	12.29	1015.1	34.91	-0.25	2304	2181	8.031	1.84	1.17	13.72	0.92	8.04
12	20.03	69.03	12.29	809.2	34.91	0.11	2303	2184	8.022	1.89	1.20	13.84	0.92	7.16
12	20.03	69.03	12.29	504.2	35.05	4.87	2315	2167	8.030	2.43	1.54	12.04	0.78	5.38
12	20.03	69.03	12.29	402.9	35.04	5.29	2315	2167	8.030	2.50	1.59	11.74	0.78	5.39
12	20.03	69.03	12.29	201.8	35.07	6.06	2324	2164	8.042	2.73	1.73	11.06	0.73	5.20
12	20.03	69.03	12.29	99.3	35.06	6.08	2319	2162	8.050	2.80	1.77	10.99	0.73	4.65
12	20.03	69.03	12.29	50.2	35.06	6.08	2315	2163	8.049	2.81	1.78	10.96	0.73	4.68
12	20.03	69.03	12.29	29.3	35.06	6.07	2315	2158	8.049	2.82	1.78	10.93	0.73	5.03
12	20.03	69.03	12.29	9.0	35.06	6.07	2314	2159	8.051	2.84	1.79	10.93	0.73	4.76
17	21.03	69.95	9.58	2438.5	34.91	-0.75	2299	2177	8.008	1.40	0.91	14.04	0.99	12.49
17	21.03	69.95	9.58	2032.8	34.91	-0.72	2301	2175	8.021	1.52	0.98	13.27	0.98	11.54
17	21.03	69.95	9.58	1520.1	34.91	-0.60	2303	2176	8.032	1.69	1.08	12.35	0.95	10.34
17	21.03	69.95	9.58	1012.1	34.91	-0.17	2303	2185	8.027	1.83	1.17	-	0.92	7.49
17	21.03	69.95	9.58	810.0	34.91	0.32	2302	2186	8.021	1.90	1.21	11.94	0.90	6.66
17	21.03	69.95	9.58	503.1	35.05	4.86	2310	2167	8.028	2.42	1.53	-	0.78	5.26
17	21.03	69.95	9.58	403.1	35.05	5.33	2311	2165	8.032	2.51	1.60	10.68	0.77	4.91
17	21.03	69.95	9.58	202.8	35.06	5.87	2312	2162	8.039	2.67	1.69	10.42	0.74	4.84
17	21.03	69.95	9.58	99.8	35.06	6.23	2312	2157	8.047	2.79	1.77	9.99	0.72	4.36
17	21.03	69.95	9.58	48.1	35.06	6.23	2311	2157	8.048	2.82	1.78	9.90	0.72	4.68
17	21.03	69.95	9.58	31.2	35.06	6.22	2315	2161	8.051	2.84	1.80	10.13	0.71	4.72
17	21.03	69.95	9.58	8.3	35.06	6.21	2315	2160	8.050	2.84	1.80	9.17	0.72	4.59
21	25.05	71.08	6.00	3124.3	34.92	-0.74	2304	2178	7.963	1.16	0.76	14.66	0.96	11.06
21	25.05	71.08	6.00	2499.8	34.92	-0.74	2298	2168	8.001	1.37	0.89	14.53	0.98	12.57
21	25.05	71.08	6.00	2000.0	34.92	-0.70	2304	2179	8.006	1.49	0.96	14.75	0.97	11.61
21	25.05	71.08	6.00	1500.6	34.91	-0.54	2301	2176	8.030	1.69	1.08	14.05	0.94	9.51
21	25.05	71.08	6.00	999.6	34.91	-0.09	2298	2176	8.032	1.86	1.18	13.65	0.91	7.43
21	25.05	71.08	6.00	800.2	34.91	0.47	2296	2178	8.021	1.91	1.21	13.22	0.88	6.38
21	25.05	71.08	6.00	499.8	35.05	4.39	2311	2172	8.010	2.29	1.45	11.67	0.77	5.13

21	25.05	71.08	6.00	199.5	35.06	5.01	2311	2178	7.992	2.36	1.49	10.97	0.73	5.00
21	25.05	71.08	6.00	101.4	35.06	5.33	2313	2173	8.027	2.60	1.64	10.73	0.72	4.97
21	25.05	71.08	6.00	50.6	35.07	5.78	2316	2184	7.988	2.46	1.56	9.59	0.66	4.61
21	25.05	71.08	6.00	30.0	35.07	5.94	2319	2184	7.993	2.51	1.59	7.60	0.62	4.29
21	25.05	71.08	6.00	9.6	35.08	5.95	2315	2143	8.096	3.09	1.95	7.50	0.58	4.34

Table 6*. Skrova coastal station; December 2018 (*) and January-November 2019.*

Date	Lat	Lon	Depth	T	S	A_T	C_T	pH_T	Ω_{Ca}	Ω_{Ar}	NO_3	PO_4	$SiOH_4$
	°N	°E	m		C°	µmol/kg	µmol/kg				µmol/kg	µmol/kg	µmol/kg
06.12*	68.12	14.53	300	34.95	7.37	2317	2181	7.965	2.40	1.53	12.21	0.77	6.16
06.12*	68.12	14.53	200	34.75	7.36	2318	2200	7.935	2.28	1.45	11.66	0.76	5.48
06.12*	68.12	14.53	150	34.32	7.38	2313	2156	8.043	2.84	1.80	8.78	0.60	3.82
06.12*	68.12	14.53	125	34.17	7.87	2304	2137	8.065	3.00	1.90	6.45	0.46	2.77
06.12*	68.12	14.53	100	33.68	7.77	2275	2098	8.078	3.02	1.91	4.24	0.34	1.96
06.12*	68.12	14.53	75	33.27	9.42	2262	2140	7.930	2.36	1.50	3.12	0.25	1.64
06.12*	68.12	14.53	50	32.93	9.96	2254	2079	8.072	3.18	2.02	3.08	0.25	1.51
06.12*	68.12	14.53	30	32.35	10.03	2205	2039	8.043	2.93	1.85	3.14	0.27	1.56
06.12*	68.12	14.53	20	32.19	8.34	2182	2025	8.050	2.76	1.74	3.17	0.28	1.29
06.12*	68.12	14.53	10	31.88	7.06	2168	2015	8.065	2.69	1.69	3.71	0.27	1.76
06.12*	68.12	14.53	5	31.88	7.15	2164	2008	8.067	2.71	1.70	3.74	0.27	1.77
06.12*	68.12	14.53	1	31.85	7.27	-	2031	-	-	-	3.00	0.22	1.73
05.01	68.12	14.53	300	34.95	7.24	2319	2199	7.932	2.24	1.42	12.27	0.84	6.40
05.01	68.12	14.53	200	34.82	7.36	2322	2204	7.930	2.26	1.44	11.29	0.76	5.55
05.01	68.12	14.53	150	34.65	7.37	2323	2168	8.025	2.76	1.75	10.26	0.64	4.64
05.01	68.12	14.53	125	34.36	7.96	2315	2150	8.049	2.94	1.87	7.87	0.55	3.56
05.01	68.12	14.53	100	34.03	8.85	2296	2156	7.973	2.58	1.64	6.16	0.48	2.90
05.01	68.12	14.53	75	33.56	9.19	2250	2120	7.953	2.45	1.55	4.09	0.32	2.12
05.01	68.12	14.53	50	32.70	7.09	2224	2061	8.088	2.92	1.84	3.57	0.28	1.87
05.01	68.12	14.53	30	32.34	5.91	2201	2043	8.089	2.77	1.74	3.35	0.26	1.82
05.01	68.12	14.53	20	32.33	5.90	2194	2044	8.076	2.69	1.69	3.31	0.27	1.82
05.01	68.12	14.53	10	32.32	5.88	2205	2102	7.932	2.01	1.27	3.42	0.27	1.91
05.01	68.12	14.53	5	32.31	5.89	2212	2051	8.102	2.86	1.80	3.33	0.27	1.91
05.01	68.12	14.53	1	32.33	5.89	2200	2043	8.053	2.58	1.62	3.16	0.27	1.84
17.02	68.12	14.53	300	34.94	7.43	2315	2199	7.924	2.21	1.41	11.95	0.81	5.75
17.02	68.12	14.53	200	34.72	7.80	2307	2144	8.036	2.83	1.79	9.74	0.64	4.19
17.02	68.12	14.53	150	34.53	7.97	2316	2145	8.051	2.95	1.87	7.81	0.55	3.36
17.02	68.12	14.53	125	34.49	8.00	2327	2160	8.035	2.89	1.83	8.62	0.59	3.65
17.02	68.12	14.53	100	34.32	7.82	2289	2130	8.026	2.77	1.76	7.70	0.56	3.33
17.02	68.12	14.53	75	34.09	7.26	2274	2138	7.989	2.51	1.59	6.15	0.44	2.76
17.02	68.12	14.53	50	33.84	6.63	2274	2112	8.062	2.84	1.79	6.28	0.45	2.83
17.02	68.12	14.53	30	33.73	6.38	2295	2127	8.091	3.01	1.90	6.99	0.49	3.06
17.02	68.12	14.53	20	33.64	6.19	2266	2112	8.059	2.77	1.75	6.14	0.45	2.76
17.02	68.12	14.53	10	33.61	6.14	2249	2097	8.056	2.73	1.72	5.79	0.42	2.69
17.02	68.12	14.53	5	33.48	5.94	2255	2103	8.068	2.78	1.75	6.00	0.43	2.75
17.02	68.12	14.53	1	33.25	5.34	2256	2106	8.031	2.52	1.59	6.02	0.45	2.75
17.03	68.12	14.53	300	34.95	7.33	2317	2180	7.970	2.42	1.54	12.55	0.82	6.08
17.03	68.12	14.53	200	34.89	7.52	2325	2174	8.002	2.65	1.68	12.32	0.79	5.31
17.03	68.12	14.53	150	34.80	7.54	-	2174	-	-	-	11.20	0.72	4.68
17.03	68.12	14.53	125	34.71	7.58	2337	2156	8.049	2.94	1.87	9.43	0.62	3.70
17.03	68.12	14.53	100	34.39	6.79	2279	2128	8.033	2.70	1.71	8.23	0.54	3.32
17.03	68.12	14.53	75	33.98	5.11	2267	2113	8.062	2.67	1.69	7.35	0.49	3.09
17.03	68.12	14.53	50	33.78	4.63	2266	2108	8.078	2.71	1.71	6.97	0.46	3.00
17.03	68.12	14.53	30	33.75	5.16	2238	2088	8.067	2.68	1.69	5.79	0.41	2.75
17.03	68.12	14.53	20	33.42	3.97	2228	2087	8.074	2.58	1.62	5.94	0.42	2.76
17.03	68.12	14.53	10	33.31	3.66	2231	2089	8.089	2.63	1.66	5.78	0.41	2.73
17.03	68.12	14.53	5	33.31	3.67	2236	2089	8.089	2.64	1.66	5.74	0.40	2.73
17.03	68.12	14.53	1	33.26	3.67	2226	2076	8.074	2.55	1.60	5.60	0.41	2.72
07.04	68.12	14.53	300	34.87	-	2322	2201	7.930	2.24	1.42	12.36	0.86	5.89
07.04	68.12	14.53	200	34.87	7.44	2314	2170	7.999	2.61	1.66	11.32	0.75	5.06

07.04	68.12	14.53	150	34.73	7.47	2326	2175	8.023	2.76	1.75	10.34	0.69	4.54
07.04	68.12	14.53	125	34.52	7.13	2303	2149	8.044	2.82	1.79	8.71	0.59	3.59
07.04	68.12	14.53	100	34.20	6.15	2289	2138	8.046	2.71	1.72	8.24	0.58	3.44
07.04	68.12	14.53	75	33.75	4.60	2269	2121	8.077	2.70	1.70	6.51	0.45	2.64
07.04	68.12	14.53	50	33.47	3.84	2264	2097	8.145	3.00	1.89	2.80	0.22	0.51
07.04	68.12	14.53	30	33.30	3.67	2251	2080	8.150	3.00	1.88	1.91	0.22	0.59
07.04	68.12	14.53	20	33.25	3.62	2246	2104	8.079	2.59	1.63	2.63	0.19	0.72
07.04	68.12	14.53	10	33.15	3.46	2251	2139	8.004	2.21	1.39	0.78	0.14	0.58
07.04	68.12	14.53	5	33.10	3.45	2244	2075	8.167	3.07	1.93	0.91	0.16	0.76
07.04	68.12	14.53	1	-	-	2240	2041	8.240	3.54	2.22	0.03	0.07	0.25
12.05	68.12	14.53	300	34.96	7.36	2320	2190	7.961	2.38	1.51	12.68	0.79	6.18
12.05	68.12	14.53	200	34.90	7.40	2322	2180	8.000	2.62	1.66	11.75	0.74	5.54
12.05	68.12	14.53	150	34.84	7.39	2316	2169	8.013	2.69	1.71	11.09	0.70	5.15
12.05	68.12	14.53	125	34.77	7.35	2310	2170	8.013	2.69	1.71	9.30	0.67	4.76
12.05	68.12	14.53	100	34.62	7.03	2306	2165	7.995	2.56	1.62	9.28	0.66	4.36
12.05	68.12	14.53	75	34.48	6.58	2298	2153	8.037	2.74	1.73	5.21	0.47	3.76
12.05	68.12	14.53	50	34.04	5.56	2285	2172	7.968	2.27	1.43	5.02	0.32	2.82
12.05	68.12	14.53	30	33.22	5.05	2234	2061	8.143	3.07	1.94	0.18	0.09	0.82
12.05	68.12	14.53	20	32.70	5.31	2196	2032	8.143	3.03	1.91	0.08	0.08	0.88
12.05	68.12	14.53	10	32.39	5.51	2188	2016	8.162	3.15	1.98	0.09	0.07	1.03
12.05	68.12	14.53	5	32.37	5.59	2195	2024	8.151	3.10	1.95	0.09	0.07	0.91
12.05	68.12	14.53	1	32.43	5.78	2209	2087	7.973	2.20	1.38	0.13	0.07	0.90
15.06	68.12	14.53	300	34.97	7.34	2316	2186	7.958	2.36	1.50	12.09	0.79	6.19
15.06	68.12	14.53	200	34.89	7.35	2307	2162	8.010	2.65	1.68	11.41	0.73	5.38
15.06	68.12	14.53	150	34.75	7.05	2312	2156	8.028	2.74	1.74	10.04	0.64	4.30
15.06	68.12	14.53	125	34.70	7.03	2320	2163	8.034	2.78	1.76	10.00	0.65	4.28
15.06	68.12	14.53	100	34.51	6.53	2301	2157	8.024	2.66	1.68	9.23	0.60	3.69
15.06	68.12	14.53	75	34.23	5.85	2263	2105	8.086	2.89	1.83	8.24	0.54	2.62
15.06	68.12	14.53	50	33.97	6.03	2276	2109	8.092	2.96	1.87	3.73	0.34	1.80
15.06	68.12	14.53	30	33.53	7.53	2291	2144	8.019	2.70	1.71	0.49	0.16	1.07
15.06	68.12	14.53	20	33.11	9.19	2230	2033	8.130	3.46	2.19	0.14	0.11	0.58
15.06	68.12	14.53	10	32.68	9.38	2195	2029	8.067	3.01	1.90	0.13	0.07	0.28
15.06	68.12	14.53	5	32.60	9.61	2205	2044	8.053	2.96	1.87	0.14	0.08	0.30
15.06	68.12	14.53	1	32.57	-	2192	2011	8.080	3.11	1.97	0.11	0.08	0.32
01.07	68.12	14.53	300	34.96	7.34	2319	2184	7.982	2.49	1.58	12.69	0.82	6.60
01.07	68.12	14.53	200	34.84	7.28	2306	2174	7.986	2.52	1.60	11.85	0.73	5.49
01.07	68.12	14.53	150	34.68	7.02	2328	2187	8.010	2.65	1.68	10.80	0.66	4.72
01.07	68.12	14.53	125	34.61	6.81	2289	2166	7.975	2.41	1.53	10.19	0.64	4.46
01.07	68.12	14.53	100	34.52	6.64	-	-	-	-	-	10.17	0.64	4.02
01.07	68.12	14.53	75	34.24	6.10	2302	2167	8.014	2.57	1.62	7.21	0.41	3.19
01.07	68.12	14.53	50	34.07	6.28	2260	2061	8.180	3.52	2.23	0.23	0.14	0.83
01.07	68.12	14.53	30	33.94	7.82	2279	2107	8.092	3.16	2.00	3.66	0.35	1.81
01.07	68.12	14.53	20	33.74	8.08	2255	2063	8.142	3.47	2.20	0.14	0.13	0.79
01.07	68.12	14.53	10	33.37	8.87	2250	2057	8.134	3.49	2.21	0.23	0.14	0.34
01.07	68.12	14.53	5	33.32	9.16	2241	2037	8.155	3.65	2.31	0.20	0.10	0.42
01.07	68.12	14.53	1	33.33	9.66	2240	2077	8.047	3.01	1.91	0.27	0.10	0.43
20.08	68.12	14.53	300	34.97	7.30	2315	2183	7.968	2.41	1.53	12.62	0.81	6.65
20.08	68.12	14.53	200	34.82	7.24	2324	2172	8.017	2.69	1.71	11.81	0.74	5.56
20.08	68.12	14.53	150	34.65	6.90	2312	2165	8.021	2.68	1.70	10.45	0.62	4.43
20.08	68.12	14.53	125	34.54	6.64	2297	2159	8.007	2.57	1.63	10.32	0.66	4.04
20.08	68.12	14.53	100	34.39	6.44	2299	2150	8.039	2.73	1.72	8.96	0.55	3.32
20.08	68.12	14.53	75	34.28	6.56	2282	2137	8.032	2.68	1.70	7.20	0.50	2.72
20.08	68.12	14.53	50	34.17	6.89	2285	2125	8.066	2.91	1.84	3.79	0.25	2.14
20.08	68.12	14.53	30	33.94	8.49	2261	2074	8.117	3.37	2.13	1.80	0.21	1.27

20.08	68.12	14.53	20	33.50	11.14	2239	2042	8.093	3.47	2.20	0.18	0.10	0.33
20.08	68.12	14.53	10	32.41	14.17	2173	1963	8.107	3.77	2.40	0.20	0.06	0.43
20.08	68.12	14.53	5	32.38	14.23	2166	1961	8.086	3.61	2.30	0.13	0.05	0.44
20.08	68.12	14.53	1	32.38	14.23	2165	1961	8.086	3.62	2.31	0.14	0.05	0.43
18.09	68.12	14.53	300	34.97	7.25	2307	2189	7.947	2.30	1.46	12.59	0.85	6.72
18.09	68.12	14.53	200	34.83	7.21	2310	2172	7.992	2.54	1.61	12.23	0.83	5.44
18.09	68.12	14.53	150	34.56	6.79	2309	2159	8.047	2.81	1.78	9.56	0.65	3.35
18.09	68.12	14.53	125	34.31	6.69	2267	2158	7.939	2.20	1.39	8.23	0.55	2.85
18.09	68.12	14.53	100	34.06	7.62	2236	2134	7.935	2.22	1.41	5.46	0.43	2.14
18.09	68.12	14.53	75	33.72	10.87	2254	2049	8.121	3.63	2.31	0.57	0.33	0.73
18.09	68.12	14.53	50	33.49	12.47	2270	2091	8.039	3.30	2.10	0.30	0.12	0.67
18.09	68.12	14.53	30	33.24	12.31	2215	2023	8.086	3.50	2.23	0.10	0.11	0.70
18.09	68.12	14.53	20	32.94	12.32	2196	2004	8.066	3.33	2.12	0.05	0.04	0.69
18.09	68.12	14.53	10	32.90	12.31	2206	2001	8.110	3.64	2.31	0.07	0.08	0.77
18.09	68.12	14.53	5	32.69	12.08	2188	1997	8.102	3.52	2.24	0.18	0.08	0.77
18.09	68.12	14.53	1	32.67	12.07	2199	2052	7.980	2.79	1.77	0.03	0.08	0.77
16.10	68.12	14.53	300	34.94	7.27	2330	2197	7.975	2.45	1.56	12.40	0.82	6.31
16.10	68.12	14.53	200	34.80	7.17	-	2185	-	-	-	11.87	0.80	5.73
16.10	68.12	14.53	150	34.55	6.76	2294	2163	8.019	2.63	1.67	10.05	0.71	4.00
16.10	68.12	14.53	125	34.29	7.11	2286	2139	8.045	2.80	1.77	7.31	0.54	3.02
16.10	68.12	14.53	100	34.14	7.75	2288	2127	8.069	3.00	1.90	5.36	0.40	2.33
16.10	68.12	14.53	75	33.93	10.88	2287	2094	8.089	3.48	2.22	2.16	0.20	1.29
16.10	68.12	14.53	50	33.41	11.50	2257	2066	8.078	3.42	2.18	0.45	0.12	1.02
16.10	68.12	14.53	30	33.03	10.40	2222	2034	8.128	3.56	2.26	0.41	0.10	0.90
16.10	68.12	14.53	20	33.02	10.36	2229	2036	8.124	3.54	2.25	0.07	0.09	1.21
16.10	68.12	14.53	10	33.01	10.34	2227	2041	8.101	3.39	2.15	0.28	0.11	0.95
16.10	68.12	14.53	5	33.01	10.34	2217	2053	8.060	3.11	1.98	0.32	0.16	0.97
16.10	68.12	14.53	1	-	-	2223	2033	8.112	3.46	2.19	0.36	0.12	0.99
14.11	68.12	14.53	300	34.94	7.23	2319	2171	8.005	2.59	1.65	12.98	0.89	6.56
14.11	68.12	14.53	200	34.83	7.19	2323	2172	8.016	2.68	1.70	12.68	0.85	5.95
14.11	68.12	14.53	150	34.66	6.96	2333	2177	8.040	2.82	1.78	11.56	0.76	4.82
14.11	68.12	14.53	125	34.43	6.80	2312	2155	8.047	2.82	1.78	9.24	0.63	3.48
14.11	68.12	14.53	100	34.23	8.18	2291	2134	8.029	2.82	1.79	6.30	0.52	2.59
14.11	68.12	14.53	75	33.41	8.50	2249	2070	8.098	3.19	2.02	2.20	0.21	1.23
14.11	68.12	14.53	50	33.29	8.14	2255	2072	8.118	3.29	2.08	2.27	0.21	1.33
14.11	68.12	14.53	30	33.26	8.03	2255	2076	8.112	3.25	2.05	1.64	0.20	1.24
14.11	68.12	14.53	20	33.27	8.13	2250	2090	8.064	2.96	1.87	1.62	0.19	1.23
14.11	68.12	14.53	10	33.25	8.16	2263	2083	8.111	3.27	2.07	2.34	0.20	1.24
14.11	68.12	14.53	5	33.24	8.16	2269	2080	8.128	3.39	2.14	2.27	0.20	1.24

Table 7. *Fugløya-Bjørnøya; January 2019.*

Stn	Date	Lat	Lon	Depth	S	T	A_T	C_T	pH_T	Ω_{Ca}	Ω_{Ar}	NO_3	PO_4	$SiOH_4$
		°N	°E	m		C°	µmol/kg	µmol/kg				µmol/kg	µmol/kg	µmol/kg
20	26.01	74.25	19.16	52.6	34.49	-0.87	2279	2160	8.060	2.17	1.36	7.77	0.58	2.91
20	26.01	74.25	19.16	31.7	34.48	-0.88	2280	2159	8.062	2.19	1.37	7.11	0.53	2.95
20	26.01	74.25	19.16	20.8	34.47	-0.90	2287	2160	8.053	2.16	1.35	6.89	0.53	2.92
20	26.01	74.25	19.16	10.3	34.47	-0.89	2280	2160	8.062	2.19	1.38	7.05	0.53	2.95
20	26.01	73.67	19.30	344.9	35.03	3.22	2314	2181	8.020	2.29	1.45	11.97	0.79	5.52
16	26.01	73.67	19.30	100.0	34.98	4.58	2321	2164	8.056	2.68	1.69	10.25	0.69	4.14
16	26.01	73.67	19.30	73.1	34.98	4.59	2309	2158	8.059	2.70	1.71	10.52	0.69	4.14
16	26.01	73.67	19.30	48.7	34.98	4.58	2316	2167	8.043	2.63	1.66	10.43	0.68	4.11
16	26.01	73.67	19.30	27.9	34.98	4.58	2316	2162	8.061	2.73	1.73	10.42	0.69	4.13
16	26.01	73.67	19.30	19.1	34.98	4.58	2312	2159	8.063	2.74	1.73	10.24	0.69	4.09
16	26.01	73.67	19.30	11.0	34.98	4.58	2316	2163	8.062	2.75	1.73	10.48	0.69	4.14
12	26.01	72.75	19.52	394.6	35.03	3.22	2317	2182	8.018	2.27	1.44	11.95	0.80	5.72
12	26.01	72.75	19.52	300.7	34.97	4.54	2319	2171	8.031	2.48	1.57	10.59	0.70	4.16
12	26.01	72.75	19.52	200.9	34.99	5.22	2319	2177	8.011	2.47	1.57	10.82	0.70	4.17
12	26.01	72.75	19.52	150.5	34.99	5.40	2313	2155	8.053	2.72	1.72	10.43	0.69	4.13
12	26.01	72.75	19.52	101.0	35.00	5.44	2310	2154	8.055	2.75	1.74	10.51	0.70	4.14
12	26.01	72.75	19.52	76.3	35.00	5.48	2309	2153	8.055	2.76	1.75	10.41	0.70	4.16
12	26.01	72.75	19.52	51.1	35.00	5.57	2311	2155	8.054	2.78	1.76	10.55	0.70	4.18
12	26.01	72.75	19.52	31.4	35.00	5.57	2312	2155	8.055	2.79	1.76	10.45	0.70	4.19
12	26.01	72.75	19.52	20.9	35.00	5.57	2310	2156	8.053	2.79	1.76	10.49	0.70	4.20
12	26.01	72.75	19.52	10.0	35.00	5.57	2311	2157	8.054	2.79	1.77	9.91	0.70	4.18
8	26.01	71.75	19.74	262.4	35.04	6.15	2311	2162	8.021	2.58	1.64	11.66	0.78	4.87
8	26.01	71.75	19.74	200.0	35.04	6.50	2321	2185	7.978	2.43	1.54	11.69	0.77	4.76
8	26.01	71.75	19.74	153.7	34.97	6.47	2319	2173	8.002	2.56	1.62	10.15	0.68	3.88
8	26.01	71.75	19.74	101.1	34.94	6.42	-	2143	-	-	-	8.43	0.58	3.17
8	26.01	71.75	19.74	76.6	34.91	6.26	2320	2167	8.021	2.67	1.69	9.77	0.65	3.70
8	26.01	71.75	19.74	50.9	34.90	6.23	2318	2166	8.023	2.68	1.70	9.52	0.65	3.66
8	26.01	71.75	19.74	30.1	34.91	6.38	2312	2148	8.053	2.86	1.81	9.70	0.65	3.64
8	26.01	71.75	19.74	21.4	34.90	6.47	2311	2145	8.054	2.88	1.82	9.46	0.64	3.58
8	26.01	71.75	19.74	10.3	34.64	5.60	2303	2140	8.070	2.86	1.81	8.40	0.58	3.15
2	27.01	70.67	19.97	151.3	34.86	7.05	2310	2144	8.041	2.81	1.78	9.18	0.63	3.63
2	27.01	70.67	19.97	99.6	34.50	6.73	2297	2132	8.058	2.86	1.81	7.64	0.54	2.90
2	27.01	70.67	19.97	73.2	34.26	6.60	2288	2124	8.060	2.85	1.80	7.13	0.50	2.76
2	27.01	70.67	19.97	48.4	34.07	6.02	2282	2120	8.067	2.83	1.78	6.50	0.46	2.52
2	27.01	70.67	19.97	28.5	33.91	5.30	2276	2116	8.079	2.82	1.78	5.76	0.42	2.32
2	27.01	70.67	19.97	19.0	33.90	5.31	2269	2114	8.078	2.80	1.77	5.85	0.42	2.31
2	27.01	70.67	19.97	9.6	33.90	5.31	2271	2115	8.080	2.82	1.78	5.73	0.42	2.32

***Table 8**. Barents Sea; September 2019.*

Stn	Date	Lat °N	Lon °E	Depth m	S	T C°	A_T µmol/kg	C_T µmol/kg	pH_T	Ω_{Ca}	Ω_{Ar}	NO_3 µmol/kg	PO_4 µmol/kg	$SiOH_4$ µmol/kg
23	29.09	77.00	34.00	123.4	34.84	-0.13	2304	2207	8.150	2.70	1.70	12.24	0.86	6.73
23	29.09	77.00	34.00	100.8	34.74	-1.00	2293	2204	8.091	2.31	1.45	6.57	0.59	2.39
23	29.09	77.00	34.00	74.9	34.72	-1.14	2299	2184	8.108	2.39	1.50	6.64	0.58	2.33
23	29.09	77.00	34.00	30.5	34.08	1.83	2266	2095	8.054	2.35	1.48	0.15	0.12	0.20
23	29.09	77.00	34.00	21.3	34.08	1.84	2270	2119	8.078	2.48	1.56	0.22	0.09	0.22
23	29.09	77.00	34.00	8.8	34.08	1.84	2270	2126	8.099	2.59	1.63	0.10	0.09	0.24
24	29.09	77.51	34.00	180.8	34.81	-0.82	2301	2216	8.189	2.81	1.77	10.71	0.80	6.38
24	29.09	77.51	34.00	126.3	34.75	-1.33	2295	2198	8.078	2.21	1.39	9.77	0.71	3.88
24	29.09	77.51	34.00	100.3	34.73	-1.46	2297	2198	8.084	2.24	1.41	9.66	0.72	3.30
24	29.09	77.51	34.00	75.9	34.69	-1.46	2300	2201	8.088	2.27	1.43	9.65	0.73	2.56
24	29.09	77.51	34.00	50.7	34.54	-0.82	2292	2185	8.087	2.32	1.45	6.58	0.60	1.69
24	29.09	77.51	34.00	30.7	34.10	1.54	2272	2102	8.047	2.30	1.44	0.62	0.14	0.52
24	29.09	77.51	34.00	18.9	34.11	1.54	2268	2103	8.091	2.52	1.58	0.50	0.14	0.51
24	29.09	77.51	34.00	10.1	34.11	1.54	2268	2096	8.156	2.88	1.81	0.46	0.11	0.41
25	28.09	78.00	34.00	182.7	34.85	-0.55	2303	2201	8.204	2.93	1.85	11.71	0.82	6.88
25	28.09	78.00	34.00	149.1	34.85	-0.28	2300	2198	8.151	2.68	1.68	11.55	0.84	6.59
25	28.09	78.00	34.00	123.6	34.81	-0.67	2296	2192	8.066	2.22	1.39	10.30	0.74	4.18
25	28.09	78.00	34.00	97.8	34.79	-0.19	2301	2187	8.064	2.27	1.42	10.90	0.74	3.80
25	28.09	78.00	34.00	74.8	34.73	-0.53	2296	2181	8.080	2.31	1.45	9.91	0.70	3.38
25	28.09	78.00	34.00	50.3	34.66	-0.51	2300	2179	8.059	2.22	1.40	6.91	0.59	2.49
25	28.09	78.00	34.00	29.9	34.23	1.03	2284	2152	8.060	2.34	1.47	2.07	0.31	1.06
25	28.09	78.00	34.00	19.4	34.19	1.25	2276	2133	8.121	2.66	1.67	0.65	0.15	0.60
25	28.09	78.00	34.00	9.4	34.19	1.25	2278	2149	8.177	2.98	1.87	0.88	0.18	0.65
27	27.09	78.75	34.00	293.0	34.84	-1.63	-	2201	-	-	-	9.35	0.69	6.06
27	27.09	78.75	34.00	124.8	34.68	-1.25	2290	2177	8.073	2.19	1.38	9.58	0.67	3.96
27	27.09	78.75	34.00	99.3	34.64	-1.57	2294	2183	8.087	2.24	1.41	9.30	0.64	3.47
27	27.09	78.75	34.00	74.3	34.61	-1.73	2290	2177	8.088	2.23	1.40	9.29	0.64	3.22
27	27.09	78.75	34.00	49.4	34.56	-1.69	2291	2184	8.215	2.91	1.83	7.75	0.61	2.68
27	27.09	78.75	34.00	30.0	34.36	-1.01	2292	2137	8.062	2.19	1.37	2.23	0.35	1.63
27	27.09	78.75	34.00	19.6	33.83	1.47	2281	2108	8.125	2.69	1.69	0.71	0.20	1.13
27	27.09	78.75	34.00	9.3	33.83	1.51	2247	2098	8.150	2.80	1.76	0.43	0.10	0.66
28	27.09	79.00	34.00	258.8	34.75	-1.76	2298	2174	8.216	2.83	1.78	8.39	0.62	4.50
28	27.09	79.00	34.00	198.8	34.72	-1.52	2295	2174	8.058	2.08	1.31	8.63	0.63	4.03
28	27.09	79.00	34.00	122.8	34.68	-1.00	2289	2172	8.064	2.17	1.37	8.86	0.64	3.51
28	27.09	79.00	34.00	99.4	34.66	-1.28	-	2087	-	-	-	0.21	0.13	0.43
28	27.09	79.00	34.00	49.1	34.58	-1.78	2289	2176	8.071	2.16	1.36	8.18	0.61	2.94
28	27.09	79.00	34.00	29.3	33.96	0.67	2283	2137	8.037	2.19	1.37	2.56	0.35	1.20
28	27.09	79.00	34.00	19.1	33.86	0.58	2266	2105	8.152	2.74	1.72	1.05	0.16	0.62
28	27.09	79.00	34.00	9.3	33.87	0.56	2256	2094	8.208	3.05	1.91	0.15	0.09	0.43
31	27.09	79.75	34.00	318.8	34.86	-1.81	2304	2187	8.187	2.65	1.67	7.68	0.63	4.88
31	27.09	79.75	34.00	200.1	34.74	-0.65	2300	2182	8.008	1.95	1.23	9.81	0.70	4.96
31	27.09	79.75	34.00	150.2	34.70	-1.05	2298	2178	8.017	1.97	1.24	9.20	0.66	4.28
31	27.09	79.75	34.00	75.1	34.61	-1.74	2288	2179	8.053	2.07	1.30	7.93	0.61	2.94
31	27.09	79.75	34.00	50.3	34.54	-1.36	2286	2166	8.067	2.17	1.36	7.30	0.63	3.03
31	27.09	79.75	34.00	29.4	34.05	0.06	2278	2162	8.058	2.23	1.40	3.56	0.43	1.86
31	27.09	79.75	34.00	20.4	33.75	0.30	2252	2091	8.072	2.28	1.43	0.45	0.14	0.59
31	27.09	79.75	34.00	10.8	33.67	0.03	2241	2073	8.128	2.52	1.58	0.22	0.10	0.51
32	27.09	80.00	34.00	203.1	34.71	-0.97	2294	2177	8.156	2.60	1.63	9.81	0.70	5.02
32	27.09	80.00	34.00	150.3	34.67	-1.01	2295	2179	8.123	2.45	1.54	9.52	0.67	4.23
32	27.09	80.00	34.00	125.3	34.63	-1.03	2288	2171	7.988	1.85	1.16	9.33	0.67	4.36

32	27.09	80.00	34.00	101.4	34.56	-1.20	2288	2164	8.010	1.93	1.21	8.25	0.65	3.89
32	27.09	80.00	34.00	75.3	34.50	-1.31	2285	2165	8.020	1.97	1.23	8.01	0.65	3.93
32	27.09	80.00	34.00	50.2	34.25	-1.15	2272	2142	8.016	1.95	1.22	5.27	0.53	3.06
32	27.09	80.00	34.00	30.4	33.84	0.40	2252	2092	8.030	2.10	1.32	1.32	0.24	1.16
32	27.09	80.00	34.00	20.3	33.68	-0.04	2241	2073	8.192	2.86	1.79	0.35	0.13	0.57
32	27.09	80.00	34.00	10.3	33.52	-0.67	2226	2086	8.196	2.80	1.75	0.64	0.15	0.74
33	26.09	80.50	34.00	163.6	34.70	-0.56	-	2076	-	-	-	9.82	0.70	4.98
33	26.09	80.50	34.00	150.2	34.70	-0.54	2291	2163	7.999	1.92	1.21	8.63	0.66	4.16
33	26.09	80.50	34.00	100.1	34.52	-1.11	2278	2152	7.987	1.84	1.15	9.68	0.68	4.83
33	26.09	80.50	34.00	74.7	34.40	-1.42	2289	2158	8.066	2.15	1.35	6.90	0.56	3.57
33	26.09	80.50	34.00	49.9	34.28	-1.51	2271	2139	8.233	2.99	1.88	5.16	0.45	2.62
33	26.09	80.50	34.00	30.2	33.97	-1.51	2249	2112	8.185	2.69	1.68	2.64	0.20	0.84
33	26.09	80.50	34.00	9.8	33.53	-1.71	2222	2073	8.156	2.47	1.55	2.59	0.24	0.80

***Table 9**. Tromsø-Longyearbyen; March, June, August, November 2019.*

Station	Date	Lat °N	Lon °E	S		T C°	A_T µmol/kg	C_T µmol/kg	pH_T	pCO2 µatm	Ω_{Ca}	Ω_{Ar}	NO_3 µmol/kg	PO_4 µmol/kg	$SiOH_4$ µmol/kg
NB1	12.3	69.72	19.07	33.50	3.07	12.3	2257	2109	8.065	367	2.63	1.65	7.89	0.92	6.67
NB2	12.3	70.26	19.45	33.92	4.08	12.3	2297	2134	8.075	364	2.87	1.81	7.82	0.60	4.72
NB3	12.3	70.97	18.88	34.85	6.18	12.3	2316	2151	8.046	396	2.91	1.84	10.81	0.79	5.85
NB4	13.3	71.58	18.49	34.92	6.15	13.3	2323	2150	7.995	454	3.02	1.91	11.16	0.79	5.69
NB5	13.3	72.20	18.05	35.00	6.39	13.3	2315	2148	8.044	398	2.92	1.85	11.51	0.82	5.85
NB6	13.3	72.81	17.49	35.02	5.87	13.3	2312	2155	8.052	389	2.78	1.76	11.86	0.82	5.85
NB7	13.3	73.30	17.08	35.00	5.83	13.3	2309	2153	8.039	401	2.77	1.75	11.51	0.82	5.69
NB8	13.3	74.52	16.02	35.02	5.79	13.3	2310	2154	8.040	401	2.76	1.75	11.86	0.82	5.85
NB9	13.3	75.28	15.28	35.03	5.55	13.3	2312	2155	8.050	390	2.78	1.76	12.21	0.85	6.01
NB10	14.3	75.87	14.72	35.00	5.07	14.3	2313	2153	8.055	385	2.81	1.77	12.21	0.85	6.01
NB11	14.3	76.36	14.27	35.01	5.22	14.3	2311	2157	8.057	383	2.74	1.73	11.86	0.85	5.85
NB12	14.3	76.90	13.75	34.72	2.75	14.3	2288	2152	8.071	363	2.47	1.56	11.51	0.82	6.18
NB13	14.3	77.49	13.14	34.94	3.48	14.3	2303	2162	8.077	360	2.53	1.60	11.86	0.85	6.18
NB14	14.3	78.09	13.60	34.95	2.96	14.3	2302	2167	8.074	362	2.46	1.55	11.86	0.85	6.18
NB15	14.3	78.26	15.50	34.75	0.06	14.3	2304	2166	8.114	324	2.48	1.56	9.91	0.76	5.85
NB1	7.6	69.72	19.07	32.44	7.19	7.6	2229	2042	8.139	304	3.25	2.05	0.42	0.32	1.79
NB2	7.6	70.26	19.45	34.07	6.75	7.6	2270	2082	8.105	335	3.21	2.03	9.28	1.67	4.72
NB3	8.6	70.97	18.97	34.49	7.53	8.6	2302	2109	-	-	3.32	2.10	0.07	0.19	1.30
NB4	8.6	71.58	18.54	34.60	7.38	8.6	2304	2099	8.131	317	3.50	2.21	0.07	0.16	0.88
NB5	8.6	72.20	18.09	34.77	7.13	8.6	2319	2099	8.133	317	3.72	2.35	9.56	0.79	5.04
NB6	8.6	72.81	17.64	34.91	7.12	8.6	2329	2111	8.119	330	3.69	2.34	1.47	0.32	2.11
NB7	8.6	73.30	17.27	35.01	6.67	8.6	2321	2129	8.106	340	3.28	2.08	9.70	0.69	4.88
NB8	8.6	74.52	16.29	35.00	6.57	8.6	2337	2140	8.095	352	3.37	2.13	7.67	0.66	4.55
NB9	9.6	75.28	15.65	34.88	4.53	9.6	2319	2152	8.113	332	2.91	1.84	7.19	0.57	4.23
NB10	9.6	75.87	15.14	34.79	3.99	9.6	2326	2092	8.211	256	3.90	2.46	4.54	0.47	3.58
NB11	9.6	76.36	14.69	35.03	5.09	9.6	2321	2146	8.147	304	3.03	1.91	1.67	0.32	2.28
NB12	9.6	76.90	14.15	34.24	1.85	9.6	2296	2038	8.317	190	4.23	2.66	1.54	0.35	2.44
NB13	9.6	77.49	13.57	34.76	3.34	9.6	2318	2046	8.323	189	4.47	2.81	1.40	0.32	2.11
NB14	9.6	78.08	13.60	35.01	4.13	9.6	2321	2141	8.173	283	3.10	1.96	3.63	0.44	2.44
NB15	9.6	78.25	15.50	34.78	3.97	9.6	2306	2026	8.322	188	4.57	2.88	2.30	0.41	4.06
NB1	30.8	69.72	19.06	32.68	9.03	30.8	2229	2055	8.091	346	3.06	1.94	0.98	0.41	7.33
NB2	30.8	70.26	19.44	34.15	9.89	30.8	2278	2072	8.111	332	3.52	2.24	0.42	0.44	5.04
NB3	30.8	70.97	18.97	34.11	9.70	30.8	2281	2068	8.135	312	3.63	2.30	0.35	0.41	4.23
NB4	31.8	71.58	18.53	34.48	10.09	31.8	2305	2091	8.130	319	3.66	2.32	0.63	0.25	1.46
NB5	31.8	72.20	18.10	34.50	10.12	31.8	2308	2086	8.134	316	3.78	2.40	2.65	0.41	1.79
NB6	31.8	72.81	17.65	34.64	10.24	31.8	2302	2077	8.131	317	3.81	2.42	1.95	0.41	1.79
NB7	31.8	73.30	17.30	34.79	7.98	31.8	2313	2093	8.155	298	3.72	2.36	1.05	0.54	4.88
NB8	31.8	74.52	16.25	34.76	9.32	31.8	2293	2081	8.097	346	3.61	2.29	0.14	0.22	1.27
NB9	31.8	75.28	15.63	34.64	6.95	31.8	2281	2095	8.155	293	3.20	2.02	0.49	0.28	2.28
NB10	1.9	75.87	15.12	34.50	6.70	1.9	2266	2081	8.138	305	3.18	2.01	0.07	0.19	0.41
NB11	1.9	76.36	14.67	34.85	8.05	1.9	2307	2081	8.122	324	3.82	2.42	0.07	0.22	1.28
NB12	1.9	76.90	14.15	32.86	3.93	1.9	2180	1971	8.159	279	3.50	2.20	0.07	0.19	0.72
NB13	1.9	77.49	13.54	32.61	4.88	1.9	2149	1923	8.116	310	3.75	2.35	0.07	0.22	0.64
NB14	1.9	78.08	13.60	32.59	6.12	1.9	2199	2006	8.137	301	3.30	2.08	0.70	0.57	1.55
NB15	1.9	78.26	15.50	31.38	6.01	1.9	1969	1802	8.136	272	2.80	1.76	3.29	0.66	5.70
NB1	22.11	69.72	19.06	33.07	6.40	22.11	2243	2100	8.031	403	2.61	1.64	5.80	0.57	4.56
NB2	22.11	70.26	19.44	33.69	7.43	22.11	2267	2099	8.105	335	2.98	1.88	3.70	0.38	2.12
NB3	22.11	70.97	18.95	34.11	6.89	22.11	2280	2121	8.065	374	2.83	1.79	5.37	0.50	3.25
NB4	23.11	71.58	18.53	34.33	6.44	23.11	2282	2132	8.090	349	2.69	1.70	6.00	0.50	2.76
NB5	23.11	72.20	18.16	34.63	6.12	23.11	2296	2138	8.084	356	2.80	1.77	6.70	0.57	2.93

NB6	23.11	72.81	17.66	34.67	6.05	23.11	2301	2144	8.047	393	2.78	1.76	7.68	0.63	3.25
NB7	23.11	73.30	17.27	34.90	5.80	23.11	2300	2152	8.051	388	2.66	1.68	9.42	0.73	4.06
NB8	23.11	74.52	16.26	34.95	6.02	23.11	2310	2155	8.059	382	2.75	1.74	9.63	0.76	4.06
NB9	23.11	75.28	15.60	34.88	4.26	23.11	2291	2149	8.067	369	2.54	1.60	9.49	0.73	4.23
NB10	23.11	75.87	15.06	34.84	4.09	23.11	2297	2152	8.055	381	2.59	1.64	9.70	0.73	4.23
NB11	24.11	76.36	14.60	34.95	5.37	24.11	2306	2150	8.063	376	2.76	1.74	10.05	0.76	4.39
NB12	24.11	76.90	14.12	33.43	-1.36	24.11	2211	2093	8.091	330	2.18	1.37	5.03	0.54	3.25
NB13	24.11	77.49	13.49	33.37	-1.55	24.11	2214	2095	8.100	323	2.18	1.37	5.10	0.57	3.42
NB14	24.11	78.08	13.60	33.59	-0.59	24.11	2221	2099	8.096	328	2.23	1.40	4.75	0.47	2.77
NB15	24.11	78.26	15.50	33.42	-0.19	24.11	2226	2183	8.119	311	1.31	0.82	2.86	0.38	2.44

***Table 10**. Oslo-Kiel; February, May, August, November 2019.*

Station	Date	Lat °N	Lon °E	S	T C°	A_T µmol/kg	C_T µmol/kg	pH_T	pCO2 µatm	Ω_{Ca}	Ω_{Ar}	NO_3 µmol/kg	PO_4 µmol/kg	$SiOH_4$ µmol/kg
DK1	25.2	59.808	10.577	26.45	2.84	1947	1857	8.016	2207	1.80	1.11	13.34	0.51	14.40
OF2	25.2	59.199	10.636	21.60	3.15	1712	1675	7.983	2204	1.07	0.64	20.43	0.35	20.85
OF1	25.2	58.998	10.659	28.08	3.91	2139	2051	8.108	2184	1.87	1.16	4.28	0.35	5.07
SK1	25.2	58.846	10.642	31.75	4.49	2222	2135	-	2095	1.85	1.16	5.38	0.38	4.40
SK2	25.2	58.648	10.643	31.55	4.40	2204	2121	8.057	2119	1.80	1.13	4.48	0.38	4.07
SK3	25.2	58.446	10.646	31.27	4.27	2245	2116	8.074	2126	2.44	1.53	4.27	0.38	3.75
SK4	25.2	58.248	10.883	31.17	4.20	2244	2113	8.066	2216	2.48	1.55	4.27	0.38	3.75
SK5	25.2	58.046	10.951	31.19	4.31	2245	2113	8.055	2198	2.49	1.56	4.27	0.38	3.75
SK6	25.2	57.849	11.162	33.44	4.79	2348	2190	8.051	2198	2.87	1.80	6.50	0.44	5.37
DK1	30.5	59.806	10.577	24.59	12.10	1863	1698	-	2201	3.01	1.86	2.25	0.16	7.04
OF2	28.5	59.198	10.630	18.51	14.07	1625	1535	8.033	2185	1.90	1.14	5.72	0.13	15.63
OF1	28.5	58.998	10.638	24.50	13.29	2067	1934	8.058	2102	2.67	1.66	0.14	0.10	1.23
SK1	28.5	58.848	10.635	27.38	12.24	2160	1997	8.061	2103	3.08	1.93	0.14	0.10	1.19
SK2	28.5	58.646	10.701	27.49	12.02	2163	2000	8.079	2096	3.08	1.93	0.07	0.10	1.29
SK3	28.5	58.449	10.655	28.16	11.69	2128	2015	8.084	2201	2.29	1.44	0.07	0.10	0.88
SK4	28.5	58.247	10.906	28.62	11.99	2184	2017	8.060	2198	3.12	1.96	0.07	0.10	1.63
SK5	28.5	58.047	11.050	28.26	11.73	2139	2019	8.074	2192	2.39	1.50	0.07	0.13	1.96
SK6	28.5	57.850	11.101	28.37	11.61	2141	2002	8.067	2187	2.68	1.68	0.07	0.10	0.80
DK1	22.8	59.807	10.577	22.96	18.49	1761	1624	8.016	2181	2.64	1.64	0.21	0.29	3.44
OF2	22.8	59.198	10.633	23.96	18.07	1951	1801	7.995	2179	2.94	1.83	0.07	0.19	2.62
OF1	22.8	59.000	10.618	25.54	17.40	2077	1913	8.029	2152	3.18	2.00	0.07	0.22	1.80
SK1	22.8	58.848	10.670	30.13	16.90	2211	2009	8.037	2133	3.67	2.34	0.07	0.28	2.28
SK2	22.8	58.647	10.693	31.02	17.04	2290	2007	8.058	2149	4.99	3.19	-	0.22	-
SK3	22.8	58.447	10.811	27.77	17.17	2127	1947	8.048	2201	3.38	2.14	0.07	0.29	1.80
SK4	22.8	58.247	10.936	30.13	16.81	2199	2004	8.038	2177	3.56	2.27	0.14	0.28	1.96
SK5	22.8	58.049	11.048	30.59	16.76	-	2008	8.025	2183	-	-	0.07	0.25	1.53
SK6	22.8	57.846	11.216	30.70	17.07	2212	2029	7.997	2177	3.36	2.15	0.14	0.35	2.45
DK1	30.11	59.808	10.578	25.98	5.21	1962	1895	7.954	2184	1.53	0.94	13.69	0.48	15.38
OF2	28.11	59.198	10.631	22.84	6.91	1997	1906	8.030	2137	1.95	1.19	2.89	0.35	5.41
OF1	28.11	58.998	10.670	22.71	6.87	1859	1782	7.981	2108	1.67	1.01	4.58	0.32	9.35
SK1	30.11	58.849	10.716	22.94	6.53	1950	1865	8.004	2098	1.82	1.11	3.45	0.35	6.72
SK2	30.11	58.647	10.773	23.90	6.98	1967	1873	7.995	2174	1.95	1.19	3.87	0.38	7.87
SK3	28.11	58.449	10.865	21.53	8.10	2011	1926	8.000	2174	1.91	1.16	1.06	0.38	3.78
SK4	28.11	58.248	10.951	21.04	8.25	1995	1914	7.995	2172	1.86	1.12	1.27	0.41	4.76
SK5	28.11	58.047	11.044	20.76	8.46	-	-	7.950	2087	-	-	1.20	0.41	5.09
SK6	28.11	57.847	11.188	18.72	8.32	1962	1889	7.977	2176	1.78	1.06	0.92	0.38	5.26

Table 11. Water column station in Hardanger; Korsfjorden (VT69) at 60.19°N 5.24°E, 2019.

Date	Depth	S	T C°	A_T µmol/kg	C_T µmol/kg	pH_T	pCO_2 µatm	Ω_{Ca}	Ω_{Ar}	NO_3 µmol/kg	PO_3 µmol/kg	$SiOH_4$ µmol/kg
23.7	667	35.11	7.17	2321.2	2189.8	7.934	490.2	2.14	1.36	-	-	-
23.7	302	35.14	7.65	2319.5	2160.7	8.01	420.4	2.66	1.70	-	-	-
23.7	202	35.07	7.66	2318.9	2171.6	7.986	452.8	2.57	1.63	-	-	-
23.7	126	34.94	7.62	2316.8	2165.9	8.000	440.2	2.66	1.69	-	-	-
23.7	101	34.82	7.54	2312.3	2159.6	8.008	431.3	2.70	1.71	-	-	-
23.7	76	34.72	7.44	2317.1	2158.2	8.027	413.0	2.80	1.78	-	-	-
23.7	51	34.57	7.47	2306.5	2159.8	8.000	442.7	2.65	1.68	-	-	-
23.7	31	34.26	7.88	2297.1	2149.2	8.002	440.8	2.68	1.70	-	-	-
23.7	21	33.55	9.07	2259.6	2086.1	8.06	376.7	3.06	1.94	-	-	-
23.7	11	31.77	13.72	2225.1	2026.6	8.072	367.1	3.53	2.24	-	-	-
23.7	6	31.71	13.84	2222.8	2025.2	8.07	369.7	3.52	2.24	-	-	-
23.7	0	34.92	7.75	2217.6	2019.8	8.125	307.4	3.33	2.11	-	-	-
30.8	302	35.07	7.57	2315.9	2163.2	7.995	435.9	2.57	1.64	9.1	0.7	4.4
30.8	202	34.97	7.68	2314.1	2171.3	7.974	466.5	2.50	1.59	9.7	0.8	5.1
30.8	127	34.62	7.98	2309.2	2167.8	7.973	472.1	2.53	1.60	8.9	0.7	4.8
30.8	102	34.34	8.29	2302.4	2153.7	7.992	450.3	2.65	1.68	6.9	0.6	3.6
24.9	50	34.17	10.09	2299.9	2149.8	7.972	479.7	2.72	1.73	5.0	0.5	3.2
24.9	30	34.17	10.09	2286.5	2124.8	7.973	482.7	2.94	1.88	5.0	0.5	3.2
24.9	20	33.40	12.73	2252.5	2089.0	7.98	470.5	2.99	1.90	-	-	-
24.9	10	33.40	12.73	2117.0	1959.5	7.993	436.2	2.90	1.84	-	-	-
24.9	5	32.59	13.48	1898.4	1745.3	8.05	345.8	2.78	1.75	-	-	-
24.9	1	32.59	13.48	1863.5	1715.0	8.056	336.4	2.71	1.70	-	-	-
18.10	664	35.11	7.36	2321.1	2187.7	7.933	491.0	2.15	1.37	10.9	0.8	7.2
18.10	303	35.11	7.71	2318.0	2168.9	7.983	450.2	2.53	1.61	9.6	0.7	4.9
18.10	303	35.11	7.71	2320.7	2172.5	7.981	453.8	2.52	1.60	9.7	0.7	4.9
18.10	202	35.05	7.85	2314.3	2169.9	7.974	466.2	2.52	1.60	9.0	0.7	4.4
18.10	102	34.69	8.58	2310.2	2169.9	7.961	489.2	2.53	1.61	8.2	0.7	4.9
18.10	77	34.37	9.59	2302.4	2156.4	7.966	485.2	2.64	1.68	6.3	0.5	3.8
18.10	52	33.74	12.91	2287.2	2113.7	7.992	456.4	3.09	1.97	2.3	0.2	2.2
18.10	31	32.90	13.13	2269.8	2070.3	8.062	380.4	3.50	2.23	0.5	0.1	1.7
18.10	21	32.70	13.15	2265.1	2065.4	8.065	377.1	3.52	2.24	0.3	0.1	1.7
18.10	11	31.93	12.62	2208.4	2040.8	8.017	420.6	3.03	1.93	1.4	0.1	1.5
18.10	5	30.26	11.93	-	-	-	-	-	-	-	-	-

18.10	1	29.99	11.75	2086.6	1920.3	8.069	351.3	2.99	1.89	0.1	0.0	0.5
12.11	662	35.12	7.39	2319.5	2186.2	7.933	491.3	2.15	1.37	0.1	0.0	0.5
12.11	302	35.07	7.86	2314.2	2170.2	7.969	466.8	2.46	1.57	10.3	0.8	7.2
12.11	127	34.58	9.27	2304.6	2162.6	7.955	494.9	2.55	1.62	9.5	0.7	4.5
12.11	102	34.42	10.76	2301.3	2142.9	7.977	470.6	2.81	1.79	7.4	0.6	4.3
12.11	76	34.26	12.06	2300.5	2127.3	7.996	451.4	3.05	1.95	4.8	0.4	3.1
12.11	51	33.49	12.25	2274.7	2105.8	7.996	449.9	3.01	1.92	2.9	0.3	2.2
12.11	31	32.67	12.11	2258.3	2080.6	8.032	409.4	3.17	2.01	3.2	0.3	2.3
12.11	21	31.96	11.08	2225.4	2053.4	8.049	388.1	3.08	1.95	2.3	0.2	1.8
12.11	11	31.64	10.51	2179.5	2016.9	8.045	384.7	2.93	1.85	2.6	0.2	1.5
12.11	6	31.19	9.17	2157.9	1994.1	8.077	349.9	2.93	1.85	2.1	0.1	1.1
12.11	1	31.13	9.03	2150.9	1989.9	8.075	351.6	2.89	1.82	1.5	0.1	1.0

Table 12. Water column station in Hardanger; ytre Hardangerfjord (H7) at 59.74°N 5.49°E, 2019.

Date	Depth m	S	T C°	A_T µmol/kg	C_T µmol/kg	pH_T	pCO_2 µatm	Ω_{Ca}	Ω_{Ar}	NO_3^- µmol/kg	PO_3^4 µmol/kg	$SiOH_4$ µmol/kg
23.7	332	35.04	7.55	2317.4	2169.4	7.985	447.0	2.51	1.60	-	-	-
23.7	98	34.78	7.62	2307.9	2161.4	7.993	448.6	2.61	1.66	-	-	-
23.7	48	34.36	8.27	2298.9	2141.1	8.019	422.2	2.81	1.78	-	-	-
23.7	28	33.93	9.51	2285.2	2097.7	8.077	363.3	3.26	2.07	-	-	-
23.7	8	32.40	12.70	2226.9	2021.7	8.094	344.1	3.59	2.28	-	-	-
23.7	0	31.52	13.25	2161.5	1965.4	8.087	343.8	3.46	2.20	-	-	-
30.8	332	35.04	7.57	2315.9	2172.9	7.97	464.2	2.43	1.55	9.8	0.7	5.6
30.8	100	34.63	8.38	2305.2	2163.9	7.968	479.3	2.54	1.62	8.2	0.6	4.6
30.8	50	32.91	13.77	2265.0	2095.3	7.983	466.4	3.06	1.95	1.4	0.2	1.6
30.8	32	31.00	16.65	2211.9	2014.6	8.036	405.7	3.55	2.27	0.1	0.1	0.9
30.8	11	30.90	16.91	2213.5	2005.6	8.057	384.5	3.74	2.39	0.0	0.0	1.0
30.8	1	30.80	17.06	2203.6	1999.8	8.049	392.2	3.68	2.35	0.0	0.1	1.0
18.10	331	35.01	7.60	2313.4	2176.8	7.953	484.1	2.35	1.50	9.7	0.8	5.6
18.10	101	34.61	8.73	2303.3	2165.8	7.953	498.5	2.49	1.58	8.2	0.7	4.9
18.10	50	33.27	12.42	2270.5	2098.0	8.006	438.9	3.07	1.96	2.4	0.2	2.4
18.10	29	32.92	12.84	2261.0	2075.7	8.035	406.3	3.28	2.09	1.1	0.2	1.7
18.10	10	31.53	12.48	2144.2	1976.3	8.033	392.1	3.00	1.91	1.1	0.1	1.2
18.10	2	28.04	11.49	1943.5	1798.3	8.064	337.6	2.64	1.65	0.6	0.1	0.6
12.11	331	35.01	7.63	2317.1	2181.9	7.948	490.6	2.33	1.49	10.2	0.8	6.5
12.11	99	34.45	10.31	2302.6	2149.0	7.972	477.4	2.74	1.74	6.0	0.5	3.8
12.11	49	33.70	12.17	2288.7	2108.7	8.019	425.2	3.18	2.02	2.6	0.2	2.1
12.11	29	32.87	12.00	2257.7	2087.7	8.013	429.4	3.05	1.94	2.8	0.2	2.0
12.11	10	30.85	9.06	2137.1	1965.9	8.105	323.0	3.03	1.91	1.3	0.1	0.5
12.11	2	30.77	9.45	2125.9	1966.2	8.073	350.8	2.87	1.81	1.5	0.1	0.6

Table 13. Cold water coral reefs: Huglhammaren, Straumsneset (Hardanger), Hola, Steinavær, Fugløya, Stjernsund, Korallen (Troms/Finnmark); June, July, September, October 2019 and October 2018 (*).

Date	Site	Station	Lat	Lon	Depth	S	T	A_T	C_T	pH_T	Ω_{Ca}	Ω_{Ar}
			°N	°E	m		C°	µmol/kg	µmol/kg			
20.06.	Huglhammaren	Hugl1	59.815	5.594	206	34.96	7.54	2312	2174	7.988	2.56	1.62
20.06.	Huglhammaren	Hugl1	59.815	5.594	132	34.88	7.82	2311	2180	7.964	2.48	1.57
20.06.	Huglhammaren	Hugl1	59.815	5.594	81	34.68	7.97	2304	2182	7.952	2.43	1.54
20.06.	Huglhammaren	Hugl1	59.815	5.594	51	32.86	10.20	2250	2084	8.046	3.04	1.93
20.06.	Huglhammaren	Hugl1	59.815	5.594	10	30.83	12.35	2212	2034	8.071	3.29	2.09
20.06.	Huglhammaren	Hugl1	59.815	5.594	1	30.75	12.49	2204	2028	8.077	3.33	2.11
20.06.	Huglhammaren	Hugl2	59.815	5.593	203	34.96	7.54	2312	2173	7.989	2.56	1.63
20.06.	Huglhammaren	Hugl2	59.815	5.593	130	34.89	7.79	2311	2182	7.966	2.49	1.58
20.06.	Huglhammaren	Hugl2	59.815	5.593	81	34.40	7.86	2296	2170	7.966	2.47	1.57
20.06.	Huglhammaren	Hugl2	59.815	5.593	51	33.07	9.69	2253	2098	8.034	2.93	1.86
20.06.	Huglhammaren	Hugl2	59.815	5.593	10	30.93	12.18	2211	2036	8.074	3.30	2.09
20.06.	Huglhammaren	Hugl2	59.815	5.593	1	30.67	12.66	2203	2025	8.077	3.35	2.12
20.06.	Huglhammaren	Hugl3	59.815	5.594	206	34.92	7.64	2297	2177	7.979	2.50	1.59
20.06.	Huglhammaren	Hugl3	59.815	5.594	134	34.88	7.78	2289	2178	7.967	2.47	1.57
20.06.	Huglhammaren	Hugl3	59.815	5.594	82	34.50	7.94	2289	2171	7.966	2.48	1.57
20.06.	Huglhammaren	Hugl3	59.815	5.594	52	33.13	9.60	2251	2090	8.045	2.98	1.89
20.06.	Huglhammaren	Hugl3	59.815	5.594	11	30.78	12.24	2192	2033	8.074	3.27	2.07
20.06.	Huglhammaren	Hugl3	59.815	5.594	1	30.66	12.56	2193	2025	8.077	3.32	2.10
21.10.	Huglhammaren	Hugl1	59.815	5.594	180	35.14	7.96	2315	2179	7.969	2.52	1.60
21.10.	Huglhammaren	Hugl1	59.815	5.594	130	35.22	8.62	2311	2175	7.962	2.55	1.62
21.10.	Huglhammaren	Hugl1	59.815	5.594	80	34.26	10.23	2299	2152	7.973	2.73	1.74
21.10.	Huglhammaren	Hugl1	59.815	5.594	50	33.08	14.01	2262	2087	8.010	3.25	2.08
21.10.	Huglhammaren	Hugl1	59.815	5.594	10	29.28	14.12	2019	1871	8.013	2.77	1.75
21.10.	Huglhammaren	Hugl2	59.815	5.593	180	35.15	7.98	2313	2177	7.965	2.50	1.59
21.10.	Huglhammaren	Hugl2	59.815	5.593	130	35.22	8.65	2309	2172	7.963	2.56	1.63
21.10.	Huglhammaren	Hugl2	59.815	5.593	80	34.26	10.45	2300	2154	7.958	2.67	1.70
21.10.	Huglhammaren	Hugl2	59.815	5.593	50	33.07	14.12	2258	2089	7.989	3.12	2.00
21.10.	Huglhammaren	Hugl2	59.815	5.593	10	29.27	14.35	2065	1904	8.013	2.86	1.81
22.10.	Huglhammaren	Hugl3	59.815	5.594	180	35.14	7.96	2313	2182	7.964	2.49	1.58
22.10.	Huglhammaren	Hugl3	59.815	5.594	130	35.22	8.70	2309	2181	7.954	2.52	1.60

22.10.	Huglhammaren	Hugl3	59.815	5.594	80	34.27	10.37	2305	2183	7.909	2.42	1.54
22.10.	Huglhammaren	Hugl3	59.815	5.594	50	33.08	14.17	2276	2124	7.945	2.89	1.85
22.10.	Huglhammaren	Hugl3	59.815	5.594	10	29.28	14.52	2200	2028	8.029	3.17	2.00
20.06.	Straumsneset	Strau1	59.940	5.470	206	35.00	7.58	2314	2169	7.990	2.57	1.63
20.06.	Straumsneset	Strau1	59.940	5.470	134	34.89	7.67	2313	2169	7.982	2.56	1.62
20.06.	Straumsneset	Strau1	59.940	5.470	83	34.62	7.86	2303	2169	7.976	2.54	1.61
20.06.	Straumsneset	Strau1	59.940	5.470	52	33.08	9.90	2261	2100	8.036	2.97	1.89
20.06.	Straumsneset	Strau1	59.940	5.470	11	30.81	12.32	2209	2035	8.071	3.28	2.08
20.06.	Straumsneset	Strau1	59.940	5.470	1	30.69	12.51	2204	2026	8.074	3.31	2.10
20.06.	Straumsneset	Strau2	59.940	5.470	206	35.01	7.59	2315	2173	7.993	2.59	1.65
20.06.	Straumsneset	Strau2	59.940	5.470	134	34.89	7.66	2300	2157	8.003	2.65	1.68
20.06.	Straumsneset	Strau2	59.940	5.470	83	34.65	7.84	2302	2168	7.976	2.54	1.61
20.06.	Straumsneset	Strau2	59.940	5.470	52	33.25	9.61	2258	2095	8.043	2.98	1.89
20.06.	Straumsneset	Strau2	59.940	5.470	11	30.74	12.37	2209	2033	8.075	3.31	2.09
20.06.	Straumsneset	Strau2	59.940	5.470	1	30.65	12.52	2208	2026	8.075	3.33	2.10
21.06.	Straumsneset	Strau3	59.940	5.470	206	35.03	7.58	2316	2171	7.999	2.63	1.67
21.06.	Straumsneset	Strau3	59.940	5.470	133	34.89	7.66	2313	2175	7.984	2.57	1.63
21.06.	Straumsneset	Strau3	59.940	5.470	82	34.64	7.85	2303	2167	7.977	2.55	1.62
21.06.	Straumsneset	Strau3	59.940	5.470	52	33.11	9.87	2256	2088	8.049	3.04	1.93
21.06.	Straumsneset	Strau3	59.940	5.470	10	30.73	12.39	2212	2030	8.075	3.32	2.10
21.06.	Straumsneset	Strau3	59.940	5.470	1	30.70	12.43	2208	2027	8.078	3.33	2.11
23.10.	Straumsneset	Strau1	59.940	5.470	180	34.94	7.85	2312	2179	7.972	2.51	1.59
23.10.	Straumsneset	Strau1	59.940	5.470	130	34.69	8.50	2303	2170	7.966	2.53	1.61
23.10.	Straumsneset	Strau1	59.940	5.470	80	33.53	9.87	2277	2118	8.027	2.94	1.87
23.10.	Straumsneset	Strau1	59.940	5.470	50	32.67	13.60	2258	2082	8.019	3.24	2.07
23.10.	Straumsneset	Strau1	59.940	5.470	10	31.14	14.21	2178	2010	8.022	3.15	2.00
23.10.	Straumsneset	Strau2	59.940	5.470	180	34.95	7.90	2315	2180	7.972	2.52	1.60
23.10.	Straumsneset	Strau2	59.940	5.470	130	34.69	8.62	2305	2171	7.962	2.53	1.61
23.10.	Straumsneset	Strau2	59.940	5.470	80	33.52	10.23	2284	2132	8.001	2.84	1.80
23.10.	Straumsneset	Strau2	59.940	5.470	50	32.67	14.02	2257	2084	8.011	3.23	2.07
23.10.	Straumsneset	Strau2	59.940	5.470	10	31.13	14.35	2172	2005	8.020	3.14	2.00
24.10.	Straumsneset	Strau3	59.940	5.470	180	34.95	7.91	2313	2183	7.969	2.50	1.59
24.10.	Straumsneset	Strau3	59.940	5.470	130	34.69	8.59	2308	2176	7.958	2.51	1.59
24.10.	Straumsneset	Strau3	59.940	5.470	80	33.52	10.17	2284	2133	7.999	2.82	1.79

24.10.	Straumsneset	Strau3	59.940	5.470	10	31.13	14.27	2195	2077	7.878	2.38	1.51
19.10.*	Hola	Hola1	68.913	14.913	235	34.78	8.17	2306	2143	8.034	2.84	1.81
19.10.*	Hola	Hola2	68.915	14.432	236	34.76	8.17	-	-	-	-	-
19.10.*	Hola	Hola3	68.914	14.435	229	34.76	8.18	2304	2141	8.035	2.85	1.81
14.07.	Hola	Hola4	68.908	14.389	264	34.98	7.09	2311	2156	8.023	2.68	1.70
15.07.	Hola	Hola5	68.921	14.396	261	34.99	7.09	2310	2157	8.022	2.67	1.70
15.07.	Hola	Hola6	68.935	14.379	241	34.99	7.09	2312	2156	8.023	2.69	1.71
15.07.	Hola	Hola7	68.914	14.396	263	34.98	7.09	2310	2156	8.019	2.66	1.69
13.07.	Steinavaer	Stein1	69.233	16.682	370	34.93	6.77	2306	2151	8.022	2.60	1.65
13.07.	Steinavaer	Stein2	69.247	16.639	226	34.82	6.68	2305	2154	8.021	2.63	1.67
13.07.	Steinavaer	Stein3	69.248	16.638	233	35.02	6.86	2311	2155	8.028	2.70	1.71
12.07.	Stjernsund	Stj1	70.256	22.523	426	34.87	5.37	2303	2162	8.025	2.46	1.56
12.07.	Stjernsund	Stj1	70.256	22.523	310	34.84	5.40	2303	2158	8.030	2.52	1.60
12.07.	Stjernsund	Stj1	70.256	22.523	274	34.81	5.41	2300	2157	8.030	2.54	1.61
12.07.	Stjernsund	Stj1	70.256	22.523	235	34.75	5.46	2296	2156	8.036	2.58	1.63
12.07.	Stjernsund	Stj1	70.256	22.523	99	34.36	6.23	2283	2124	8.072	2.87	1.81
12.07.	Stjernsund	Stj1	70.256	22.523	49	34.25	6.94	2280	2104	8.105	3.15	1.99
12.07.	Stjernsund	Stj1	70.256	22.523	29	33.80	6.63	2273	2090	8.127	3.23	2.04
12.07.	Stjernsund	Stj1	70.256	22.523	10	33.18	7.17	2244	2066	8.114	3.15	1.99
12.07.	Stjernsund	Stj2	70.272	22.454	345	34.93	5.38	2306	2161	8.029	2.52	1.60
12.07.	Stjernsund	Stj2	70.272	22.454	308	34.91	5.37	2304	2157	8.029	2.52	1.60
12.07.	Stjernsund	Stj2	70.272	22.454	274	34.88	5.39	2303	2160	8.031	2.54	1.61
12.07.	Stjernsund	Stj2	70.272	22.454	234	34.80	5.42	2302	2153	8.035	2.58	1.63
12.07.	Stjernsund	Stj2	70.272	22.454	99	34.40	6.02	2287	2130	8.069	2.84	1.79
12.07.	Stjernsund	Stj2	70.272	22.454	49	34.20	7.06	2278	2097	8.115	3.22	2.04
12.07.	Stjernsund	Stj2	70.272	22.454	29	33.70	6.30	2262	2078	8.136	3.23	2.04
12.07.	Stjernsund	Stj2	70.272	22.454	10	33.34	6.84	2231	2050	8.133	3.22	2.03
22.09.	Stjernsund	Stj5	70.274	22.495	192	34.39	5.80	2283	2147	8.033	2.58	1.63
22.09.	Stjernsund	Stj5	70.274	22.495	152	34.43	7.03	2282	2130	8.039	2.74	1.74
22.09.	Stjernsund	Stj5	70.274	22.495	101	34.37	8.02	2280	2123	8.057	2.96	1.88
22.09.	Stjernsund	Stj5	70.274	22.495	76	34.35	8.59	2280	2114	8.062	3.06	1.94
22.09.	Stjernsund	Stj5	70.274	22.495	50	34.28	9.32	2279	2102	8.078	3.25	2.06
22.09.	Stjernsund	Stj5	70.274	22.495	31	34.11	9.49	2270	2082	8.104	3.42	2.17
22.09.	Stjernsund	Stj5	70.274	22.495	10	33.87	9.08	2254	2064	8.118	3.44	2.18

22.09.	Stjernsund	Stj4	70.267	22.472	227	34.57	5.66	2289	2153	8.028	2.54	1.61
22.09.	Stjernsund	Stj4	70.267	22.472	151	34.37	6.68	2280	2132	8.039	2.71	1.71
22.09.	Stjernsund	Stj4	70.267	22.472	101	34.39	8.26	2283	2121	8.057	2.99	1.90
22.09.	Stjernsund	Stj4	70.267	22.472	50	34.16	9.17	2274	2097	8.082	3.24	2.06
22.09.	Stjernsund	Stj4	70.267	22.472	30	33.99	9.26	2264	2080	8.105	3.38	2.15
22.09.	Stjernsund	Stj4	70.267	22.472	12	33.77	8.99	2252	-	8.117	3.41	2.16
22.09.	Stjernsund	Stj3	70.258	22.459	200	34.61	5.73	2290	-	8.034	2.59	1.64
22.09.	Stjernsund	Stj3	70.258	22.459	151	34.44	6.91	2282	2135	8.039	2.74	1.73
22.09.	Stjernsund	Stj3	70.258	22.459	100	34.36	8.67	2281	2120	8.058	3.04	1.93
22.09.	Stjernsund	Stj3	70.258	22.459	50	34.19	9.36	2274	2085	8.083	3.27	2.08
22.09.	Stjernsund	Stj3	70.258	22.459	29	34.01	9.26	2265	2075	8.113	3.44	2.18
22.09.	Stjernsund	Stj3	70.258	22.459	12	33.74	8.87	2243	2049	8.122	3.42	2.17
22.09.	Stjernsund	Stj1	70.255	22.523	443	34.88	5.49	2300	2170	8.010	2.39	1.52
22.09.	Stjernsund	Stj1	70.255	22.523	312	34.86	5.48	2302	-	8.021	2.48	1.58
22.09.	Stjernsund	Stj1	70.255	22.523	274	34.81	5.52	2298	2160	8.021	2.50	1.58
22.09.	Stjernsund	Stj1	70.255	22.523	236	34.70	5.59	2297	2162	8.022	2.52	1.59
22.09.	Stjernsund	Stj1	70.255	22.523	100	34.42	8.25	2286	2122	8.055	2.98	1.89
22.09.	Stjernsund	Stj1	70.255	22.523	50	34.24	9.33	2280	2096	8.086	3.30	2.09
22.09.	Stjernsund	Stj1	70.255	22.523	31	34.05	9.34	2269	2076	8.116	3.48	2.21
22.09.	Stjernsund	Stj1	70.255	22.523	10	33.94	9.21	2262	2069	8.117	3.46	2.20
22.09.	Stjernsund	Stj2	70.271	22.454	357	34.91	5.60	2306	2166	8.015	2.46	1.56
22.09.	Stjernsund	Stj2	70.271	22.454	313	34.87	5.63	2305	2166	8.017	2.48	1.57
22.09.	Stjernsund	Stj2	70.271	22.454	278	34.78	5.60	2300	2162	8.020	2.50	1.58
22.09.	Stjernsund	Stj2	70.271	22.454	101	34.42	8.36	2287	2121	8.053	2.98	1.89
22.09.	Stjernsund	Stj2	70.271	22.454	50	34.20	9.18	2277	2100	8.082	3.25	2.06
22.09.	Stjernsund	Stj2	70.271	22.454	29	34.00	9.27	2269	2073	8.107	3.41	2.16
22.09.	Stjernsund	Stj2	70.271	22.454	10	33.77	8.95	2248	2058	8.117	3.40	2.16
11.07.	Fugløya	Fugl1	70.330	20.551	174	34.65	6.00	2296	2145	8.041	2.67	1.69
11.07.	Fugløya	Fugl2	70.328	20.623	164	34.77	5.77	2297	2150	8.033	2.62	1.66
11.07.	Fugløya	Fugl3	70.343	20.534	136	34.54	6.32	2289	2133	8.049	2.75	1.74
12.07.	Korallen	Koral1	70.929	22.189	145	34.71	6.40	2295	2143	8.043	2.73	1.73
12.07.	Korallen	Koral2	70.932	22.190	203	34.86	6.40	2301	2147	8.035	2.68	1.70
12.07.	Korallen	Koral3	70.932	22.190	200	34.82	6.33	2301	2155	8.038	2.69	1.70

Table 14. Water column station in Troms/Finnmark; Straumsfjorden (VR54) at 69.50°N 18.34°E, 2019.

Date	Depth	S	T	A_T	C_T	pH_T	pCO_2	Ω_{Ca}	Ω_{Ar}	NO_3^-	PO_3^4	$SiOH_4$
	m		C°	µmol/kg	µmol/kg		µatm			µmol/kg	µmol/kg	µmol/kg
10.02	0	25.39	3.75	2212.5	2114.4	8.050	399.4	2.10	1.28	6.9	0.6	5.5
10.02	5	33.74	3.77	2253.5	2104.7	8.081	350.5	2.65	1.67	7.2	0.6	5.5
10.02	10	33.75	3.77	2253.3	2103.5	8.083	348.2	2.66	1.67	7.2	0.6	5.7
10.02	20	33.76	3.71	2252.8	2114.6	8.053	375.7	2.49	1.57	7.5	0.6	5.4
10.02	30	33.53	3.79	2256.2	-	-	-	-	-	7.1	0.5	5.2
02.03	0	27.83	0.45	1846.7	1848.2	7.691	770.1	0.74	0.46	8.6	0.5	12.0
02.03	5	30.07	2.65	2051.8	1950.2	8.030	371.0	1.95	1.22	8.1	0.5	8.8
02.03	10	32.94	3.25	2224.5	2089.8	8.064	361.9	2.45	1.54	7.7	0.6	6.0
02.03	20	33.48	3.86	2238.7	2103.0	8.049	378.2	2.46	1.55	7.8	0.6	6.0
02.03	30	32.97	3.98	-	2045.3	-	-	-	-	7.7	0.6	6.0
06.04	0	30.83	2.41	2106.9	1928.9	8.235	223.0	3.06	1.91	0.5	0.1	3.7
06.04	5	31.03	2.64	2122.0	1941.1	8.233	225.4	3.10	1.94	0.5	0.1	3.4
06.04	10	32.04	3.31	2172.9	1995.6	8.192	255.2	3.05	1.91	0.8	0.2	2.4
06.04	20	33.84	4.40	2259.5	2075.2	8.155	289.2	3.15	1.98	6.3	0.5	3.7
06.04	30	33.98	4.47	2263.9	2106.0	8.088	345.2	2.77	1.74	6.5	0.5	4.2
26.04	0	14.23	5.39	1156.2	1103.9	8.143	192.2	1.09	0.62	6.6	0.2	28.3
26.04	5	30.92	4.96	2155.8	1971.6	8.199	252.2	3.19	2.00	1.9	0.3	4.7
26.04	10	33.17	4.79	2233.6	2055.2	8.147	294.0	3.08	1.94	3.1	0.4	3.9
26.04	20	33.81	4.71	2251.9	2083.7	8.113	322.2	2.92	1.84	5.3	0.5	3.7
26.04	30	33.76	4.69	2256.9	2091.3	8.107	328.2	2.88	1.81	5.1	0.5	3.9
21.05	0	20.56	6.03	1528.9	1433.5	8.164	220.0	1.79	1.07	0.3	0.1	18.3
21.05	5	31.5	5.70	2174.4	1983.8	8.192	258.2	3.29	2.06	0.1	0.1	4.5
21.05	10	32.64	5.35	2194.8	2006.5	8.174	270.4	3.22	2.03	0.1	0.1	4.2
21.05	20	33.76	5.28	2252.5	2090.9	8.088	344.6	2.83	1.78	4.3	0.4	3.9
21.05	30	33.82	5.28	2253.5	2095.1	8.079	352.6	2.78	1.75	4.2	0.4	3.9
23.06	0	18.21	10.17	1380.3	1298.0	8.111	238.6	1.61	0.95	0.1	0.1	9.4
23.06	5	29.73	7.64	2106.5	1897.0	8.238	225.1	3.62	2.27	0.2	0.1	1.1
23.06	10	32.22	6.79	2134.3	2006.8	8.007	408.9	2.35	1.48	1.7	0.2	1.3
23.06	20	32.04	6.42	2149.2	1983.3	8.115	311.0	2.89	1.82	5.3	0.4	2.6
23.06	30	33.39	6.25	2228.4	2066.7	8.080	349.2	2.83	1.79	3.2	0.3	1.9

21.07	0	19.26	12.01	1489.6	1386.6	8.131	242.6	1.98	1.19	0.1	0.1	9.3
21.07	5	30.13	9.28	2090.4	1907.7	8.146	285.7	3.20	2.01	1.2	0.2	2.9
21.07	10	32.7	8.56	2194.6	2016.6	8.097	333.4	3.10	1.96	1.5	0.3	1.9
21.07	20	33.55	7.96	2237.1	2049.8	8.111	324.4	3.22	2.04	2.8	0.4	1.8
21.07	30	33.79	7.88	2245.4	2062.0	8.099	335.5	3.15	2.00	3.2	0.4	1.9
31.08	0	32.16	10.85	2153.0	1980.1	8.062	362.6	3.05	1.93	1.4	0.3	1.8
31.08	5	32.56	10.55	2169.4	1988.9	8.076	349.8	3.15	1.99	1.7	0.3	1.8
31.08	10	33.04	9.61	2208.0	2041.2	8.047	382.6	2.95	1.87	3.3	0.4	2.6
31.08	20	33.57	8.93	2234.8	2064.3	8.056	375.5	2.99	1.89	3.8	0.4	2.3
31.08	30	33.7	8.61	2236.6	2062.1	8.069	362.7	3.03	1.92	3.4	0.4	1.9
31.08	50	34.09	8.44	2260.3	2088.6	8.057	375.8	2.99	1.89	-	-	-
31.08	75	34.22	8.29	2268.6	2092.8	8.065	368.5	3.02	1.92	3.8	0.5	1.8
31.08	100	34.35	7.13	2272.0	2108.1	8.051	379.5	2.83	1.79	5.2	0.5	3.1
31.08	125	34.37	6.44	2275.2	2118.2	8.043	386.1	2.71	1.71	7.0	0.7	4.4
31.08	150	34.73	-	2324.9	2115.4	-	-	-	-	7.1	0.7	4.5
26.09	0	30.61	8.65	2075.8	1908.4	8.113	307.4	2.94	1.85	0.7	0.2	3.4
26.09	5	31.66	9.04	2134.1	1961.0	8.099	325.4	3.03	1.91	0.6	0.2	2.4
26.09	10	32.89	9.07	2196.3	2017.8	8.087	342.4	3.11	1.97	1.2	0.3	2.1
26.09	20	33.37	8.97	2218.7	2057.3	8.038	391.7	2.85	1.81	2.6	0.4	2.3
26.09	30	32.58	8.79	-	2006.6	-	-	-	-	1.4	0.3	2.1
26.09	50	33.91	9.89	2255.9	2073.5	8.062	372.5	3.15	2.00	1.9	0.3	1.3
26.09	75	34.28	9.84	2268.6	2094.5	8.036	398.8	3.01	1.92	3.3	0.5	1.8
26.09	100	34.11	8.99	-	2082.0	-	-	-	-	3.6	0.4	2.1
26.09	125	34.2	7.51	2262.5	2101.9	8.039	389.8	2.77	1.75	5.0	0.6	2.8
26.09	150	34.3	-	2267.6	2110.0	-	-	-	-	5.2	0.6	3.1
30.10	0	25.39	3.75	2231.6	2062.9	8.077	354.5	2.95	1.87	3.4	0.4	3.4
30.10	5	33.74	3.77	2232.1	2062.9	8.078	353.7	2.96	1.87	3.4	0.4	3.4
30.10	10	33.75	3.77	-	2067.4	-	-	-	-	3.5	0.4	3.4
30.10	20	33.76	3.71	2234.9	2061.0	8.086	345.6	3.02	1.91	3.6	0.4	3.1
30.10	30	33.53	3.79	2249.2	2057.8	8.116	321.4	3.27	2.07	3.6	0.4	3.1
30.10	50	27.83	0.45	2240.2	2056.4	8.090	342.2	3.15	2.00	3.2	0.4	2.6
30.10	75	30.07	2.65	2259.1	2080.1	8.066	366.9	3.07	1.95	3.4	0.4	2.8
30.10	100	32.94	3.25	2271.9	2077.1	8.098	337.7	3.29	2.09	3.3	0.4	2.6

30.10	125	33.48	3.86	2260.3	2095.6	8.041	388.3	2.83	1.80	4.2	0.5	3.1
30.10	150	32.97	3.98	2259.5	2094.4	8.052	375.3	2.81	1.78	6.3	0.7	4.5
28.11	0	30.83	2.41	2246.8	2081.3	8.087	346.3	2.90	1.83	4.9	0.5	3.2
28.11	5	31.03	2.64	2241.6	2085.0	8.065	365.4	2.77	1.75	4.9	0.5	3.2
28.11	10	32.04	3.31	2239.8	2086.3	8.057	373.0	2.73	1.72	4.9	0.5	3.2
28.11	20	33.84	4.40	2244.5	2088.6	8.062	368.5	2.76	1.74	5.1	0.5	3.2
28.11	30	33.98	4.47	2240.4	2087.9	8.053	376.1	2.70	1.70	5.1	0.5	3.4
28.11	50	14.23	5.39	2250.4	2089.7	8.069	361.3	2.81	1.77	4.7	0.5	2.9
28.11	75	30.92	4.96	2249.3	2092.0	8.052	377.2	2.75	1.74	4.7	0.5	2.9
28.11	100	33.17	4.79	2249.9	2083.9	8.074	355.1	2.86	1.81	-	-	-
28.11	125	33.81	4.71	2265.9	2115.8	8.020	409.5	2.63	1.66	6.3	0.6	4.1
28.11	150	33.76	4.69	2267.3	2117.7	8.013	416.2	2.61	1.65	7.1	0.7	4.5

Table 15. Water column station in Svalbard; Isfjorden (IsA station) at 78.26 °N 15.53°E, 2019.

Date	Station	Depth	S	T	A_T	C_T	pH_T	Ω_{Ca}	Ω_{Ar}
		m		C°	µmol/kg	µmol/kg			
10.05.	IsA	63	34.93	1.97	2306	2159	8.085	2.59	1.63
10.05.	IsA	50	34.94	2.16	2306	2155	8.092	2.65	1.67
10.05.	IsA	25	34.95	2.24	2305	2153	8.096	2.68	1.69
10.05.	IsA	10	34.95	2.25	2307	2155	8.097	2.70	1.70
10.05.	IsA	2	34.84	2.24	2305	2156	8.088	2.65	1.67
05.08.	IsA	2	31.20	8.89	2125	1926	8.179	3.49	2.20
05.08.	IsA	5	31.52	8.91	2153	1951	8.177	3.54	2.23
05.08.	IsA	10	32.48	7.70	2193	1992	8.183	3.55	2.24
05.08.	IsA	20	33.37	6.16	2232	2032	8.192	3.53	2.23
05.08.	IsA	30	34.21	4.80	2270	2078	8.189	3.44	2.17
05.08.	IsA	50	34.55	4.11	2292	2099	8.185	3.37	2.13
11.09.	IsA	2	32.71	4.98	2193	1921	8.172	3.18	2.00
11.09.	IsA	15	32.90	4.92	2195	1937	8.155	3.07	1.93
11.09.	IsA	68	34.00	4.82	2263	1985	8.156	3.19	2.01
03.10.	IsA	80	34.47	4.27	2289	2147	8.153	3.16	2.00
03.10.	IsA	50	33.95	4.23	2259	2123	8.155	3.12	1.96
03.10.	IsA	30	33.46	3.52	2238	2100	8.164	3.06	1.92
03.10.	IsA	10	33.09	3.38	2226	2090	8.167	3.03	1.90
03.10.	IsA	4	33.08	3.36	2217	2084	8.166	3.01	1.89
12.11.	IsA	100	34.65	4.26	-	-	-	-	-
12.11.	IsA	50	33.77	1.43	2242	2096	8.126	2.64	1.66
12.11.	IsA	30	33.49	0.12	2237	2083	8.140	2.57	1.61
12.11.	IsA	10	33.46	0.07	2212	2085	8.142	2.56	1.61
12.11.	IsA	5	33.46	0.64	2229	2082	8.134	2.59	1.62
28.11.	IsA	81	34.21	3.40	2254	2106	8.106	2.74	1.73
28.11.	IsA	50	34.07	2.95	-	2105	-	-	-
28.11.	IsA	30	33.89	1.90	2236	2101	8.123	2.67	1.68
28.11.	IsA	11	33.66	0.23	2253	2097	8.138	2.61	1.63

Table 16. Water column station in Svalbard; Isfjorden/Grønnefjorden (SVR1) at 78.13°N 14.00°E, 2019.

Date	Depth	S	T	A_T	C_T	pH_T	pCO_2	Ω_{Ca}	Ω_{Ar}	NO_3^-	PO_3^4	$SiOH_4$
	m		C°	µmol/kg	µmol/kg		µatm			µmol/kg	µmol/kg	µmol/kg
21.8	0	33.9	5.254	2241.7	2029.1	8.207	250.6	3.57	2.25	0.3	0.3	2.4
21.8	5	33.92	5.262	2241.4	2038.0	8.187	264.6	3.43	2.16	0.3	0.3	2.4
21.8	10	33.98	5.232	2242.7	2031.7	8.203	253.4	3.54	2.23	0.4	0.3	2.6
21.8	20	34.38	4.822	2267.4	2073.0	8.164	282.8	3.29	2.07	1.1	0.3	2.4
21.8	30	34.65	4.515	2284.7	2087.9	8.168	280.8	3.31	2.09	1.1	0.4	2.4
21.8	50	34.49	3.797	-	2072.4	-	-	-	-	1.9	0.4	2.8
21.8	75	34.85	3.751	2297.0	2114.5	8.142	299.7	3.07	1.94	3.5	0.5	3.6
21.8	100	34.95	3.484	2300.2	2121.4	8.135	304.4	3.00	1.89	4.9	0.6	3.6
21.8	125	35.07	3.401	2307.3	2132.4	8.124	313.4	2.92	1.85	6.4	0.7	4.1
21.8	200	35.12	3.19	2308.7	2153.4	8.076	352.1	2.61	1.65	8.6	0.9	4.5
21.8	275	35.12	-	2309.8	2160.4	8.113	313.4	2.47	1.56	-	-	-
06.09	0	33.19	4.928	2200.3	2012.3	8.172	271.1	3.21	2.02	0.2	0.2	1.4
06.09	5	33.19	4.934	2200.0	2009.9	8.177	267.5	3.23	2.04	0.2	0.2	1.4
06.09	10	33.21	4.957	2199.2	2015.6	8.161	278.7	3.14	1.97	0.3	0.2	1.3
06.09	20	33.54	4.952	2222.4	2031.8	8.170	274.2	3.23	2.04	0.5	0.3	1.3
06.09	30	34.18	4.914	2254.9	2066.2	8.153	289.3	3.20	2.02	1.3	0.3	1.6
06.09	50	34.69	4.545	2282.3	2096.9	8.141	300.6	3.13	1.98	2.8	0.5	2.3
06.09	75	34.96	4.025	2291.0	2121.3	8.107	328.0	2.89	1.82	3.8	0.5	2.6
06.09	125	35.14	3.669	2308.0	2142.3	8.097	336.6	2.80	1.77	7.5	0.7	3.4
06.09	200	35.24	3.416	-	2157.9	-	-	-	-	11.1	0.9	5.0
06.09	290	35.19	5.254	-	2167.9	-	-	-	-	-	-	-

Table 17. Discrete underway stations in Svalbard (Isfjorden, ISF) in November 2019.

Date	Station	Lat	Lon	Depth	S	T	A_T	C_T	pH_T	Ω_{Ca}	Ω_{Ar}
		°N	°E	m		C°	µmol/kg	µmol/kg			
12.11.	ISF-1	78.26	15.23	5	33.50	0.47	2239	2080	8.139	2.62	1.64
12.11.	ISF-2	78.24	15.04	5	33.51	0.58	2235	2084	8.137	2.61	1.64
12.11.	ISF-3	78.21	14.77	5	33.40	0.48	2237	2078	8.141	2.62	1.64
12.11.	ISF-4	78.18	14.51	5	33.38	0.41	2232	2078	8.142	2.61	1.64
12.11.	ISF-5	78.16	14.26	5	33.37	0.30	2219	2079	8.142	2.58	1.62
12.11.	ISF-6	78.13	13.96	5	33.43	-0.34	2228	2084	8.116	2.41	1.51
12.11.	ISF-7	78.11	13.71	5	33.37	-0.34	2204	2083	8.113	2.36	1.48
12.11.	ISF-8	78.08	13.47	5	33.46	-0.36	2212	2090	8.108	2.35	1.47
12.11.	ISF-9	78.07	13.07	5	33.64	0.21	2228	2099	8.106	2.42	1.52
12.11.	ISF-10	78.07	12.12	5	34.15	1.74	2260	2122	8.102	2.59	1.63
28.11.	ISF-1	78.26	15.23	5	33.48	-0.53	-	2095	-	-	-
28.11.	ISF-2	78.24	15.04	5	33.55	-0.33	2215	2092	8.134	2.49	1.56
28.11.	ISF-3	78.21	14.77	5	33.50	-0.53	2212	2093	8.135	2.47	1.55
28.11.	ISF-4	78.18	14.51	5	33.48	-0.44	2220	2093	8.137	2.50	1.56
28.11.	ISF-5	78.16	14.26	5	33.55	-0.82	-	2100	-	-	-
28.11.	ISF-6	78.13	13.96	5	33.59	-0.46	2220	2096	8.120	2.41	1.51
28.11.	ISF-7	78.11	13.71	5	33.57	-1.04	2223	2105	8.104	2.29	1.43
28.11.	ISF-8	78.08	13.47	5	33.58	-0.91	2218	2102	8.099	2.27	1.42
28.11.	ISF-9	78.07	13.07	5	33.69	-0.74	2227	2108	8.092	2.27	1.42
28.11.	ISF-10	78.07	12.12	5	34.01	-0.06	2238	2116	8.101	2.39	1.50

6.3 Definitions

A_T = [HCO_3^-] + 2[CO_3^{2-}] + [$B(OH)_4^-$] + [OH^-]+[HPO_4^{2-}] + 2[PO_4^{3-}] + [$SiO(OH)_3^-$] + [NH_3] + [HS^-] - [H^+] - [HSO_4^-] + [HF^-] + [$H_3 PO_4$] -…..

Equation 4

C_T = [CO_2*] + [HCO_3^-] + [CO_3^{2-}] *Equation 5*

[H^+] ~ [H^+]$_f$ +[HSO_4^-],
der [H^+]$_f$ er den frie hydrogenkonsentrasjonen

pH = -log10 ([H^+]) *Equation 6*

pCO_2 = [CO_2*]/K_0 *Equation 7*

6.4 Organic alkalinity

A_T is defined according to Dickson (1981) as "*… the number of moles of hydrogen ion equivalent to the excess of proton acceptors (bases formed from weak acids with a dissociation constant $K \leq 10^{-4.5}$, at 25 °C and zero ionic strength) over proton donors (acids with $K > 10^{-4.5}$) in one kilogram of sample*". This is ***Eq. 4*** (***Chapter 6.3***) in written text, and it represents the measured A_T. ***Eq. 4*** is, in contrast to the other definitions in this chapter, an ambiguous definition, because it includes unknown acids and bases (represented by the ellipses in the equation) that are not part of the CO_2 system. This could be e.g. weak organic acids from terrestrial humic substances transported to the coastal areas by rivers (Ulfsbø et al. 2015). These unknown substances are interpreted as organic alkalinity, A_{org} simply because there are no other potential sources of excess A_T in oxic water.

In the literature, we find reports on experiments where the measured A_T (according to Eq. 4) is larger than the A_T calculated by two of the other carbon variables: C_T and pH or C_T and pCO_2. This excess A_T, which equals the A_{org}, appears because the A_T analyse includes both inorganic and organic substances, while the current calculation software, like CO2SYS (Pierrot et al., 2006), only include the inorganic part of the carbonate system. In the open ocean, where the amount of organic matter is assumed to be low, A_{org} is also assumed to be low. On the contrary, A_{org} is assumed to play a significant role in coastal waters, where the amount of organic matter is large. Studies from the Baltic Sea have shown that A_{org} amounts to 25-35 µmol kg^{-1} in the surface waters, which represents 1.5-3.5% of the measured A_T. The Baltic Sea receives huge amounts of terrestrial organic matter and the eutrophication is large due to nutrient supply from land (Kuliński et al., 2017).

The nature of the organic acids is not well known, which makes it difficult to fully understand how they affect the carbonate system. The A_T and C_T pair is frequently used in biogeochemical models to calculate the remaining variables of the carbonate system (e.g. Edman and Omstedt, 2013). The A_T-C_T pair is attractive due to the conservative behaviour with respect to temperature and pressure. If the measured A_T used in a coastal model is not corrected for A_{org}, the calculated pH and pCO_2 will also be erroneous. A sensitivity study from the Baltic Sea reported that pCO_2 was underestimated by 27-56% and pH was overestimated by up to 0.4 when A_T data which were not corrected for A_{org} was used (Kuliński et al., 2014). Thus, it is important to consider the A_{org} when the carbonate system is calculated from coastal data.

However, these calculations are not straight forward and there are a number of sources for uncertainty: e.g. uncertainty in the dissociation constants and uncertainty in the measured C_T, pH and A_T. According to Orr et al. (2018), calculating A_T from the pair C_T-pH introduces an uncertainty of 0.6% in the A_T value, given that uncertainty of the dissociation constants are included and the standard uncertainty of C_T is 0.5% and that of pH is 0.01. Following from this, if the A_T value is calculated from C_T and pH to be about 2300 μmol kg^{-1}, this value has an uncertainty interval of ± 15 μmol kg^{-1}. This has to be taken into consideration when the A_{org} is estimated in the following paragraphs.

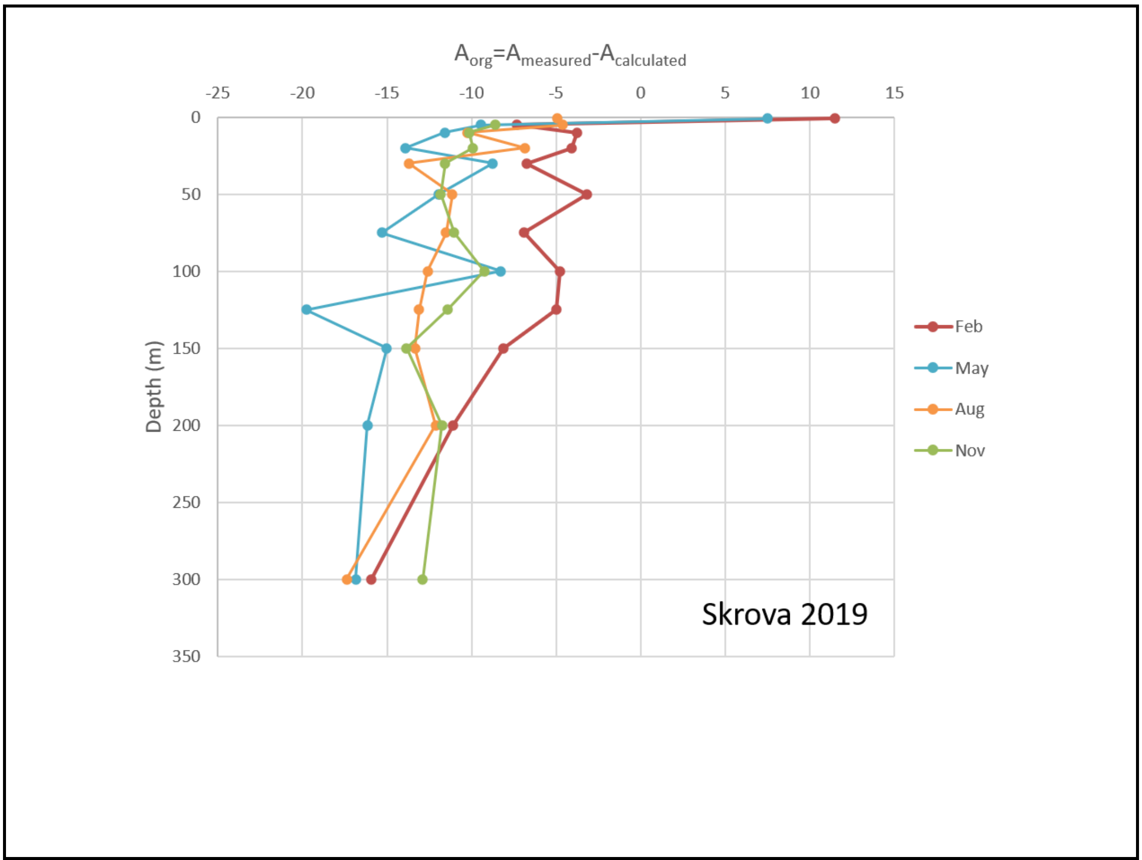

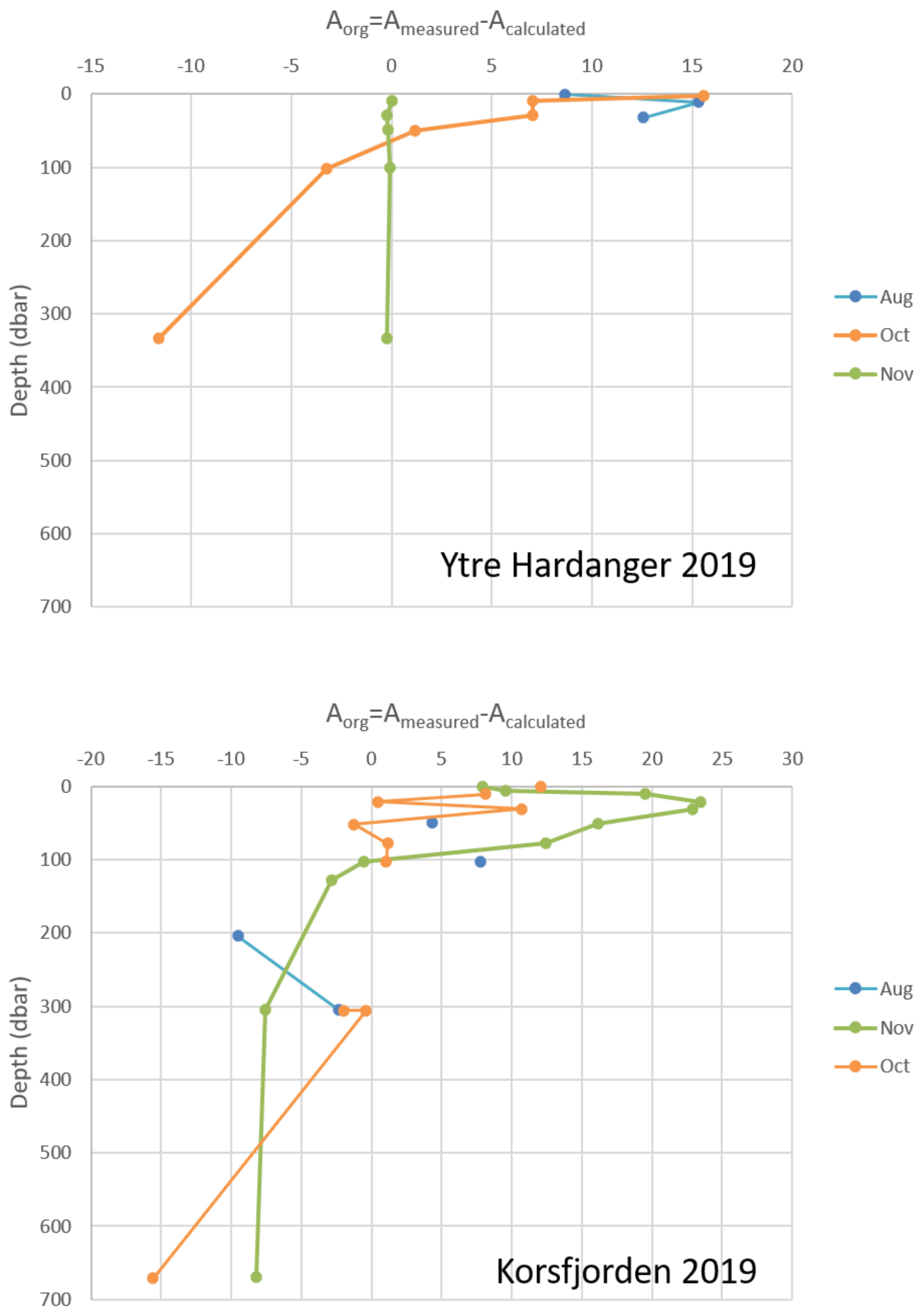

***Figure 77**. Organic alkalinity (A_{org}) as a function of depth (dbar and m is almost interchangeable in this context) from coastal areas at Skrova (upper plot, HI data) and in Hardanger (two lower plots, NORCE data).*

***Figur 77**. Organisk alkalinitet (A_{org}) som funksjon av dyp (dbar og m er nærmest ensbetydende i denne konteksten) fra kystnære områder ved Srova (øverst, HI-data) og i Hardanger (to nederste figurer, NORCE-data).*

Here, we have performed a first attempt to estimate the organic alkalinity, A_{org}, in some of the regions included in the ocean acidification program, and we have used data collected by NORCE-UiB and HI. We have focussed on data material where three of the carbon variables have been analysed from the same water sample: C_T, pH, and A_T, and we have calculated A_T from the two other carbon variables: C_T and pH. The excess A_T is the difference between analysed A_T and calculated A_T, and this is interpreted as A_{org}. For comparison, we have included data from both coastal areas and the open ocean.

Figure 77 shows the A_{org} as a function of depth in a few coastal areas: the Skrova area (upper plot) and the Hardanger are (two lower plots). The surface A_{org} varies between -10 and 25 µmol kg^{-1} at the different coastal stations (approximately 0 to 1% of the measured A_T values), while the deeper A_{org} values at these stations vary between -20 and 0 µmol kg^{-1}. At Skrova, there seems to be a seasonality in A_{org}, but this is hard to see in the Hardanger data due to few data points.

Figure 78 shows the A_{org} from the open ocean: the Greenland Sea (upper plot) and along the Svinøy section (lower plot). The amount of A_{org} in the surface waters is low: from -30 to 10 µmol kg^{-1} in the Greenland Sea and -10 to 5 µmol kg^{-1} at the Svinøy section. The A_{org} also seems to decrease with depth in both open ocean areas, which cannot be explained by organic matter. One explanation might be that pH from large depths are losing CO_2 during sampling and analysis, which will lead to an overestimation of the pH and thus, the calculated A_T will be too large. Another explanation might be that the deeper water is rich in calcite particles, which will overestimate the C_T values, and thus the calculated A_T will be too high. A third explanation for the negative deep water A_{org} might be that some of the pH samples were poisoned with $HgCl_2$ and analysed at a later stage, which might affect the pH, either by losing CO_2 to the surroundings or by $HgCl_2$ directly influencing the pH. Correction for this is difficult.

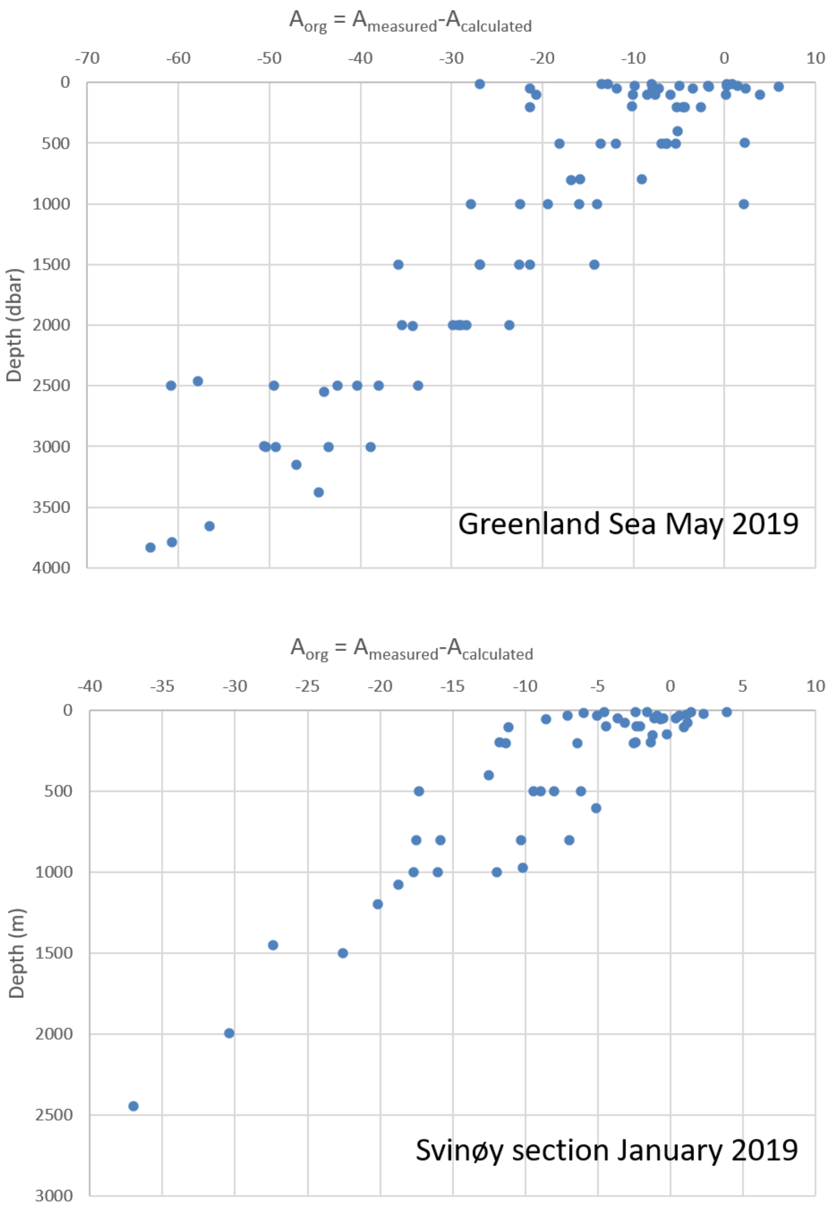

Figure 78. *Organic alkalinity (A_{org}) as a function of depth (dbar and m is almost interchangeable in this context) from open ocean areas in the Greenland Sea (upper plot, NORCE-UiB data) and at the Svinøy section (lower plot, HI data).*

Figur 78. *Organisk alkalinitet (A_{org}) som funksjon av dyp (dbar og m er nærmest ensbetydende i denne konteksten) fra åpne havområder i Grønlandshavet (øverst, NORCE-UiB-data) og langs Svinøysnittet (nederst, HI-data).*

To conclude, estimating A_{org} in coastal waters is important but difficult, since there are large uncertainties connected to the estimates. More knowledge is needed regarding this topic, and a way forward is to analyse three carbon variables (C_T, A_T, and pH) instead of only two (C_T and A_T) from the same water sample. Currently, this is not feasible for all stations and depths, but it could be performed for selected stations if funding and personnel were available.

Norwegian Environment Agency
Telephone: +47 73 58 05 00 | Fax: +47 73 58 05 01
E-mail: post@miljodir.no
Web: www.miljødirektoratet.no
Postal address: Postboks 5672 Torgarden, N-7485 Trondheim
Visiting address Trondheim: Brattørkaia 15, 7010 Trondheim
Visiting address Oslo: Grensesvingen 7, 0661 Oslo

The Norwegian Environment Agency is working for a clean and diverse environment. Our primary tasks are to reduce greenhouse gas emissions, manage Norwegian nature, and prevent pollution.

We are a government agency under the Ministry of Climate and Environment and have 700 employees at our two offices in Trondheim and Oslo and at the Norwegian Nature Inspectorate's more than sixty local offices.

We implement and give advice on the develop-pment of climate and environmental policy. We are professionally independent. This means that we act independently in the individual cases that we decide and when we communicate knowledge and information or give advice.

Our principal functions include collating and communicating environmental information, exercising regulatory authority, supervising and guiding regional and local government level, giving professional and technical advice, and participating in international environmental activities.